Development, Testing, and Sensitivity and Uncertainty Analyses of a Transport and Reaction Simulation Engine (TaRSE) for Spatially Distributed Modeling of Phosphorus in the Peat Marsh Wetlands of Southern Florida

By James W. Jawitz, Rafael Muñoz-Carpena, Stuart Muller, Kevin A. Grace, and Andrew I. James

Prepared in Cooperation with the South Florida Water Management District

Scientific Investigations Report 2008-5029

U.S. Department of the Interior
U.S. Geological Survey

U.S. Department of the Interior
DIRK KEMPTHORNE, Secretary

U.S. Geological Survey
Mark D. Myers, Director

U.S. Geological Survey, Reston, Virginia: 2008

For product and ordering information:
World Wide Web: http://www.usgs.gov/pubprod
Telephone: 1-888-ASK-USGS

For more information on the USGS--the Federal source for science about the Earth, its natural and living resources, natural hazards, and the environment:

World Wide Web: http://www.usgs.gov
Telephone: 1-888-ASK-USGS

Suggested citation:

Jawitz, J.W., Muñoz-Carpena, Rafael, Muller, Stuart, Grace, K.A., and James A.I., 2008, Development, Testing, and Sensitivity and Uncertainty Analyses of a Transport and Reaction Simulation Engine (TaRSE) for Spatially Distributed Modeling of Phosphorus in the Peat Marsh Wetlands of Southern Florida: U.S. Geological Survey Scientific Investigations Report 2008-5029, 109 p.

Contents

Figures

Tables

Conversion Factors

Multiply	By	To Obtain
micrometer (μm)	0.03937	inch
centimeter (cm)	0.3937	inch
meter (m)	3.281	foot
kilometer (km)	0.6214	mile
square meter (m^2)	0.0002471	acre
hectare (ha)	2.471	acre
square kilometer (km^2)	247.1	acre
centimeter per second (cm/s)	0.3937	inch per second
centimeter per day (cm/d)	0.3937	inch per day
meter per second (m/s)	3.281	foot per second
meter per square second (m/s^2)	3.281	foot per square second
square meter per second (m^2/s)	10.76	square foot per second
meter per day (m/d)	3.281	foot per day
meter per year (m/yr)	3.281	foot per year
gram per square meter (g/m^2)	10.76	gram per square foot
gram per square meter per day $g/m^2/d$	10.76	gram per square foot per day
gram per square meter per second $g/m^2/s$	10.76	gram per square foot per second
gram per cubic centimeter (g/cm^3)	62.4220	pound per cubic foot
gram per cubic meter (g/m^3)	35.32	gram per cubic foot

Abbreviations and Acronyms

CDF	cumulative distribution function
EAA	Everglades Agricultural Area
FAST	Fourier Amplitude Sensitivity Test
DMSTA	Dynamic Stormwater Treatment Area Design Model
DOM	dissolved organic matter
HRT	hydraulic retention time
HSE	hydrologic simulation engine
OAT	one parameter at a time
PDF	probabilistic distribution function
PNG	pseudorandom number generation
PP	particulate phosphorus
r-LHS	replicated Latin hypercube sampling
RSM	Regional Simulation Model
RSM/WQ	Regional Simulation Model/Water Quality Model
SAV	submerged aquatic vegetation
SFWMD	South Florida Water Management District
SRP	soluble reactive phosphorus
STA	stormwater treatment area
TaRSE	Transport and Reaction Simulation Engine
TSS	Total Suspended Solids
USGS	U.S. Geological Survey
WCA	Water Conservation Area
XML	extensible markup language

Additional abbreviated units

L/kg	liter per kilogram
mg/kg	milligram per kilogram
mg/L	milligram per liter
mg/m^2	milligram per square meter
$mg/m^2/yr$	milligram per square meter per year
mg/m^3	milligram per cubic meter
µg/L	microgram per liter

Temperature in degrees Celsius (°C) may be converted to degrees Fahrenheit (°F) as follows:

$°F = (1.8 \times °C) + 32$

Vertical coordinate information is referenced to the National Geodetic Vertical Datum of 1929 (NGVD 29)

Horizontal coordinate information is referenced to the North American Datum of 1983 (NAD 83)

Altitude, as used in this report, refers to distance above the vertical datum.

Development, Testing, and Sensitivity and Uncertainty Analyses of a Transport and Reaction Simulation Engine (TaRSE) for Spatially Distributed Modeling of Phosphorus in the Peat Marsh Wetlands of Southern Florida

By James W. Jawitz[1], Rafael Muñoz-Carpena[2] , Stuart Muller[2], Kevin A. Grace[1], and Andrew I. James[1]

Abstract

Alterations to the predevelopment delivery of water and nutrients into the Everglades of southern Florida have been occurring for nearly a century. Major regional drainage projects, large-scale agricultural development, and changes to the hydrology of the Kissimmee River-Lake Okeechobee watershed have resulted in substantial phosphorus transport increases by surface waters. Excess phosphorus has accumulated in the soils of northern Everglades marshes to levels that have impaired the natural resources of the region. Regulations now limit the amount of phosphorous that enters the Everglades through an extensive network of water-control structures.

This study involved the development and application of water-quality modeling components that may be applied to existing hydrologic models of southern Florida to evaluate the effects of different management scenarios. The result of this work is a spatially distributed water-quality model for phosphorus transport and cycling in wetlands. The model solves the advection-dispersion equation on an unstructured triangular mesh and incorporates a wide range of user-selectable mechanisms for phosphorus uptake and release parameters. In general, the phosphorus model contains transfers between stores; examples of stores that can be included are soil, water column (solutes), pore water, macrophytes, suspended solids (plankton), and biofilm. Examples of transfers are growth, senescence, settling, diffusion, and so forth, described with first order, second order, and Monod types of transformations. Local water depths and velocities are determined from an existing two-dimensional, overland-flow hydrologic model. The South Florida Water Management District Regional Simulation Model was used in this study.

The model is applied to three case studies: intact cores of wetland soils with water, outdoor mesocosoms, and a large constructed wetland; namely, Cell 4 of Stormwater Treatment Area 1 West (STA-1W Cell 4). Different levels of complexity in the phosphorus cycling mechanisms were simulated in these case studies using different combinations of phosphorus reaction equations. Changes in water column phosphorus concentrations observed under the controlled conditions of laboratory incubations, and mesocosm studies were reproduced with model simulations. Short-term phosphorus flux rates and changes in phosphorus storages were within the range of values reported in the literature, whereas unknown rate constants were used to calibrate the model output.

In STA-1W Cell 4, the dominant mechanism for phosphorus flow and transport is overland flow. Over many life cycles of the biological components, however, soils accrue and become enriched in phosphorus. Inflow total phosphorus concentrations and flow rates for the period between 1995 and 2000 were used to simulate Cell 4 phosphorus removal, outflow concentrations, and soil phosphorus enrichment over time. This full-scale application of the model successfully incorporated parameter values derived from the literature and short-term experiments, and reproduced the observed long-term outflow phosphorus concentrations and increased soil phosphorus storage within the system.

A global sensitivity and uncertainty analysis of the model was performed using modern techniques such as a qualitative screening tool (Morris method) and the quantitative, variance-based, Fourier Amplitude Sensitivity Test (FAST) method. These techniques allowed an in-depth exploration of the effect of model complexity and flow velocity on model outputs. Three increasingly complex levels of possible application to southern Florida were studied corresponding to a simple soil pore-water and surface-water system (level 1), the addition of plankton (level 2), and of macrophytes (level 3). In the analysis for each complexity level, three surface-water velocities were considered that each correspond to residence times for the selected area (1-kilometer long) of 2, 10, and 20 days. Various of model outputs were studied that could be potentially useful to the model user: surface-water soluble reactive phosphorus (SRP) outflow, soil pore-water SRP variation, soil organic accretion, soil adsorbed phosphorus, plankton outflow, and macrophyte variation.

[1]Soil and Water Science Department, University of Florida, Gainesville, FL 32611

[2]Department of Agricultural and Biological Engineering, University of Florida, Gainesville, FL 32611

Results show that a simple soil pore-water and surface-water system modeled with and without plankton exhibits little change in sensitivity, owing to the plankton-based processes. Effects in both cases are primarily linear (additive), and the degree of interactions among parameters is minimal. The sensitivity ranking of the parameters, however, changes with the introduction of plankton-related modeling processes, because the plankton growth parameters dominate the simulated response of the system for most outputs studied. The introduction of macrophytes substantially alters the parameter sensitivity, tempering much of the linear effects and generating nonlinear interactions among all components. Although it is possible to reduce the number of important parameters to about half of the total model parameters for levels 1 and 2, the presence of interactions prevents such simplification for level 3.

Among the important parameters for level 1, the organic soil oxidation rate, k_{ox}, was consistently ranked most important followed by three other parameters: diffusion coefficient, k_{df}, soil bulk density, ρ_b, and mass fraction of phosphorus in organic soil, $X_{so}{}^{P}$. These results agree well with current understanding of the physical system, because the principal source of new phosphorus to the level-1 system is from oxidation of the soil (controlled by k_{ox}) and the pore-water SRP and, hence, the adsorbed phosphorus is controlled by the other three parameters. The SRP in the water column is more sensitive to k_{df} because this parameter represents the limiting process of diffusion through which the surface water gains new phosphorus. These trends across outputs persist in the level-2 results, with the only notable difference being the prominence of plankton growth parameters in the ranking for mobile outputs (outflow of surface-water SRP and plankton biomass). Level-3 results do not exhibit any pattern of parameter dominance across the different outputs.

Model sensitivity to velocity is correlated with model complexity; that is, as velocity increases, the model sensitivity to the important parameters changes the most for the most complex case. The complex interactions that occur in level 3 complicate the process of identifying sensitive parameters with the Morris screening method. This technique, however, was found to be computationally efficient for qualitatively evaluating global model sensitivity and linear or nonlinear effects of important parameters. In cases where many parameters appear to be important, as when interactions predominate, the extended FAST method provides quantitative measures of the linear and nonlinear contributions of each parameter to the observed global output variance.

Introduction

Freshwater wetlands serve a variety of needs by providing habitat, flood control, and water treatment as well as recreational opportunities. The ability to predict surface-water phosphorus concentrations in freshwater wetlands is of great interest to resource managers charged with maintaining water quality. Phosphorus is an essential element for all known life forms and is the limiting nutrient for biological growth in most freshwater ecosystems (Hecky and Kilham, 1988). Excessive external inputs of phosphorus can stimulate biological productivity in wetlands to a degree that negatively affects these resources. This overstimulation is often accompanied by an increase in surface-water phosphorus concentration. The Everglades in southern Florida has been found to be especially sensitive to phosphorous enrichment (Noe and others, 2001). Monitoring and predicting phosphorus concentration changes are, therefore, important approaches for maintaining water quality and natural resources of freshwater systems.

Several investigators have developed simple predictive models of phosphorus cycling, including Walker (1995) and Kadlec and Knight (1996), although these steady-state models cannot simulate changes over time. Walker and Kadlec (2005) extended these steady-state models to account for event-driven behavior of treatment wetlands by also incorporating nutrient storage in biota in the Dynamic Stormwater Treatment Area Design Model (DMSTA). Other efforts have produced ecological models that are relatively complex (that is, not restricted to only one or two parameters) at one- or two-dimensional spatial resolution (Kadlec and Hammer, 1988; Martin and Reddy, 1997; Sklar and others, 2001). In these wetland models, however, solute exchange between neighboring computational cells is based solely on a water mass balance. Each cell is, thus, considered to be completely mixed, which can be a severely limiting assumption as the model spatial and temporal discretization interval increases. A preferred, but more computationally intensive approach is to fully couple water flow and solute transport. This approach recently has been implemented for phosphorus cycling in a eutrophic lake (Chen and Sheng, 2005), but has yet to be implemented in wetlands.

In 2003, the University of Florida and the U.S. Geological Survey (USGS), in cooperation with the South Florida Water Management District (SFWMD), initiated a study to develop a transport and reaction simulation engine (TaRSE) to simulate phosphorus transport and cycling in wetlands. The model developed in this study solves the advection-dispersion equation on an unstructured triangular mesh and incorporates a wide range of user-selectable mechanisms for biogeochemical cycling between water, plants, and soils (A.I. James, University of Florida, written commun., 2008).

This model was developed to help assess the effects of management alternatives on large freshwater marsh treatment wetlands in southern Florida. Important features of the model include the following: (1) ability to select different combinations of phosphorus cycling mechanisms to suit the complexity of the problem under consideration, (2) ability to couple the phosphorus biogeochemical model to a hydrologic model, and (3) capability for two-dimensional spatially distributed parameterization and prediction.

Purpose and Scope

The purpose of this report is to describe the development, testing, and sensitivity and uncertainty analysis of a transport and reaction simulation engine (TaRSE) designed to simulate phosphorus transport and cycling in wetlands. Model calibration, validation, and application are discussed, with several combinations of phosphorus cycling mechanisms applied to data sets of varying scales, culminating with an application of the model to several years of field data from a large constructed wetland-Cell 4 of Stormwater Treatment Area 1West (STA-1W Cell 4).

A complete global sensitivity and uncertainty analysis of the full model is performed using the Morris method as a screening tool and the variance-based Fourier Amplitude Sensitivity Test (FAST) method. These techniques can be used to explore the effects of model complexity on model outputs. In flow-driven systems, such as the Everglades in southern Florida, it is also important to verify the effect of water velocity on model results. A statistical framework is, therefore, applied in which the sensitivity and uncertainty of the model are evaluated at three increasingly complex model structures and three surface-water flow velocities (or residence times). This model evaluation further reinforces the validity of the model, while guiding the potential user in the parameter selection and application process.

Description of Study Area

The STA-1W study area is a constructed treatment wetland on the eastern perimeter of the Everglades Agricultural Area (EAA), adjacent to Water Conservation Area (WCA) 1 as shown in figure 1. Cell 4 encompasses 147 ha and acts as a "polishing" cell before water is discharged into the adjacent WCAs. The cell was constructed in the early 1990s and became operational in August 1994 (Newman and Pietro, 2001). The spatially uniform vegetation community (dominated by submerged aquatic vegetation), well-characterized hydrology, and simple geometry of Cell 4 made it a preferable test case for coupled nutrient-hydrodynamic model development.

Previous Studies

The biogeochemical cycling of phosphorus in wetlands has been studied extensively, and many of the fundamental physical, chemical, and biological processes involved in the transfer of phosphorus between wetland soil, biomass, and water column are well documented (Reddy and others, 2005). One approach to mathematical modeling of phosphorus cycling in wetlands has been to combine mechanistic representations of the fundamental biogeochemical processes into what has been termed a "detailed ecosystem model" (Wang and Mitsch, 2000). This approach, however, often is considered cumbersome because of the large number of process parameters required. A second and more common approach to modeling wetland phosphorus dynamics is to group all phosphorus cycling processes into a single parameter, usually referred to as either an uptake coefficient or settling velocity (Mitsch and others, 1995; Walker, 1995; Kadlec and Knight, 1996). Models of intermediate complexity that combine some process lumping and some mechanistic representations also have been employed (Kadlec, 1997).

Although the modeling efforts, just described, represent the phosphorus biogeochemical cycling in wetlands with varying degrees of complexity, surface-water flow through the wetlands was simulated in these studies as simply a water mass balance (Walker, 1995; Wang and Mitsch, 2000) or as nondispersive, unidirectional plug flow (Kadlec, 1997). The spatial variability in the wetland interior of water depth and velocity arising from irregular wetland geometry or irregular water flow inlet and outlet locations (Persson and others, 1999) are, thus, not captured by such models. Furthermore, these models treat the entire wetland as a lumped bioreactor with no capability to describe spatial heterogeneity of wetland components or processes. Examples of such variables that would be desirable to represent in a spatially distributed manner include soil phosphorus concentration, vegetation type or density, and process rate coefficients such as biological uptake.

Coupling biogeochemical complexity with hydrologic and spatial simplicity is consistent with most ecological models designed to predict dynamic behavior while treating the system as spatially homogeneous (Costanza and others, 1990). Similarly, wetland models that have captured hydrologic complexity and include spatially distributed parameters generally have been restricted to biogeochemical simplicity. For example, Raghunathan and others (2001) used a spatially distributed regional-scale hydrologic model coupled with a simple one-parameter settling rate to describe phosphorus transport in the Everglades. Worman and Kronnas (2005) also used a spatially distributed hydrologic model coupled with a one-parameter, first-order kinetic model to describe nitrogen transport in a treatment wetland.

Recently, ecological models have been converging toward coupled biogeochemical and spatial complexity. As noted by Costanza and others (1990), this trend is related to the increased availability of spatial data and advances in computational power.

Concerning the area of study, the STA-1W wetland has been the focus of detailed studies on wetland restoration (Chimney and Goforth, 2001), surface- and ground-water hydrology (Guardo and Tomasello, 1995; Guardo, 1999; Choi and Harvey, 2000; Harvey and others, 2004), and nutrient dynamics (Moustafa, 1999; Nungesser and Chimney, 2001). In particular, STA-1W Cell 4 (147 ha) has been investigated for soil response to flooding (Newman and Pietro, 2001) and internal hydrodynamics (Dierberg and others, 2005).

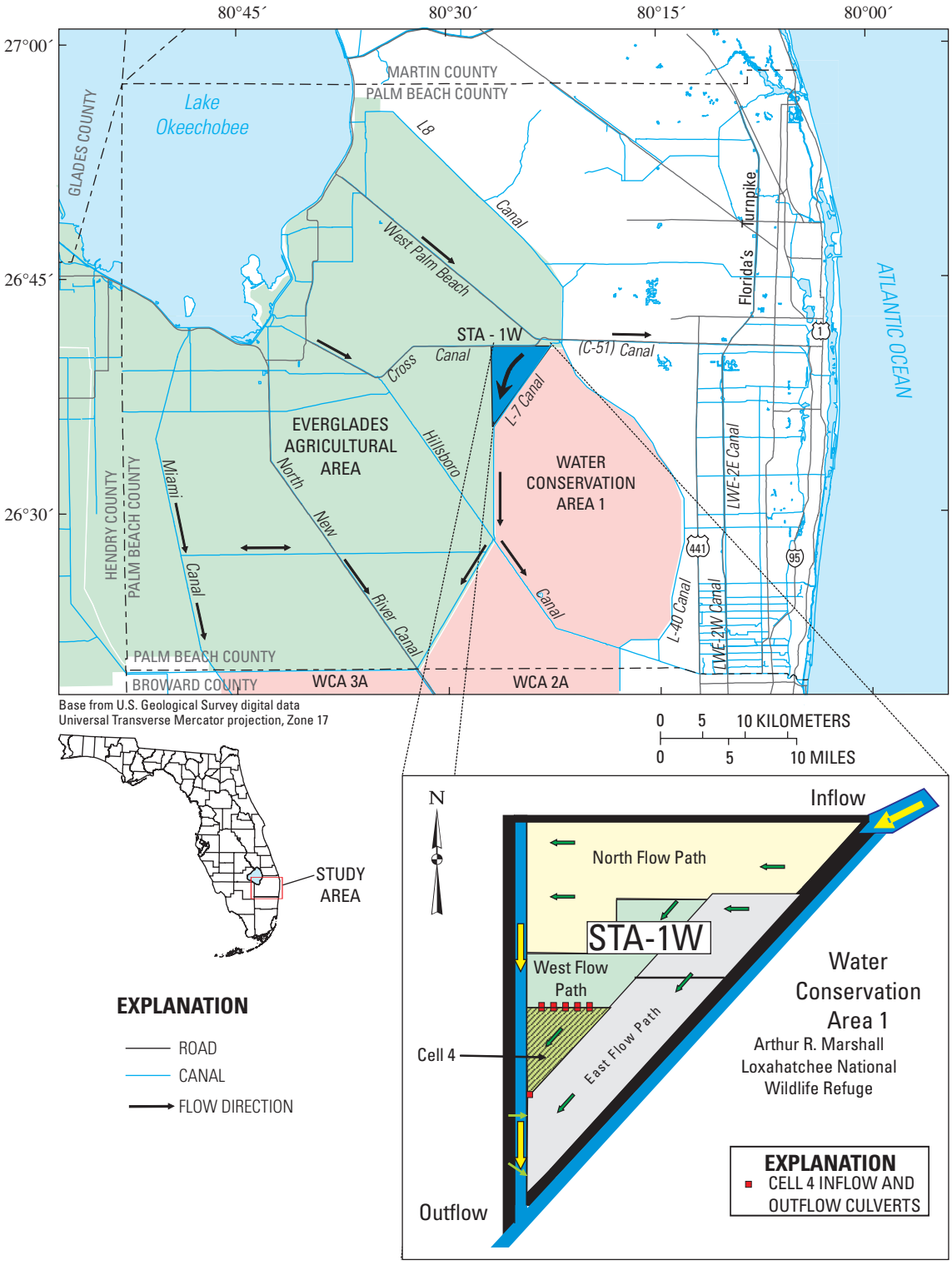

Figure 1. Study area, including Cell 4, Stormwater Treatment Area-1W (STA-1W).

Acknowledgments

The authors would like to acknowledge the contributions of the following individuals to this project: U.S. Geological Survey employees Ronnie Best, Alyssa Dausman, Mike Deacon, Rhonda Howard, Barbara Howie, Maggie Irizarry, Christian Langevin, Robert Renken, Kimberly Swidarski, and Arturo Torres; South Florida Water Management employees Cynthia Gefvert, Eric Flaig, Zacki Moustafa, Jayahtha Obeysekera, Ken Tarboton and Naiming Wang; and University of Florida staff Ken Campbell and Yuncong Li.

Model Conceptualization

Phosphorus cycling in wetlands is the transfer of this element in various forms between biota (micro and macro), water (surface and subsurface), and soil. Various mass stores exist within each of these compartments, and modeled processes basically are transfers between these stores. Phosphorus may be transferred as a solute in water or as a component of another material. Modeled water flows, including inflow and outflow, are shown in figure 2, and material flows, such as settling of particulate matter or decay of plant matter, are shown in figure 3. Figure 4 shows the movement of phosphorus between the various stores, in either dissolved form or associated with material flow. Each store and transfer process is described in the following discussion.

The modeled phosphorus cycling mechanisms are user selectable and may include subsets of the processes shown in figures 2 to 4 in many possible combinations. Three combinations are selected for demonstration and comparison to measured data.

Model Notation

The basic notation used for the model is presented in table A1 (app. 1). Storage in surface water, pore water, and biomass is represented by C, whereas storage in the soil (such as sorbed solutes) is denoted by S. Both terms have dimensions of $[ML^{-2}]$ (in the model, the default units are grams per square meter), which is the standard dimension for storage in wetland modeling (for example, Kadlec and Hammer, 1988; Martin and Reddy, 1997). The mass fractions of phosphorus in some storage is denoted by X $[MM^{-1}]$, and a material flux is denoted by J $[ML^{-2}T^{-1}]$.

The symbols for storages and mass fractions are modified by superscripts and subscripts (table A1) to indicate what (for example, P for phosphorus) and where the substance is, respectively. For example, the concentration of particulate organic matter (*po*) in the water column is written C^{po}, whereas the concentration of phosphorus in that particulate organic matter is denoted $C_{po}{}^{P}$. Material fluxes J are modified by superscripts indicating what the material is and subscripts indicating the mechanism involved. For example, the notation for particulate organic material settling (*st*) from the water column to the soil is $J_{st}{}^{po}$, and the phosphorus transferred by this settling process to the organic soil (*so*) is indicated by the product $X_{so}{}^{P}\, J_{st}{}^{po}$, where X is a mass fraction.

When volumetric concentration is required in dimensions of $[ML^{-3}]$, such as for determining growth rates, square brackets are used around the symbol. For example, $[C_{sw}{}^{P}]$ is the mass of phosphorus per volume of surface water. Mass concentration $[MM^{-1}]$, such as the sorbed phosphorus concentration in soils, is similarly denoted (for example $[S_{si}{}^{P}]$).

Stores

Living organisms obtain phosphorus during growth and release some of this phosphorus after senescence, death, and decomposition. The residual partially decomposed biomass may either be exported from the system in flowing water or contribute to soil accretion. The phosphorus cycle in wetlands may, thus, be characterized as sedimentary instead of, for example, the gaseous export pathways for nitrogen cycling in wetlands (Mitsch and Gosselink, 2000). Phosphorus that is accreted in soil, however, may be released to soil pore water and consequently reenter the biogeochemical cycle. The biomass, water, and soil constituents tracked by the model each contain phosphorus (table A2, app. 1).

Biomass

Wetland biota of interest include small organisms such as bacteria, phytoplankton, algae, and periphyton, as well as macrophytes such as sawgrass, cattail, and water hyacinth. In the model, biological organisms are classified as either phytoplankton (small organisms suspended in the water column), biofilm (primarily periphyton in floating, epiphytic, or benthic forms), or macrophytes. Phosphorus cycling in the wetland biotic community, which includes phytoplankton, periphyton, and macrophytes, is closely coupled (Sand-Jensen and Borum, 1991; Havens and others, 2001). Periphyton removes phosphorus from the water

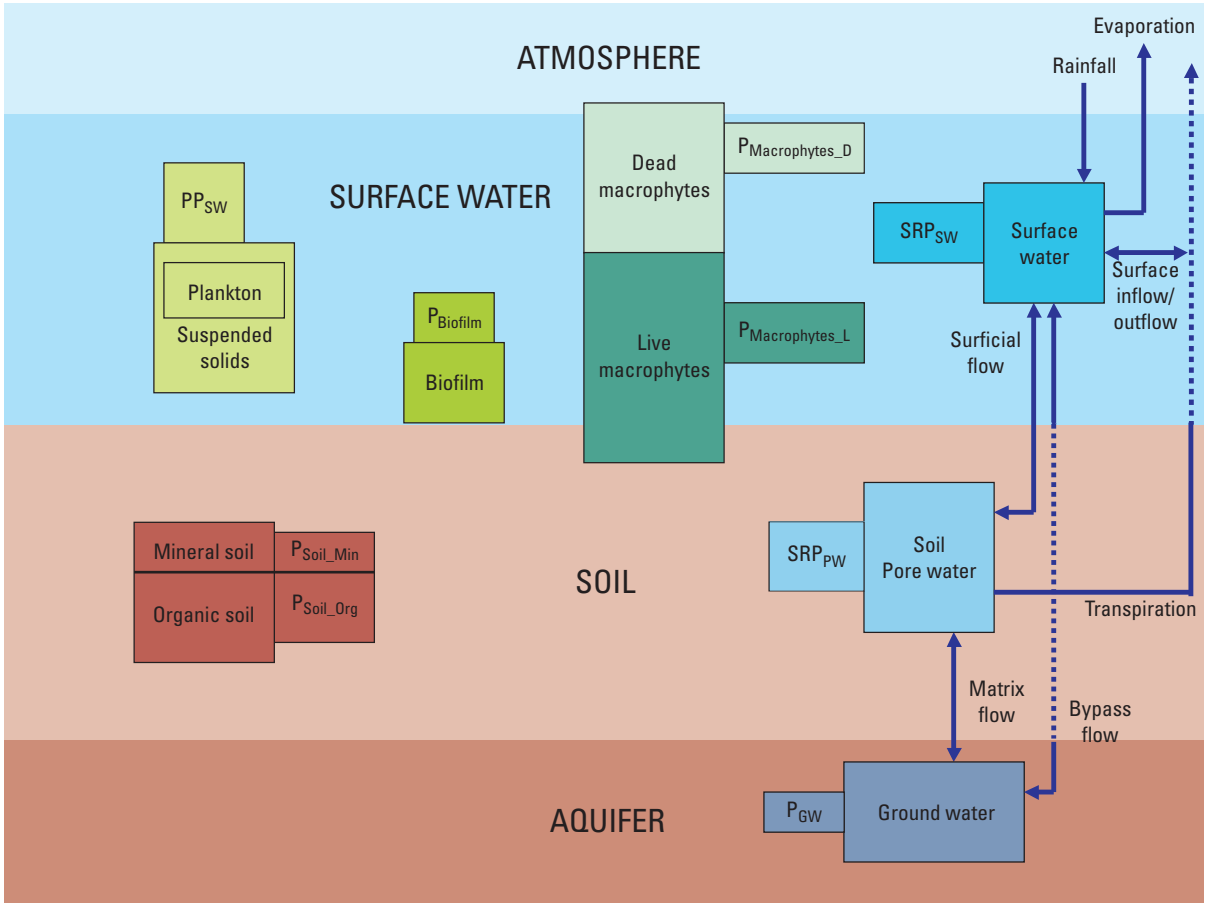

EXPLANATION

———	DIRECT TRANSFERS OF WATER
·····	DIRECT TRANSFERS THAT BYPASS THE ACTIVE SOIL
$P_{Biofilm}$	PHOSPHORUS MASS FRACTION OF BIOFILM
P_{GW}	TOTAL PHOSPHORUS CONCENTRATION IN THE GROUND WATER
$P_{Macrophytes\_D}$	PHOSPHORUS MASS FRACTION OF THE DEAD MACROPHYTE MATERIAL
$P_{Macrophytes\_L}$	PHOSPHORUS MASS FRACTION OF THE LIVING MACROPHYTE MATERIAL
P_{Soil_Min}	PHOSPHORUS MASS FRACTION OF THE MINERAL SOIL
P_{Soil_Org}	PHOSPHORUS MASS FRACTION OF THE ORGANIC SOIL
PP_{SW}	PARTICULATE PHOSPHORUS CONCENTRATION IN THE SURFACE WATER
SRP_{PW}	SOLUBLE REACTIVE PHOSPHORUS CONCENTRATION IN THE PORE WATER
SRP_{SW}	SOLUBLE REACTIVE PHOSPHORUS CONCENTRATION IN THE SURFACE WATER

Figure 2. Water flows considered in the conceptual model.

column and may suppress plankton biomass, whereas high densities of plankton can limit light penetration and suppress the growth of algae. Macrophytes provide structural support for epiphytic periphyton. Because these classifications are generalizations, their names can be considered operationally defined; for example, many types of small organisms besides phytoplankton may be suspended in the water column.

The biological stores considered here are classified as either mobile or stabile (nonmobile). The former includes organisms that are suspended in the water column such as plankton, algae, and floating plants, whereas the latter include rooted macrophytes and epiphytic and benthic periphyton. Of the latter, only rooted macrophytes access phosphorus in the pore water and, therefore, are capable of translocating soil nutrients.

The turnover rates for phosphorus cycling among wetland stores often are conceptualized as “fast” for water column organisms, “intermediate” for rooted macrophytes, and “slow” for soil (for example, Kadlec, 1997; Wang and Mitsch, 2000). Consequently, the relative importance of each of these stores may depend on the temporal scale under consideration.

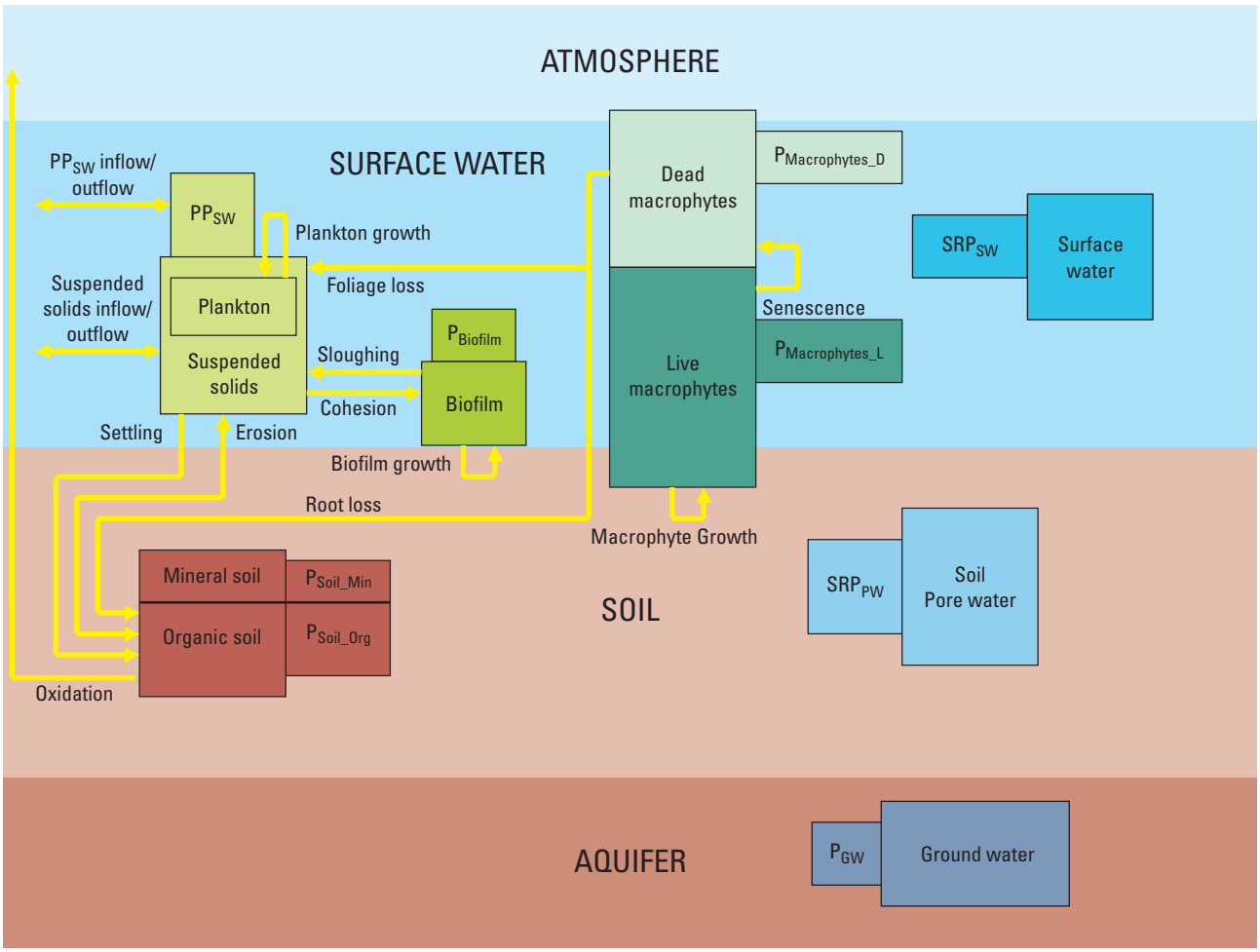

EXPLANATION

	DIRECT TRANSFERS OF MATERIAL
$P_{Biofilm}$	PHOSPHORUS MASS FRACTION OF BIOFILM
P_{GW}	TOTAL PHOSPHORUS CONCENTRATION IN THE GROUND WATER
$P_{Macrophytes\_D}$	PHOSPHORUS MASS FRACTION OF THE DEAD MACROPHYTE MATERIAL
$P_{Macrophytes\_L}$	PHOSPHORUS MASS FRACTION OF THE LIVING MACROPHYTE MATERIAL
P_{Soil_Min}	PHOSPHORUS MASS FRACTION OF THE MINERAL SOIL
P_{Soil_Org}	PHOSPHORUS MASS FRACTION OF THE ORGANIC SOIL
PP_{SW}	PARTICULATE PHOSPHORUS CONCENTRATION IN THE SURFACE WATER
SRP_{PW}	SOLUBLE REACTIVE PHOSPHORUS CONCENTRATION IN THE PORE WATER
SRP_{SW}	SOLUBLE REACTIVE PHOSPHORUS CONCENTRATION IN THE SURFACE WATER

Figure 3. Material flows considered in the conceptual model.

Phytoplankton (C_{sw}^{pl}, but incorporated into particulate organic material) acquires phosphorus solely from the water column, and is transported by surface-water flow as a component of suspended solids. Plankton growth is self-limiting because of competition for light and nutrients with existing phytoplankton. Macrophyte growth also restricts phytoplankton growth by limiting light and nutrients.

Macrophytes (C^{mp}) are slower growing organisms than phytoplankton, with slower decay and longer turnover times. These organisms can obtain nutrients from both water column and pore-water phosphorus stores. Rooted macrophytes obtain the majority of their required phosphorus from pore water (Carignan and Kalff, 1980), whereas floating macrophytes obtain phosphorus solely from the water column. Above- and below-ground processes for macrophytes are managed in the model using foliage and root mass fractions, f_f and f_r, respectively, where $f_r = 1 - f_f$. The root fraction becomes incorporated into the soil upon death, and the foliage fraction decays directly to the water column. The foliage fraction also may restrict light availability in the water column and at the soil surface.

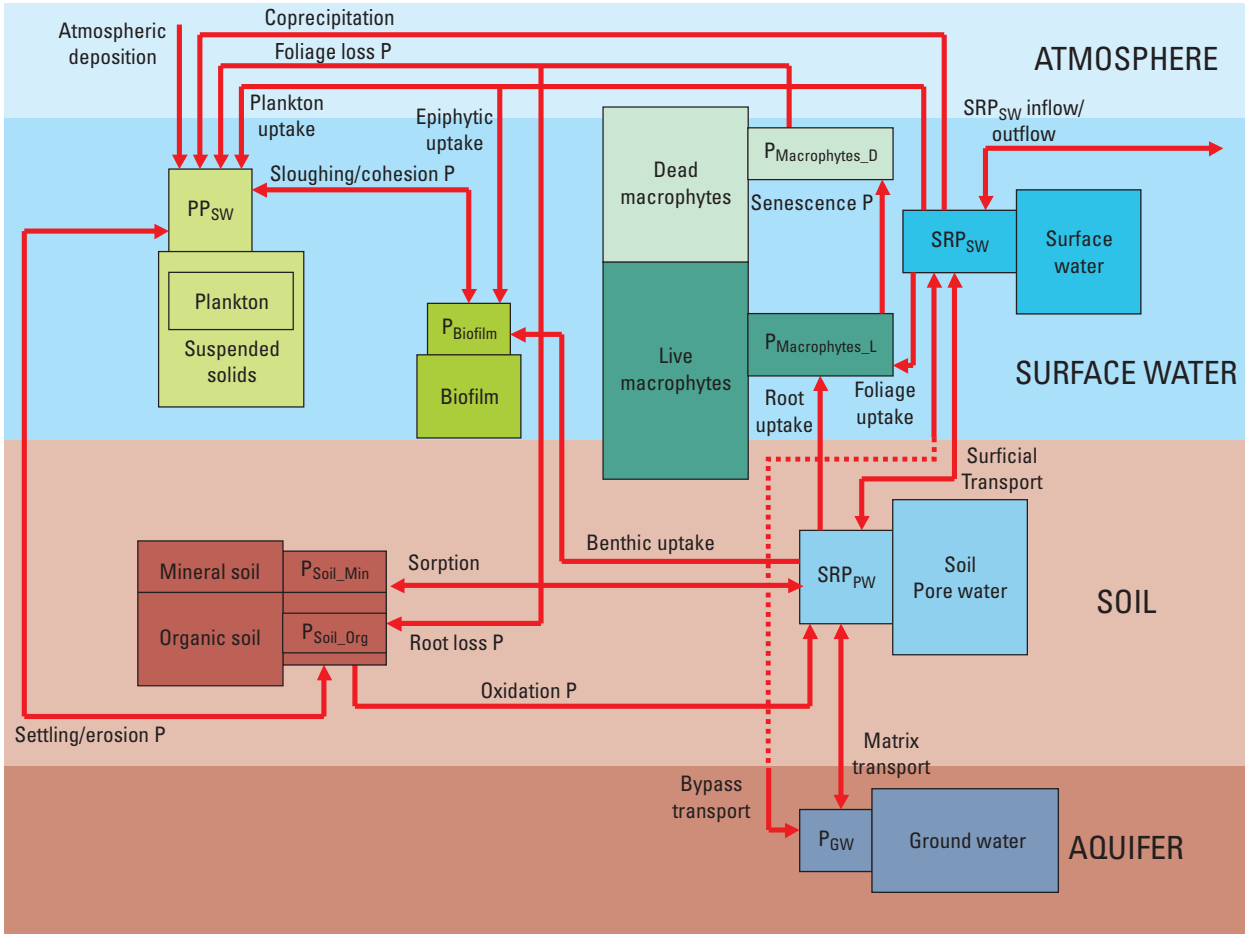

EXPLANATION

———	DIRECT TRANSFERS OF PHOSPHORUS
·····	DIRECT TRANSFERS THAT BYPASS THE ACTIVE SOIL
$P_{Biofilm}$	PHOSPHORUS MASS FRACTION OF BIOFILM
P_{GW}	TOTAL PHOSPHORUS CONCENTRATION IN THE GROUND WATER
$P_{Macrophytes\_D}$	PHOSPHORUS MASS FRACTION OF THE DEAD MACROPHYTE MATERIAL
$P_{Macrophytes\_L}$	PHOSPHORUS MASS FRACTION OF THE LIVING MACROPHYTE MATERIAL
P_{Soil_Min}	PHOSPHORUS MASS FRACTION OF THE MINERAL SOIL
P_{Soil_Org}	PHOSPHORUS MASS FRACTION OF THE ORGANIC SOIL
PP_{SW}	PARTICULATE PHOSPHORUS CONCENTRATION IN THE SURFACE WATER
SRP_{PW}	SOLUBLE REACTIVE PHOSPHORUS CONCENTRATION IN THE PORE WATER
SRP_{SW}	SOLUBLE REACTIVE PHOSPHORUS CONCENTRATION IN THE SURFACE WATER

Figure 4. Phosphorus flows considered in the conceptual model.

For this study, stabile epiphytic and benthic nonrooted organisms are classified as biofilm. Epiphytic and benthic environments provide large surface area and structural support for organisms that lack differentiated structural tissues. Epiphytic forms, C_{ep}^{bf}, obtain phosphorus from the water column, rather than from the supporting plants (Carignan and Kalff, 1982). In the littoral zone of Lake Okeechobee, Havens and others (2001) measured total phosphorus in the combined communities of water column plankton and epiphytic periphyton to be about 150 mg/m^2; about 90 percent of the phosphorus was associated with epiphyton.

Benthic forms, C_{be}^{bf}, also may intercept nutrients diffusing from pore water to the water column (Carlton and Wetzel, 1988); however, biofilms readily become limited by nutrients in static waters and by light in productive waters. Fast-moving water can support biofilm growth, but sloughing losses of biofilm tissues can occur when flow velocity changes.

Water Column

The water column contains dissolved and particulate constituents. Dissolved components are assumed to be homogeneously mixed within the water column, and are transported through advection and dispersive fluxes. Suspended particles include inert sediments as well as living phytoplankton, bacteria, and other dislodged biological constituents that are transported with advective water flows.

Total phosphorus in the water column can be partitioned into phosphorus that is or is not directly available for biological uptake. Soluble reactive phosphorus (SRP), C_{sw}^{P}, is well correlated to the biologically available phosphate pool in freshwaters (Murphy and Riley, 1962), and in standard determinations SRP is measured as filtrate (0.45 μm) that reacts with an ascorbic acid-molybdenum color reagent (American Public Health Association, 1992). This method of determination is useful in surface water and pore water because dissolved organic matter (DOM) does not interfere with the reaction (Watanabe and Olsen, 1965). Phosphorus associated with DOM may be biologically unavailable. The importance of these compounds to phosphorus cycling currently is not well understood (Turner and others, 2005); therefore, they are not included in the model at this stage.

Organic and inorganic particulate phosphorus molecules, C_{po}^{P} and C_{pi}^{P}, are larger than DOM. Because SRP and biologically unavailable phosphorus compounds have different reactivities, it is necessary to consider the process equations for these compounds separately. Operationally defined phosphorus fractions are highly exchangeable; for example, when plankton cells release bioavailable phosphorus upon senescence (Lehman, 1980).

Other dissolved constituents are known to affect phosphorus cycling dynamics. For instance, hydrogen ion concentration (pH), ionic strength, and alkalinity all describe the chemical environment in which biological processes occur, including phosphorus uptake and biomass growth. Nutrients other than phosphorus, such as nitrogen, calcium, and iron, are essential nutrients for biological growth. Because phosphorus is the predominant limiting nutrient in freshwater systems, other constituents were assumed to have a minimal influence on phosphorus fate and transport in the model. This simplifying assumption was made recognizing that other dissolved constituents may be more or less important in specific applications.

Surface-water flow transports suspended matter (especially under turbulent flow conditions), measured as total suspended solids ($C^{ss} = C^{po} + C^{pi}$). Much of the suspended load in low-gradient systems, such as those in southern Florida, is either living plankton (*pl*), or biological material consisting of nonliving plankton or other organic matter (*pn*) (Daroub and others, 2002). Some inorganic content, C^{pi}, can also be attributed to the remains of siliceous and carbonate exteriors of plankton (for example, diatoms). These remains typically settle out of the water column, but can be resuspended by turbulent flow. High-gradient systems (for example, mountain streams and large rivers) with large hydraulic potentials have higher maximum flow velocities, more erosion of inorganic components from the watershed, and a greater portion of inorganic matter in the suspended solids. Because tracking the three forms of suspended solids is data intensive and may not be warranted by existing data, these forms either may be lumped into two forms, C^{po} and C^{pi} (organic and inorganic), or the single form, C^{ss}.

Soil

In peat-forming wetlands, soil organic matter can accumulate to depths of several meters. Such high amounts of organic matter in the soil represent only a narrow range of hydrologic conditions in which the water table is at or near the land surface. When drained, peat soils may be depleted completely to expose the underlying mineral bedrock (Davis, 1946). Changes in hydrology can influence the development and long-term stability of such soils, and can ultimately control soil phosphorus stability. In southern Florida, surface soils such as Everglades muck and Loxahatchee peat can be composed almost entirely of organic matter. Drainage of Everglades soils during the past century has resulted in the oxidation (and loss) of more than 2 m of soil in some areas (Allison, 1956; Snyder, 2005).

Soil pore water is an important nutrient store for macrophyte growth, and as such, can control the distribution of vegetation in wetland ecosystems. When pore-water phosphorus concentration, C_{pw}^{P}, is high, opportunistic emergent vegetation such as cattails may have a competitive advantage over phytoplankton, periphyton, and nonrooted or slower growing macrophytes. This competition is especially acute when column phosphorus is scarce. Pore-water phosphorus may be transported directly to the water column by molecular diffusion and advection, as with bioturbation for example. Finally, pore-water phosphorus also is exchanged with solid-phase soil phosphorus, S_{si}^{P}, through sorption-desorption reactions. Sources of pore-water phosphorus include surface-water exchange and the mineralization of phosphorus in soil.

Soil solids are composed of eroded and settled minerals, and the remains of biological tissues undergoing decomposition. The heterogeneous nature of biomass turnover in diverse ecosystems, together with multiple limiting factors (such as space, energy, nutrient, and moisture availability) on decomposer activities, allow for the continuous decomposition of soil constituents. Mineralization rates can be modified by large changes in nutrient supply, as with soil phosphorus enrichment, or by large changes in water-table altitude. For the current study, it is assumed that only a portion of deep soil is active in which processes occur, such as phosphorus uptake by roots and diffusive exchange with the surface water. The active soil depth, z_{as}, is the thickness of soil modified by these processes, and can be considered as some function of root biomass.

In marsh wetlands, unconsolidated decaying plant matter (sometimes called floc) can accumulate at the soil surface. This layer has been shown to be important in phosphorus dynamics in southern Florida marsh wetlands (Corstanje and others, 2006). Floc depths of up to 17 cm with an average total phosphorus concentration of 632 mg/kg (about 50 percent higher than in the surface soils) was found in WCA 1, which is part of the northern Everglades. Noe and Childers (2007) found that the floc layer is the second largest store of phosphorus after soil. In the model applications described here, the floc layer is not considered separately; however, the dynamics in this layer could be considered either as a separate soil layer, or as dead macrophytes.

Physical and Biological Transfer Mechanisms

Each of the transfer mechanisms considered here involve movement of either material or phosphorus between various stores. The transfer mechanisms and associated stores used in the model are listed in table A1. All transfer rates are modeled as either zero order, first order, or Michaelis-Menten (Monod equation). Rate constants and half-saturation constants used in the model are listed in table A3 (app. 1); all other model symbols and parameters are listed in tables A1 and A3 (app. 1).

Physical Transfer Processes

Physical transfers of phosphorus or phosphorus-containing materials include particle settling and resuspension, solute transfer between pore water and surface water (advection and diffusion), solute sorption and desorption, biofilm cohesion and sloughing, and mineral precipitation. Ground-water and surface-water inflow and atmospheric deposition are also considered physical transfers, but are only user-defined system inputs. However, the outflow of phosphorus with ground water or surface water is calculated.

Water Flows

The length of time that a given amount of water is retained within a wetland area is known as hydraulic retention time (HRT), and can influence the potential for phosphorus exchange between flowing water and the other storages (Dierberg and others, 2002; Dierberg and others, 2005). The nominal HRT is the ratio of wetland water storage to flow rate; however, water storage and flow distribution may change during transient conditions. For example, floodplain wetlands that receive stormwater pulses can experience conditions of variable flow (including zero flow).

Surface-flow velocities within the wetland are not directly dependent on phosphorus concentrations in the water column. Indirectly, water column phosphorus may influence macrophyte density, and thus, affect flow velocity (Nepf, 1999; Green, 2006) and sedimentation rates. Water flowing along paths of least resistance preferentially travels toward areas of low macrophyte biomass density or greater water depths. Open-water zones can be maintained by continuous or periodic high-flow velocities that prevent the establishment of macrophytes, creating positive feedback for “channel” creation and maintenance (Riis and Biggs, 2003). Extensive preferential flow paths in wetlands result in low retention times and concomitant low phosphorus removal effectiveness (Martinez and Wise, 2003b; Dierberg and others, 2005; Wang and others, 2006). Additionally, the prevailing hydraulic conditions can influence accrued soil properties that affect phosphorus dynamics, such as water content, hydraulic conductivity, and particle size distribution.

Atmospheric Deposition

Atmospheric deposition along with surface-water inputs and ground-water exchange define the conditions under which a wetland ecosystem develops. Bulk atmospheric phosphorus deposition, including both wet (rainfall) and dry (pollen, dust, and plant matter) components, is denoted by J_{atm}^{P}. Hendry and others (1981) reported a mean bulk atmospheric phosphorus deposition rate in Florida of 59 mg/m^2/yr, with a range from 27 mg/m^2/yr in nonagricultural rural areas to 96 mg/m^2/yr at Belle Glade, Florida. The latter is an area of intensive agricultural activity where sugar cane fields are burned prior to harvesting. In addition, dry matter accounted for about 80 percent of the bulk phosphorus deposition, and about 65 percent of the deposited phosphorus was inorganic. Ahn and James (2001) also reported that bulk atmospheric phosphorus deposition in southern Florida was dominated by dry deposition, with a range from 11 mg/m^2/yr in a remote portion of Everglades National Park, to 77 mg/m^2/yr in an area surrounded by improved pastures. The average from all stations monitored in southern Florida was 40 ± 33 mg/m^2/yr. Grimshaw and Dolske (2002) reported wet atmospheric phosphorus deposition in Florida as 1.3 ± 0.3 mg/m^2/yr, with nearly 90 percent of this as SRP. Volume-average phosphorus concentrations in measured rainfall in Florida were 1.3 ± 0.1 µg/L, nearly all of which was SRP.

Based on these data, atmospheric deposition in the model for the current study comprises constant SRP concentration in rainfall and constant dry phosphorus deposition that is not dependent on rainfall, but may vary depending on surrounding land use. Influx of atmospheric deposition is a user-defined input to this model. The particulate deposition is partitioned as 60 percent inorganic (J_{atm}^{pi}) and 40 percent (nonliving) organic (J_{atm}^{pn}) particles.

Pore-Water/Surface-Water Transfer

Three mechanisms may enable transfer of phosphorus between pore water and surface water: (1) advective transport with vertically flowing water, (2) Fickian diffusive transport caused by concentration gradients, and (3) biologically enhanced transport (bioturbation).

Limestone beneath the southern Florida wetlands is responsible for the high connectivity between surface water and the surficial aquifer system, although peat sediments underlying the wetlands may restrict surface- and ground-water exchange. During wet and dry periods, wetland stage is typically above and below land surface, respectively. In the latter case, the wetland may serve as a recharge basin for the aquifer. A 4-year water budget conducted in STA-1W showed that about 30 percent of the surface water that is pumped into the wetland is lost to recharge, and that ground-water discharge to the wetland is relatively minor (Choi and Harvey, 2000). A follow-up study (Harvey and others, 2004) showed that most of the recharge measured in large wetlands in southern Florida originates near levees separating the wetlands from adjacent water bodies that often have dissimilar water levels. Ground-water exchange in the central portions of these large wetlands was found to be relatively small—almost always less than 1 cm/d. Harvey and others (2004) also suggested that traveling waves from inflow water pulsing may be related to periods of infrequent but substantial recharge to the interior of large wetlands.

These studies highlight the importance of including spatially distributed information for accurate modeling of phosphorus transport. In the current model, vertical advective flux and horizontal seepage through berms to connecting canals or adjacent water bodies are determined using Darcy's Law.

Diffusive flux of phosphorus across the soil-water interface is based on Fick's Law and concentration gradients between pore water and surface water (for example, Fisher and Reddy, 2001). Phosphorus concentrations are typically greater in pore water than in the water column and, therefore, diffusion is usually from the pore water. Diffusive flux is inversely proportional to diffusion distance, z_{df}, which is considered here to be 4 cm, based on concentration gradients observed in the northern Everglades (Fisher and Reddy, 2001; Newman and Pietro, 2001).

Biological components may cause deviations from predicted phosphorus exchange rates that rely strictly on physical processes such as diffusion. Rooted macrophytes can deplete soil pore-water nutrients, and benthic biofilms can intercept phosphorus diffusing from soil to water. Chironomids can increase water exchange across the soil-water interface with filter-feeding activities, and can alter soil porosity by creating macropores. Holdren and Armstrong (1980) found phosphorus flux rates from lake sediment intact cores to be at least an order of magnitude greater than would be expected from diffusion alone. When the cores were exposed to a poison to kill any chironomids present, phosphorus flux rates were dramatically reduced to levels consistent with molecular diffusion. Hansen and others (1998) have shown chironomids can increase decomposition of sediment organic matter and increase sediment phosphorus release.

The pooled contributions of molecular diffusion and enhanced solute mixing due to macrobenthos activity have been quantified using a Fickian model, with effective diffusion coefficient (D) values of up to 15 times greater than would be expected from diffusion alone (Van Rees and others, 1996). The flux of phosphorus from pore water to surface water induced by bioturbation can constitute a substantial portion of the phosphorus budget. In the current model, diffusion and bioturbation are represented with a Fickian diffusion model, where the diffusion coefficient, D, is multiplied by a bioturbation factor, BF.

Settling and Entrainment of Particulate Material

Suspended particles in wetlands include inorganic particles and organic material such as algae, plankton, or plant debris. The settling velocity, ω, of many inorganic particles is directly related to particle size and can be determined for sand-like particles using common semianalytic relations such as the following (Sturm, 2001):

$$\omega = \frac{8\nu}{d_s}\left[\left(1+\frac{0.0139*(SG-1)gd^3}{\nu^2}\right)^{0.5}-1\right], \quad (1)$$

where:

ν is the kinematic viscosity of water (10^{-6} m^2/s at standard temperature and pressure),
SG is the particle specific gravity,
d is the particle diameter (meters),
g is gravitational acceleration (9.81 m/s^2), and
d_s is the geometric mean (meters) of the sieve sizes just passing and retaining the particle; this value is often close to d.

Empirically determined values for ω are commonly used for wetlands. Kadlec and Knight (1996) have suggested a value of 10 m/d, based on a reported range of 3 to 30 m/d from several wetland studies. Based on equation 1, ω = 10 m/d corresponds to $d \approx 10$ µm (silt-size particles).

Particle depositional flux, J_{st}^{po} or J_{st}^{pi} for organic and inorganic material respectively, is the product of ω and suspended sediment concentration. This mechanism only applies to nonliving particles, C^{pn}, because living suspended organic material (such as plankton) can exhibit complex behavior such as motility or changing buoyancy.

The flux of sediment particles entrained or resuspended into the water column from the soil, J_{en}^{S}, is strongly dependent on water velocity and sediment characteristics. Sediment erosion has been the subject of numerous investigations, and resuspension has been shown not to occur until the water velocity reaches a minimum threshold with enough energy to erode the sediment bed (Miller and others, 1977; Wiberg and Smith, 1987). The threshold for sediment erosion is measured as the critical shear stress $\tau_c = \rho_w u_c^2$, where ρ_w is the density of water and u_c is the critical shear velocity, measured just above the viscous no-flow sublayer at the sediment-water interface.

Critical shear stress has been measured for a range of particle sizes in numerous studies and these data are summarized in the Shields diagram (Sturm, 2001, p. 384). For silts and sands with d = 10 μm and 100 μm, this diagram and the relations above may be used to determine critical shear velocities u_c = 0.006 m/s and 0.01 m/s, respectively (assuming SG = 2.65, ρ_w = 1 g/cm^3, and $\nu = 10^{-6}$ m^2/s). Shear velocities, however, are always less than mean velocities and often substantially less. The depth-averaged critical velocity for resuspension, v_c, is then substantially higher than u_c, and can be determined from empirical relations. Two examples of empirical relations are briefly compared:

$$v_c = \frac{1}{0.0475}\left(\frac{\tau_c}{g}\right)^{0.5}\left(\frac{y}{d}\right)^{1/6}, \text{ and} \tag{2}$$

$$v_{c,100} = 122.6 d^{0.29} \quad d < 0.2 \text{ cm}, \tag{3}$$

where y is the flow depth, in meters; $v_{c,100}$ is the velocity (in centimeters per second) 100 cm above the sediment interface, and d is depth, in centimeters. Equations 2 and 3 are from Sturm (2001) and Miller and others (1977), respectively. Using the diameters given earlier (10 and 100 μm) and an assumed flow depth of 1 m, these two equations provide nearly identical values for v_c and $v_{c,100}$, as noted below:

Diameter (μm)	v_c (m/s)	$v_{c,100}$ (m/s)	$v_{c,100}$ (m/d)
10	0.18	0.17	1.4 x 10^3
100	0.34	0.32	2.7 x 10^3

Constructed wetlands typically are designed to have low velocities. For example, at a large treatment wetland in Florida, velocities of 72 ± 44 m/d were measured in 15 treatment cells based on mean travel lengths and hydraulic retention times reported by Martinez and Wise (2003a,b). A multiyear water budget for the Everglades Nutrient Removal Project (Guardo, 1999) suggested velocities of about 400 m/d, based on a mean hydraulic retention time of 20 days and an average travel length of about 8 km. These velocities are substantially lower than the v_c values determined earlier. Steady-flow conditions in treatment wetlands, therefore, are highly unlikely to generate flow-induced bottom shear stresses sufficient to induce bed erosion and resuspend particles.

Extreme transient conditions can induce resuspension of even cohesive sediments. Such conditions include high winds, high hydraulic loading rates, or hydraulic "shocks" in areas near pumps. For example, Stuck (1996) found that cohesive organic sediments in EAA canals were relatively resistant to erosion under steady-flow conditions, but were entrained quickly after sudden changes in velocity during pump startup. In shallow lakes, wind speed has been found to be a primary driver of sediment particle entrainment in the water column (Carrick and others, 1993; Hanlon, 1999; Schelske and others, 2000). The presence of emergent vegetation, however, substantially alters the hydrodynamic conditions. Wind-induced waves and the corresponding bottom shear stresses are expected to be damped in well-vegetated wetlands compared to shallow lakes. Under equivalent forcing conditions, such as bed slope or wind speed, water velocities in vegetated systems are substantially less than in unvegetated systems, even at moderate vegetation densities (Nepf, 1999).

Observations of steady-state, spatially uniform background concentrations, C^*, of total suspended solids (TSS) in wetlands suggest that a balance exists between settling and the sum of resuspension and internally generated particles, such as from biological processes (Kadlec and Knight, 1996). For example, J_{st} = 25 g/m^2/d in a wetland with TSS C^* = 5 g/m^3 and ω = 5 m/d. Suspended solid generation from the combined effects of internal growth and resuspension must equal this value for the steady-state background concentration to be maintained. Using this logic for a well-characterized wetland, Kadlec and Knight (1996) found J_{en}^{S} = 46 g/m^2/d. Because the wetland water velocity was well below the critical erosive value, other processes such as bioturbation were identified as contributing to the observed sediment flux.

Erosive flux has been found to increase linearly with bed shear stress above the critical value, τ_c (Ariathurai and Arulanandan, 1978). Wetland flow velocities are assumed herein to be less than v_c, however, and the flux of sediments entrained by flowing water is zero. A mechanism is included in the present model to enable sediment resuspension enhancement through bioturbation (discussed later).

Sloughing and Cohesion of Biofilm

Benthic biofilms in southern Florida typically are described as periphyton—a combination of benthic algae, bacteria, and extracellular mucilage (McCormick and Stevenson, 1998). Periphyton can also grow epiphytically on macrophyte leaves and stems, although these forms can be considered an extension of macrophyte storage. The cohesive properties of the extracellular matrix of benthic biofilms can minimize sloughing losses and substrate erosion (Sutherland and others, 1998), and cause the film to grow by trapping particulates suspended in flowing water. This growth can be counteracted by shearing forces that cleave overextended macrophytes and biofilms. Benthic biofilms can also slough during large velocity changes (Stuck, 1996). Biofilm cohesion and sloughing are hypothesized here to be first-order rate processes that (1) exchange material between biofilms and particulate organic material, and (2) depend on the amount of particulate organic material and biofilm, respectively.

Sorption/Desorption

Dissolved phosphorus adsorbs onto the reactive surfaces of soil solids in a dynamic equilibrium that maintains a relatively constant ratio of liquid and solid phases within the soil pore-water matrix. This partitioning is accomplished through: (1) desorption reactions when the liquid phase is depleted, as with root phosphorus uptake; and (2) soil sorption when dissolved concentration increases, as with soil OM mineralization. In the current model, linear sorption relations are used to "instantaneously" partition soil phosphorus between pore-water and solid phases. This partitioning is applied as follows, beginning with the equation for equilibrium sorption/desorption:

$$\left[C_{si}{}^{P}\right] = k_d{}^{sr}\left[C_{pw}{}^{P}\right], \tag{4}$$

where $k_d{}^{sr}$ is the sorption distribution coefficient, $\left[C_{pw}{}^{P}\right]$ is the mass of adsorbed phosphorus per unit volume of soil, and $\left[C_{pw}{}^{P}\right]$ is the mass of pore-water SRP in per unit volume of soil. To convert to mass of adsorbed phosphorus per area (expressed as $S_{si}{}^{P}$), the active soil depth, z_{as}, bulk density, ρ_b, and inorganic fraction, f_i, are multiplied:

$$S_{si}{}^{P} = z_{as}\rho_b f_i k_d{}^{sr}\left[C_{pw}{}^{P}\right]. \tag{5}$$

Multiplying $\left[C_{pw}{}^{P}\right]$ by the porosity, θ, and the active soil depth, z_{as} yields $C_{pw}{}^{P}$ in grams per square meter and, thus, equation 5 is rewritten as:

$$S_{si}{}^{P} = \frac{\rho_b f_i k_d{}^{sr}}{\theta} C_{pw}{}^{P}. \tag{6}$$

Taking the derivative of equation 6 with respect to time yields:

$$\frac{\mathrm{d}S_{si}{}^{P}}{\mathrm{d}t} = \frac{\rho_b f_i k_d{}^{sr}}{\theta}\frac{\mathrm{d}C_{pw}{}^{P}}{\mathrm{d}t}. \tag{7}$$

Mineral Precipitation

Carbonates can be precipitated from hard waters by algae, periphyton, and submerged aquatic vegetation (SAV) during daytime photosynthesis (Otsuki and Wetzel, 1972; Murphy and others, 1983; Scinto and Reddy, 2003). The formation of stable calcium phosphates from calcium carbonate-phosphate coprecipitates can be hindered by excess humic acid compounds in solution (Alvarez and others, 2004) produced by decomposing organic matter in soils.

Scinto and Reddy (2003) showed that abiotic uptake (precipitation) of phosphorus by periphyton represents a relatively small fraction (about 10 percent) of total uptake. The current model computes coprecipitation using the same Michaelis-Menten reaction kinetics as for biological uptake, with a maximum uptake rate of about 10 percent of the biological value.

Biological Transfer Processes

Because carbon dioxide is exchanged with the atmosphere, aquatic systems may act as either net OM sinks that fix carbon through photosynthetic productivity, or net sources that emit carbon dioxide following metabolic respiration. Wetlands often are considered sinks of phosphorus through the accumulation of OM, if OM and nutrient storage increase continuously. Phosphorus storage capacity in a wetland is finite if OM stores do not increase, whether phosphorus removal is primarily through soil sorption or biomass uptake (Richardson and Qian, 1999).

Gains to biological storage include growth and import, whereas losses include death and washout (in the case of algae and other nonrooted organisms). The difference between growth and decay rates for algae, macrophytes, and biofilms determines the relative contribution of each to soil phosphorus cycling within wetlands. Biological transfers include the uptake and release of phosphorus during growth and senescence, and mineralization of soil phosphorus.

Growth of Biological Tissues

Biological growth is assumed to be phosphorus limited, as is often the case for algae (Grover, 1989), macrophytes, and periphyton in freshwater systems. Growth rates are proportional to the existing biomass, with submaximal rates achieved under limiting conditions. The Michaelis-Menten kinetic formulation for particulate organic growth, G^{po}, allows algal growth rates to be limited by SRP concentration, $C_{sw}{}^{P}$. Specifically, the growth of plankton in the water column, $G_{sw}{}^{pl}$, based on maximum growth rate, $k_g{}^{pl}$, and half-saturation constant, $k_{1/2}{}^{pl}$, can, therefore, be expressed as:

$$G_{sw}{}^{pl} = k_g{}^{pl} C_{sw}{}^{pl} \frac{C_{sw}{}^{P}}{C_{sw}{}^{P} + k_{1/2}{}^{pl}} . \quad (8)$$

This formulation has been widely used to simulate the effect of phosphorus limitation on algal growth in the absence of other limiting factors, and also has been used to describe phosphorus limitation of periphyton in southern Florida (Hwang and others, 1998; Dong and others, 2002; Scinto and Reddy, 2003).

The Michaelis-Menton formulation was also used in this study to describe phosphorus-limited growth rates for macrophytes and biofilms as well as plankton. In the current model, new growth is assumed to have a constant phosphorus mass fraction such that gains in biological storage cause a proportional increase in phosphorus within the storage. Similarly, the decay of living biomass causes a loss of both organic material and phosphorus storage at a fixed concentration.

Uptake rates for phytoplankton have been found to always be greater than those of periphyton, indicating that the former are more efficient in assimilating phosphorus (Hwang and others, 1998). Plankton uptake rates may be higher than those for other organisms because of their large specific surface areas. Although dissolved organic phosphorus usually is considered relatively unavailable biologically, phosphorus-deficient plankton and periphyton communities have been observed to use this form of phosphorus at rates about equal to those for SRP uptake (Havens and others, 2001). For applications in which periphyton are discretized into epiphytic and benthic pools, the epiphytic periphyton maximum uptake rates and half-saturation constants have been found, respectively, to be about double and half those of epipelon (Scinto and Reddy, 2003). The greater uptake rates for epiphyton probably result from its ability to obtain a large portion of its required phosphorus from pore water (Havens and others, 2001).

Factors other than phosphorus also may limit the growth of aquatic organisms (Hecky and Kilham, 1988). Many biological reaction rates are temperature dependent (Goldman and Carpenter, 1974). Light availability changes with water column attenuation characteristics and seasonal fluctuations in incoming solar radiation and biomass shading, and can also limit photosynthesis and growth rates (Carr and others, 1997). Nutrients other than phosphorus, such as nitrogen or potassium, can also limit biological growth.

Senescence and Decay of Biological Tissues

Turnover rates for cattail leaves in southern Florida have been estimated to be about 0.011 d^{-1} (4 yr^{-1}) (Kadlec, 1999; Grace, 2003). For algal components, losses caused by mortality may average 0.1 d^{-1} for diatoms and green algae (Asaeda and Van Bon, 1997). First-order decay coefficients have been reported for standing dead biomass and fallen leaf litter of cattail and sawgrass in Everglades peat in the range of 10^{-4} to 10^{-3} d^{-1} (DeBusk and Reddy, 1998). Godshalk and Wetzel (1978) reported macrophyte decomposition rates between 0.002 and 0.06 d^{-1} under anaerobic conditions, and between 0.004 and 0.085 d^{-1} under aerobic conditions.

Such large differences in decomposition rates between organic detrital materials may be caused by differences in fiber content, nutrient content, or conditions within the decompositional environment (DeBusk and Reddy, 1998). For this reason, it is necessary to consider OM sources that have different turnover (decomposition) rates. First-order decay relations are used in the current model for plankton and macrophytes, with exchanges occurring between plankton, nonplankton particulate OM, macrophytes, and organic soil:

$$\frac{dC_{sw}^{pl}}{dt} = -k_{sn}^{pl} C_{sw}^{pl}, \quad (9)$$

$$\frac{dC_{sw}^{pn}}{dt} = k_{sn}^{pl} C_{sw}^{pl} + k_{de}^{fo} f_f C^{mp}, \quad (10)$$

$$\frac{dC^{mp}}{dt} = -\left(k_{de}^{fo} f_f + k_{de}^{fo} f_r\right) C^{mp}, \text{ and} \quad (11)$$

$$\frac{dS^o}{dt} = k_{de}^{fo} f_r C^{mp}, \quad (12)$$

where rate constants (k_{xx}^{xx}) and fractions (f_x) are as defined in table A3. Macrophytic foliage decay increases the particulate organic store and root decay increases the organic soil store.

Soil Oxidation and Mineralization and Burial

Soil oxidation results from soil drainage and exposure to air or fire, and causes a loss of organic soil, S^o, primarily through the conversion of organic carbon to carbon dioxide. Under these conditions, a wetland typically exports phosphorus mineralized from the OM store as it is depleted. In general, soil mineralization rates are lower than macrophyte and planktonic matter decay rates because the majority of soil materials are residual compounds resistant to decomposition (Turner and others, 2005). In the current model when the soil is saturated, oxidation loss is treated as a first-order removal of material from the system, with the phosphorus contained in the organic soil transferred directly to the pore water, C_{pw}^{P}. The oxidation of organic soil and the mineralization of phosphorus contained in the organic soil, respectively, are modeled as:

$$\frac{dS^o}{dt} = -k_{ox}^{so} S^o, \quad (13)$$

$$\frac{dS_{so}^{P}}{dt} = -X_{so}^{P} k_{ox}^{so} S^o, \text{ and} \quad (14)$$

$$\frac{dC_{pw}^{P}}{dt} = X_{so}^{P} k_{ox}^{so} S^o, \quad (15)$$

where k_{ox}^{so} is the rate of soil oxidation, and X_{so}^{P} is the phosphorus mass fraction of the organic soil.

Measured mineralization rates of phosphorus from wetland soils range from 1×10^{-6} d^{-1} for low-productivity meadowlands to 1.5×10^{-6} d^{-1} for bogs (Bridgham and others, 1998). The volume of active soil is assumed to be constant over time in the current model, and additions caused by settling and decay balance the loss caused by burial (that is, movement to deep storage). The amount buried, therefore, is set equal to the change in soil volume.

Feedbacks and External Environmental Factors

External factors other than phosphorus concentration that may affect the aforementioned physical and biological processes include hydrology, temperature, and light. The timing, magnitude, duration, and spatial extent of flooding will dictate whether plankton is present or which macrophytes are prevalent. The absence of water would expose organic soil to the atmosphere, causing rapid oxidation. Temperature affects the growth rates of many biota, increasing metabolism as well as decomposition. Macrophytes and some plankton require light for photosynthesis, a process that can be inhibited by particulate matter in the water and shading from foliage.

Light Limitation

Incident light above the water surface is available to suspended phytoplanktonic and floating and emergent plants. After some light is reflected by the water surface, light intensity is further reduced by scattering and absorption by suspended matter, submerged plants and algae, and the bed. The remaining light is reflected upward by the bed surface. In general, light is available according to the following equation:

$$PAR = I_0 e^{-k_e z_{ws}}, \tag{16}$$

where *PAR* is photosynthetically active radiation; I_0 is incident light just below the air-water interface (that is, maximum available light); k_e is the light extinction coefficient for the aquatic system, and z_{ws} is depth below the water surface (Carr and others, 1997). The temporal variability of the limiting control that light has on plant growth has also been modeled dynamically using coefficients from empirical relations; specifically, Secchi depth and turbidity relations (Carr and others, 1997). An additional extinction coefficient, k_{wb}, can be used to determine the *PAR* accounting for further loss due to plant biomass, C^{mp}, in the water column:

$$PAR = I_0 e^{-k_e z_{ws} - k_{wb} C^{mp}}. \tag{17}$$

Equation 17 shows that submerged, floating, and emergent macrophyte biomass limits the light available to benthic periphyton. The formulation also can be used to calculate light availability for organisms such as benthic periphyton—a biotic layer that can affect phosphorus dynamics strongly across the sediment-water interface.

Because light decreases exponentially with depth and biomass shading and linearly with total suspended solids, C^{SS} (Krause-Jensen and Sand-Jensen, 1998), k_e can be used to limit growth and equation 8 is adjusted as follows:

$$G_{sw}{}^{pl} = k_g{}^{pl} C_{sw}{}^{pl} \frac{C_{sw}{}^{P}}{C^{SS}\left(C_{sw}{}^{P} + k_{1/2}{}^{pl}\right)} e^{-k_e z_{ws} - k_{wb} C^{mp}}. \tag{18}$$

Temperature Effects

Temperature, *T*, affects biological activities that range from cell and plant growth to decomposition and respiration reactions and, consequently, is a primary controlling factor on wetland productivity. Shelef and others (1970) showed that the half-saturation constants used to describe nutrient uptake reactions are temperature dependent. Goldman and Carpenter (1974) related temperature to maximum algal growth rate, $k_g{}^{po}$, based on a broad range of empirical growth data and the Arrhenius equation:

$$k_g{}^{po} = ab^T = 0.851(1.066)^T, \tag{19}$$

where *a* and *b* are empirical constants, and *T* is in degrees Celsius. The effect of temperature on the algal growth rate is expressed as:

$$G_{sw}{}^{pl} = k_g{}^{pl} ab^T C_{sw}{}^{pl} \frac{C_{sw}{}^{P}}{C^{SS}\left(C_{sw}{}^{P} + k_{1/2}{}^{pl}\right)} e^{-k_e z_{ws} - k_{wb} C^{mp}}. \tag{20}$$

Vegetation Effects on Flow Restriction

Sessile organisms reduce wave energy in bottom waters near the soil-water interface and increase flow resistance in the water column. The effect of vegetation density on Manning's *n* values can be estimated using common approximations shown in the following table (Dingman, 1984). More sophisticated methods for relating vegetation and flow restrictions are emerging, including regressions of Manning's *n* with vegetation surface area (Green, 2006). The current model is capable of tracking changes in Manning's *n* as a function of vegetation density and providing this parameter as feedback to coupled hydrologic models.

Vegetation density	Manning's n values as affected by vegetation of the channel bed surface (from Dingman, 1984)
High	.025 – 0.050
Low	0.005 – 0.010
Medium	.010 – 0.025
Very high	.050 – 0.100

Reaction Equations

The mechanisms described earlier were used to develop a set of reactions among the different constituents, and where possible, the reactions were simplified by grouping terms. Most of the equations for phosphorus content in materials such as plankton, ${C_{pl}}^{P}$, are redundant if the mass fractions remain constant over time. The phosphorus content equations can be obtained simply by multiplying the material content by the appropriate mass fraction. For example, ${C_{pl}}^{P}$ can be obtained by multiplying C^{pl} by ${X_{pl}}^{P}$. The number of equations, therefore, can be reduced substantially by eliminating the equations for phosphorus content in materials where changes in phosphorus are due solely to the movement of material.

The reaction equations for the materials are as follows (variables and parameters are defined in appendixes 1 and 2):

$$\frac{\mathrm{d}C_{sw}^{\ pl}}{\mathrm{d}t} = G_{sw}^{\ pl} - \left(k_{sn}^{\ pl} + k_{ch}^{\ pl}\right)C_{sw}^{\ pl} + k_{sl}^{\ bf}C^{bf}, \tag{21}$$

$$\frac{\mathrm{d}C_{sw}^{\ pn}}{\mathrm{d}t} = k_{sn}^{\ pl}C_{sw}^{\ pl} - k_{st}^{\ pn}\left[C_{sw}^{\ pn}\right] + J_{en}^{\ so} + k_{de}^{\ fo}f_f C^{mp} + J_{atm}^{\ pn}, \tag{22}$$

$$\frac{\mathrm{d}C_{sw}^{\ pi}}{\mathrm{d}t} = -k_{st}^{\ pi}\left[C_{sw}^{\ pi}\right] + J_{en}^{\ si} + J_{ppt}^{\ sw} + J_{atm}^{\ pi}, \tag{23}$$

$$\frac{\mathrm{d}S^{o}}{\mathrm{d}t} = k_{st}^{\ pn}\left[C_{sw}^{\ pn}\right] - k_{ox}^{\ so}S^{o} - J_{en}^{\ so} + k_{de}^{\ ro}f_f C^{mp}, \tag{24}$$

$$\frac{\mathrm{d}S^{i}}{\mathrm{d}t} = k_{st}^{\ pi}\left[C_{sw}^{\ pi}\right] - J_{en}^{\ si}, \tag{25}$$

$$\frac{\mathrm{d}C^{mp}}{\mathrm{d}t} = G_{fo}^{\ mp} + G_{ro}^{\ mp} - \left(k_{de}^{\ fo}f_f + k_{de}^{\ ro}f_r\right)C^{mp}, \text{ and} \tag{26}$$

$$\frac{\mathrm{d}C^{bf}}{\mathrm{d}t} = k_{ch}^{\ pl}C_{sw}^{\ pl} + G_{ep}^{\ bf} + G_{be}^{\ bf} - k_{sl}^{\ bf}C^{bf}. \tag{27}$$

The reaction equations for the solutes are as follows (variables and parameters are defined in appendixes 1 and 2):

$$\frac{\mathrm{d}C_{sw}^{\ P}}{\mathrm{d}t} = -X_{pl}^{\ P} G_{sw}^{\ pl} + X_{fo}^{\ P} G^{fo} + X_{bf}^{\ P} G_{ep}^{\ bf} - k_{df} \frac{\left[C_{sw}^{\ P}\right] - \left[C_{pw}^{\ P}\right]}{z_{df}} - X_{ppt}^{\ P} J_{ppt}^{\ sw}, \tag{28}$$

$$\frac{\mathrm{d}C_{pw}^{\ P}}{\mathrm{d}t} = X_{so}^{\ P} k_{ox}^{\ so} S^{o} - X_{ro}^{\ P} G^{ro} - X_{bf}^{\ P} G_{bn}^{\ bf} + k_{df} \frac{\left[C_{sw}^{\ P}\right] - \left[C_{pw}^{\ P}\right]}{z_{df}} - \frac{\theta}{\rho_b f_i k_d} \frac{\mathrm{d}S_{si}^{\ P}}{\mathrm{d}t}, \tag{29}$$

$$\frac{\mathrm{d}C_{pl}^{\ P}}{\mathrm{d}t} = X_{pl}^{\ P} G_{sw}^{\ pl} - X_{pl}^{\ P} \left(k_{sn}^{\ pl} + k_{ch}^{\ pl}\right) C_{sw}^{\ pl} + X_{bf}^{\ P} k_{sl}^{\ bf} C_{sl}^{\ bf}, \tag{30}$$

$$\frac{\mathrm{d}C_{pn}^{\ P}}{\mathrm{d}t} = X_{pl}^{\ P} k_{sn}^{\ pl} C_{sw}^{\ pl} + X_{pn}^{\ P} k_{st}^{\ pn} C_{sw}^{\ pn} + X_{so}^{\ P} J_{en}^{\ so} + X_{fo}^{\ P} k_{de}^{\ fo} f_f C^{mp} + X_{atm,pn}^{\ P} J_{atm}^{\ pn}, \tag{31}$$

$$\frac{\mathrm{d}C_{pi}^{\ P}}{\mathrm{d}t} = -X_{pi}^{\ P} k_{st}^{\ pi} \left[C_{sw}^{\ pi}\right] + X_{si}^{\ P} J_{en}^{\ si} + X_{ppt}^{\ P} J_{ppt}^{\ sw} + X_{atm,pi}^{\ P} J_{atm}^{\ pi}, \tag{32}$$

$$\frac{\mathrm{d}S_{so}^{\ P}}{\mathrm{d}t} = X_{pn}^{\ P} k_{st}^{\ P} \left[C_{sw}^{\ pn}\right] - X_{so}^{\ P} k_{ox}^{\ so} S^{o} - X_{so}^{\ P} J_{en}^{\ so} + X_{ro}^{\ P} k_{de}^{\ ro} f_r C^{mp}, \tag{33}$$

$$\frac{\mathrm{d}S_{si}^{\ P}}{\mathrm{d}t} = X_{pi}^{\ P} k_{st}^{\ pi} \left[C_{sw}^{\ pi}\right] - X_{si}^{\ P} J_{en}^{\ si} + \frac{\rho_b f_i d_d}{\theta} \frac{\mathrm{d}C_{pw}^{\ P}}{\mathrm{d}t}, \tag{34}$$

$$\frac{dC_{mp}^{\ P}}{dt} = X_{fo}^{\ P} G^{fo} + X_{ro}^{\ P} G^{ro} - \left(X_{fo}^{\ P} k_{de}^{\ fo} f_f + X_{ro}^{\ P} k_{de}^{\ ro} f_r\right) C^{mp}, \text{ and} \tag{35}$$

$$\frac{\mathrm{d}C_{bf}^{\ P}}{\mathrm{d}t} = X_{pl}^{\ P} k_{ch}^{\ pl} C_{sw}^{\ pl} + X_{ep}^{\ P} G_{ep}^{\ bf} + X_{bn}^{\ P} G_{bn}^{\ bf} - X_{bf}^{\ P} k_{sl}^{\ P} C^{bf}. \tag{36}$$

The full suite of growth rates is given by the following:

$$G_{sw}^{\ pl} = k_g^{\ pl} C_{sw}^{\ pl} \frac{\left[C_{sw}^{\ P}\right]}{\left[C_{sw}^{\ P}\right] + k_{1/2}^{\ pl}}, \tag{37}$$

$$G^{fo} = k_g^{\ fo} C^{fo} \frac{\left[C_{sw}^{\ P}\right]}{\left[C_{sw}^{\ P}\right] + k_{1/2}^{\ fo}}, \tag{38}$$

$$G^{ro} = k_g{}^{ro} C^{ro} \frac{\left[C_{pw}{}^{P}\right]}{\left[C_{pw}{}^{P}\right] + k_{1/2}{}^{ro}}, \quad (39)$$

$$G_{ep}{}^{bf} = k_g{}^{bf} C^{bf} \frac{\left[C_{sw}{}^{P}\right]}{\left[C_{sw}{}^{P}\right] + k_{1/2}{}^{bf}}, \text{ and} \quad (40)$$

$$G_{bn}{}^{bf} = k_g{}^{bf} C^{bf} \frac{\left[C_{pw}{}^{P}\right]}{\left[C_{pw}{}^{P}\right] + k_{1/2}{}^{bf}}. \quad (41)$$

Model Calibration and Validation

In this study, model performance and flexibility are demonstrated with applications to laboratory and field experimental data sets from the following sources, each representing a specific scale and level of complexity.

- *Level 1*—A laboratory core study that measured the flux of SRP released from wetland soils to the water column without interactions influenced by plants or phytoplankton (Grace, 2003).
- *Level 2*—An outdoor mesocosm study that measured phosphorus release to the water column from flooded soils with different initial phosphorus contents under a natural light environment (DB Environmental, Inc., written commun., 2004). Both suspended and dissolved phosphorus concentrations were measured.
- *Level 3*—Analysis of data collected from field operations at STA-1W Cell 4 (147 ha) for the period February 1995-June 2000, and stored in the SFWMD DBHYDRO database: *http://my.sfwmd.gov/dbhydroplsql/show_dbkey_info.main_menu*

Some of the important Cell 4 simulation complexities not represented in the first two levels include through-flowing water, suspended and dissolved components, and active periphyton and macrophtye communities. The level-3 period was considerably longer (5.4 years) than the 14-day simulation periods for levels 1 and 2. Two model implementations are presented for level 3: one in which the field-scale system was treated as homogeneous, and another in which the model was coupled with a spatially distributed hydrologic model.

Level 1—Soil Cores

In this study, five intact soil cores (0.1 m deep and 0.07 m in diameter) were collected from STA-1W Cell 1 outflow region and incubated with 0.45-μm filtered water (initial SRP less than 2 μg L^{-1}) for 28 days (Grace, 2003). The SRP concentrations were measured in the water column over time to determine the phosphorus flux from the soil. Soil and pore-water phosphorus concentrations and soil bulk density also were measured during the level-1 study. No periphyton, water column plankton, or macrophytes were present in the cores, which were incubated in the dark with air continuously stirring the water column but not resuspending surficial sediments.

The important mechanisms controlling phosphorus flux to the water column included the following:

- Soil phosphorus mineralization to the pore water, estimated by the first-order coefficient for organic soil oxidation, k_{ox};
- Sorption-desorption equilibrium between pore-water phosphorus and soil surface-exchange sites, estimated by the partitioning coefficient, $k_d{}^{sr}$;
- Phosphorus diffusion from the pore water to the water column, estimated by the diffusion coefficient, D; and
- Biologically enhanced phosphorus transfer from the pore water to the water column (bioturbation), estimated by the bioturbation factor, BF.

All other transfer mechanisms were assumed to be inactive.

The initial measured soil and water column conditions and model parameters are summarized in table 1. The sorption partitioning coefficient, k_d^{sr}, was 10 L/kg, based on the study of Richardson and Vaithiyanathan (1995) conducted on soils from southern Florida wetlands. The value for D is based on results from Fisher and Reddy (2001), and values for k_{ox} and BF (table 1) were calibrated. The bulk density of highly organic soils is often low at the soil surface and increases with depth. Bulk density values reported for the soils in these core studies were between 0.1 and 0.25 g/cm^3 (Grace, 2003). Irons (2001) reported a bulk density in Cell 4 of 0.29 g/cm^3 for cultivated soils, and bulk densities from 0.047 to 0.179 g/cm^3 for newly accrued soils; a value of 0.2 g/cm^3 was used for all simulations.

Because the timescale in the level-1 study was only a few weeks, the primary constraints were that soil phosphorus storage could not be depleted substantially, and that pore-water phosphorus concentrations remained relatively stable. For pore-water phosphorus concentrations to be stable, the mineralization flux of phosphorus from soil to pore water must be balanced with the flux of phosphorus from pore water to the water column. Mineralization rates reported in the literature are relatively slow, being on the order of 10^{-3} to 10^{-5} days (Bridgham and others, 1998); a value of $k_{ox} = 0.0001$ d^{-1} was used in the level-1 study.

Fickian diffusive fluxes of phosphorus calculated from pore water concentration gradients in wetland soils generally have been lower than fluxes measured from intact core studies (Fisher and Reddy, 2001). Van Rees and others (1996) estimated that bioturbation increased phosphorus exchange between soil pore water and surface water from 1.5 to 15 times above rates expected solely from diffusion.

Observed water column SRP concentrations are compared to simulated values in figure 5A. Figure 5a shows comparisons between predicted water column SRP concentrations based solely on diffusion ($BF = 1$), and those that consider the combined effects of diffusion and bioturbation (BF greater than 1). The best fit of these data corresponds to a bioturbation factor of 2.7. Figure 5B shows the associated change in pore-water SRP concentrations due to the exchange with the water column. This change is presented relative to the overall soil phosphorus storage for perspective.

Table 1. Initial conditions and calibrated parameter values for level-1 model application.

[Symbols are defined in appendixes 1 and 2. Unit abbreviations are defined on the Conversion Factors page; BF, bioturbation factor]

Symbol	Value
Initial Conditions – Soil	
$[C_{pw}^P]$	500 µg/L
$[S_{si}^P]$	3.75 mg/kg
$[S_{so}^P]$	800 mg/kg
k_d^{sr}	10 L/kg
z_{as}	.10 m
z_{df}	.04 m
θ	.8 [-]
ρ_b	.2 g/cm^3
Initial conditions – water column	
$[C_{sw}^P]$	1 µg/L
z_{wc}	.30 m
Calibrated parameters	
BF	2.7
k_{oxso}	.0001 1/d

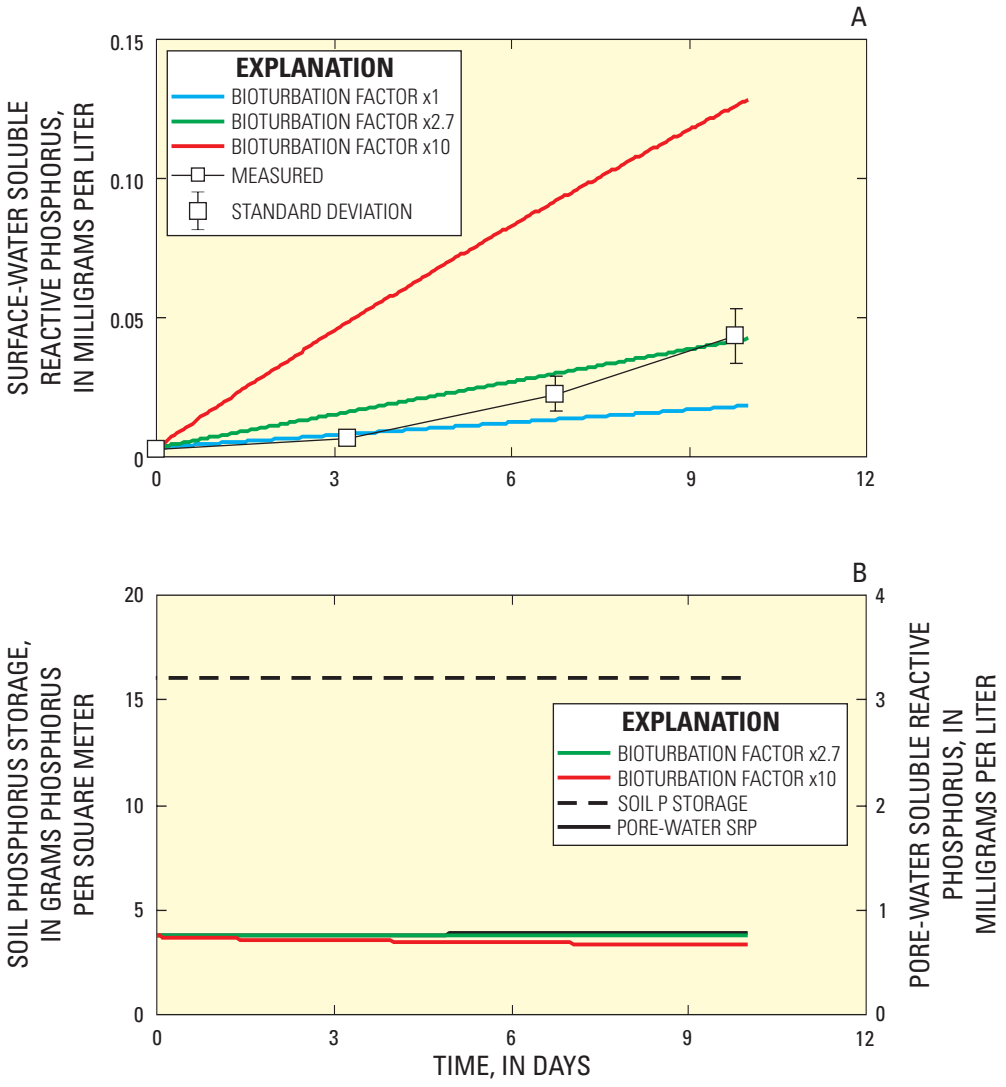

Figure 5. (A) Measured water column soluble reactive phosphorus (SRP) concentrations compared to model level-1 predictions, including a range of bioturbation factors, and (B) simulated changes in soil phosphorus storage and pore-water soluble reactive phosphorus.

Level 2—Outdoor Mesocosms

Four replicate mesocosms (0.2-m deep soils, 0.4-m deep water column, and 1-m^2 surface area) were established for each of two treatments using soils collected from within STA-1W. The first was a muck soil retrieved during recent excavations for a new gate structure, which represented "low-P" soils typical of the area prior to STA operations. The second treatment was a "high-P" soil collected during 2005 near the Cell 4 inlet, where 10 years of flow-through operations at the STA had enriched the phosphorus content of the soil. The STA-treated water was applied to the soil and allowed to equilibrate for 14 days.

Although no macrophytes nor periphyton were present at the beginning of these mesocosm studies, planktonic communities did develop from the initial water column population during the experiments. The mechanisms controlling phosphorus flux to the water column were the same as for level 1, although phosphorus cycling mechanisms influenced by phytoplankton growth also were included. Additionally, the mesocosms were outdoors rather than in a temperature-controlled laboratory as in level 1. All other transfer mechanisms were assumed to be inactive.

Table 2. Initial conditions and calibrated parameter values for level-2 high phosphorus model application.

[Symbols are defined in appendixes 1 and 2. Unit abbreviations are defined on the Conversion Factors page. Where a range of values is listed, the smallest value is for low phosphorus soil and largest value is for high phosphorus soil. Additional components not included in previous level of model application are shaded in blue. BF, bioturbation factor]

Symbol	Value	Condition or Parameter Type
	Initial Conditions	
$[C_{pw}{}^{P}]$	45-700 µg/L	Soil
$[S_{si}{}^{P}]$	.25 – 7.0 mg/kg	Soil
$[S_{so}{}^{P}]$	342- 852 mg/kg	Soil
$k_d{}^{sr}$	10 L/kg	Soil
z_{as}	.20 m	Soil
z_{df}	.04 m	Soil
θ	.8 [-]	Soil
ρ_b	.2	Soil
$[C_{sw}{}^{P}]$	43 µg/L	Water Column
$C_{sw}{}^{pl}$	243 µg/L	Water Column
z_{wc}	.3 m	Water Column
	Calibrated Parameters	
BF	2.7 – 20	Soil
$k_{ox}{}^{so}$	.0001 1/d	Soil
$^{1}k_{1/2}{}^{pl}$	2.005 mg/L	Algae
$^{1}k_{g}{}^{pl}$	2.25 1/d	Algae
$^{1}k_{sn}{}^{pl}$	2.1 1/d	Algae

Initial soil and water column phosphorus storages were based on measured values, but the parameters regulating transfer mechanisms used in level 1 were maintained for level 2 (table 2). Because the timescale in this case also was only a few weeks, soil phosphorus storage and pore-water phosphorus concentration were constrained to be relatively stable. Total phosphorus and SRP concentrations were both measured in the water column over time. Particulate phosphorus (PP) was assumed to be represented by total phosphorus minus SRP. Concentrations of SRP and PP were measured in the initial floodwater, again 24 hours after the mesocosms were flooded and after 3, 7, and 14 days. The 24-hour concentrations represent the initial condition for model simulation, because of possible disturbances to the system during the flooding process. This shortened the simulation time to 13 days.

Observed water column PP and SRP concentrations are compared to simulated values in figure 6, and the best fits to these data indicate that a bioturbation factor of 12 is appropriate. This bioturbation factor is larger than that required to fit the level-1 data, which indicates an increased bioturbation effect with the increased scale of the experiment. Both the simulated SRP and PP dynamics generally matched the observed trends in the data. The simulation started on day 1 rather than day 0 because of potential disturbances caused by water additions to the system on day 1.

Level 3—Stormwater Treatment Area 1W, Cell 4

Application of the model to a field-scale system was demonstrated using STA-1W performance data from a 5.4-year period between February 1995 and June 2000. Some of the important complexities of the field system in level 3, not represented in levels 1 and 2, include flowing water and active macrophtye communities. Although phosphorus concentrations, flow rates, and biomass dynamics fluctuated during this period, the long-term performance characteristics of soil, macrophyte, and water column storages provided a basis for comparison to model output.

Two field-scale model applications are presented: (1) a homogeneous, steady-state flow case that included a more complex representation of phosphorus cycling, and (2) a spatially distributed, transient flow case that included only a simple representation of phosphorus cycling. The spatially distributed transport model was validated against known analytical solutions using nonreactive and reactive solutes (James and Jawitz, 2007).

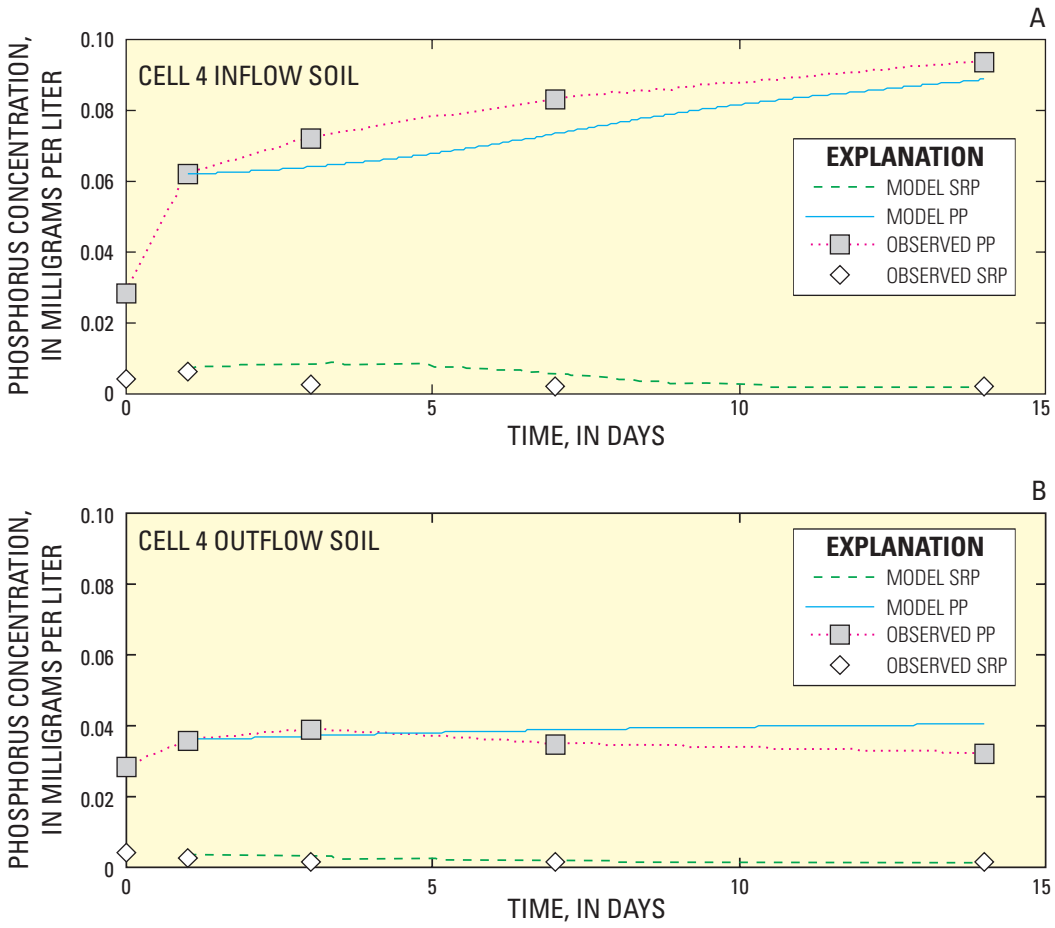

Figure 6. Comparison between observed and simulated water column particulate phosphorus (PP) and soluble reactive phosphorus (SRP) concentrations for level-2 simulations.

A study of the soils within STA-1W prior to construction showed that the average phosphorus content in the upper 10 cm of soil was about 8.3 g/m^2 (Reddy and Graetz, 1991), and this was used as the initial condition for soil phosphorus concentration. In June 2000, soils were sampled again in the inflow region and outflow region of Cell 4 (Irons, 2001). These data provided a basis for comparing the predicted increase in soil phosphorus storage.

Shortly after flooding the Cell 4 region of STA-1W in August 1993, pore-water SRP concentrations increased to nearly 4 mg/L at a 10-cm depth, and decreased to less than 1 mg/L by January 1994 (Newman and Pietro, 2001). The simulation was started in February 1995 so that the effects of cultivation practices would be minimal, and the wetland soil, water, and biomass dynamics would be more representative of a typical wetland.

In 1995, SFWMD scientists resampled soil and pore-water phosphorus concentrations in 0- to 5-cm and 5- to 10-cm depth intervals at four locations within Cell 4. The average values for these two depth intervals were used as initial conditions for the level-3 calibration (table 3). Pore-water SRP concentrations were 346 ± 280 µg/L, and soil total phosphorus concentrations were 355 ± 23 mg/kg. These values are between the high- and low-phosphorus soils of the level-2 calibration (mesocosm) study.

The particulate settling processes simulated in level 2 were limited to representing algal biomass and suspended particulate transfer from the water column to soil storage. In level 3, the production of particulate phosphorus from macrophyte turnover also was included. The growth rate coefficient and half saturation concentration for algal biomass growth functions were consistent between level-2 and level-3 simulations to limit the number of new parameters in level 3.

Model results indicate that 6.2 g/m^2 of new soil phosphorus had accumulated over the period of simulation, a value between the upper and lower estimates of soil phosphorus accrual determined by Irons (2001) (figs. 5 and 6). The predicted biomass phosphorus storage ranged from 0.1 to 0.31 g/m^2, which compared favorably with measurements (0.07-2.0 g/m^2) reported in an assessment of the SAV communities of Cell 4 during winter and summer periods (DB Environmental Inc., 2004). No spatial

Table 3. Initial conditions and calibrated and algae parameter values for level-3 field-scale model application.

[Symbols are defined in appendixes 1 and 2, except where noted; HLR, hydraulic loading rate; BF, bioturbation factor. Unit abbreviations are defined on the Conversion Factors page]

Symbol	Value	Condition or parameter type
	Initial Conditions	
$[C_{pw}{}^{P}]$	346 µg/L	Soil
$[S_{si}{}^{P}]$	3.75 mg/kg	Soil
$[S_{so}{}^{P}]$	355 mg/kg	Soil
$k_d{}^{sr}$	10 L/kg	Soil
$k_{ox}{}^{so}$	.0001 1/d	Soil
z_{as}	.20 m	Soil
z_{df}	.04 m	Soil
θ	.8 [-]	Soil
ρ_b	.2 g/cm^3	Soil
$C_{pl}{}^{P}$	30 µg/L	Water column
$C_{sw}{}^{P}$	14 µg/L	Water column
HLR	.15 m/d	Water column
z_{wc}	.8 m	Water column
$^{1}C_{mp}{}^{P}$	.1-1.0 g/m^2 phosphorus	Biomass (phosphorus)
	Calibrated Parameters	
BF	3	Soil
$k_{sn}{}^{pl}$	.3 1/d	Algae
$^{1}k_{1/2}{}^{fo}$	.050 mg/L	Macrophytes
$^{1}k_{1/2}{}^{ro}$	1.0 mg/L	Macrophytes
$^{1}k_{g}{}^{fo}$	.01 1/d	Macrophytes
$^{1}k_{g}{}^{ro}$	.01 1/d	Macrophytes
$^{1}k_{sn}{}^{fo}$	.002 1/d	Macrophytes
$^{1}k_{sn}{}^{ro}$	.002 1/d	Macrophytes
	Algae Parameters	
$k_{1/2}{}^{pl}$	.005 mg/L	Algae
$k_{g}{}^{pl}$	.25 1/d	Algae

[1]Additional components not included in previous level of model application conditions.

trends in SAV phosphorus storage were observed in that assessment, although higher phosphorus storage was reported for summer periods than for winter periods. Higher biomass phosphorus storage was typical in areas dominated by water hyacinth (1.5-4.0 g/m^2), although these floating macrophytes were not commonly found in Cell 4 during the calibration period and were restricted to the inflow region (DB Environmental Inc., 2004). Macrophyte biomass in Cell 4 is dominated by SAV, but also includes minor amounts of emergent cattails and water hyacinth. The biomass of these plant communities appears to be dynamic and probably is affected by hydraulics, nutrient loads, and seasonal light and temperature variation. The primary forcing functions that control macrophyte vegetation dynamics, however, have not been determined. Additional datasets are necessary if interannual variation in macrophyte biomass and species-specific effects are to be incorporated into the model.

Some of the important complexities of the field system not represented in the first two cases include flowthrough of water and any suspended or dissolved components, and active periphyton and macrophyte communities. The calibrated results and validation for the homogeneous, steady-state field scenario are presented in figures 7 to 10.

For the spatially distributed exercise, removal of phosphorus (total phosphorus) from the water column and storage within Cell 4 was modeled using a first-order uptake parameter with coefficient k_u. Conversely, phosphorus release from storage into the water column was modeled using a second first-order parameter, k_r. The uptake parameter is assumed to represent a grouping of several different processes including the settling of particulate phosphorus, SRP uptake by macrophytes, sorption onto soil, and so forth. The release parameter is assumed to combine such effects as senescence, desorption, resuspension, and so forth. The uptake was assumed to be proportional to phosphorus content in the water column, whereas the release was proportional to the phosphorus content in the soil.

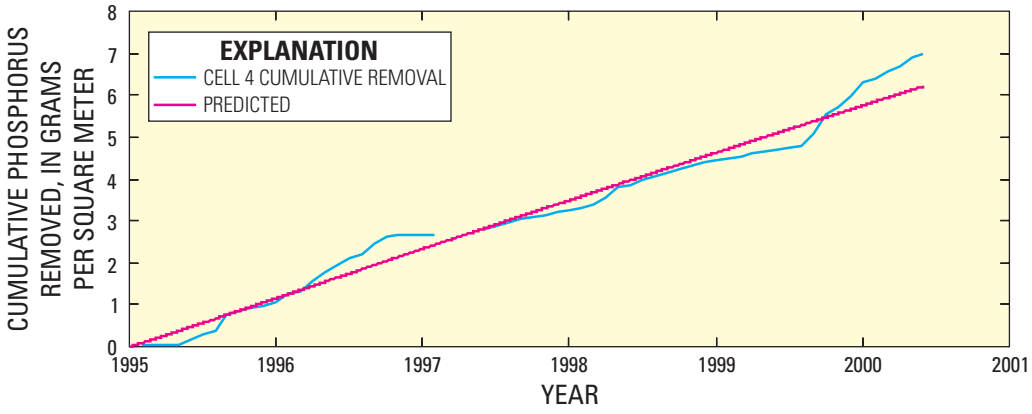

Figure 7. Comparison of cumulative phosphorus removal from South Florida Water Management District water sampling of inflow and outflow waters in Cell 4, to the phosphorus removal predicted by the model.

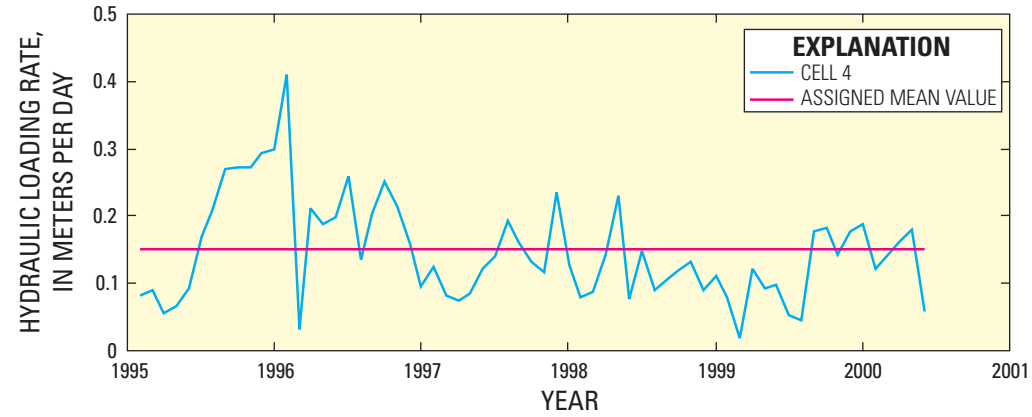

Figure 8. Hydraulic loading rate to Cell 4 for the February 1995 to June 2000 period, relative to the mean hydraulic loading rate applied during level-3 calibration.

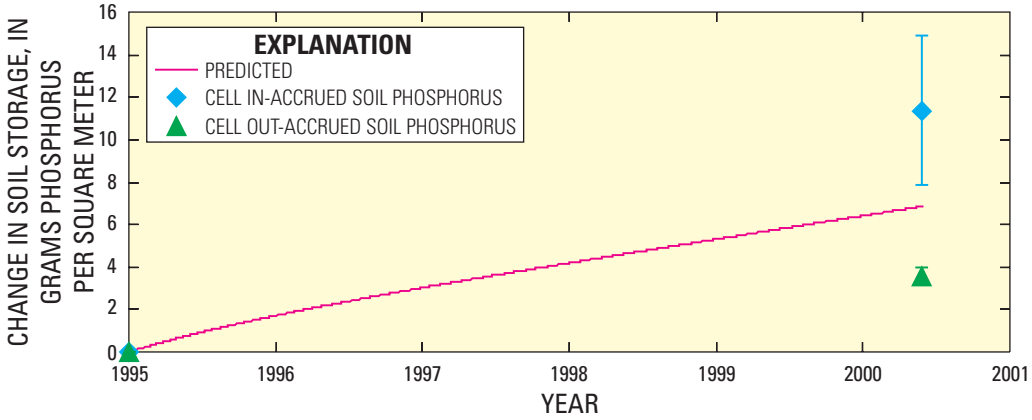

Figure 9. Measured and predicted change in soil phosphorus storage over time in the inflow and outflow region of Cell 4, as determined from soil phosphorus content and bulk density measurements of the newly accrued soil material (Irons, 2001). Values are mean ± 1 standard deviation of four soils per region.

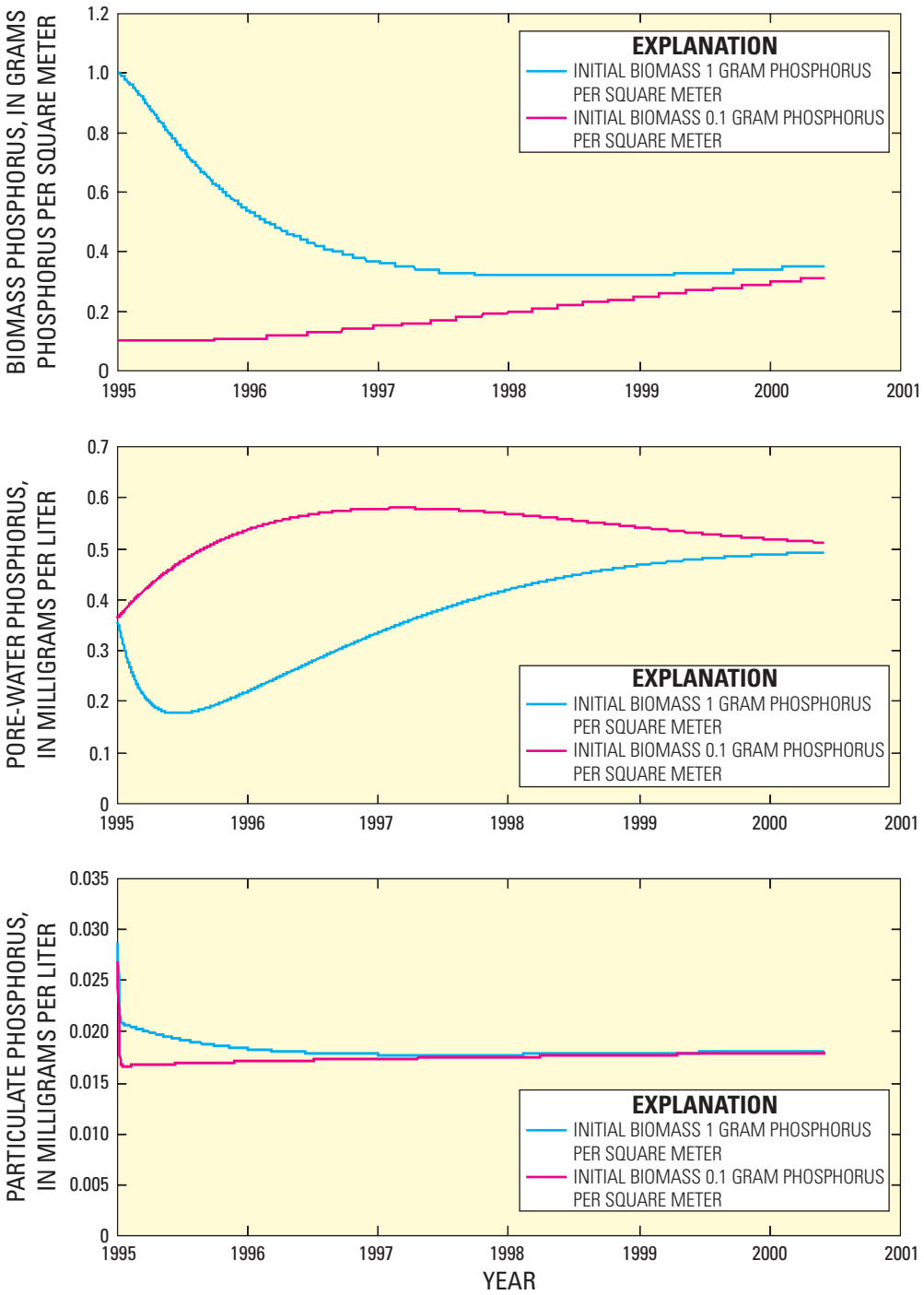

Figure 10. Effect of initial biomass on particulate phosphorus and pore-water concentrations in the calibrated model.

A finite-element mesh with 208 elements and 130 element vertices was used (fig. 11). Data were obtained from a USGS digital elevation map, and the hydrodynamics were provided by the SFWMD Regional Simulation Model (RSM). Water enters along the northern edge of Cell 4 at structures G-254A-E, flows southward along a gentle altitude gradient, and exits at structure G-256. Daily inflow and outflow water volumes were obtained for the simulation period from DBHYDRO, along with weekly or bimonthly phosphorus concentrations.

The parameters k_u and k_r were chosen to match the first 6 months of 1995; the best-fit values are 2.4 d^{-1} and 2.4×10^{-4} d^{-1}, respectively. The inflow and outflow total phosphorus concentrations, as well as simulated total phosphorus outflow concentrations at G-256, are shown for 1995-97 period in figure 12 and the 1998-2000 period in figure 13. Because of the mechanisms of

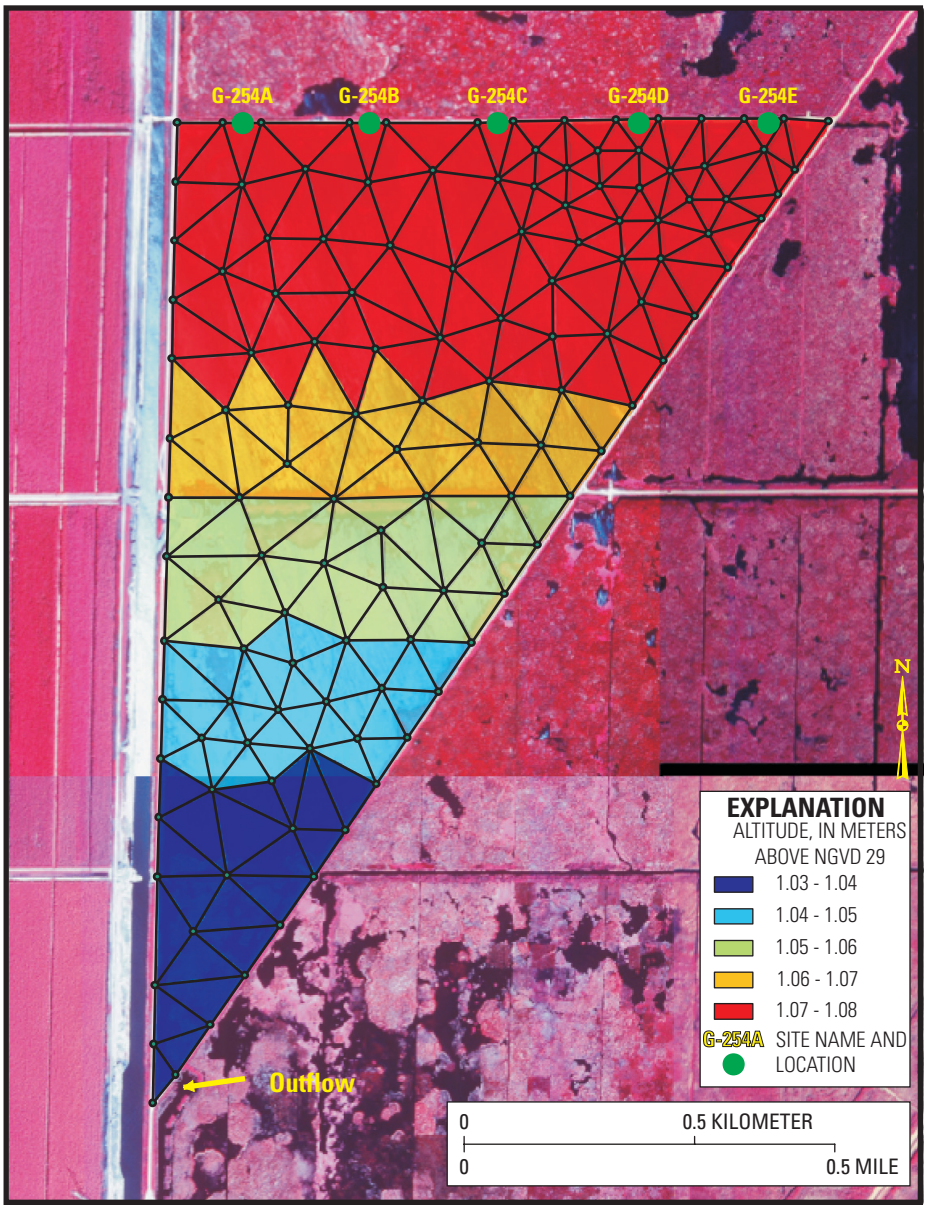

Figure 11. Aerial photograph of the modeled Stormwater Treatment Area 1W (STA-1W), Cell 4, including elevations within the cell, and the model mesh.

phosphorus release from soil included in this application of the model, phosphorus would be in the outflow, as long as phosphorus were still present in the soil even if the phosphorus inflow were zero. The simulated outflow total phosphorus concentrations match the measured outflow values for the first 2 years (1995-96) of the simulation (fig. 12), but subsequently overestimate the values for the majority of the rest of the modeling period (fig. 13).

Maps of spatially distributed values generated from the measured and simulated total accumulated soil phosphorus are shown in figures 14 and 15, respectively. The basic pattern of accumulation is the same in both cases, with the greatest amount of accumulated phosphorus in the soil present in the northern part of Cell 4, close to the inflow gages. Although not shown, phosphorus uptake had a moderately strong influence on the distribution of accumulated soil phosphorus within Cell 4 during the calibration phase. Lower values of k_u resulted in more evenly distributed patterns of soil phosphorus. This information was not used to calibrate the model, although it may be used for future refinement of the Cell 4 model. Overall, the amount of soil phosphorus estimated by the simulation underestimates the measured values within the cell. This is expected because the model overestimated total phosphorus outflow concentrations. Phosphorus, therefore, did not accumulate sufficiently within Cell 4 during the simulation. This overestimation illustrates a limitation of relying on only two temporally and spatially constant parameters to simulate processes within the cell.

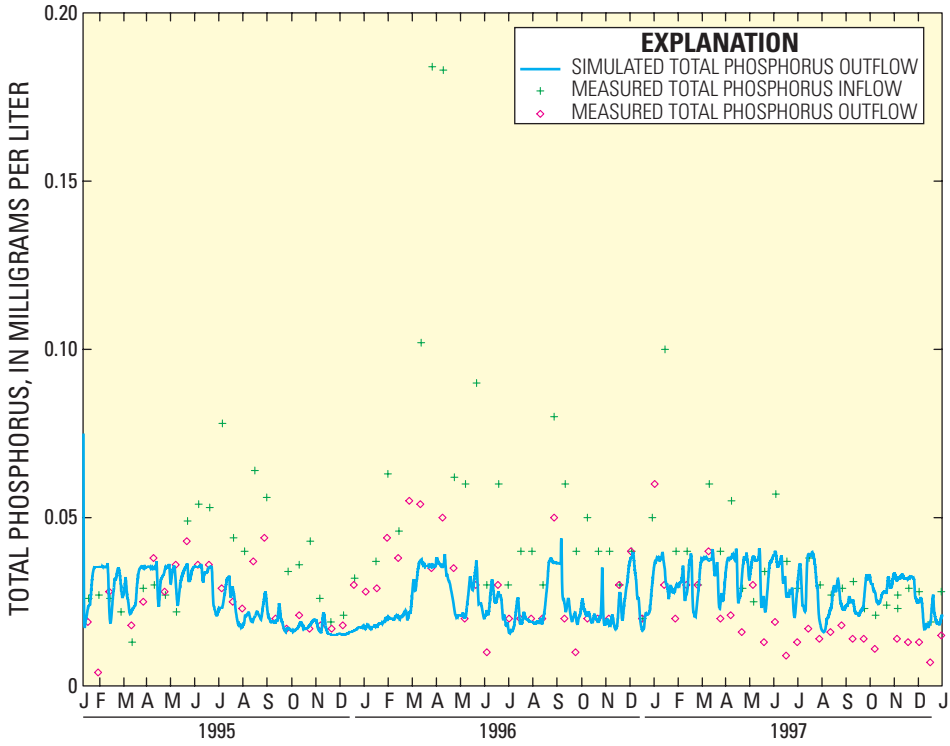

Figure 12. Measured inflow and outflow of total phosphorus, and simulated outflow from Cell 4 from 1995 to 1997.

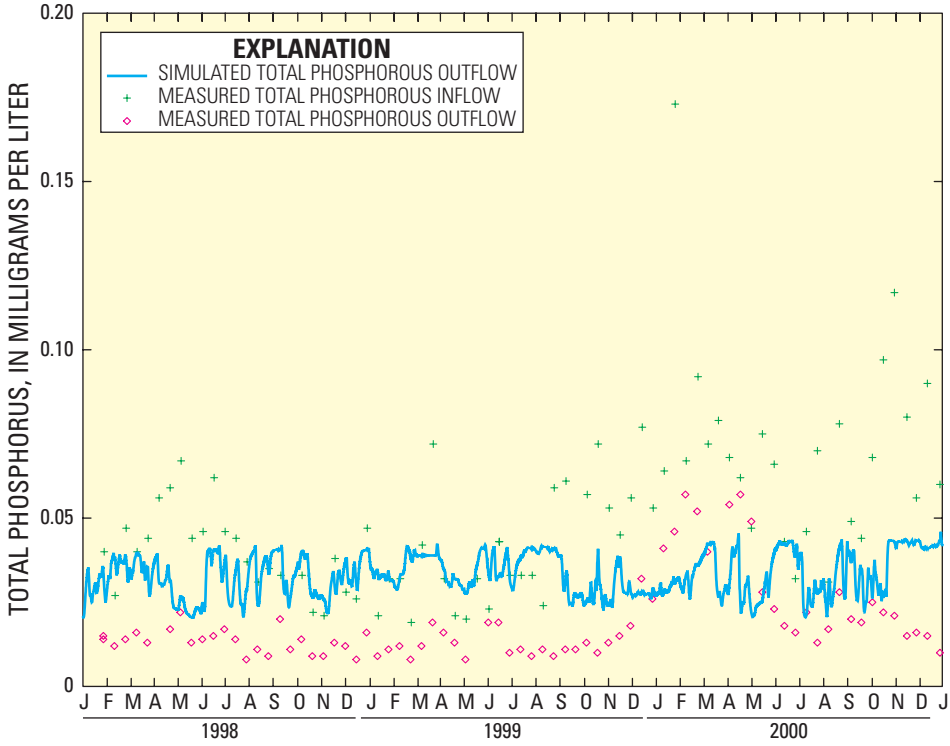

Figure 13. Measured inflow and outflow of total phosphorus, and simulated outflow from Cell 4 from 1998 to 2000.

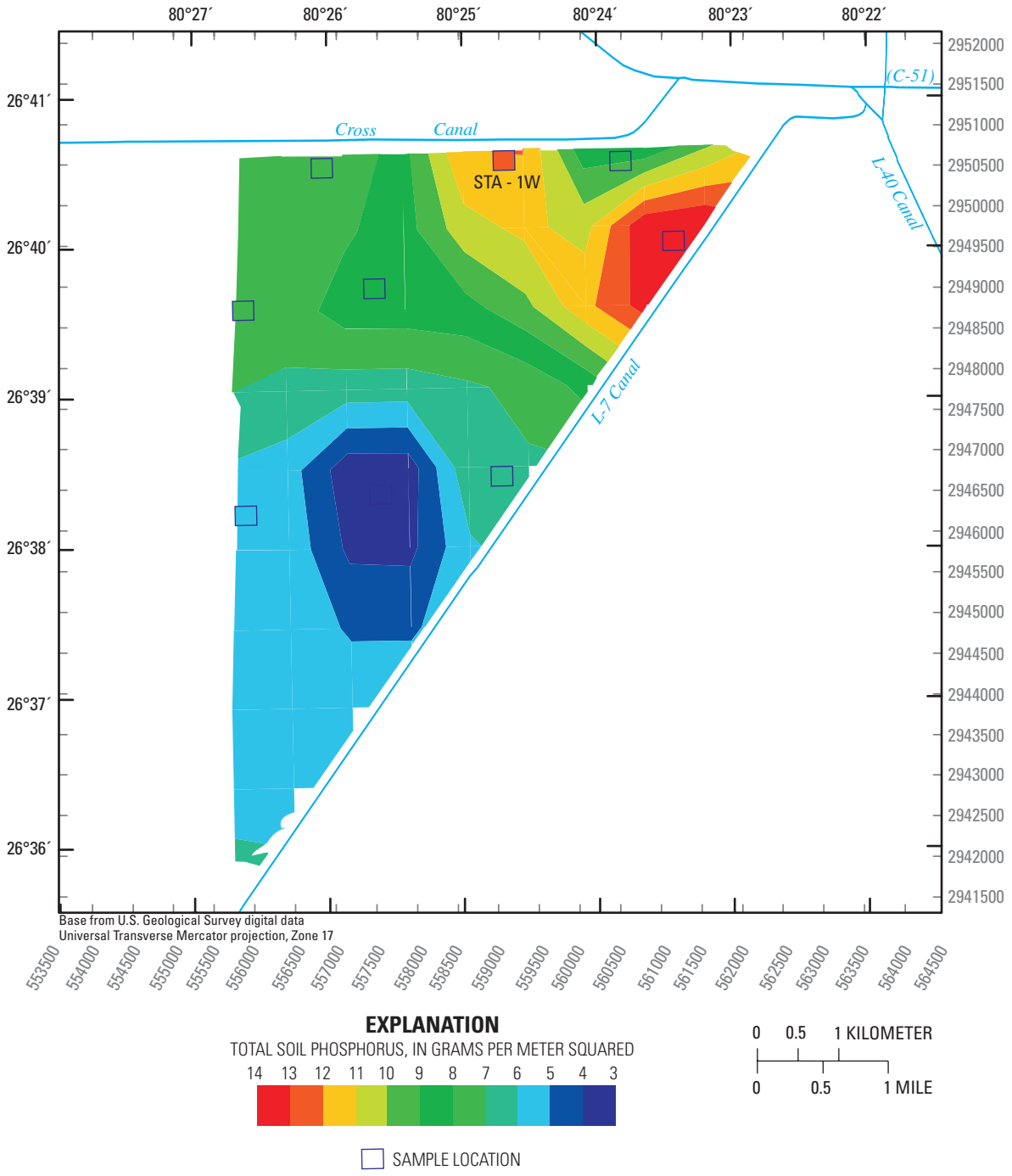

Figure 14. Accumulated total soil phosphorus from samples collected at the end of 2000.

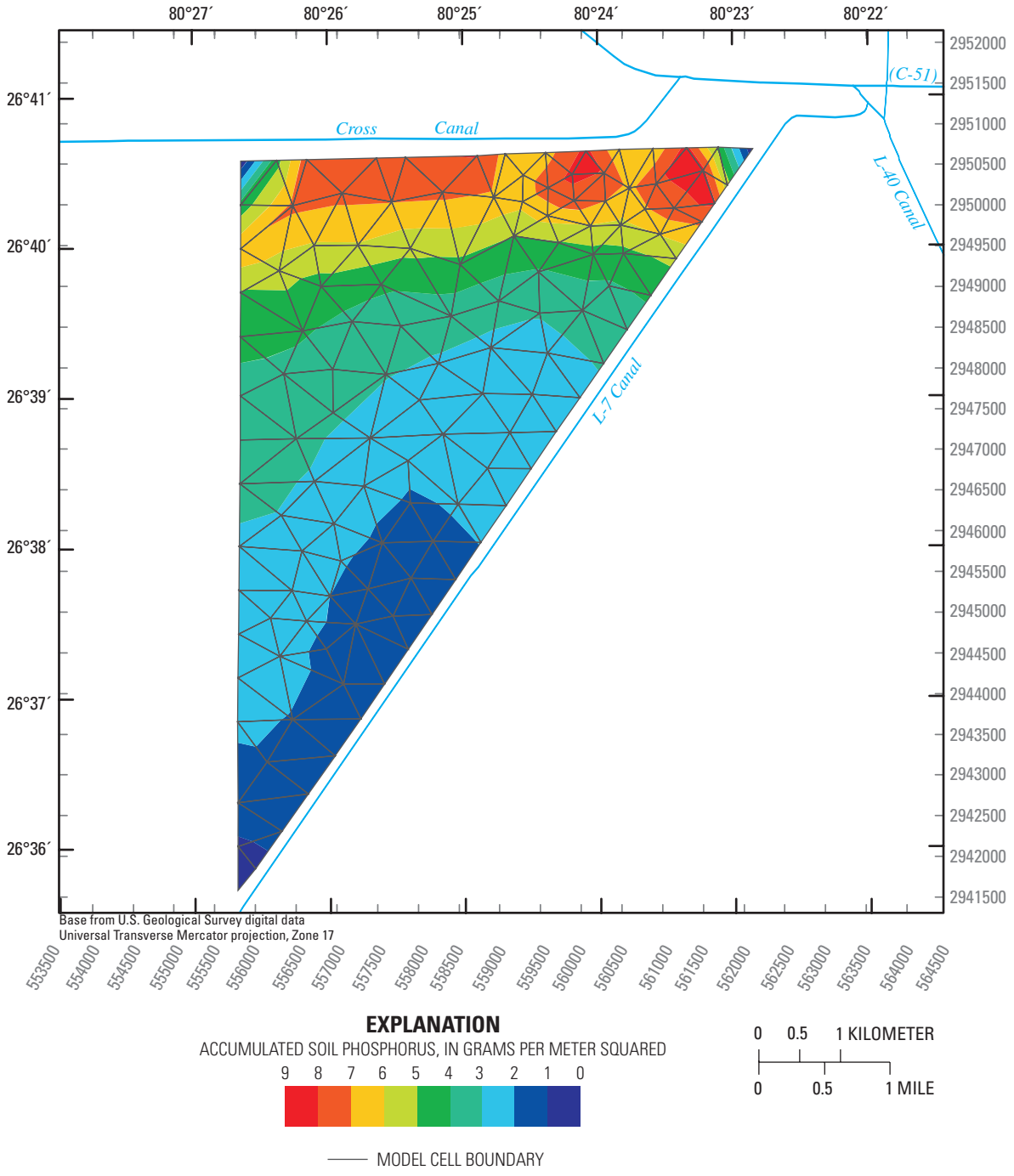

Figure 15. Estimated accumulated soil phosphorus at the end of 2000.

Global Sensitivity Analysis

Mathematical models are built in the presence of uncertainties of various types, such as input variability, model algorithms, model calibration data, and scale (Beven, 1989; Haan, 1989; Luis and McLaughlin, 1992). Uncertainty analysis is used to propagate all such uncertainties, using the model, onto the model output of interest. Sensitivity analysis is used to determine the strength of the relation between a given uncertain input and the output (Saltelli and others, 2004). The evaluation of model sensitivity and uncertainty is an essential part of the model development and application process (Reckhow, 1994; Beven, 2006). Although sensitivity analysis is useful in selecting proper parameters and models, and model uncertainty analysis provides an informative assessment of results, these tools are frequently ignored in current water-quality modeling efforts (Beven, 2006; Muñoz-Carpena and others, 2006). Complex mathematical models, such as the model described herein, often contain a large number of input parameters and are computationally intensive. To facilitate the evaluation and application of these models, it is important to identify a subset of parameters that strongly affect model output for several reasons:

- *Model Simplification*—If only a few parameters are important, the model typically can be simplified by eliminating parts that appear superfluous, or by grouping discrete processes.
- *Quality Assurance*—If the model shows a strong or weak dependence on parameters initially expected to be unimportant or important, respectively, the model structure may need to be revised.
- *Additional Research*—The process may clarify whether important parameters require more accurate quantification (Saltelli, 2002).

Concerning global sensitivity, an "input factor" broadly refers to anything that changes the model prior to execution. This not only includes the model parameters, input data, and boundary conditions, but also entirely different conceptualizations of the system. The model described herein allows for user-defined model complexity through a flexible XML user interface as described by A.I. James (University of Florida, written commun., 2008). Of particular concern is how model complexity affects global sensitivity and the uncertainty of different model outputs, especially for those biogeochemical processes that are present at different complexity levels. Furthermore, in flow-driven systems such as the Everglades, it is necessary to account for the effect of water velocity in the analysis. A statistical framework applied here follows that presented by Muñoz-Carpena and others (2007) to evaluate a test system at three increasingly complex model structures and three surface-water flow velocities (or residence times).

Techniques and Screening Methods

Input factors of interest in the sensitivity analysis are those that are uncertain; that is, their value lies within a finite interval of nonzero width. Traditionally, model sensitivity has been expressed mathematically as the derivative of a model output with respect to an input variation. These derivatives are typically normalized by either the central value where the derivative is calculated, or by the standard deviations of the input parameter and output values. These sensitivity measurements are "local" because they are fixed to a point or narrow range where the derivative is taken. Local sensitivities are used widely and are the basis of many applications, such as the solution of inverse problems. These local sensitivity indexes, used in "one parameter at a time" (OAT) methods, quantify the effect of a single parameter, X_i, by assuming all others are fixed (Saltelli and others, 2005). Sometimes a crude variational approach is selected whereby, instead of a derivative, incremental ratios are taken by moving factors one at a time from the baseline by a fixed amount (for example, 5 percent) without prior knowledge of the factor uncertainty range.

Local sensitivity indexes are only valid and useful if all factors in a model are linear, or if some type of average can be used over the parametric space. In the current model, because some of the proposed model equations (or equation combinations) are nonlinear, an alternative "global" sensitivity approach is more appropriate. Exploring the entire parametric space of the model may help determine (1) which of the uncertain input parameters largely determine the uncertainty of a specific output, or (2) which input parameter, if fixed, would reduce output uncertainty by the greatest amount (Saltelli and others, 2005).

Different types of global sensitivity methods can be selected based on the objective of the analysis. For computationally expensive models or the simultaneous evaluation of many parameters, it is usually most efficient to apply a screening method. This type of method provides a qualitative parameter ranking in terms of relative effect over output variation and allows the user to focus the calibration or development effort on the most sensitive parameters. If quantitative information is desired, an analysis of variance technique usually is required. Each of these methods is applied to the new wetland phosphorus model presented herein, and the results are compared.

Morris Method

The screening method proposed by Morris (1991), herein referred to as "Morris method" or "Morris," and later modified by Campolongo and others (2005) was used in this study because it is relatively easy to apply, requires very few simulations, and its results are easily interpreted (Saltelli and others, 2005). Morris (1991) proposed conducting individually randomized experiments that evaluate the elementary effects (relative output differences) of changing one parameter at a time. Each input may assume a discrete number of values, called levels, that are selected within an allocated range of variation for the parameter. For each parameter, two sensitivity measures are proposed: (1) the mean of the elementary effects (μ), which estimates the overall effect of the parameter on a given output; and (2) the standard deviation of the effects (σ), which estimates the higher order characteristics of the parameter, such as curvatures and interactions. Because the model output can be nonmonotonic, Campolongo and others (2005) suggested considering the distribution of absolute values of the elementary effects (μ^*) to avoid the canceling of effects of opposing signs. The number of simulations required (N) to perform the Morris analysis is expressed as:

$$N = r\,(k + 1) \tag{42}$$

where r is the sampling size for search trajectory ($r = 10$ produces satisfactory results), and k is the number of factors. Although elementary effects are local measures, the method is considered global because the final measure, μ^*, is obtained by averaging the elementary effects, and this eliminates the need to consider the specific points at which they are computed (Saltelli and others, 2005). Morris (1991) recommended applying μ (or μ^* thereof) to rank parameters in order of importance, and Saltelli and others (2004) suggested applying the original Morris measure, σ, when examining the effects induced by interactions. To interpret the results in a manner that simultaneously provides insight about the parameter ranking and potential presence of interactions, Morris (1991) suggested plotting the points on a $\mu(\mu^*)$-σ Cartesian plane. Because the Morris method is qualitative in nature, it should only be used to assess the relative parameter ranking.

Extended Fourier Amplitude Sensitivity Test (FAST)

A variance-based method such as FAST can be used to obtain a quantitative measure of sensitivity (Cukier and others, 1973, 1978; Koda and others, 1979). This technique decomposes the total variance ($V = \sigma^2_Y$) of the model output $Y = f(X_1, X_2, ..., X_k)$ in terms of the individual factors X_i, using spectral analysis so that:

$$V = \sigma^2_Y = V_1 + V_2 + V_3 + ... + V_k + R\,, \tag{43}$$

where V_i is the part of the variance that can be attributed to the input factor X_i alone, k is the number of uncertain factors, and R is a residual corresponding to higher order terms. The first-order sensitivity index, S_i, which is defined as a fraction of the total output variance attributed to a single factor, can then be taken as a measure of global sensitivity of Y with respect to X_i; that is:

$$S_i = V_i / V\,. \tag{44}$$

To calculate S_i, the FAST technique randomly samples the k-dimensional space of the input parameters using the replicated Latin hypercube sampling (r-LHS) design (McKay and others, 1979; McKay, 1995). The number of evaluations required in the analysis can be expressed as:

$$N = M\,(k + 2)\,, \tag{45}$$

where M is a number between 500 and 1,000. For a perfectly additive model, $\Sigma S_i = 1$; that is, no interactions are present and total output variance is explained as a summation of the individual variances introduced by varying each parameter alone. In general, models are not perfectly additive, and $\Sigma S_i < 1$.

The FAST analysis was extended to incorporate the calculation of the total order effects through the total sensitivity index, S_{Ti}, calculated as the sum of the first and all higher order indices for a given parameter X_i (Saltelli, 1999; Saltelli and others, 2000). For example, for X_1:

$$S_{T1} = S_1 + S_{1i} + S_{1jk}, + ... + S_{1\,...\,n} \quad \text{and} \quad S_{T1} - S_1 = S_{1i} + S_{1jk}, + ... + S_{1\,...\,n}\,. \tag{46}$$

For a given parameter X_i, interactions can be isolated by calculating S_{Ti} - S_i, which makes the extended FAST technique a powerful method for quantifying the individual effect of each parameter alone (S_i) or through interaction with others (S_{Ti} - S_i). An additional benefit of the extended FAST analysis is that because the results are derived from a randomized sampling procedure, they can be used as the basis for the uncertainty evaluation by constructing cumulative distribution functions (CDFs) for each of the selected outputs. This could lead to an efficient Monte Carlo type of uncertainty analysis, if only the sensitive parameters identified by the Morris screening method are considered as the source of uncertainty (Muñoz-Carpena and others, 2007).

Effects of Changing Model Structure and Flow Velocity on Global Model Output Sensitivity

A.I. James (University of Florida, written commun., 2008) present the implementation of the phosphorus conceptual water-quality model, TarSE, in the Hydrologic Simulation Engine (HSE) of the SFWMD Regional Simulation Model (RSM). Documentation of the SFWMD/RSM is available on the RSM web site at *https://my.sfwmd.gov/portal/page?_pageid=1314,2555966,1314_2554338&_dad=portal&_schema=PORTAL&navpage=rsm*. The RSM/HSE runs on Linux platforms, as does TaRSE, which is compiled into a static library that can be linked to the RSM. The resulting combined model is referred to as Regional Simulation Model/Water-Quality model (RSM/WQ). Input data are provided to the RSM/WQ through flexible extensible markup language (XML) input files that define the control parameters, hydrologic boundary conditions, sources, initial conditions, and so forth. The RSM/WQ is used in the global sensitivity analysis of the proposed phosphorus conceptual model. Descriptions of the specific water-quality input files used in this evaluation are provided in appendix 3.

Analysis Procedure

A software package, SimLab v2.2 (Saltelli and others, 2004), was used in the global sensitivity analysis. SimLab is designed for uncertainty and sensitivity analyses using pseudorandom number generation (PNG). The emphasis of the analysis is to sample a set of points from joint probability distributions of the selected model input factors; that is, the "sample distribution." PNG-based uncertainty and sensitivity analyses involve performing multiple model evaluations with stochastically selected values for model inputs, and using the results of these evaluations to determine: (1) degree of uncertainty in model predictions, and (2) input variables responsible for the uncertainty. The general protocol is as follows:

- *Step 1*—Range and probabilistic distribution functions (PDFs) are selected for each input variable (input factor). If the analysis is preliminary, then "rough" distribution assumptions may be adequate.
- *Step 2*—A sample of points is generated from the distribution of the inputs specified in Step 1, resulting in a sequence of sample elements. The SimLab Statistical Pre-Processor module executes this step based on PDFs provided by the user.
- *Step 3*—Simulations are run with the sample elements, yielding a set of model outputs. The model evaluations map the input space to the result space, which provides a basis for subsequent uncertainty and sensitivity analyses. A series of UNIX scripts were prepared to run the RSM/WQ model with a new set of sampled input values for each simulation. These scripts automatically substitute the new parameter set into the input XML files, run the model, and perform the necessary postprocessing to obtain the selected model outputs for the analysis. The outputs for each simulation are stored in a matrix containing the same number of lines as the number of samples generated in Step 2.
- *Step 4*—Sensitivity and uncertainty analysis of the model outputs. The Statistical Post Processor module of Simlab is used to calculate sensitivity indexes for the Morris and extended FAST methods.

Flow Domain

A 1,000 × 200-m flow domain was selected and discretized into 160 equal rectangular triangles (cells) as shown in figure 16. Flow was set from left to right so that the inflow boundary consisted of cells 1, 41, 81 and 121, and the outflow boundary consisted of cells 40, 80, 120, 160. A no-flow boundary was used for the top and bottom (longer) sides of the rectangle. A constant velocity across the domain was fixed with an average water depth of 1.0 m. To test the effect of flow velocity on the transformation and transport of phosphorus in wetlands, three fixed longitudinal flow velocities (0.00579, 0.00116, and 0.000579 m/s) were considered for each batch of sensitivity analysis simulations. These velocities correspond to residence times of 2, 10 and 20 days, respectively, representative of operational flows within STA-1W Cell 4 (fig. 1).

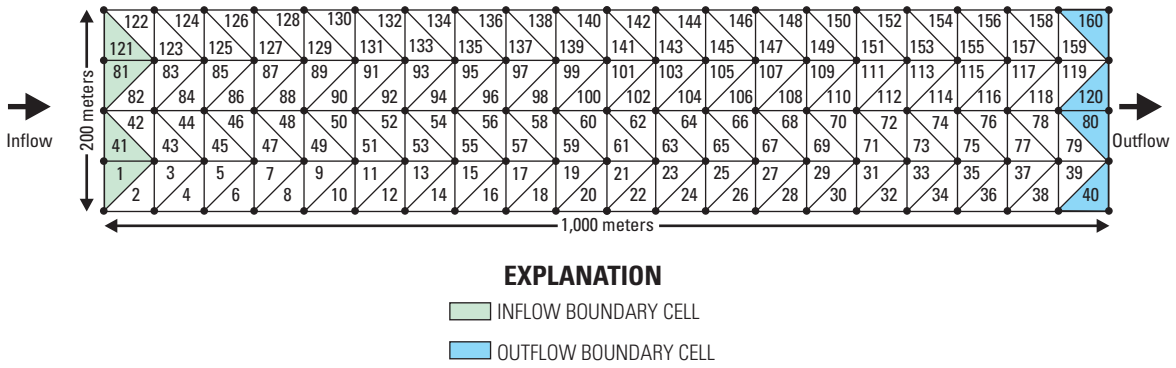

Figure 16. Testing domain for global sensitivity. The total simulation time for all model runs was 30 days and the initial time increment selected was $\Delta t = 3$ hour.

Description of Inputs and Outputs

Three model-complexity levels similar to the ones described earlier for model calibration were used in the global sensitivity analysis. Details of formulation and RSM/WQ model input files used in each case are given in appendix 3. Schematics of the transfer and transformation processes involved in each complexity level are presented in figures 17 to 19.

The field-scale ambient variability of many inputs has been reported to be modeled adequately using normal or log-normal distributions (Jury and others, 1991; Haan and others, 1998). Because of the lack of data needed to estimate mean and standard deviations for PDFs assumed to be Gaussian, the β-distribution was used to assign proper values so that shape factors fit an approximate log-normal distribution. The β-distribution is generally used as a rough model in the absence of sufficient data (Wyss and Jørgensen, 1998). When only the range and a base (effective) value are known, a simple triangular distribution can be used (Kotz and van Dorp, 2004). To characterize sensitivity and uncertainty, each input parameter was assigned a PDF based on the range of values obtained from a comprehensive literature review summarized in appendix 2. The range for each parameter was selected to cover all physically realistic values, and all parameters were assigned β-distributions except for λ_l and λ_t. These two parameters are related to the composition of the physical system (that is, vegetation density, domain dimensions, velocity, and so forth), rather than natural variation, so that the probability of the different values within their range can be considered constant. This corresponds to the uniform distribution (U-distribution) that was selected for them. Table 4 summarizes the sensitivity parameters selected for all complexity levels studied, and table 5 shows the values of the rest of the fixed model parameters used in the simulations.

Several outputs were selected in the analysis for each one of the conceptual model "stores" considered for each complexity level. For mobile quantities discussed earlier, averages across the outflow domain were calculated at the end of the simulation as an average over the entire simulation. Because trends in the results were similar, the average at the end of the simulation (subscript "*o,tf*") was chosen for discussion. For stabile quantities, variation at the end of the simulation was estimated as the difference across the entire domain between the mean value at the beginning and end of the simulation. Table 6 summarizes the details of the outputs calculated for the global sensitivity and uncertainty analysis.

Six pseudorandom parameter sample sets were created—one for each complexity level for the Morris and FAST methods. Each sample set was run three times for each velocity. The number of Morris method runs was selected according to the number of parameters in each complexity level based on equation 42. For the FAST method, a sufficiently large number of simulations were selected to allow for both the global sensitivity index calculation and the uncertainty analysis. After some experimentation, the number of runs for each set of simulations was set to 5,000. The number of simulations run for each level (table 7) illustrates one of the potential advantages of the Morris method over the FAST method. For an average simulation time of 15 seconds per run, the total required time to evaluate the model increased from about 15 hours for the Morris method to 16 days with the FAST method.

Morris Method Results

Results of the global sensitivity analysis obtained from the screening Morris method are presented for each of the selected model outputs identified in table 6. The rankings of importance of parameters for each respective output, based on the relative value of Morris μ^*, are presented in tables 8 to 13. As suggested by Morris, only parameters separated from the origin of the μ^*-σ plane were considered important. Figures 20 to 25 graphically present the Morris method results for the selected outputs. As previously noted, the choice of parameters deemed to be important for sensitivity when using the Morris method is subjective. The decision is based on using this graphical presentation, and the user must decide whether a parameter is sufficiently far from the origin to warrant ranking. Choosing parameters becomes increasingly difficult when the parameters are more widely distributed throughout the μ^*-σ plane, as was the case for many level-3 results (for example, fig. 22G-I). Consequently, without quantified measures to more accurately compare the contribution of each parameter, it becomes challenging to identify their true importance in these complex cases, and the advantages of an alternate approach such as the extended FAST method become apparent. Though the number of key parameters identified is an important outcome (sensitivity to parameters), so too are any noticeable changes in the ranking of these parameters across either velocities (sensitivity to environmental structure) or levels of complexity (sensitivity to model structure), noting the limitations described above.

These initial screening results illustrate four products of the global sensitivity analysis: (1) an indication of the importance of some common parameters for all outputs; (2) an indication of how changing the modeling structure affects the sensitivity of the model outputs to parameters, environment conditions, and the model structure itself; (3) a verification of model behavior and absence of errors; and (4) an indication of how important parameters influence the model outputs, either directly or through their interaction with other parameters. Results are discussed in terms of four broad considerations that include screening of parameters, ranking of parameters, effect of flow velocity on sensitivity, and effect of complexity on sensitivity.

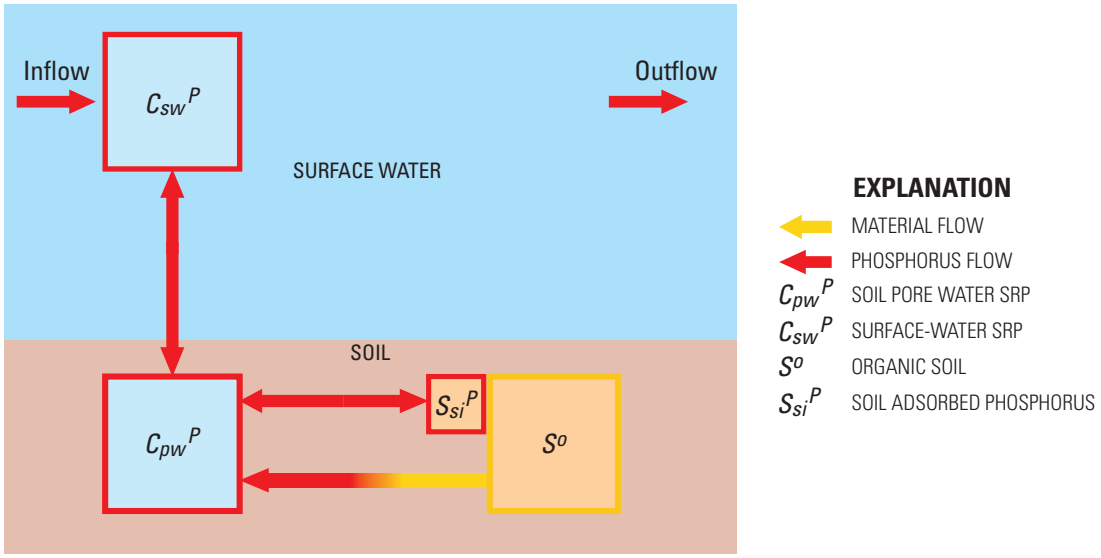

Figure 17. Conceptual model for complexity level 1. SRP is soluble reactive phosphorus. Notation definitions are presented in table 6.

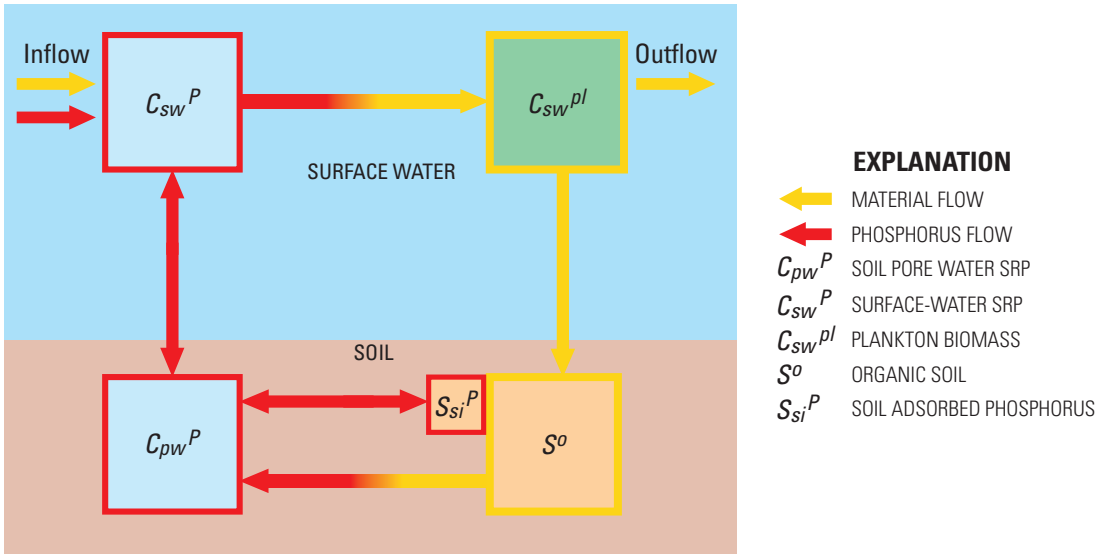

Figure 18. Conceptual model for complexity level 2. SRP is soluble reactive phosphorus. Notation definitions are presented in table 6.

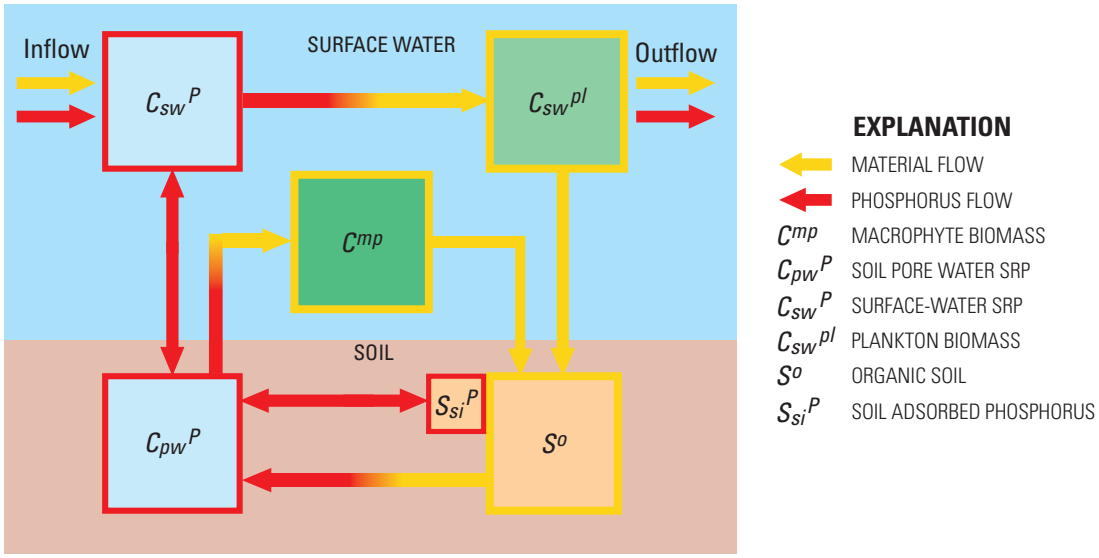

Figure 19. Conceptual model for complexity level 3. SRP is soluble reactive phosphorus. Notation definitions are presented in table 6.

Table 4. Parameters used in the global sensitivity and uncertainty analyses, including probability distribution functions and parameter use in levels 1 to 3.

[Ranges and distributions are based on the literature review presented in appendix 2. Complete parameter descriptions are provided in the model calibration and validation section and appendix 1 of this report. Unit abbreviations are defined on the Conversion Factors page]

Parameter	Coded notation[1]	Parameter description	Distribution	Units	Parameter present in		
					Level 1	Level 2	Level 3
ρ_b	bulk density	Bulk density	β (0.05, 0.5)	Unitless	x	x	x
X_{mp}^{P}	chi_mp	Mass fraction of phosphorus in macrophytes	β (0.0002, 0.005)	Unitless			x
X_{so}^{P}	chi_org_soil	Mass fraction of phosphorus in organic soil	β (0.0006, 0.0025)	Unitless	x	x	x
X_{pl}^{P}	chi_pl	Mass fraction of phosphorus in plankton	β (0.0008, 0.015)	Unitless		x	x
k_d	k_d	Coefficient of adsorption	β (8×10^{-6}, 11×10^{-6})	m^3/g	x	x	x
k_{df}	k_df	Coefficient of diffusion	β (7×10^{-10}, 4×10^{-9})	m^2/s	x	x	x
$k_{1/2}^{mp}$	k_halfsat_mp	Half saturation constant for macrophyte growth	β (0.001, 0.01)	g/m^3			x
$k_{1/2}^{pl}$	k_halfsat_pl	Half saturation constant for plankton growth	β (0.005, 0.08)	g/m^3		x	x
k_g^{mp}	k_mp_growth	Macrophyte growth rate	β (0.004, 0.17)	1/d			x
k_{sn}^{mp}	k_mp_senesc	Macrophyte senescence rate	β (0.001, 0.05)	1/d			x
k_{ox}	k_ox	Soil oxidation rate	β (0.0001, 0.0015)	1/d	x	x	x
k_g^{pl}	k_pl_growth	Plankton growth rate	β (0.2, 2.5)	1/d		x	x
k_{st}^{pl}	k_pl_settle	Plankton settling rate	β (2.3×10^{-7}, 5.8×10^{-6})	m/s		x	x
λ_l	long_disp	Longitudinal dispersivity	U (70, 270)	m	x	x	x
θ	soil_porosity	Soil porosity	β (0.7, 0.98)	Unitless	x	x	x
λ_t	tran_disp	Transverse dispersivity	U (70, 270)	m	x	x	x

[1]Code implementation is provided in appendix 2.

Table 5. Fixed model inputs used in the global sensitivity and uncertainty analyses.

[Notations are defined in appendix 1. Units: g/m^2, gram per square meter; g/m^3, gram per cubic meter; m, meter]

Type	Description (units)	Value	Level 1	Level 2	Level 3
Initial and boundary conditions	C^{mp} (g/m^2)	500			x
	$C_{sw}{}^{pl}$ (g/m^3)	.043		x	x
	$C_{pw}{}^{P}$ (g/m^2)	.071	x	x	x
	$C_{sw}{}^{P}$ (g/m^3)	.05	x	x	x
	S^o (g/m^2)	30,000	x	x	x
	$S_{si}{}^{P}$ (g/m^2)	.027	x	x	x
Parameters	k_1 (day)	1	x	x	x
	Surface porosity (unitless)	1	x	x	x
	z_{as} (m)	.1	x	x	x
	z_{df} (m)	.04	x	x	x

Table 6. Model outputs used in the global sensitivity and uncertainty analyses.

[Notations are defined in appendix 1. SRP, soluble reactive phosphorus]

Class	Type	Output	Description
Mobile	Surface-water SRP ($C_{sw}{}^{P}$) outflow	$C_{sw}{}^{P}]_{o,tf}$	Average of $C_{sw}{}^{P}$ for outlet cells (boundary cells 40, 80, 120, and 160 in fig. 16) at the final time step
		$C_{sw}{}^{P}]_{o,t}$	Average of $C_{sw}{}^{P}$ for outlet across all simulation time steps
	Plankton biomass ($C_{sw}{}^{pl}$) outflow	$C_{sw}{}^{pl}]_{o,tf}$	Average of $C_{sw}{}^{pl}$ for outlet cells at the final time step
		$C_{sw}{}^{pl}]_{o,t}$	Average of $C_{sw}{}^{pl}$ for outlet cells across all simulation time steps
Stabile	Soil pore-water SRP ($C_{pw}{}^{P}$) variation	$C_{pw}{}^{P}]_{acr}$	Difference in averages of $C_{pw}{}^{P}$ across the domain (all cells) between initial and end time step
	Organic soil (S^o) accretion	$S^o]_{acr}$	Difference in averages of S^o across the domain (all cells) between initial and end time step
	Soil adsorbed P ($S_{si}{}^{P}$) variation	$S_{si}{}^{P}]_{acr}$	Difference in averages of $S_{si}{}^{P}$ across the domain (all cells) between initial and end time step
	Macrophyte biomass (C^{mp}) accumulation	$C^{mp}]_{acr}$	Difference in averages of C^{mp} across the domain (all cells) between initial and end time step

Table 7. Regional Simulation Model/Water Quality Model (RSM/WQ) simulations run in the global sensitivity and uncertainty analyses.

[FAST, Fourier amplitude sensitivity test; RSM/WQ, Regional Simulation Model/Water Quality Model]

Level	Number of velocities	Number of parameters	Number of simulations		
			Morris	FAST	Total
1	3	8	90 × 3	5,000 × 3	15,270
2	3	12	130 × 3	5,004 × 3	15,402
3	3	16	170 × 3	5,008 × 3	15,534
Total simulations			1,170	45,046	46,206

Table 8. Morris method global sensitivity analysis parameter ranking for the surface-water soluble reactive phosphorus (SRP) outflow outputs ($C_{sw}^{P}]_{o,tf}$ and $C_{sw}^{P}]_{o,t}$).

[Parameter descriptions are provided in table 4. Numbers for each parameter represent the parameter ranking in decreasing order of importance for each output (1 = most important for that level, "--" no significant influence). Missing values or symbols indicate that they are not part of the simulation]

Complexity	Velocity (meters per day)	Output	Parameter															
			k_{df}	k_{ox}	X_{so}^{P}	k_d	θ	ρ_b	λ_l	λ_t	k_g^{pl}	$k_{1/2}^{pl}$	k_{st}^{pl}	X_{pl}^{P}	k_g^{mp}	$k_{1/2}^{mp}$	k_{sn}^{mp}	X_{mp}^{P}
Level 1	50	$C_{sw}^{P}]_{o,tf}$	2	1	4	--	--	3	--	--								
	100	$C_{sw}^{P}]_{o,tf}$	2	1	4	--	--	3	--	--								
	500	$C_{sw}^{P}]_{o,tf}$	2	1	4	--	--	3	--	--								
	50	$C_{sw}^{P}]_{o,t}$	2	1	4	--	--	3	--	--								
	100	$C_{sw}^{P}]_{o,t}$	2	1	4	--	--	3	--	--								
	500	$C_{sw}^{P}]_{o,t}$	2	1	4	--	--	3	--	--								
Level 2	50	$C_{sw}^{P}]_{o,tf}$	5	3	4	--	--	6	--	--	1	2	--	--				
	100	$C_{sw}^{P}]_{o,tf}$	5	3	4	--	--	6	7	--	1	2	--	--				
	500	$C_{sw}^{P}]_{o,tf}$	7	4	5	--	--	6	3	--	1	2	--	8				
	50	$C_{sw}^{P}]_{o,t}$	4	3	6	--	--	5	--	--	1	2	--	--				
	100	$C_{sw}^{P}]_{o,t}$	4	3	5	--	--	6	--	--	1	2	--	7				
	500	$C_{sw}^{P}]_{o,t}$	7	4	5	--	--	6	3	--	1	2	--	8				
Level 3	50	$C_{sw}^{P}]_{o,tf}$	--	7	6	1	11	9	10	--	13	5	12	--	3	2	4	8
	100	$C_{sw}^{P}]_{o,tf}$	11	--	8	--	10	--	9	6	5	12	1	4	7	--	2	3
	500	$C_{sw}^{P}]_{o,tf}$	10	4	3	--	12	9	8	--	1	2	5	6	7	--	--	11
	50	$C_{sw}^{P}]_{o,t}$	--	8	7	1	12	10	11	--	6	5	13	14	3	2	4	9
	100	$C_{sw}^{P}]_{o,t}$	12	--	9	--	10	--	11	6	4	8	1	5	7	--	2	3
	500	$C_{sw}^{P}]_{o,t}$	10	4	3	--	12	9	8	--	1	2	5	6	7	--	--	11

Table 9. Morris method global sensitivity analysis parameter ranking for the pore-water soluble reactive phosphorus variation output ($C_{pw}^{P}]_{acr}$)

[Parameter descriptions are provided in table 4. Numbers 1-6 for each parameter represents the ranking of parameter in decreasing order of importance for each output (1 = most important for that level, "--" no significant influence). Missing values or symbols indicate that they are not part of the simulation]

Complexity	Velocity (meters per day)	Output	Parameter															
			k_{df}	k_{ox}	X_{so}^{P}	k_d	θ	ρ_b	λ_l	λ_t	k_g^{pl}	$k_{1/2}^{pl}$	k_{st}^{pl}	X_{pl}^{P}	k_g^{mp}	$k_{1/2}^{mp}$	k_{sn-mp}	X_{mp}^{P}
Level 1	50	$C_{pw}^{P}]_{acr}$	4	1	2	6	5	3	--	--								
	100	$C_{pw}^{P}]_{acr}$	4	1	2	6	5	3	--	--								
	500	$C_{pw}^{P}]_{acr}$	4	1	2	6	5	3	--	--								
Level 2	50	$C_{pw}^{P}]_{acr}$	4	1	2	6	5	3	--	--	--	--	--	--				
	100	$C_{pw}^{P}]_{acr}$	4	1	2	6	5	3	--	--	--	--	--	--				
	500	$C_{pw}^{P}]_{acr}$	4	1	2	6	5	3	--	--	--	--	--	--				
Level 3	50	$C_{pw}^{P}]_{acr}$	5	--	3	--	4	--	2	--	--	--	--	--	1	--	--	--
	100	$C_{pw}^{P}]_{acr}$	1	--	4	--	--	--	3	--	--	--	--	--	2	--	--	--
	500	$C_{pw}^{P}]_{acr}$	3	--	2	--	4	--	--	--	--	--	--	--	1	--	--	--

Table 10. Morris method global sensitivity analysis parameter ranking for the organic soil accretion output *($S^0]_{acr}$).*

[Parameter descriptions are provided in table 4. Numbers 1-6 for each parameter represents the ranking of parameter in decreasing order of importance for each output (1 = most important for that level, "--" no significant influence). Missing values or symbols indicate that they are not part of the simulation]

Complexity	Velocity (meters per day)	Output	Parameter															
			k_{df}	k_{ox}	$X_{so}{}^P$	k_d	θ	ρ_b	λ_l	λ_t	$k_g{}^{pl}$	$k_{1/2}{}^{pl}$	$k_{st}{}^{pl}$	$X_{pl}{}^P$	$k_g{}^{mp}$	$k_{1/2}{}^{mp}$	$k_{sn\text{-}mp}$	$X_{mp}{}^P$
Level 1	50	$S^o]_{acr}$	--	1	--	--	--	--	--	--								
	100	$S^o]_{acr}$	--	1	--	--	--	--	--	--								
	500	$S^o]_{acr}$	--	1	--	--	--	--	--	--								
Level 2	50	$S^o]_{acr}$	--	1	--	--	--	--	--	--	--	--	--	--				
	100	$S^o]_{acr}$	--	1	--	--	--	--	--	--	--	--	--	--				
	500	$S^o]_{acr}$	--	1	--	--	--	--	--	--	--	--	--	--				
Level 3	50	$S^o]_{acr}$	--	1	4	3	10	8	9	--	--	11	--	--	5	7	2	6
	100	$S^o]_{acr}$	13	1	6	9	12	10	14	7	11	--	2	8	4	--	3	5
	500	$S^o]_{acr}$	10	1	2	--	7	5	8	--	--	--	9	--	4	--	3	6

Table 11. Morris method global sensitivity analysis parameter ranking for the soil adsorbed phosphorus variation output *($S_{si}{}^P]_{acr}$)*

[Parameter descriptions are provided in table 4. Numbers 1-6 for each parameter represents the ranking of parameter in decreasing order of importance for each output (1 = most important for that level, "--" no significant influence). Missing values or symbols indicate that they are not part of the simulation]

Complexity	Velocity (meters per day)	Output	Parameter															
			k_{df}	k_{ox}	$X_{so}{}^P$	k_d	θ	ρ_b	λ_l	λ_t	$k_g{}^{pl}$	$k_{1/2}{}^{pl}$	$k_{st}{}^{pl}$	$X_{pl}{}^P$	$k_g{}^{mp}$	$k_{1/2}{}^{mp}$	$k_{sn\text{-}mp}$	$X_{mp}{}^P$
Level 1	50	$S_{si}{}^P]_{acr}$	4	1	2	--	--	3	--	--								
	100	$S_{si}{}^P]_{acr}$	4	1	2	--	--	3	--	--								
	500	$S_{si}{}^P]_{acr}$	4	1	2	--	--	3	--	--								
Level 2	50	$S_{si}{}^P]_{acr}$	4	1	2	--	--	3	--	--	--	--	--	--				
	100	$S_{si}{}^P]_{acr}$	4	1	2	--	--	3	--	--	--	--	--	--				
	500	$S_{si}{}^P]_{acr}$	4	1	2	--	--	3	--	--	--	--	--	--				
Level 3	50	$S_{si}{}^P]_{acr}$	5	6	2	--	3	--	4	--	--	--	--	--	1	--	--	--
	100	$S_{si}{}^P]_{acr}$	1	--	3	--	--	--	4	--	--	--	--	--	2	--	--	--
	500	$S_{si}{}^P]_{acr}$	3	4	2	--	--	--	--	--	--	--	--	--	1	--	--	--

Table 12. Morris method global sensitivity analysis parameter ranking for the plankton biomass outflow outputs ($(C_{sw}^{pl}]_{o,tf}$ and $C_{sw}^{pl}]_{o,t}$).

[Parameter descriptions are provided in table 4. Numbers 1-6 for each parameter represents the ranking of parameter in decreasing order of importance for each output (1 = most important for that level, "--" no significant influence). Missing values or symbols indicate that they are not part of the simulation]

Complexity	Velocity (meters per day)	Output	Parameter															
			k_{df}	k_{ox}	X_{so}^{P}	k_d	θ	ρ_b	λ_l	λ_t	k_g^{pl}	$k_{1/2}^{pl}$	k_{st}^{pl}	X^{pl}	k_g^{mp}	$k_{1/2}^{mp}$	k_{sn}^{mp}	X_{mp}^{P}
Level 2	50	$C_{sw}^{pl}]_{o,tf}$	4	1	2	6	--	3	--	--	--	--	--	5				
	100	$C_{sw}^{pl}]_{o,tf}$	3	1	2	--	--	4	--	--	--	--	--	5				
	500	$C_{sw}^{pl}]_{o,tf}$	6	3	4	--	--	7	5	--	1	2	--	8				
	50	$C_{sw}^{pl}]_{o,t}$	3	2	4	6	--	1	--	--	--	--	--	5				
	100	$C_{sw}^{pl}]_{o,t}$	4	1	3	6	--	2	7	--	--	--	--	5				
	500	$C_{sw}^{pl}]_{o,t}$	5	4	7	--	--	6	3	--	1	2	--	8				
Level 3	50	$C_{sw}^{pl}]_{o,tf}$	7	11	5	12	2	15	1	16	8	10	3	6	4	9	13	14
	100	$C_{sw}^{pl}]_{o,tf}$	3	15	7	14	12	13	2	10	8	11	1	4	5	--	6	9
	500	$C_{sw}^{pl}]_{o,tf}$	8	4	5	--	12	10	7	--	1	3	2	9	6	--	--	11
	50	$C_{sw}^{pl}]_{o,t}$	9	10	6	8	3	15	2	--	13	12	1	5	4	7	11	14
	100	$C_{sw}^{pl}]_{o,t}$	4	14	9	15	11	12	2	8	10	13	1	3	6	--	5	7
	500	$C_{sw}^{pl}]_{o,t}$	8	4	5	--	12	10	7	--	1	3	2	9	6	--	--	11

Table 13. Morris method global sensitivity analysis parameter ranking for the macrophyte biomass accumulation output ($C^{mp}]_{acr}$)

[Parameter descriptions are provided in table 4. Numbers 1-6 for each parameter represents the ranking of parameter in decreasing order of importance for each output (1 = most important for that level, "--" no significant influence). Missing values or symbols indicate that they are not part of the simulation]

Complexity	Velocity (meters per day)	Output	Parameter															
			k_{df}	k_{ox}	X_{so}^{P}	k_d	θ	ρ_b	λ_l	λ_t	k_g^{pl}	$k_{1/2}^{pl}$	k_{st}^{pl}	X_{pl}^{P}	k_g^{mp}	$k_{1/2}^{mp}$	k_{sn}^{mp}	X_{mp}^{P}
Level 3	50	$C^{mp}]_{acr}$	--	3	4	5	9	8	10	--	--	11	--	--	6	7	2	1
	100	$C^{mp}]_{acr}$	11	4	5	10	--	7	12	9	13	--	3	8	6	--	1	2
	500	$C^{mp}]_{acr}$	9	3	1	--	7	6	8	--	--	--	10	--	5	--	4	2

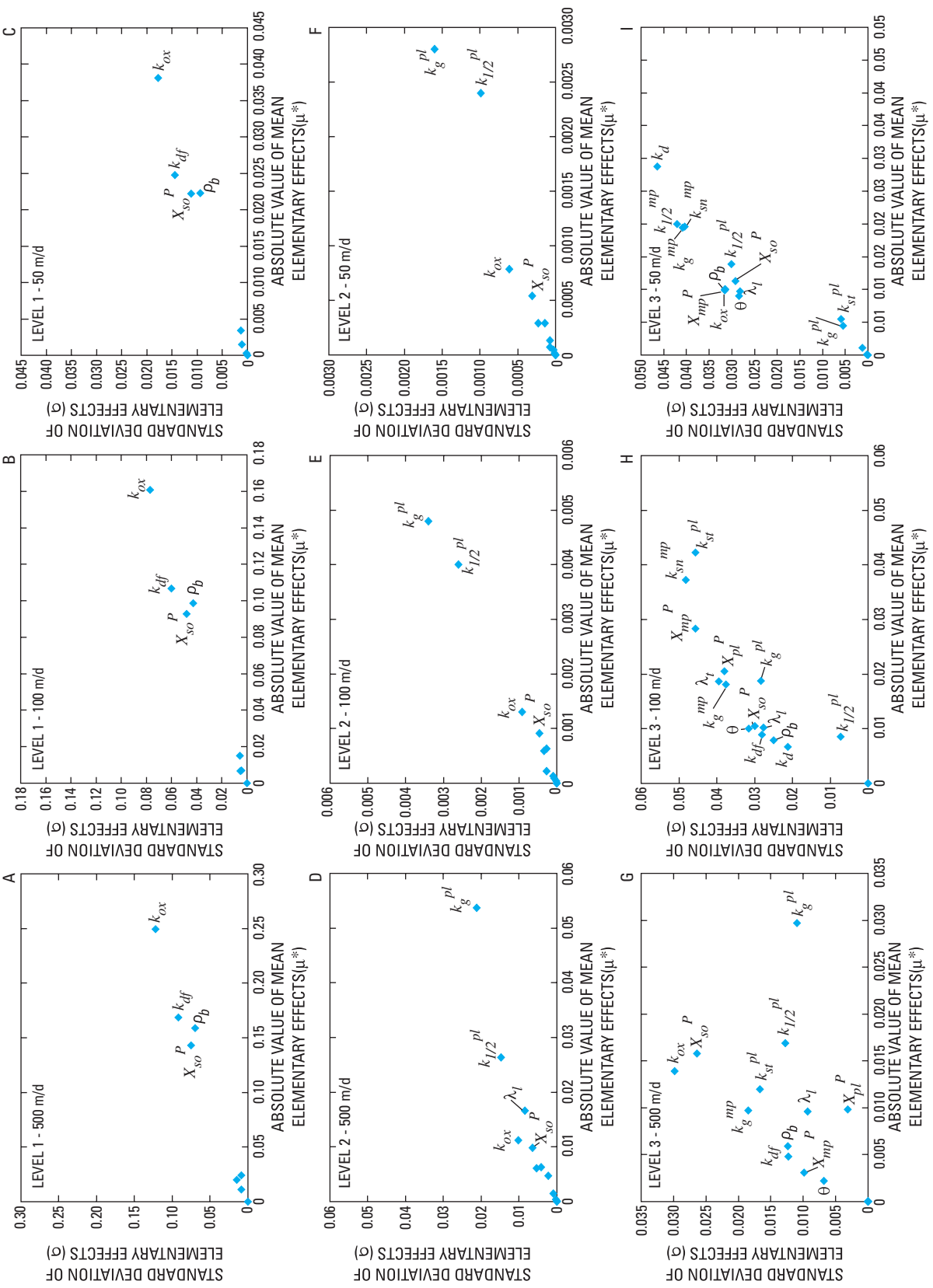

Figure 20. Morris method global sensitivity analysis results for surface-water soluble reactive phosphorus outflow ($C_{sw}{}^{Pl}{}_{Jo,tl}$) across complexity levels and velocities tested. Parameter descriptions are provided in table 4.

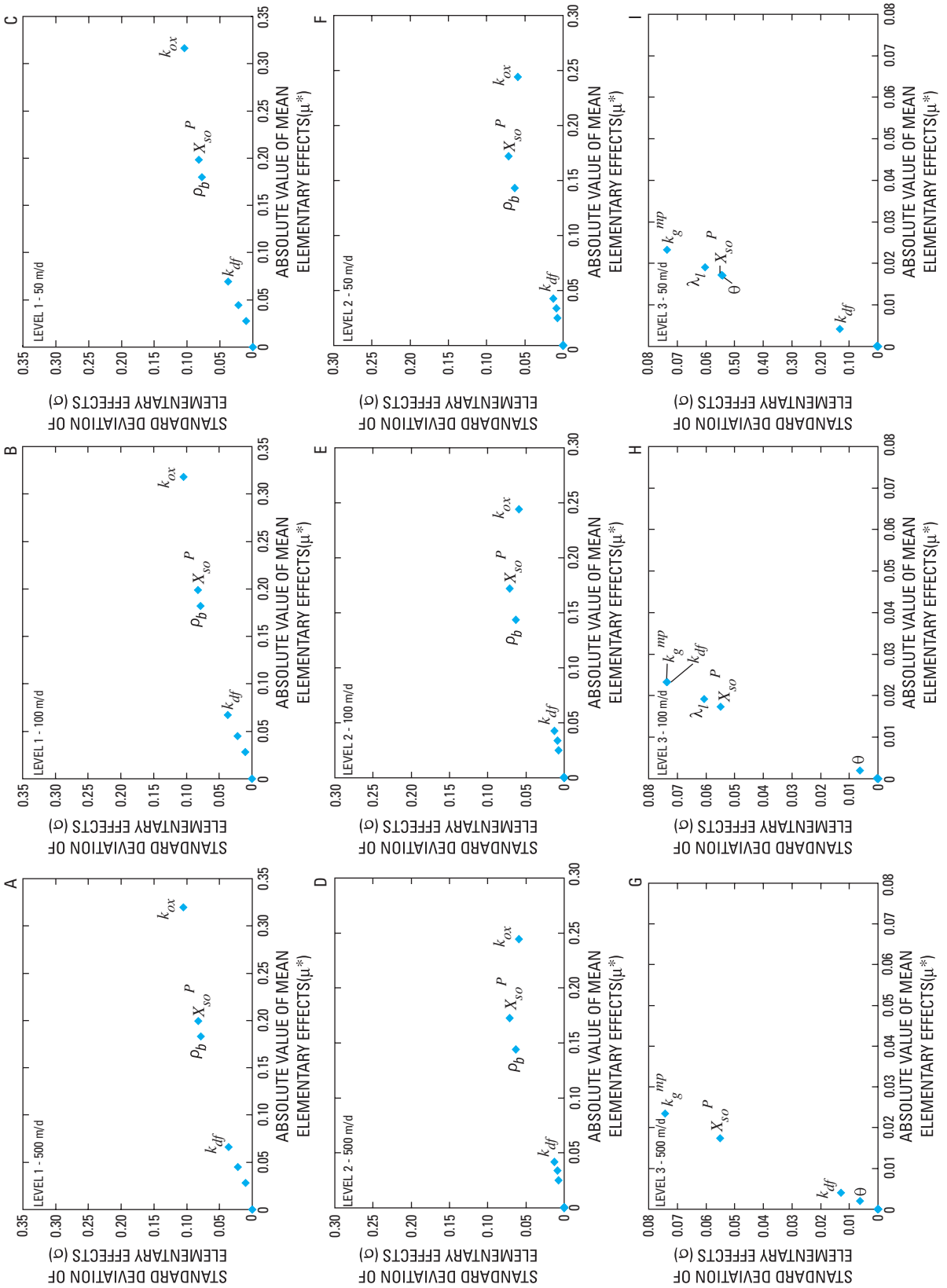

Figure 21. Morris method global sensitivity analysis results for soil pore-water soluble reactive phosphorus variation ($C_{pw}{}^{P}I_{acrl}$) across complexity levels and velocities tested. Parameter descriptions are provided in table 4.

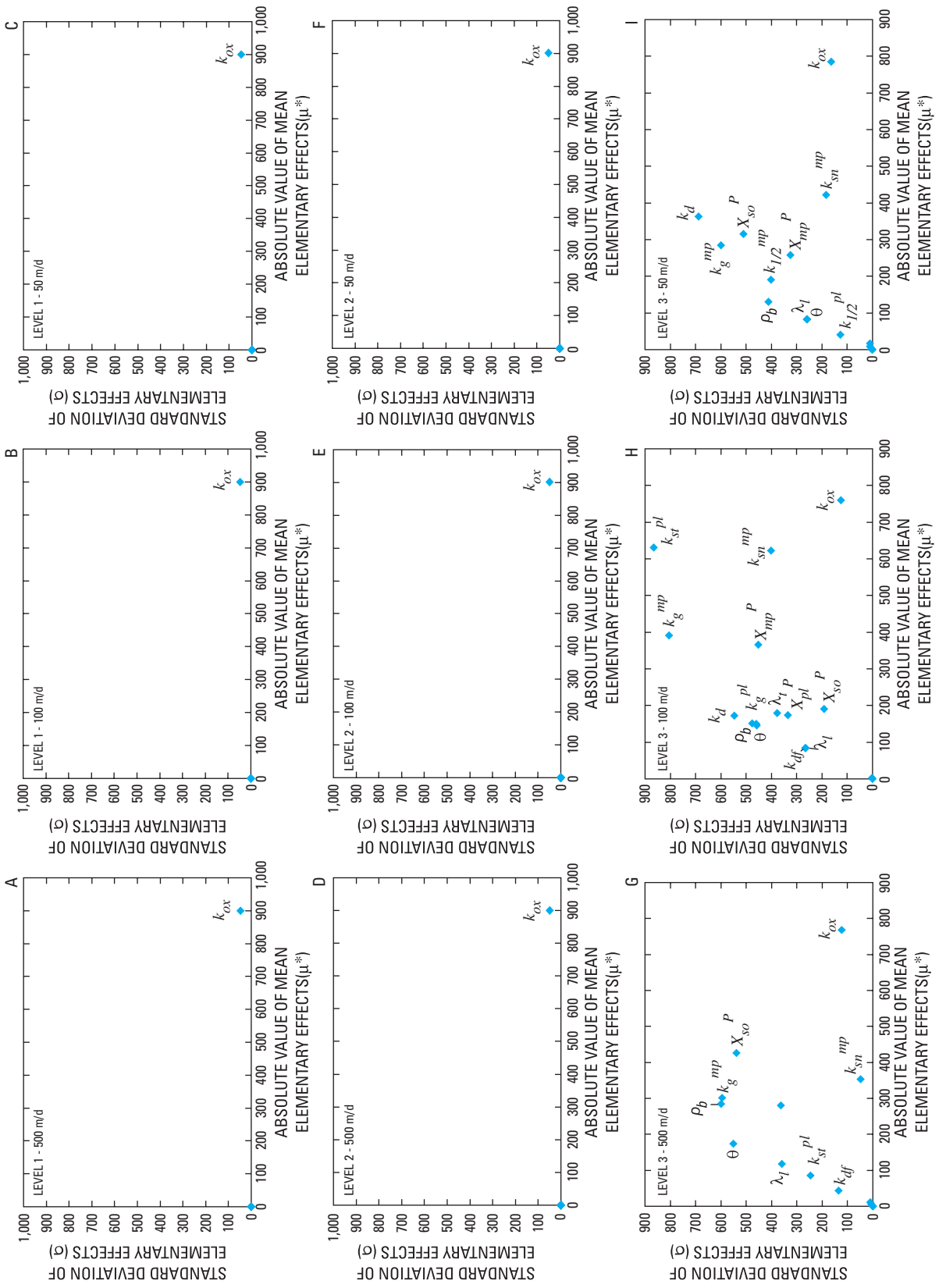

Figure 22. Morris method global sensitivity analysis results for organic soil accretion ($S^o]_{acr}$) across complexity levels and velocities tested. Parameter descriptions are provided in table 4.

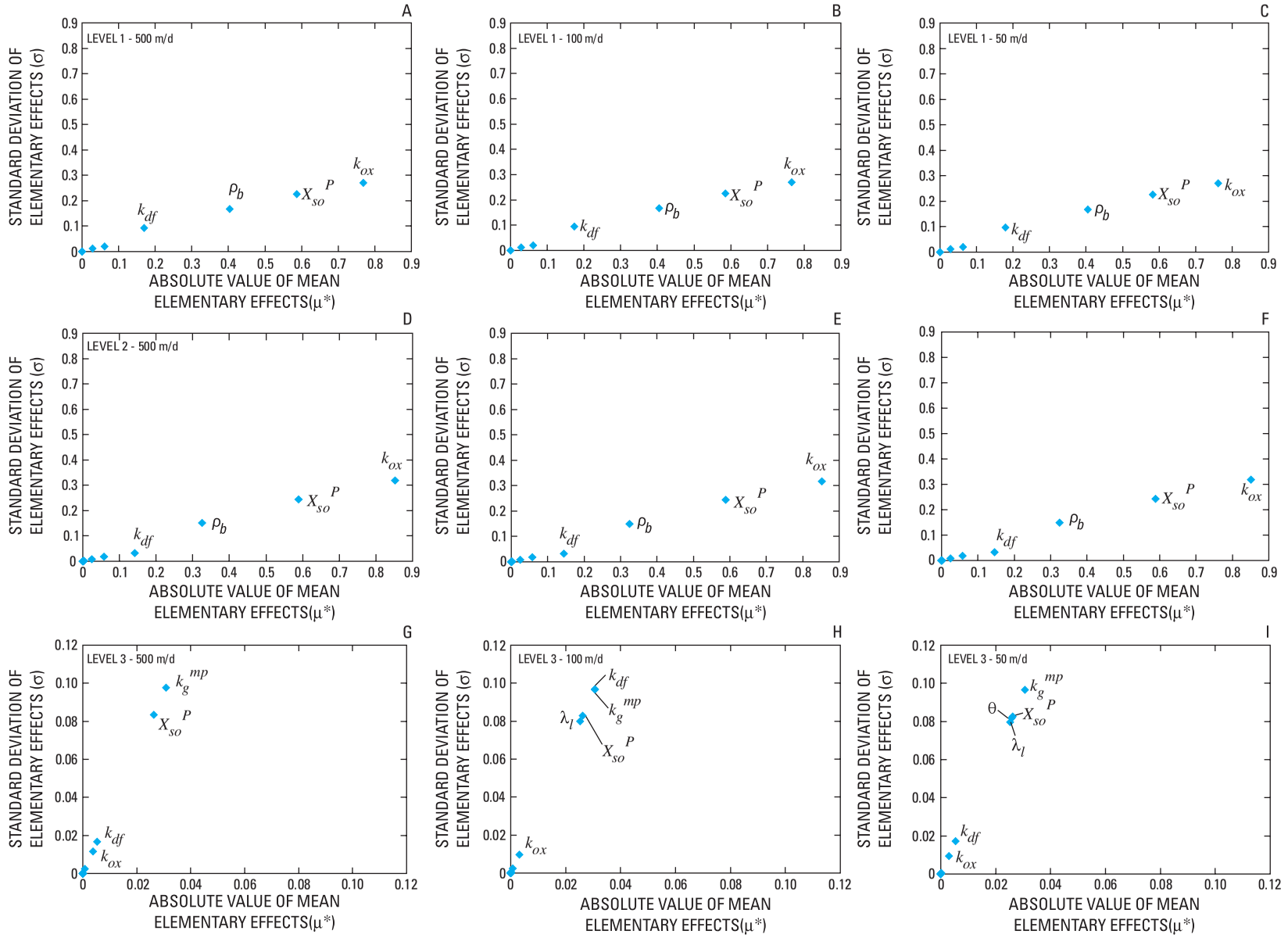

Figure 23. Morris method global sensitivity analysis results for soil adsorbed phosphorus variation ($S_{si}^P]_{acr}$) across complexity levels and velocities tested. Parameter descriptions are provided in table 4.

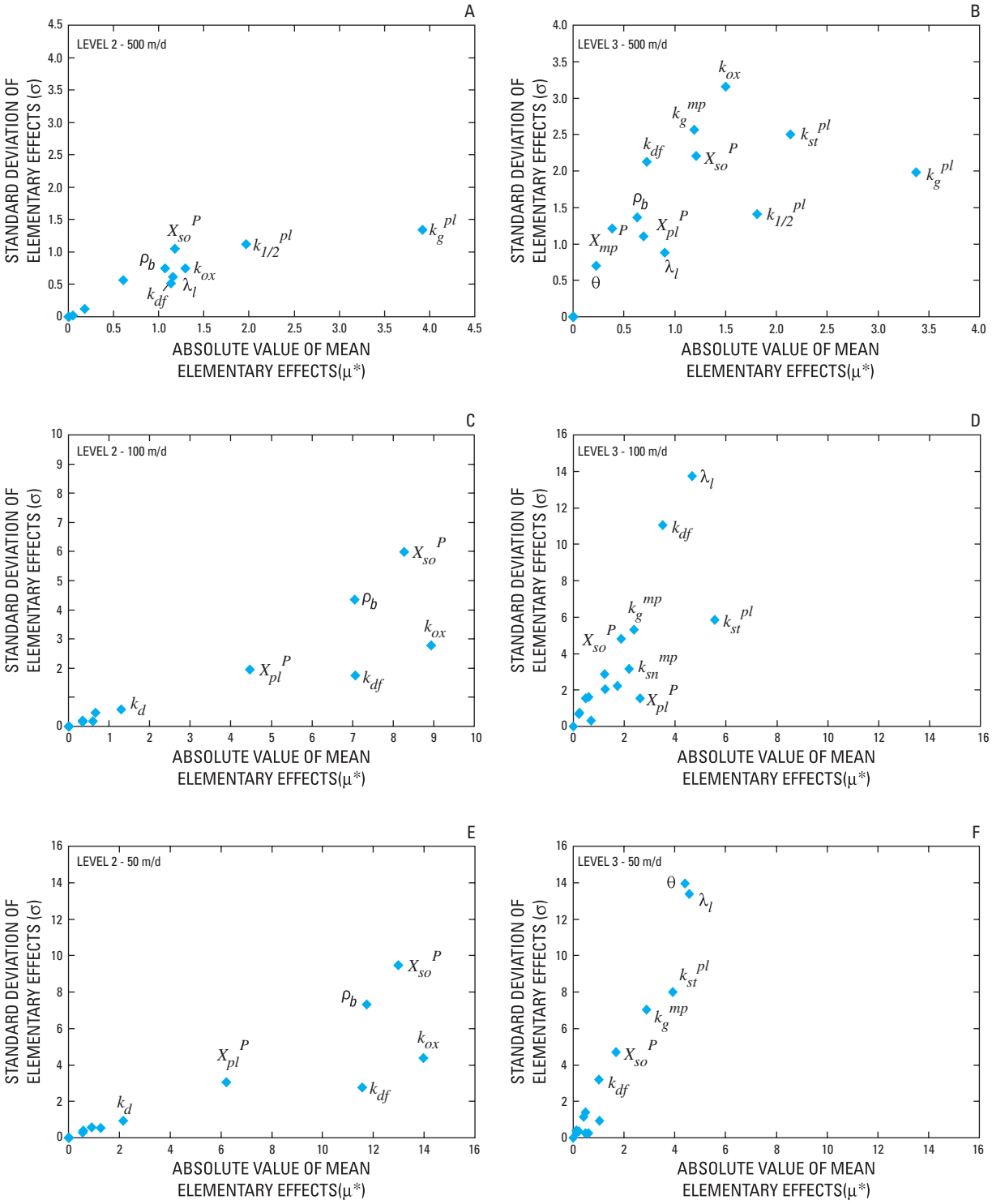

Figure 24. Morris method global sensitivity analysis results for plankton biomass outflow ($C_{sw}{}^{pl}]_{o,tf}$) across complexity levels and velocities tested. Parameter descriptions are provided in table 4.

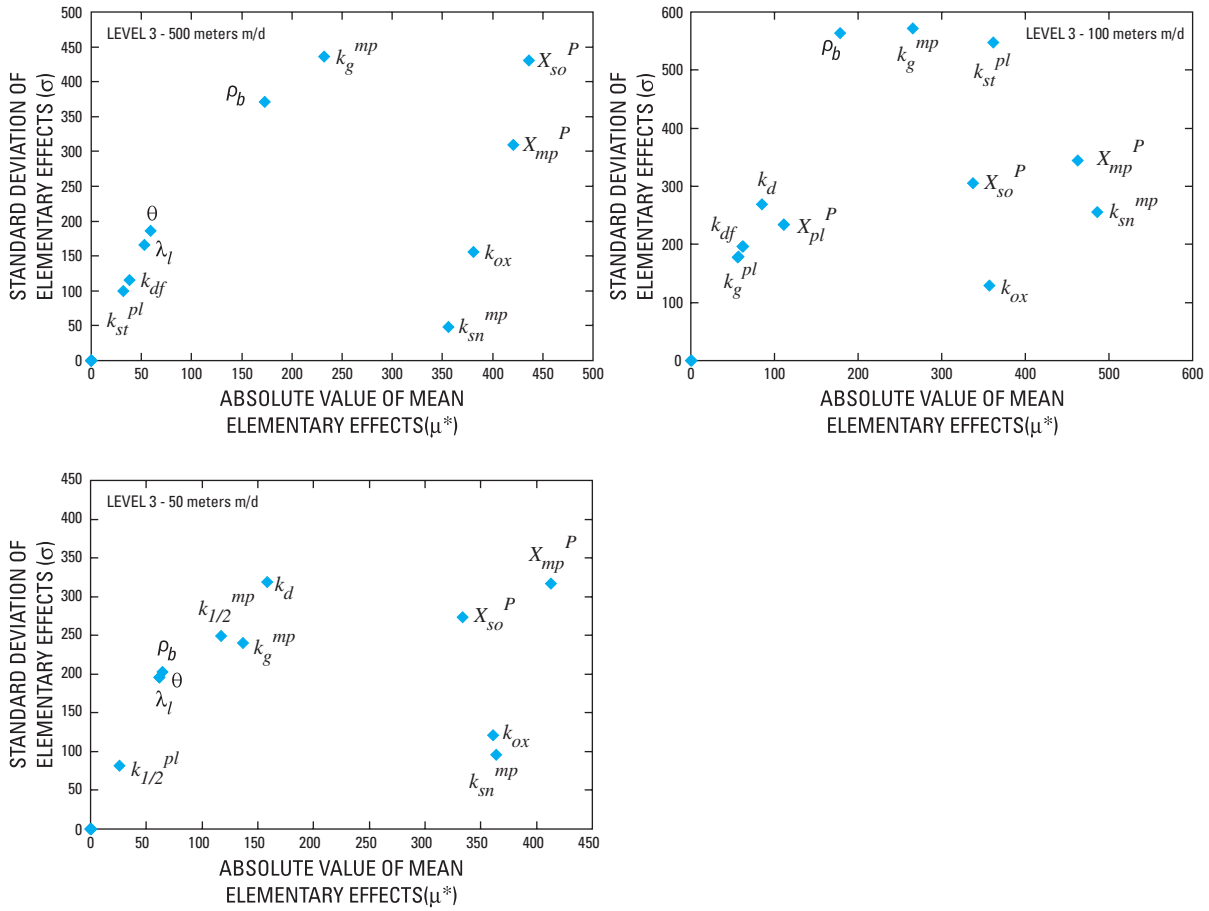

Figure 25. Morris method global sensitivity analysis results for macrophyte biomass accumulation ($C^{mp}]_{acr}$) across complexity levels and velocities tested. Parameter descriptions are provided in table 4.

Screening of Parameters

In almost all instances, the number of important parameters identified using the Morris method was substantially smaller than the full set of model parameters tested, especially for levels 1 and 2, as shown by the maximum recorded rankings for these levels in tables 8 to 13. The following summarizes the number of input parameters identified as being important for each level (range is due to variation across velocities as discussed later):

Level	Initial number of input parameters	Number of input parameters considered important (parameters defined in appendix 1)					
		$C_{sw}^{P}]_{o,tf}$	$C_{pw}^{P}]_{acr}$	$S^{o}]_{acr}$	$S_{si}^{P}]_{acr}$	$C_{sw}^{pl}]_{o,tf}$	$C^{mp}]_{acr}$
1	8	4	6	4	1	--	--
2	12	6-8[1]	6	4	1	6-8	--
3	16	11-14	4-5	10-13	4-6	12-15	10-11

Ranking of Parameters

Comparing parameter rankings in tables 8 to 11 over all outputs, by level, indicates that for level 1, soil oxidation rate, k_{ox}, is consistently ranked most important. Three other parameters, k_{df}, ρ_b and $X_{so}{}^P$, repeatedly appear to be of intermediary importance, sharing ranking positions 2 to 4 depending on the output. These results are in good agreement with current understanding of the physical system, because the principal source of new phosphorus to the level-1 system is from oxidation of the soil, controlled by k_{ox}. Of the parameters ranked 2 to 4, the stabile outputs associated with the soil, $C_{pw}{}^P]_{acr}$ and $S_{si}{}^P]_{acr}$, are sensitive to $X_{so}{}^P$ and ρ_b. These two parameters play a direct role in the amount of SRP contributed to the pore water through oxidation, and in turn to the amount of adsorbed phosphorus. The SRP concentration in the water column is more sensitive to k_{df} than $X_{so}{}^P$ and ρ_b, because this parameter represents the limiting process of diffusion through which the surface water gains new phosphorus originating from the pore water.

These trends across outputs persist in the level-2 results (tables 8-12), with the only notable difference being the previously mentioned prominence of plankton growth parameters in the ranking for mobile outputs $C_{sw}{}^P]_{o,tf}$ and $C_{sw}{}^{pl}]_{o,tf}$. Level-3 results (tables 8-13) do not exhibit any pattern of parameter dominance across the different outputs.

Effect of Flow Velocity

Changes in flow velocity appear to have no effect on the ranking of parameters for all outputs in level 1 (tables 8-11). Negligible velocity effects on ranking are also evident in level 2 for all outputs except $C_{sw}{}^{pl}]_{o,tf}$ (table 12 and fig. 24A, C, E), which shows the plankton growth parameters $k_g{}^{pl}$ and $k_{1/2}{}^{pl}$ to be the most important at 500 m/d (fig. 24A), and the soil phosphorus parameters k_{ox} and $X_{so}{}^P$ to be the most important at slower velocities of 50 and 100 m/d (fig. 24C, E). This unexpected relation is discussed later, together with the additional information provided from the extended FAST and uncertainty results. Outputs in the level-3 case exhibit a much greater sensitivity to velocity than outputs in the level 1 and 2 cases, and parameter rankings changed with velocity for all outputs (tables 8-13). As previously noted, however, the dispersed positioning of so many of the parameters in the μ^*-σ plane means that there may be little quantifiable difference between parameters that are ranked differently, as discussed later.

Effect of Model Complexity

The parameter ranking in tables 8 to 12 is the same between levels 1 and 2 for stabile outputs $C_{pw}{}^P]_{acr}$, $S^o]_{acr}$ and $S_{si}{}^P]_{acr}$, although the mobile output associated with the water column $C_{sw}{}^P]_{o,tf}$ was observed to become most sensitive to the plankton growth parameters, $k_g{}^{pl}$ and $k_{1/2}{}^{pl}$, introduced in level 2. This is to be expected because the additional complexity of level 2 is due to the incorporation of suspended solids in the form of plankton, which should have an influence on surface-water SRP concentration through uptake kinetics. Plankton grows rapidly and extracts SRP from the water column, and accordingly SRP concentration becomes more sensitive to losses from uptake by growing plankton than to parameters associated with the much slower process of diffusion, which were important when plankton was absent in level 1. Except indirectly through longitudinal dispersivity (λ_l) in the transport equation, diffusion is the only process that influences SRP concentration in the water column for level 1. This explains the importance of k_{df} and parameters such as k_{ox}, $X_{so}{}^P$ and ρ_b that directly influence pore-water SRP and, as a consequence, diffusion (fig. 20A-C).

At level 2, a subtle rise in the prominence of λ_l occurs between 100 and 500 m/d for both $C_{sw}{}^P]_{o,tf}$ and $C_{sw}{}^{pl}]_{o,tf}$ (figs. 20D and 24A). This is an informative confirmation of realistic transport dynamics because dispersion is a function of λ_l and velocity, and would directly increase the amount of SRP or plankton biomass transported to the output cells under higher velocity conditions. An increase from 50 to 100 m/d was seemingly insufficient to register a similar increase in rank.

Rankings changed markedly for nearly all outputs with the introduction of level-3 parameters associated with macrophytes. The more complicated system dynamics caused an extensive reordering of parameter rankings, although as previously mentioned, there was probably little quantifiable difference between similar positions. Many more parameters are also spread out across the μ^*-σ plane to form "clouds" that make it difficult to clearly identify truly sensitive parameters. Only $S^o]_{acr}$ maintains a similar trend in level 3 to that observed for previous levels, with k_{ox} remaining linearly dominant (fig. 22). Mobile components in the water column ($C_{sw}{}^P]_{o,tf}$ and $C_{sw}{}^{pl}]_{o,tf}$) remain sensitive to plankton growth parameters $k_{1/2}{}^{pl}$ and $k_g{}^{pl}$, as they were in level 2, but are comparably sensitive to macrophyte parameters $k_{1/2}{}^{mp}$, $k_g{}^{mp}$, and $k_{sn}{}^{mp}$ (figs. 20G-I, and 24B, D, F). As in levels 1 and 2, the remaining stabile components (figs. 21G-I, 22G-I, 23G-I and 25A-C) appear sensitive to a variety of soil parameters, such as $X_{so}{}^P$, k_{ox}, and ρ_b, but here too the macrophyte parameters become comparably important.

Compared with the level-1 and level-2 Morris results, the level-3 plots show a general parameter shift away from the μ^*-axis and toward the σ-axis, indicating an increase in the contribution of higher order effects. Results from the simpler systems for levels 1 and 2 were more closely associated with the μ^*-axis than level-3 results, with proportionately more first-order influence on sensitivity. The initial increase in complexity to level 2 does not appear to change the dominance of first-order effects substantially, but the introduction of the macrophytes for level 3 greatly reduced the additivity of the model by substantially

increasing the role of interactions. This in turn diminishes the first-order contribution to overall variance and, thus, the proportionate first-order contributions of many similarly ranked parameters are also expected to decrease. Because the quantifiable difference between closely grouped parameters is expected to be small, calculated variances (using extended FAST results) are necessary to determine the importance of the observed changes in ranking.

Extended Fourier Amplitude Sensitivity Test (FAST) Results

Results of the global sensitivity analysis obtained from the variance-based FAST method for each of the selected model outputs are discussed herein and presented in tables 14 to 19 and figures 26 to 31. Also considered are the effects of complexity level and velocity on the sensitive parameters affecting each of the model outputs. A threshold value of greater than 5 percent of total output variance was selected to distinguish sensitive from nonsensitive parameters. Significant contributions exceeding 5 percent are highlighted in blue in tables 14 to 19.

The extended FAST results reinforce and quantify those obtained with the Morris method and, in many cases, eliminate the subjectivity inherent to that qualitative approach. The list of important parameters is also further reduced in many instances.

In an effort to simplify the presentation of FAST results, one output of particular interest in the Everglades, surface-water SRP outflow ($C_{sw}{}^{P}]_{o,tf}$), is discussed here in detail. Detailed sensitivity trends for each individual output, corresponding to figures 26 to 31 as well as tables 14 to 19, are discussed in the appendix 4.

Surface-Water Soluble Reactive Phosphorus ($C_{sw}{}^{P}]_{o,tf}$) Case Study

For level 1, depending on the velocity case, 35.1 to 37.5 percent of the variance can be attributed to the first order effects of k_{ox}, 18.6 to 21.9 percent to ρ_b, 15.4 to 16.9 percent to $X_{so}{}^{P}$ and 15.4 to 15.7 percent to k_{df}. The greater number of simulations required to obtain these results, compared to the Morris method, improves their accuracy, and some reordering of parameter importance occurs as a result. Although ρ_b was previously ranked third by the Morris method, the results presented here indicate that it is in fact the second most important parameter. Conversely, k_{df} decreases in rank from second to third (at 500 m/d) or fourth (at 50 and 100 m/d), whereas $X_{so}{}^{P}$ rises from fourth to third at 50 and 100 m/d. This reordering demonstrates the fine tuning that can be performed using the extended FAST results. In this case, however, the reordering is of little importance because the actual difference between the contributions of parameters ranked second, third, or fourth is negligible relative to the actual difference of the unranked parameters. Irrespective of their order, all four of the listed parameters would typically be included for the extended FAST analysis based on the Morris results. However, if a user were required to select only two parameters to better measure in the field, then the choice of ρ_b (as per the extended FAST results) instead of k_{df} (as per the Morris results) for the second parameter could potentially reduce variance by up to 6 percent more.

Level-2 results show that $k_g{}^{pl}$ accounts for 46.7, 37.0, and 67.1 percent of the change in $C_{sw}{}^{P}]_{o,tf}$, and $k_{1/2}{}^{pl}$ for another 22.6, 10.2, and 15.8 percent for the 50, 100, and 500 m/d cases, respectively (table 14). Because the next highest contribution is only 3.4 percent (k_{ox} at 500 m/d), $k_g{}^{pl}$ and $k_{1/2}{}^{pl}$ are the critical parameters, and accordingly, the remaining parameters that were originally ranked using the Morris method can be disregarded. This reduces the number of important parameters from 6-8 to 2.

The extended FAST results also confirm the relative importance of direct effects as opposed to indirect effects through interactions. Close to 89 percent of the total variation in $C_{sw}{}^{P}]_{o,tf}$ for level 1 was consistently due to first order effects, and 73.5, 53.4, and 94.6 percent of the variation in level 2 at 50, 100, and 500 m/d, respectively. This dominance of linear effects corroborates earlier conclusions from the Morris plots, where proximity of parameters to the μ^*-axis was used to deduce the same result. Specifically, the pattern shown in table 14, of falling and then rising total first order effects over increasing velocity, is further demonstration of the high qualitative accuracy of the Morris method. Taking into account the variable scales of the μ^* and σ-axes in figures 24A, C, and E, the relative magnitudes of μ^* and σ for the two plankton parameters are found to follow the same order observed in the extended FAST results; if figure 24E was plotted within figure 24C, the points of the latter figure would be comparatively farther from the μ^*-axis (that is, less linear), and similarly so if the points of figure 24A were plotted in figure 24A. This apparent importance of interactions at 100 m/d in level 2 seems somewhat anomalous, but closer examination of the uncertainty analysis results (presented later) provides useful explanatory information.

For level 3, combined first-order effects account for only 47.2, 39.2, and 55.2 percent over increasing velocity, indicating that about 45 to 60 percent of the variation is due to interactions. Except for $k_g{}^{pl}$ and $k_{1/2}{}^{pl}$, which are responsible for 18.2 and 14.6 percent, respectively, of the total variation at 500 m/d, all the first-order contributions of the level-3 parameters are less than 6 percent. This result implies that the 500-m/d water velocity creates a unique environment; the uncertainty analysis results presented later provide further insight on this case.

This comparison between the Morris and extended FAST results demonstrates the accuracy of the Morris results for identifying qualitative trends, and for screening out unimportant parameters. It also illustrates the need, however, for quantitative measures to guarantee accurate ranking of parameters, and for further screening.

Table 14. Fourier Amplitude Sensitivity Test (FAST) results for the surface-water soluble reactive phosphorus outflow outputs ($C_{sw}^{P}]_{o,tf}$ and $C_{sw}^{P}]_{o,t}$).

[Parameter descriptions are provided in table 4. Values for all results except velocity are shown as percentages. Values greater than 5 percent of the total output variance are shaded]

Complexity	Velocity (meters per day)	Output	Parameter																Total
			k_{df}	k_{ox}	X_{so}^{P}	k_d	θ	ρ_b	λ_l	λ_t	k_g^{pl}	$k_{1/2}^{pl}$	k_{st}^{pl}	X_{pl}^{P}	k_g^{mp}	$k_{1/2}^{mp}$	k_{sn}^{mp}	X_{mp}^{P}	
First order index, S_i																			
Level 1	50	$C_{sw}^{P}]_{o,tf}$	15.4	37.5	16.9	0.3	0.1	18.6	0.0	0.0									88.8
	100	$C_{sw}^{P}]_{o,tf}$	15.6	36.2	16.1	.3	.1	20.4	.1	.0									88.8
	500	$C_{sw}^{P}]_{o,tf}$	15.7	35.1	15.4	.4	.1	21.9	.4	.0									88.9
Level 2	50	$C_{sw}^{P}]_{o,tf}$	.1	2.0	.6	.6	.1	.4	.3	.0	46.7	22.6	.1	.1					73.5
	100	$C_{sw}^{P}]_{o,tf}$	.3	1.3	.7	1.9	.3	.4	.5	.2	37.0	10.2	.3	.4					53.4
	500	$C_{sw}^{P}]_{o,tf}$	1.7	3.4	2.0	.0	.0	1.5	2.6	.0	67.1	15.8	.0	.4					94.6
Level 3	50	$C_{sw}^{P}]_{o,tf}$	2.7	1.8	3.1	5.3	4.1	4.3	4.3	2.1	4.8	1.1	1.8	2.4	2.2	2.0	2.7	2.5	47.2
	100	$C_{sw}^{P}]_{o,tf}$	3.0	1.7	1.7	3.7	1.9	2.3	1.7	1.9	4.2	3.1	5.4	1.5	2.8	.7	1.1	2.8	39.2
	500	$C_{sw}^{P}]_{o,tf}$	.8	.6	1.6	1.2	.9	.5	1.9	.8	18.2	14.6	1.2	4.2	2.6	2.2	1.3	2.7	55.2
Interactions, $S_{Ti} - S_i$																			
Level 1	50	$C_{sw}^{P}]_{o,tf}$	4.2	7.5	7.3	.5	.3	4.4	.2	.2									
	100	$C_{sw}^{P}]_{o,tf}$	4.4	7.6	7.2	.6	.3	4.7	.4	.5									
	500	$C_{sw}^{P}]_{o,tf}$	4.6	7.7	7.0	.6	.4	4.9	.7	.5									
Level 2	50	$C_{sw}^{P}]_{o,tf}$	7.8	7.3	5.0	12.6	23.3	22.6	11.8	11.8	13.7	8.2	15.6	9.4					
	100	$C_{sw}^{P}]_{o,tf}$	21.0	27.1	16.6	43.7	44.1	47.6	37.9	36.7	35.7	24.2	38.8	36.8					
	500	$C_{sw}^{P}]_{o,tf}$	2.2	3.9	2.3	.7	8.4	4.4	.8	.9	.9	2.6	1.8	.8					
Level 3	50	$C_{sw}^{P}]_{o,tf}$	88.9	85.9	84.3	82.9	85.5	83.8	87.3	86.1	74.5	85.6	82.9	83.4	84.6	85.7	78.6	81.3	
	100	$C_{sw}^{P}]_{o,tf}$	78.7	79.7	83.1	81.9	85.7	82.0	81.4	77.8	78.9	85.8	86.8	84.5	81.2	79.8	82.5	75.9	
	500	$C_{sw}^{P}]_{o,tf}$	52.1	61.7	67.1	59.5	66.8	55.0	52.9	67.3	63.9	63.1	66.0	61.0	28.4	57.7	62.6	54.7	
First order index, S_i																			
Level 1	50	$C_{sw}^{P}]_{o,t}$	18.3	32.2	14.1	.4	.1	24.1	.1	.0									89.3
	100	$C_{sw}^{P}]_{o,t}$	18.3	31.4	13.6	.4	.1	25.4	.2	.0									89.4
	500	$C_{sw}^{P}]_{o,t}$	18.4	30.7	13.2	.4	.1	26.4	.3	.0									89.6
Level 2	50	$C_{sw}^{P}]_{o,t}$	.3	.9	0.4	.5	.0	1.1	.1	.0	64.9	14.5	.0	.4					83.2
	100	$C_{sw}^{P}]_{o,t}$	.1	.8	.4	.9	.1	.9	.1	.1	59.2	11.8	.1	.3					74.7
	500	$C_{sw}^{P}]_{o,t}$	1.5	2.0	1.1	.0	.0	1.5	2.0	.0	67.9	18.7	.0	.6					95.1
Level 3	50	$C_{sw}^{P}]_{o,t}$	2.7	1.7	3.0	5.0	4.2	4.5	4.5	1.9	6.6	1.2	1.8	2.1	2.0	2.2	2.9	2.5	48.6
	100	$C_{sw}^{P}]_{o,t}$	2.9	1.7	1.7	4.0	1.8	2.1	1.6	1.8	5.6	3.1	5.2	1.5	2.4	.7	1.1	2.9	40.2
	500	$C_{sw}^{P}]_{o,t}$	1.0	.6	1.6	1.3	.9	.5	1.7	.9	18.7	14.9	1.1	4.9	1.2	2.1	1.2	2.6	55.1
Interactions, $S_{Ti} - S_i$																			
Level 1	50	$C_{sw}^{P}]_{o,t}$	5.0	7.5	6.8	.6	.4	5.1	.6	.4									
	100	$C_{sw}^{P}]_{o,t}$	5.2	7.5	6.6	.6	.4	5.3	.5	.4									
	500	$C_{sw}^{P}]_{o,t}$	5.2	7.4	6.5	.7	.4	5.4	.2	.2									
Level 2	50	$C_{sw}^{P}]_{o,t}$	4.3	5.5	4.9	9.1	14.3	16.2	10.6	8.9	10.6	8.9	11.5	8.4					
	100	$C_{sw}^{P}]_{o,t}$	7.0	11.1	8.9	17.8	23.0	24.7	19.9	15.9	17.1	14.8	17.2	18.6					
	500	$C_{sw}^{P}]_{o,t}$	2.0	2.3	1.6	.8	7.6	4.8	.9	1.0	1.0	2.3	1.6	.9					
Level 3	50	$C_{sw}^{P}]_{o,t}$	86.9	85.7	83.1	83.2	83.6	81.6	86.2	84.7	71.5	84.3	81.4	83.2	83.6	84.4	78.3	78.9	
	100	$C_{sw}^{P}]_{o,t}$	77.4	78.2	81.8	80.1	84.4	80.6	80.7	76.0	78.7	85.4	86.3	84.5	80.2	78.8	80.9	74.2	
	500	$C_{sw}^{P}]_{o,t}$	51.4	62.0	67.1	59.0	66.4	55.3	53.0	67.7	64.1	62.7	65.9	60.9	30.2	58.1	62.3	56.4	

Table 15. Fourier Amplitude Sensitivity Test (FAST) results for the pore-water soluble reactive phosphorus variation output ($C_{pw}{}^{P}]_{acr}$).

[Parameter descriptions are provided in table 4. Values for all results except velocity are shown as percentages. Values greater than 5 percent of the total output variance are shaded]

Complexity	Velocity (meters per day)	Parameter																Total
		k_{df}	k_{ox}	$X_{so}{}^{P}$	k_d	θ	ρ_b	λ_l	λ_t	$k_g{}^{pl}$	$k_{1/2}{}^{pl}$	$k_{st}{}^{pl}$	$X_{pl}{}^{P}$	$k_g{}^{mp}$	$k_{1/2}{}^{mp}$	$k_{sn}{}^{mp}$	$X_{mp}{}^{P}$	
First order index, S_i																		
Level 1	50	2.0	43.5	20.9	0.4	1.2	17.5	0.0	0.0									85.5
	100	1.9	43.5	20.9	.4	1.2	17.7	.0	.0									85.6
	500	1.8	43.5	20.9	.4	1.2	17.9	.0	.0									85.7
Level 2	50	1.6	42.4	19.7	.3	1.8	17.3	.0	.0	.0	.0	.0	.0					83.2
	100	1.6	42.4	19.7	.3	1.8	17.3	.0	.0	.0	.0	.0	.0					83.2
	500	1.6	42.4	19.7	.3	1.8	17.5	.0	.0	.0	.0	.0	.0					83.3
Level 3	50	.8	5.9	3.0	1.6	1.7	3.0	1.7	1.1	.7	1.9	1.4	.9	11.6	1.9	2.5	8.9	48.6
	100	1.2	4.6	1.2	.9	.8	1.8	2.0	1.7	1.3	.8	.9	.9	16.8	2.3	2.7	8.6	48.5
	500	1.9	2.9	2.7	1.6	.5	1.7	2.0	1.2	2.6	1.1	1.9	1.4	12.7	3.0	2.2	9.9	49.2
Interactions, $S_{Ti} - S_i$																		
Level 1	50	1.3	9.6	5.4	.6	.7	4.2	.4	.5									
	100	1.2	9.6	5.4	.6	.7	4.2	.8	.5									
	500	1.2	9.6	5.4	.6	.7	4.2	.7	.4									
Level 2	50	1.8	6.7	5.7	.6	.9	.6	.6	.6	1.0	5.1	.7	.7					
	100	1.8	6.7	5.7	.6	.9	.6	.6	.6	1.0	5.1	.7	.7					
	500	1.8	6.7	5.7	.6	.9	.6	.6	.6	1.0	5.1	.7	.7					
Level 3	50	51.4	76.3	55.8	75.9	58.0	47.6	62.2	75.2	77.6	79.9	65.5	59.1	46.3	57.3	69.7	42.6	
	100	60.6	63.8	31.6	60.8	64.0	51.2	56.4	78.6	72.3	76.0	59.7	54.0	55.8	51.5	80.6	59.1	
	500	61.9	59.5	58.0	53.1	69.2	71.4	66.2	68.1	71.3	79.2	60.2	65.0	17.3	54.4	80.3	58.9	

Table 16. Fourier Amplitude Sensitivity Test (FAST) results for the organic soil accretion output ($S^o]_{acr}$)

[Parameter descriptions are provided in table 4. Values for all results except velocity are shown as percentages. Values greater than 5 percent of the total output variance are shaded]

Complexity	Velocity (meters per day)	Parameter																Total
		k_{df}	k_{ox}	$X_{so}{}^{P}$	k_d	θ	ρ_b	λ_l	λ_t	$k_g{}^{pl}$	$k_{1/2}{}^{pl}$	$k_{st}{}^{pl}$	$X_{pl}{}^{P}$	$k_g{}^{mp}$	$k_{1/2}{}^{mp}$	$k_{sn}{}^{mp}$	$X_{mp}{}^{P}$	
First order index, S_i																		
Level 1	50	0.0	98.7	0.0	0.0	0.0	0.0	0.0	0.0									98.7
	100	.0	98.7	.0	.0	.0	.0	.0	.0									98.7
	500	.0	98.7	.0	.0	.0	.0	.0	.0									98.7
Level 2	50	.0	98.6	.0	.0	.0	.0	.0	.0	.0	.0	.0	.0					98.6
	100	.0	98.6	.0	.0	.0	.0	.0	.0	.0	.0	.0	.0					98.6
	500	.0	98.6	.0	.0	.0	.0	.0	.0	.0	.0	.0	.0					98.6
Level 3	50	1.7	13.0	3.6	3.5	4.8	3.5	3.9	2.2	3.2	.7	1.8	2.4	1.8	2.1	9.1	3.3	60.4
	100	2.7	15.1	1.6	2.9	.6	1.6	2.1	2.5	.9	1.6	3.1	2.4	2.6	.7	5.5	4.7	50.4
	500	2.8	14.6	1.7	3.6	1.6	.9	1.7	1.3	2.3	1.8	3.7	1.4	1.9	2.1	4.1	3.9	49.4
Interactions, $S_{Ti} - S_i$																		
Level 1	50	.2	1.3	.2	.2	.2	.2	.6	.5									
	100	.2	1.3	.2	.2	.2	.2	.5	.4									
	500	.2	1.3	.2	.2	.2	.2	.5	.4									
Level 2	50	.3	1.4	.3	.3	.3	.3	.3	.3	.3	.3	.3	.3					
	100	.3	1.4	.3	.3	.3	.3	.3	.3	.3	.3	.3	.3					
	500	.3	1.4	.3	.3	.3	.3	.3	.3	.3	.3	.3	.3					
Level 3	50	83.1	68.3	76.1	75.3	63.0	64.9	81.3	82.0	68.9	80.1	69.7	74.8	70.7	73.5	68.4	57.4	
	100	70.9	72.7	76.6	79.4	59.3	72.7	81.5	79.6	76.3	79.1	72.2	69.3	66.2	60.7	82.1	73.2	
	500	72.8	73.7	85.5	79.9	65.5	63.9	82.9	85.1	74.4	77.0	77.3	73.3	40.9	59.3	72.2	74.3	

Table 17. Fourier Amplitude Sensitivity Test (FAST) results for the soil adsorbed phosphorus variation output ($S_{si}{}^{P}]_{acr}$).

[Parameter descriptions are provided in table 4. Values for all results except velocity are shown as percentages. Values greater than 5 percent of the total output variance are shaded]

Complexity	Velocity (meters per day)	Parameter																Total
		k_{df}	k_{ox}	$X_{so}{}^{P}$	k_{d}	θ	ρ_{b}	λ_{l}	λ_{t}	$k_{g}{}^{pl}$	$k_{1/2}{}^{pl}$	$k_{st}{}^{pl}$	$X_{pl}{}^{P}$	$k_{g}{}^{mp}$	$k_{1/2}{}^{mp}$	$k_{sn}{}^{mp}$	$X_{mp}{}^{P}$	
First order index, S_i																		
Level 1	50	1.9	51.1	24.6	0.4	0.1	12.1	0.0	0.0									90.3
	100	1.8	51.3	24.7	.4	.1	12.1	.0	.0									90.4
	500	1.7	51.4	24.7	.4	.1	12.0	.0	.0									90.4
Level 2	50	2.5	49.4	25.5	.6	.1	12.5	.0	.0	.0	.0	.0	.0					90.4
	100	2.5	49.3	25.5	.6	.1	12.5	.0	.0	.0	.0	.0	.0					90.4
	500	2.4	49.3	25.5	.6	.1	12.6	.0	.0	.0	.0	.0	.0					90.3
Level 3	50	1.0	6.0	3.1	1.2	1.7	2.3	1.6	.9	.6	1.7	1.3	.9	18.1	1.9	2.6	9.4	54.4
	100	1.2	4.2	1.0	1.2	.8	1.8	1.8	2.1	.9	1.0	.9	1.2	23.9	2.0	2.6	9.4	56.0
	500	1.9	3.3	3.4	2.0	.5	0.9	2.0	1.2	2.2	1.4	1.9	1.4	18.2	2.7	1.9	11.3	56.3
Interactions, $S_{Ti} - S_i$																		
Level 1	50	.7	8.1	5.6	.5	0.4	2.4	0.5	0.4									
	100	.7	8.1	5.6	0.5	0.4	2.3	0.2	0.2									
	500	.7	8.1	5.6	0.5	0.4	2.3	0.4	0.5									
Level 2	50	1.0	7.9	6.7	1.2	0.3	0.6	0.7	0.5	0.5	3.1	0.6	0.6					
	100	1.0	7.9	6.7	1.2	0.3	0.6	0.7	0.5	0.5	3.1	0.6	0.6					
	500	1.0	7.9	6.7	1.2	0.3	0.6	0.7	0.5	0.5	3.1	0.6	0.6					
Level 3	50	59.4	79.3	62.0	78.6	57.6	42.1	59.1	71.1	72.1	79.3	67.4	58.6	47.0	61.3	68.2	40.7	
	100	54.1	72.6	33.8	75.8	61.2	49.9	58.1	79.5	66.6	73.7	57.8	54.1	54.7	51.8	78.1	57.3	
	500	59.6	66.1	64.5	62.4	66.0	71.7	65.3	65.9	68.2	78.7	58.0	64.2	16.8	55.9	76.2	60.3	

Table 18. Fourier Amplitude Sensitivity Test (FAST) results for the plankton biomass outflow outputs ($C_{sw}^{pl}]_{o,tf}$ and $C_{sw}^{pl}]_{o,t}$).

[Parameter descriptions are provided in table 4. Values for all results except velocity are shown as percentages. Values greater than 5 percent of the total output variance are shaded]

Complexity	Velocity (meters per day)	Output	Parameter																Total
			k_{df}	k_{ox}	X_{so}^{P}	k_d	θ	ρ_b	λ_l	λ_t	k_g^{pl}	$k_{1/2}^{pl}$	k_{st}^{pl}	X_{pl}^{P}	k_g^{mp}	$k_{1/2}^{mp}$	k_{sn}^{mp}	X_{mp}^{P}	
First order index, S_i																			
Level 2	50	$C_{sw}^{pl}]_{o,tf}$	15.2	43.1	15.8	0.4	0.1	14.7	0.3	0.0	0.5	0.0	0.0	9.4					99.6
	100	$C_{sw}^{pl}]_{o,tf}$	14.0	44.0	16.0	.0	.0	13.0	.0	.0	.0	.0	.0	11.0					98.0
	500	$C_{sw}^{pl}]_{o,tf}$	4.0	8.2	3.5	.1	.0	4.0	1.6	.0	61.8	13.6	.0	1.5					98.2
Level 3	50	$C_{sw}^{pl}]_{o,tf}$	2.4	3.8	1.2	3.9	3.6	2.3	3.0	2.4	2.3	1.8	12.2	7.5	11.8	1.4	2.6	2.7	64.9
	100	$C_{sw}^{pl}]_{o,tf}$	2.1	2.1	2.4	1.2	1.1	2.2	.6	1.6	1.4	1.7	11.2	15.9	5.3	.3	2.6	1.3	52.8
	500	$C_{sw}^{pl}]_{o,tf}$	.8	2.1	2.0	1.6	2.0	.5	1.9	1.1	12.7	11.3	3.2	3.1	1.5	2.3	2.1	4.1	52.3
Interactions, $S_{Ti} - S_i$																			
Level 2	50	$C_{sw}^{pl}]_{o,tf}$	4.5	9.0	5.7	.5	1.1	.6	.7	2.0	.5	6.0	.9	.8					32.4
	100	$C_{sw}^{pl}]_{o,tf}$	5.0	9.0	6.0	1.0	1.0	.0	.0	2.0	.0	5.0	1.0	.0					30.0
	500	$C_{sw}^{pl}]_{o,tf}$	2.7	4.5	3.9	.6	6.7	4.1	1.4	2.4	.7	4.1	1.7	.8					33.6
Level 3	50	$C_{sw}^{pl}]_{o,tf}$	72.7	71.9	58.0	67.1	49.2	66.7	69.7	77.3	71.4	65.5	74.5	72.5	57.2	65.1	65.0	62.3	
	100	$C_{sw}^{pl}]_{o,tf}$	72.1	55.7	45.7	51.0	57.4	56.7	70.8	66.3	67.1	56.0	59.3	73.9	67.4	62.5	63.8	71.3	
	500	$C_{sw}^{pl}]_{o,tf}$	62.6	73.5	76.7	66.2	71.1	69.4	64.9	72.6	73.4	74.3	61.2	67.7	51.1	47.2	65.0	50.5	
First order index, S_i																			
Level 2	50	$C_{sw}^{pl}]_{o,t}$	18.0	39.0	14.0	.0	.0	16.0	.0	.0	.0	.0	.0	13.0					100.0
	100	$C_{sw}^{pl}]_{o,t}$	17.0	40.0	14.0	.0	.0	15.0	.0	.0	.0	.0	.0	16.0					100.0
	500	$C_{sw}^{pl}]_{o,t}$	2.7	4.1	2.0	.1	.0	2.8	1.3	.0	64.8	17.8	.0	1.4					97.0
Level 3	50	$C_{sw}^{pl}]_{o,t}$	2.6	2.9	1.5	4.5	4.4	2.6	2.3	2.1	2.4	1.6	14.7	17.5	4.8	1.4	2.3	2.0	69.5
	100	$C_{sw}^{pl}]_{o,t}$	1.9	1.3	2.3	1.4	1.2	2.1	.7	1.7	1.2	2.2	11.2	17.0	2.8	.3	2.5	1.1	51.0
	500	$C_{sw}^{pl}]_{o,t}$	.7	2.2	1.7	1.8	2.1	.5	1.9	1.2	12.5	11.1	3.1	2.9	1.4	2.3	1.9	4.4	51.8
Interactions, $S_{Ti} - S_i$																			
Level 2	50	$C_{sw}^{pl}]_{o,t}$	5.2	9.5	5.6	1.1	1.6	.6	.6	2.8	.6	7.4	1.4	1.0					37.4
	100	$C_{sw}^{pl}]_{o,t}$	6.0	10.0	6.0	1.0	1.0	.0	.0	2.0	.0	6.0	1.0	1.0					34.0
	500	$C_{sw}^{pl}]_{o,t}$	2.1	2.9	2.8	.7	6.5	4.8	1.4	2.4	.8	3.5	1.5	.9					30.4
Level 3	50	$C_{sw}^{pl}]_{o,t}$	73.5	72.3	64.6	63.0	50.4	66.0	68.5	70.2	75.7	72.1	75.2	75.7	66.9	72.5	69.4	69.1	
	100	$C_{sw}^{pl}]_{o,t}$	71.9	55.2	54.4	52.3	58.6	58.3	70.4	64.8	68.4	60.8	59.0	75.0	69.2	64.7	63.5	70.1	
	500	$C_{sw}^{pl}]_{o,t}$	63.3	74.1	79.2	67.9	71.6	69.0	64.6	74.4	73.7	74.7	61.8	68.3	54.5	47.9	65.7	52.5	

Table 19. Fourier Amplitude Sensitivity Test (FAST) results for the macrophyte biomass accumulation output ($C^{mp}]_{acr}$)

[Parameter descriptions are provided in table 4. Values greater than 5 percent of the total output variance are shaded]

Complexity	Velocity (meters per day)	Parameter																Total
		k_{df}	k_{ox}	X_{so}^{P}	k_d	θ	ρ_b	λ_p	λ_t	k_g^{pl}	$k_{1/2}^{pl}$	k_{st}^{pl}	X^{pl}	k_g^{mp}	$k_{1/2}^{mp}$	k_{sn}^{mp}	X^{mp}	
First order index, S_i																		
Level 3	50	1.0	5.8	5.9	3.4	2.6	2.3	1.3	1.3	1.5	1.5	1.9	3.8	2.2	1.9	11.8	16.1	64.2
	100	2.5	4.9	3.0	1.0	1.3	1.5	1.4	1.7	.4	1.4	1.8	1.6	3.1	.6	6.6	10.3	43.0
	500	2.5	7.9	5.1	3.5	2.0	.5	1.4	1.0	2.2	1.6	2.2	1.4	3.8	2.3	4.9	29.1	71.2
Interactions, $S_{Ti} - S_i$																		
Level 3	50	65.6	60.0	75.3	61.4	60.0	65.0	57.1	70.2	73.1	85.4	59.4	73.1	78.2	72.2	55.6	58.0	
	100	58.7	55.8	76.1	80.6	39.9	65.1	59.3	69.3	73.3	75.2	68.4	73.1	65.8	65.1	64.8	62.6	
	500	67.3	64.6	63.4	65.8	56.3	59.3	78.1	78.2	54.1	71.3	70.8	57.9	54.0	71.3	62.4	60.8	

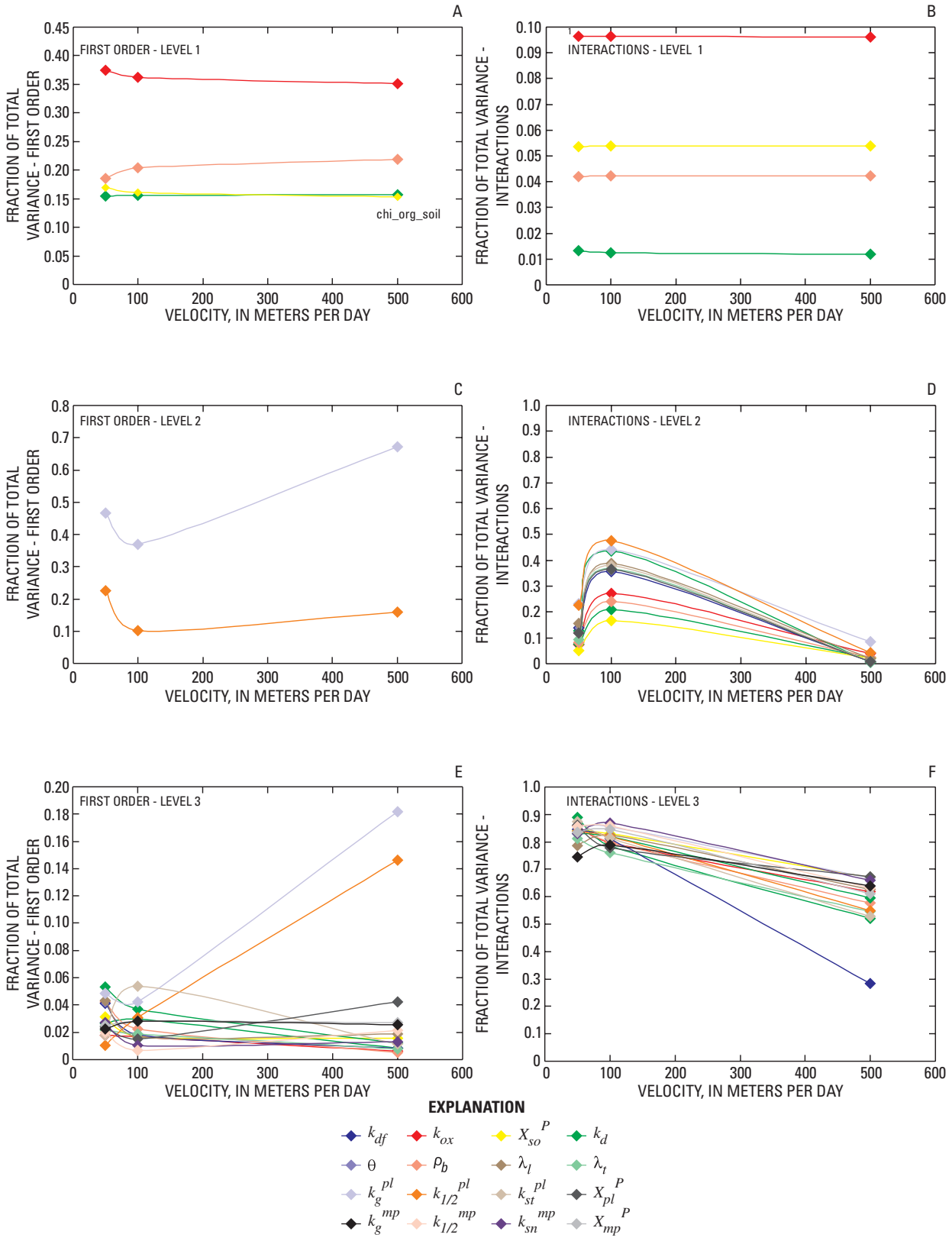

Figure 26. Fourier Amplitude Sensitivity Test (FAST) global sensitivity analysis results for surface-water soluble reactive phosphorus outflow ($C_{sw}{}^{P}]_{o,tfl}$) across complexity levels and velocities tested. Parameter descriptions are provided in table 4.

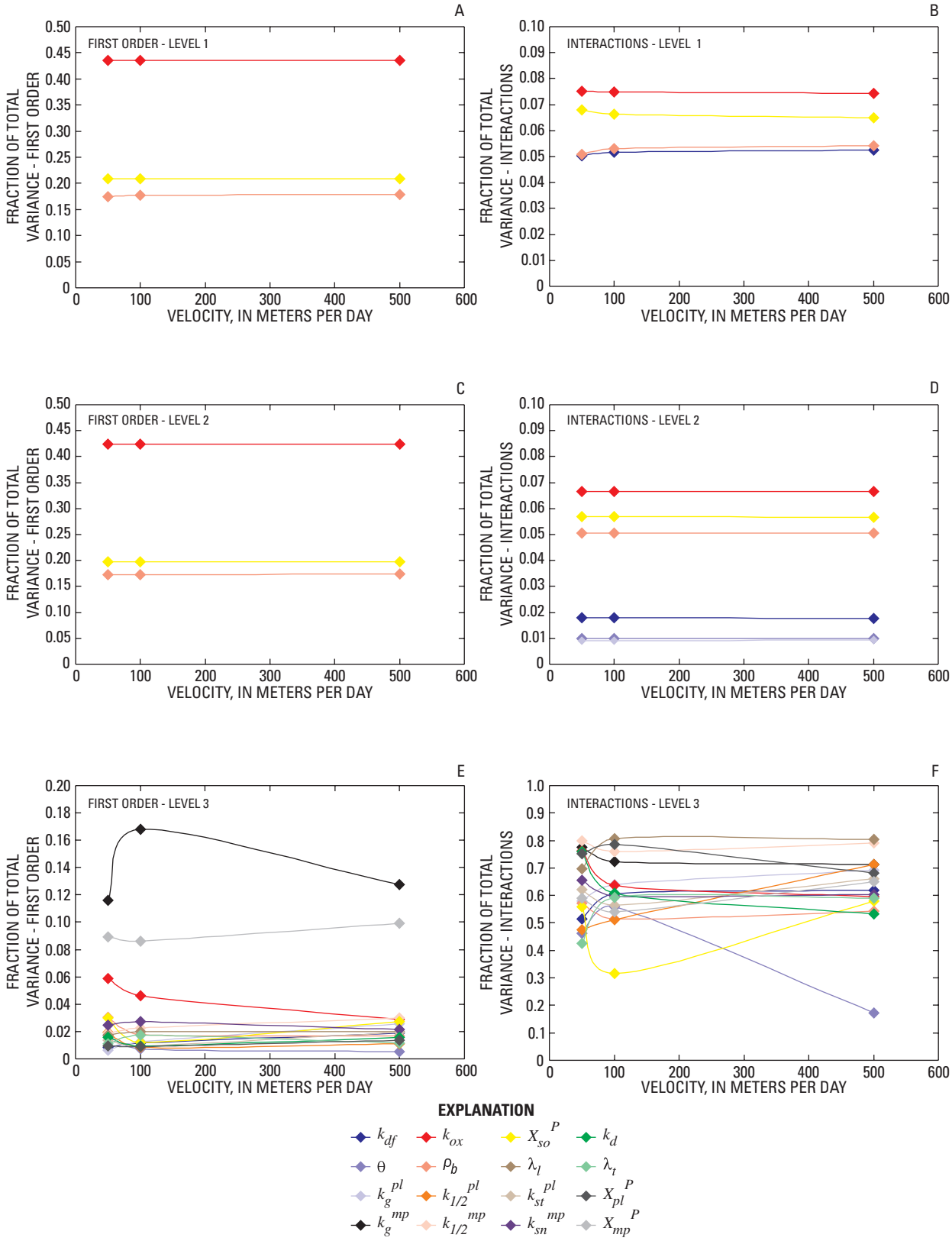

Figure 27. Fourier Amplitude Sensitivity Test (FAST) global sensitivity analysis results for soil pore-water soluble reactive phosphorus variation ($C_{pw}{}^{P}]_{acr}$) across complexity levels and velocities tested. Parameter descriptions are provided in table 4.

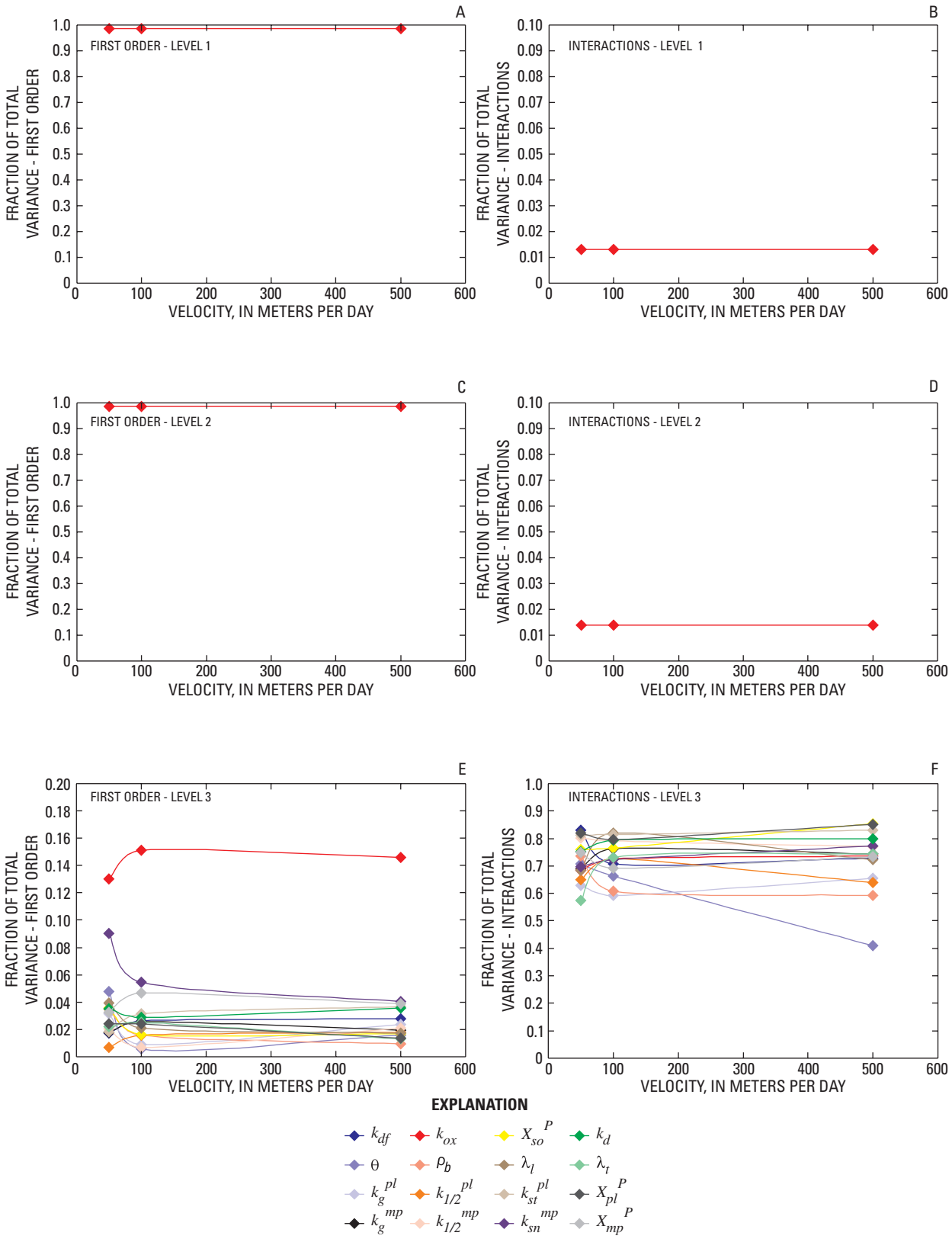

Figure 28. Fourier Amplitude Sensitivity Test (FAST) global sensitivity analysis results for organic soil accretion ($S^o]_{acr}$) across complexity levels and velocities tested. Parameter descriptions are provided in table 4.

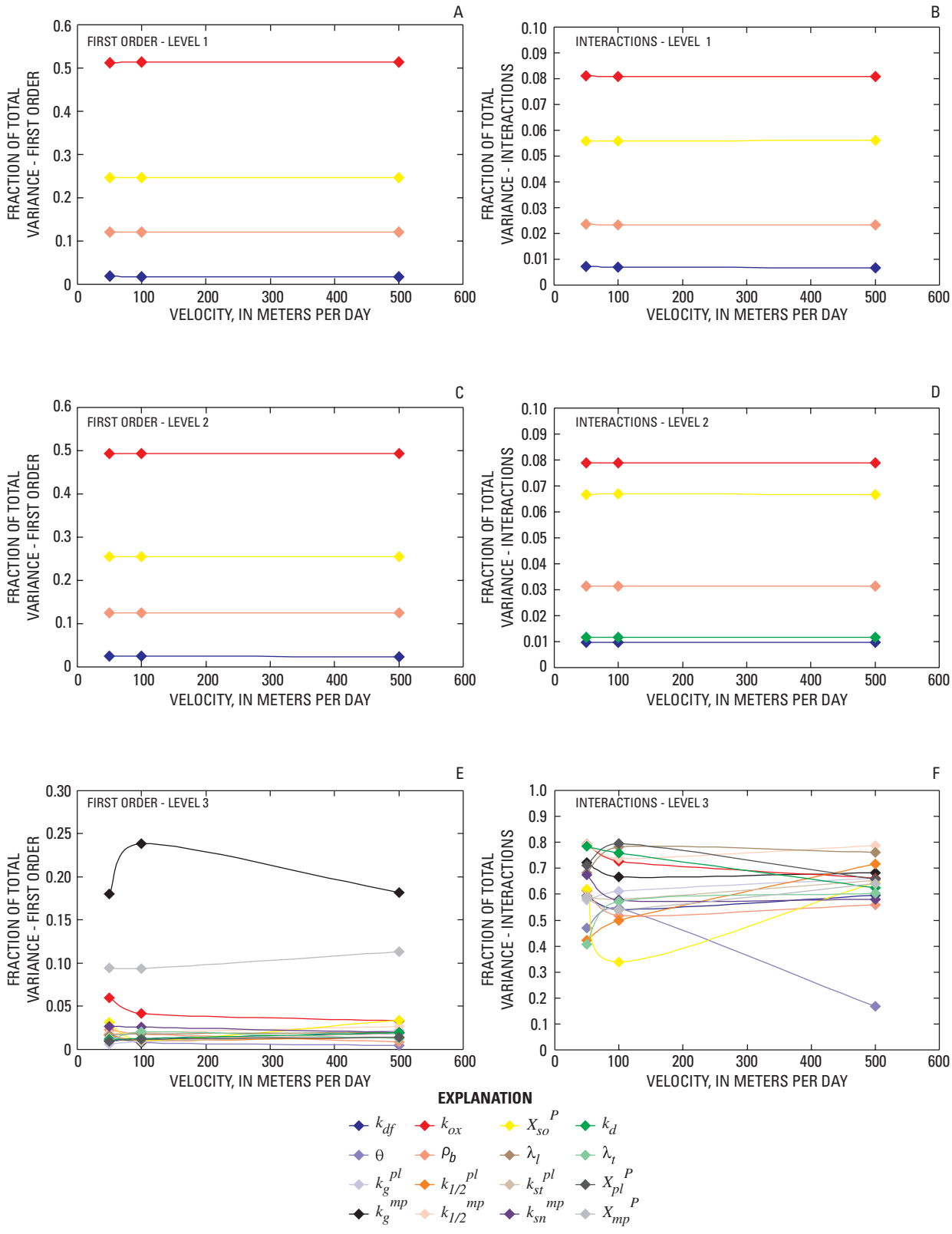

Figure 29. Fourier Amplitude Sensitivity Test (FAST) global sensitivity analysis results for soil adsorbed phophorus variation ($S_{si}{}^{P}]_{acr}$) across complexity levels and velocities tested. Parameter descriptions are provided in table 4.

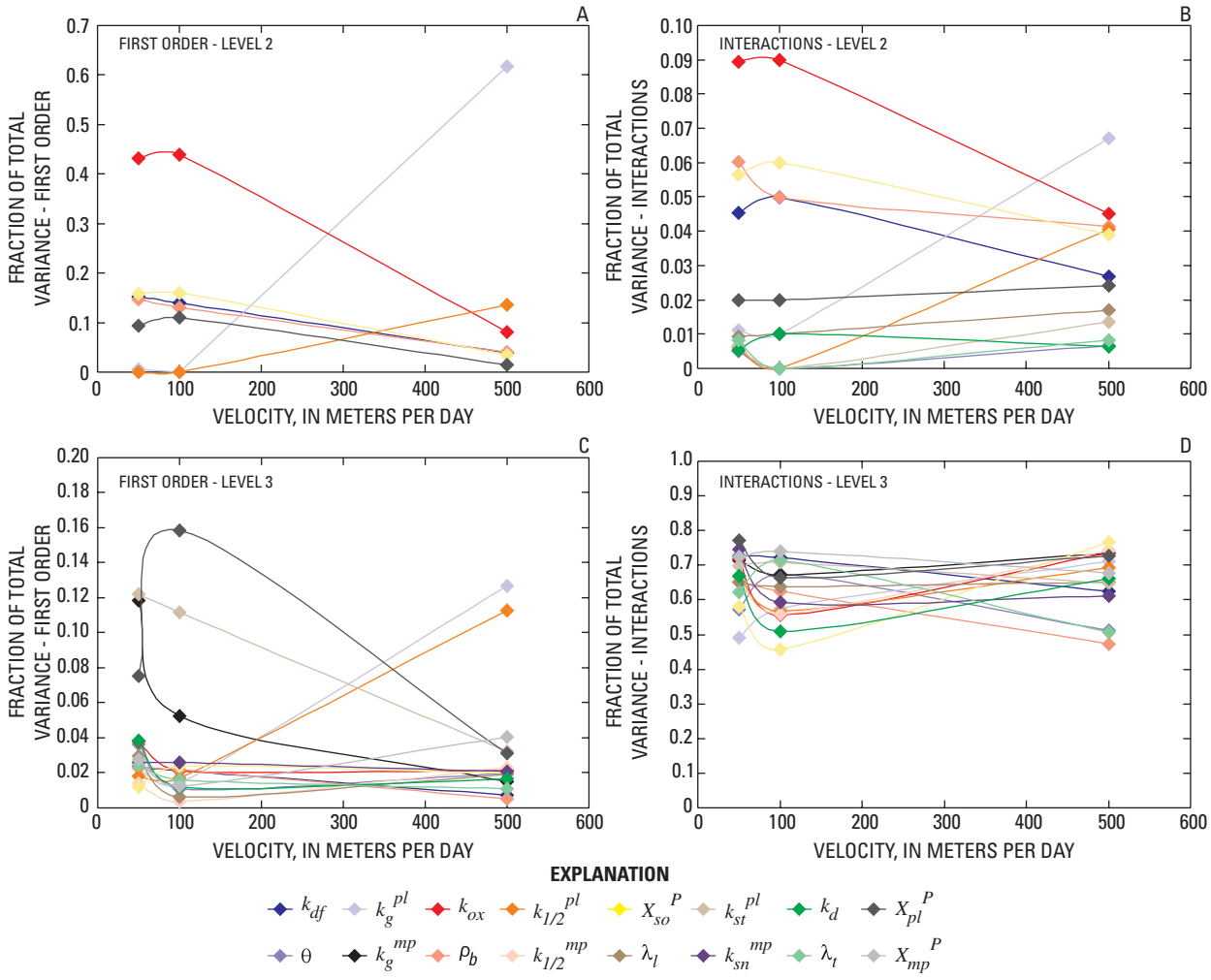

Figure 30. Fourier Amplitude Sensitivity Test (FAST) global sensitivity analysis results for plankton biomass outflow ($C_{sw}^{pl}]_{o,tf}$) across complexity levels and velocities tested. Parameter descriptions are provided in table 4.

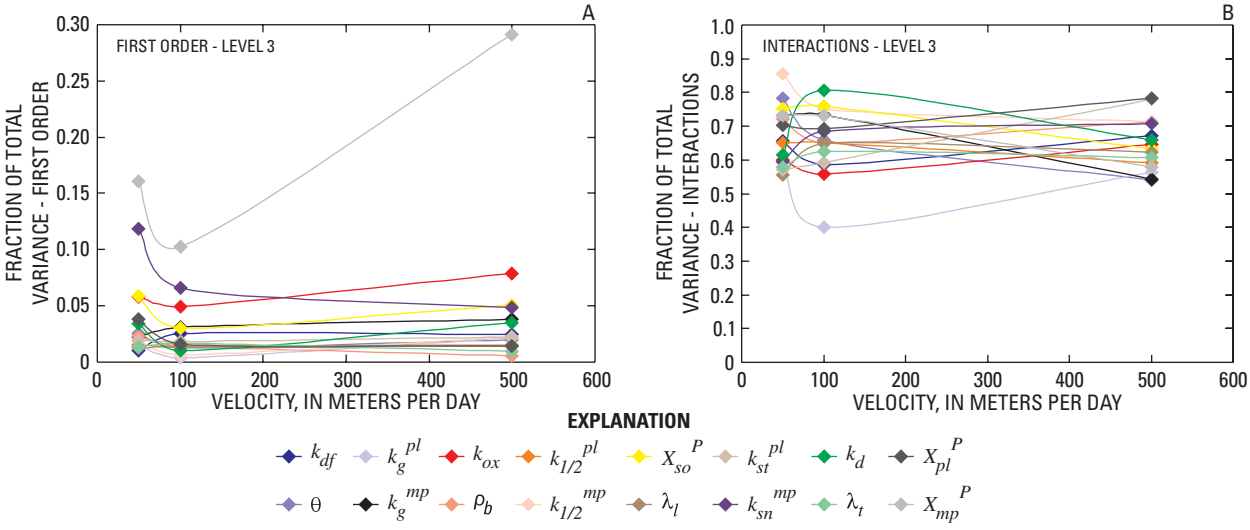

Figure 31. Fourier Amplitude Sensitivity Test (FAST) global sensitivity analysis results for macrophyte biomass accumulation ($C^{mp}]_{acr}$) across complexity levels and velocities tested. Parameter descriptions are provided in table

General Trends Observed in Sensitivity Dynamics

The model discussed herein generally appears to be additive for levels 1 and 2, and outputs are predominantly dependent on first-order effects, as indicated by the high sums of first order contributions. As noted earlier, soil pore-water SRP ($C_{sw}{}^{P}]_{o,tf}$) has 88.8 to 88.9 and 53.4 to 94.6 percent of its variation attributed to first-order effects in levels 1 and 2, respectively, depending on velocity (table 14). Between 85.5 and 85.7 percent of all variation in $C_{pw}{}^{P}]_{acr}$ in level 1 and between 83.2 and 83.3 percent in level 2 are due to linear effects (table 15). With no discernible velocity effects, $C_{pw}{}^{P}]_{acr}$ at both levels is strongly dependent on k_{ox} (43.5 percent in level 1 and 42.4 percent in level 2), followed by $X_{so}{}^{P}$ (20.9 and 19.7 percent for levels 1 and 2, respectively) and ρ_b (between 17 and 18 percent depending on level and velocity). The final number of important parameters for $C_{pw}{}^{P}]_{acr}$ was, therefore, reduced from 6 to 3 for levels 1 and 2 (table 15). Accrued organic soil ($S^{o}]_{acr}$) was almost exclusively dependent on k_{ox}; more than 98 percent of all variation in $S^{o}]_{acr}$ was attributed to this parameter for both levels and at all velocities, as predicted by the Morris results (table 16). Similarly, $S_{si}{}^{P}]_{acr}$ also showed high sensitivity to k_{ox}, which is responsible for 49.3 to 51.4 percent of the variation for both levels (table 17). Of the overall linear effects on $S_{si}{}^{P}]_{acr}$, which totaled about 90 percent, only two other parameters contributed substantially: $X_{so}{}^{P}$ (24.6 to 25.5 percent for both levels), and ρ_b (12.1 to 12.6 percent). These results indicate that k_{df} can be removed from the list of the four parameters originally identified as important by the Morris method.

The effect of the parameters on $C_{sw}{}^{pl}]_{o,tf}$ for level 2 largely appears to be additive, with first-order effects totaling 98.2 to 99.6 percent across all velocities (table 18). At 50 and 100 m/d, k_{ox} and $X_{so}{}^{P}$ consistently account for between 43.1 and 44.0 percent, and about 16 percent of the variation, respectively, with most of the remaining variation at these respective velocities accounted for by k_{df} (14.0 to 15.2 percent), ρ_b (13.0 to 14.7 percent) and $X^{P}{}_{pl}$ (9.4 to 11.0 percent). Sensitivity dynamics are very different at 500 m/d, with $k_g{}^{pl}$, $k_{1/2}{}^{pl}$, and k_{ox}, accounting for 61.8, 13.6, and 8.2 percent, respectively, of the variation.

There is a clear decrease in the role of first-order effects for all outputs in level 3. Over the three velocities, total first-order contributions were 39.2 to 55.2 percent for $C_{sw}{}^{P}]_{o,tf}$, 48.5 to 49.2 percent for $C_{pw}{}^{P}]_{acr}$, 49.4 to 60.4 percent for $S^{o}]_{acr}$, 54.4 to 56.3 percent for $S_{si}{}^{P}]_{acr}$, 52.3 to 64.9 percent for $C_{sw}{}^{pl}]_{o,tf}$, and 43.0 to 71.2 percent for $C^{mp}]_{acr}$ (tables 14-19). Although only one output at one velocity had a total first-order effect *less* than 70 percent in levels 1 and 2 (most were greater than 80 percent), only one output at one velocity had total first order effects *greater* than 70 percent in level 3, with most about or less than 50 percent. Thus, the role of interactions is substantially more important for all outputs in level 3.

Concerning sensitivity to changing velocity, level-1 outputs were found to be relatively insensitive (tables 14-17, and figs. 26-29A, B). Outputs for mobile components exhibit some sensitivity to velocity in level 2; $C_{sw}{}^{P}]_{o,tf}$ is more susceptible to higher order effects at 100 m/d than at other velocities (table 14), and $C_{sw}{}^{pl}]_{o,tf}$ is only sensitive to plankton growth parameters at 500 m/d (table 18 and fig. 30A). Noteworthy changes in sensitivity at different velocities is apparent in the level-3 results of three outputs, namely, $C_{sw}{}^{P}]_{o,tf}$, $S^{o}]_{acr}$, $C_{sw}{}^{pl}]_{o,tf}$ (tables 14, 16, and 18, respectively). Although no parameters are clearly dominant for $C_{sw}{}^{P}]_{o,tf}$ at 50 and 100 m/d, $k_g{}^{pl}$ and $k_{1/2}{}^{pl}$ account for 18.2 and 14.6 percent, respectively, at 500 m/d (fig. 26E and table 14); the minor individual first-order effects of the other 14 parameters together account for the remaining 22 parameters. As for levels 1 and 2, level-3 first-order effects for $S^{o}]_{acr}$ were dominated by k_{ox} (table 16 and fig. 28E), but to a lesser extent (13.0 to 15.1 percent in level 3 compared with more than 98 percent in levels 1 and 2). Furthermore, at the slowest velocity, $k_{sn}{}^{mp}$ contributes almost 10 percent of the total variation, but only 5.5 and 4.1 percent at 100 and 500 m/d, respectively (table 16). This result presumably is due to the greater role of settling on soil storage in slow-flowing water; faster flowing water carries more of the decomposing material out of the simulation cell before it has time to settle in the soil. About half of the variation in $S^{o}]_{acr}$ at 100 and 500 m/d is due to interactions, but only 40 percent at 50 m/d.

The first-order effects on $C_{sw}{}^{pl}]_{o,tf}$ (table 18) are dominated at 50 and 100 m/d by $k_{sf}{}^{pl}$ (12.2 and 11.2 percent, respectively), $X_{pl}{}^{P}$ (7.5 and 15.9 percent, respectively) and $k_g{}^{mp}$ (11.8 and 5.3 percent, respectively). At 500 m/d, $k_g{}^{pl}$ and $k_{1/2}{}^{pl}$ become the major contributors (12.7 and 11.3 percent, respectively). $C^{mp}]_{acr}$ is subject to stronger first-order influence at 50 and 500 m/d, for which $X_{mp}{}^{P}$ contributes the largest portion of the total variation at these velocities (64.2 and 71.2 percent, respectively) (table 19). At 100 m/d, contributions are more diffuse; linear effects total 43 percent, of which only $X_{mp}{}^{P}$ accounts for more than 10 percent.

The tabulated values for the interaction effects of each parameter represent their total contribution to output variation through interactions with *all* other parameters, and shading indicates exceedence of a relatively low threshold value of 5 percent. The comparative lack of shaded cells for the interactions portion of level 1 and 2 results (tables 14-18) is indicative of a substantially lower contribution to variability from interactions at these levels. Level-3 results differ greatly in that interaction effects for every parameter are shaded for all outputs at this level (tables 14-19), corroborating the strong dominance of interactions at this level noted from the Morris method results and lower first-order totals. In one exception, extensive shading of level-2 results of interaction effects for $C_{sw}{}^{P}]_{o,tf}$ (table 14) show the increased role of such interactions at this level under slower velocities. This trend was expected given the reduced total first-order contributions at the lower velocities.

Analysis and Assessment of Model Uncertainty from Fourier Amplitude Sensitivity Test (FAST) Simulations

Mathematical models provide an alternative to field monitoring that potentially can save time, reduce cost, and minimize the need for testing management alternatives, although the uncertainty of the model results is a major concern. If model uncertainty is not evaluated formally, the science and value of the model will be undermined (Beven, 2006). The issue of uncertainty of model outputs has implications for policy, regulation, and management, but the source and magnitude of uncertainty and its effect on water-quality assessment has not been studied comprehensively (Beven, 2006; Muñoz-Carpena and others, 2006; Shirmohammadi and others, 2006). Reckhow (1994) proposed that although uncertainty assessment can improve risk assessment and decision making, it does not eliminate uncertainty nor change the fact that, because of uncertainty, some decisions will have consequences other than those anticipated. Rather, the explicit integration of uncertainty in water-quality modeling studies should help improve environmental management and decision making.

Following the approach used in Morgan and Henrion (1990), probabilistic and cumulative distribution functions (PDFs and CDFs, respectively) were constructed to communicate the uncertainty graphically. The CDFs are useful for depicting probabilities of exceedance and confidence. The model was applied to a generic site, however, and parameters were tested over the entire range of feasible values for southern Florida wetland ecosystems, with the purpose of evaluating the sensitivity and uncertainty trends across the range of possible conditions. Given the intentional generality of this sensitivity and uncertainty analysis, meaningful interpretation of specific outcomes, such as the chance of exceeding a particular output value or defining confidence intervals, is not practically useful, and a separate uncertainty analysis is needed for each individual application of the model (Muñoz-Carpena and others, 2007). The application herein remains important, however, and is included to (1) guide future such applications in which uncertainty measures are the goal, and (2) complement the exploration of the wetland system dynamics achieved during the global sensitivity analysis of the model.

The primary focus of this particular uncertainty analysis is the PDFs, which help provide the insight needed to explain some unexpected trends previously mentioned in the sensitivity analysis, and to further explore how model structure and flow velocity affect sensitivity and uncertainty. Results of this analysis correspond to a "worst case scenario" in which all of the potentially sensitive model parameters, from 8 to 16 depending on complexity level, are allowed to vary across the complete parametric space identified in an extensive literature review; parameters and their associated distributions are presented in table 4.

Measures of output uncertainty were obtained directly from the FAST analysis conducted to quantify sensitivity. Figures 32 to 34 depict both the probability and cumulative distribution functions for the outputs of levels 1, 2 and 3, respectively, and table 20 presents summary statistics of the uncertainty results. Three main elements can be observed and interpreted from the probability distributions obtained. First, the slope and range of the PDFs are indicative of the uncertainty and range in the model output results. In addition, any shifting between PDFs for different velocities provides information about the effects of velocity on output uncertainties. Finally, any apparent discontinuities in the PDFs, indicating bimodality of output distributions, also will be helpful for interpreting model results.

Level-1 Uncertainty

The sensitivity analysis provides insight about the strength of the relation between a parameter and an output, and how that relation may vary with changing flow velocity or structure; it does not identify the actual relation between an output and the velocity or structure itself. Results of the earlier Morris and extended FAST analyses indicated no apparent influence of velocity on the sensitivity of outputs to parameters in level 1. Although the sensitivity to parameters may not have changed significantly, the uncertainty analysis results show that in the case of $C_{sw}{}^{P}]_{o,tf}$, the output itself is indeed sensitive to velocity (fig. 32A); as velocity increases, so too does the uncertainty of $C_{sw}{}^{P}]_{o,tf}$. This effect on uncertainty is absent for the remaining outputs at this level ($C_{pw}{}^{P}]_{acr}$, $S^{o}]_{acr}$, and $S_{si}{}^{P}]_{acr}$) (figs. 32B-D), which can be explained by the fact that they represent the stabile components. These components do not move with the flowing water and are largely isolated from the water column in level 1 by the slow process of diffusion. Consequently, velocity effects are secondary, whereas the mobile SRP concentration in the surface water is directly affected by changes in velocity through the dispersion term of the transport equation (A.I. James, University of Florida, written commun., 2008).

The process of dispersion is embodied by the dispersion coefficient (D_l), which is itself a function of the product of dispersivity (predominantly λ_l) and flow velocity ($D_l = \lambda_l v_l$). Because the distribution and range of the dispersivity are consistent across velocities, the dispersion becomes a function of velocity. At low velocities, there is little dispersive spreading of the SRP that enters through the boundary; the phosphorus remains "together" as it moves through the model in a quasi-plug flow manner. With increased velocity, and hence, dispersion, some of the SRP travels through the system at different rates, introducing the log-normal effect seen in the PDF for this output in level 1 (fig. 32). Further increasing the velocity increases this spread and associated skewness, hence the observed difference between CDFs and PDFs with velocity. The observed spread in $C_{sw}{}^{P}]_{o,tf}$ and the absence of this spread for the stabile components is, therefore, an important validation of the dispersion mechanics in the transport code of the model, further illustrating the usefulness of this analysis as a general verification of model performance.

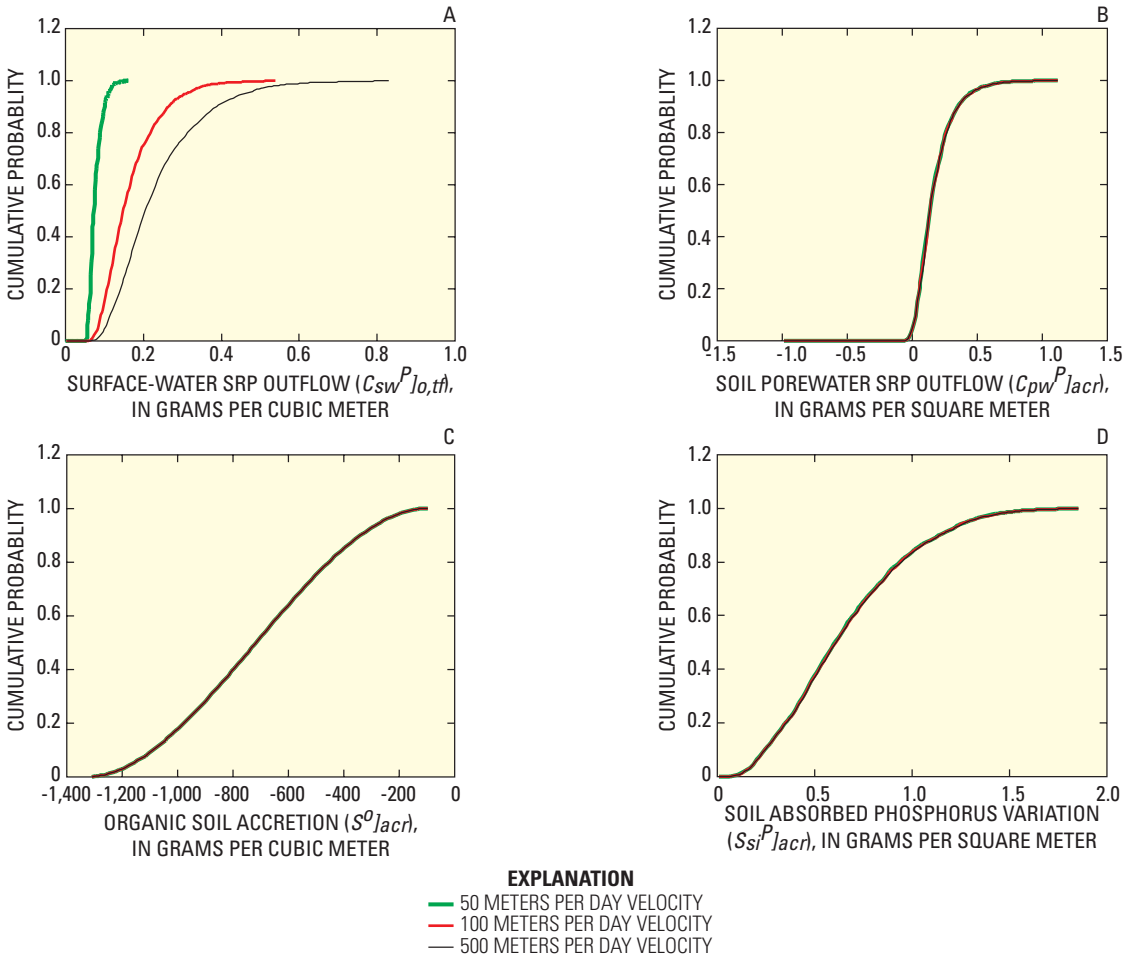

Figure 32. Probability distributions for level-1 outputs obtained from the global analysis of uncertainty based on Fourier Amplitude Sensitivity Test (FAST) results. SRP is soluble reactive phosphorus. Parameters are defined in appendix 1.

For level 1, the results indicate that the CDF slope for surface-water SRP decreases as velocity increases. The sharp rise in surface-water SRP at 50 m/d indicates a narrow range of possible outcomes, with nearly 100-percent certainty that the output will be less than 0.1 g/cm^3. As velocity increases, so too does the uncertainty and possibility of exceeding an arbitrary value for $C_{sw}{}^{P}]_{o,tf}$, such as 0.2 g/m^3. For 100 m/d, about 80 percent of the outcomes will be less than this value, whereas at 500 m/d this likelihood drops to about 40 percent. Because no values as large as 0.2 g/m^3 were obtained at 50 m/d, there is no possibility of exceeding the stipulated value at this velocity.

Level-2 Uncertainty

These fundamental relations with velocity would be expected to persist in the level-2 results, and figure 33 shows this is indeed the case. Outputs for stabile components remain insensitive to velocity changes; mobile outputs, which include $C_{sw}{}^{pl}]_{o,tf}$ at this level, are again seen to be affected by velocity. The change in complexity appears to have no effect on the uncertainty of any stabile outputs, and their range and distribution for level 2 appear almost identical to those observed for level 1 (table 20). The influence of velocity on $C_{sw}{}^{P}]_{o,tf}$ persists, but the distinction is substantially less obvious between 50 and 100 m/d than between 100 and 500 m/d (fig. 33). The uncertainty in $C_{sw}{}^{P}]_{o,tf}$ is reduced at all velocities in level 2, as indicated by the reduced standard deviations listed in table 20, but the general trend of increasing uncertainty with increasing velocity is still evident. Initially, this result was unexpected because increasing the number of parameters, each with their own intrinsic uncertainty, should increase uncertainty in the model output. Also unexpected is the large change in the profile of the distributions. Specifically, the respective skewness for the 50- and 100-m/d cases increases from 1.3 and 1.4 in level 1 to 3.4 and 7.9 in level 2; for the 500 m/d case, skewness drops from 1.4 to 0.2. This latter observation indicates that the high velocity creates a system with very different phosphorus dynamics than those for lower velocities.

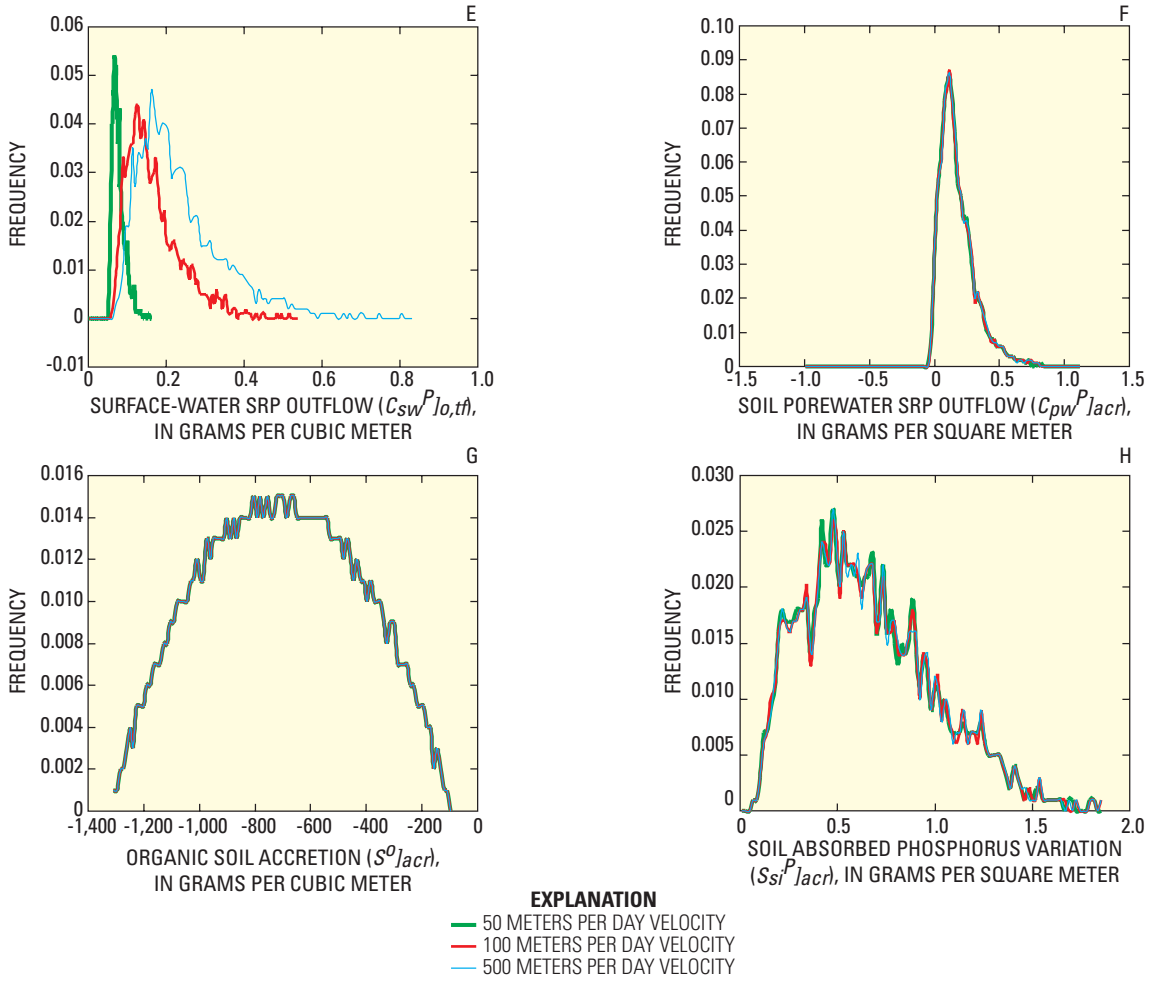

Figure 32. Probability distributions for level-1 outputs obtained from the global analysis of uncertainty based on Fourier Amplitude Sensitivity Test (FAST) results—Continued. SRP is soluble reactive phosphorus. Parameters are defined in appendix 1.

These unexpected trends can be explained through close examination of figure 33. As noted for the sensitivity analysis results, $C_{sw}{}^{P}]_{o,tf}$ sensitivity dynamics in level 2 changed substantially with velocity, as indicated by the output uncertainty results. Although the quantified differences mean little given the generality of the application, the trends are important. The PDF at 500 m/d is clearly diverging from those of the lesser velocities, and ultimately becomes negatively skewed relative to them in level 3 (table 20). This inversion of output dynamics is due to the introduction of an interdependent sink for surface-water SRP in the form of uptake by plankton. Compared with the observed results for $C_{sw}{}^{P}]_{o,tf}$, plankton mass ($C_{sw}{}^{pl}]_{o,tf}$) has an inverted relation with velocity, and actually exhibits decreased uncertainty with increasing velocity. At slower velocities (50 and 100 m/d) planktons take longer to reach the output cells when exiting the modeled domain and, thus, remain in the system longer and consume more SRP. A slower flow rate also means slower replenishment of SRP supplied to the modeled system by means of the boundary conditions. Because a constant concentration for $C_{sw}{}^{P}$ of 0.05 g/m^3 was set for the initial and boundary conditions, a faster flow rate inputs more SRP to the system.

This combination of less supply and greater uptake depleted nearly all of the SRP in the water column in many of the simulations, as indicated by the means for level 2 $C_{sw}{}^{P}]_{o,tf}$ in table 20. The initial mass of plankton selected would also have influenced these dynamics; specifically, a larger population would deplete the SRP more quickly than a smaller population. However, this initial condition was consistent for all cases studied, and meaningful conclusions can, therefore, be made. A velocity of 500 m/d appears sufficient to maintain SRP levels in the water column throughout the simulation by supplying more SRP at the boundary, given the faster flow at the same concentration, and by transporting plankton away before the population in a given cell grows large enough to consume all of the available SRP. This conclusion appears to be supported by the results for $C_{sw}{}^{pl}]_{o,tf}$, which show that at 500 m/d, the mean for $C_{sw}{}^{pl}]_{o,tf}$ is substantially less than that obtained at 50 and 100 m/d (table 20).

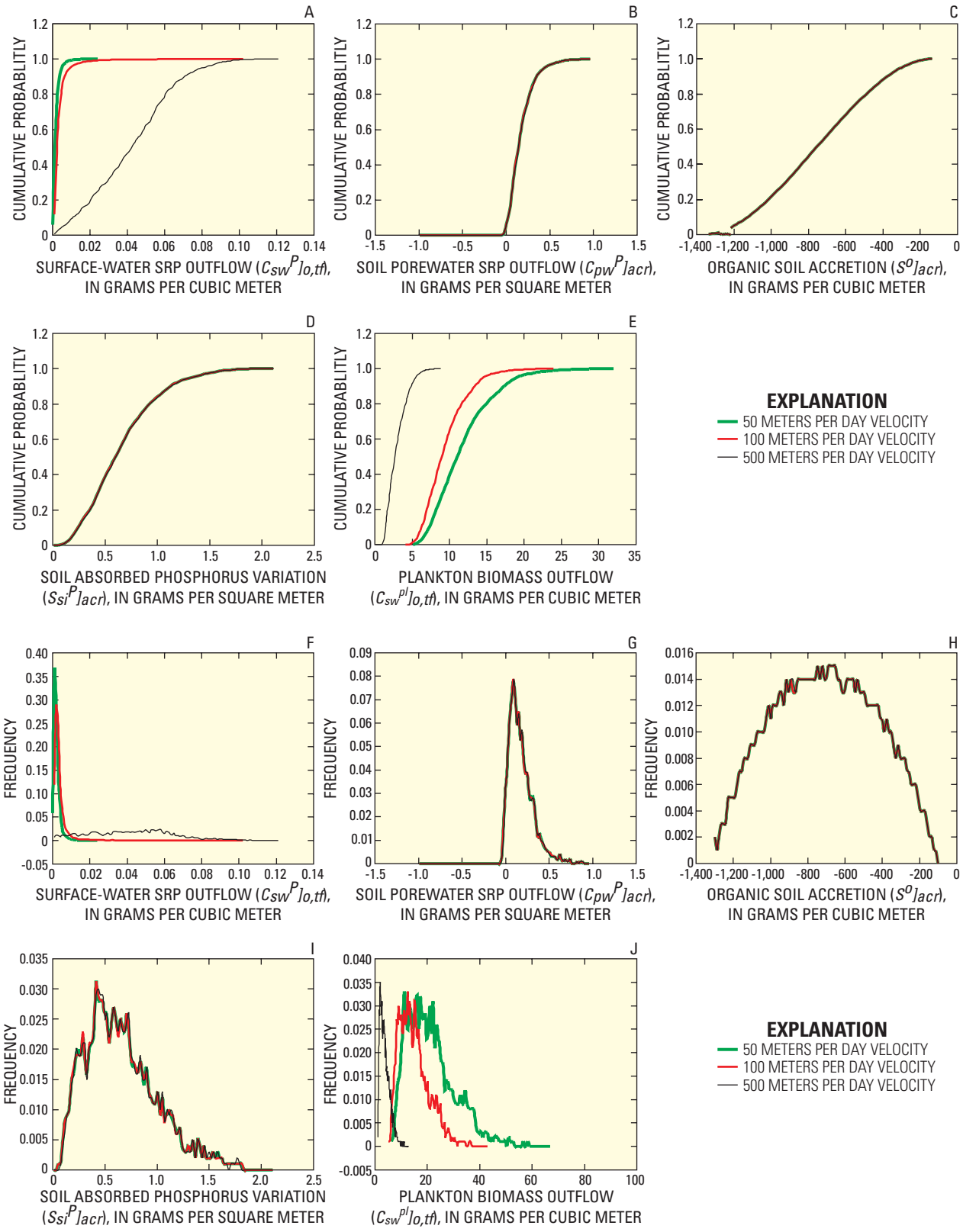

Figure 33. Probability distributions for level-2 outputs obtained from the global analysis of uncertainty based on Fourier Amplitude Sensitivity Test (FAST) results. SRP is soluble reactive phosphorus. Parameters are defined in appendix 1.

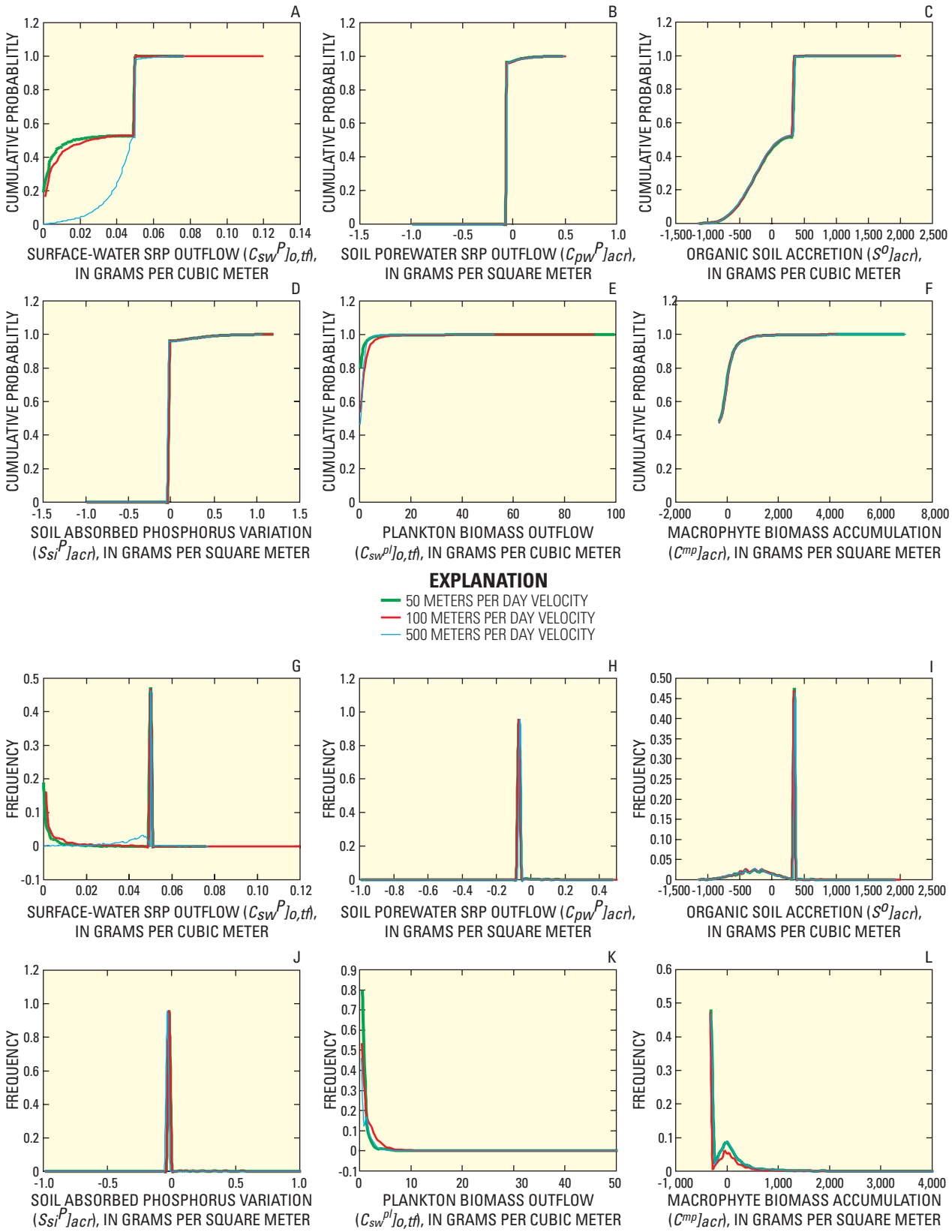

Figure 34. Probability distributions for level-3 outputs obtained from the global analysis of uncertainty based on Fourier Amplitude Sensitivity Test (FAST) results. SRP is soluble reactive phosphorus. Parameters are defined in appendix 1.

Table 20. Summary statistics for output probability distributions.

[Parameter descriptions are provided in table 4. Units for mobile outputs are grams per cubic meter ($C_{sw}{}^{P}]_{o,tf}$, $C_{sw}{}^{P}]_{o,t}$, $C_{sw}{}^{pl}]_{o,tf}$, $C_{sw}{}^{pl}]_{o,t}$). Units for stabile outputs are grams per square meter ($C_{pw}{}^{P}]_{acr}$, $S^{o}]_{acr}$, $S_{si}{}^{P}]_{acr}$, $C^{mp}]_{acr}$). SD, standard deviation; SE, standard error; Q, quartile]

Output	Level	Velocity (m/d)	Range	Mean	Median	SD	SE mean	Minimum	Q1	Q2	Q3	Maximum	Skew	Kurtosis
$C_{sw}{}^{P}]_{o,tf}$	1	50	0.11	0.08	0.07	0.02	0.00	0.05	0.07	0.07	0.09	0.16	1.3	5.0
	1	100	.47	.17	.15	.07	.00	.06	.12	.15	.20	.54	1.4	5.4
	1	500	.77	.24	.21	.11	.00	.07	.16	.21	.29	.84	1.4	5.7
	2	50	.02	.00	.00	.00	.00	.00	.00	.00	.00	.02	3.4	24.4
	2	100	.10	.00	.00	.01	.00	.00	.00	.00	.00	.10	7.9	104.7
	2	500	.12	.04	.04	.02	.00	.00	.02	.04	.06	.12	.2	2.5
	3	50	.08	.03	.02	.02	.00	.00	.00	.02	.05	.08	.0	1.1
	3	100	.12	.03	.03	.02	.00	.00	.00	.03	.05	.12	.0	1.2
	3	500	.08	.04	.05	.01	.00	.00	.04	.05	.05	.08	-1.8	6.7
$C_{sw}{}^{P}]_{o,t}$	1	50	.07	.07	.06	.01	.00	.05	.06	.06	.07	.12	1.4	5.5
	1	100	.25	.11	.10	.04	.00	.06	.08	.10	.13	.30	1.5	5.8
	1	500	.35	.13	.12	.05	.00	.06	.10	.12	.15	.41	1.5	5.9
	2	50	.05	.01	.01	.00	.00	.00	.01	.01	.01	.05	2.6	15.4
	2	100	.08	.01	.01	.01	.00	.00	.01	.01	.01	.08	3.8	27.2
	2	500	.09	.04	.04	.02	.00	.00	.03	.04	.05	.09	-.1	2.4
	3	50	.07	.03	.03	.02	.00	.00	.01	.03	.05	.07	.0	1.1
	3	100	.08	.03	.03	.02	.00	.00	.01	.03	.05	.08	-.1	1.2
	3	500	.06	.04	.05	.01	.00	.00	.04	.05	.05	.06	-2.0	7.0
$C_{pw}{}^{P}]_{acr}$	1	50	1.16	.18	.15	.14	.00	-.04	.08	.15	.24	1.13	1.6	7.1
	1	100	1.17	.18	.15	.14	.00	-.04	.08	.15	.25	1.13	1.6	7.1
	1	500	1.17	.18	.15	.14	.00	-.04	.08	.15	.25	1.13	1.6	7.1
	2	50	1.01	.18	.15	.14	.00	-.04	.08	.15	.25	.97	1.4	5.9
	2	100	1.01	.18	.15	.14	.00	-.04	.08	.15	.25	.97	1.4	5.9
	2	500	1.01	.18	.15	.14	.00	-.04	.08	.15	.25	.97	1.4	5.9
	3	50	.56	-.07	-.07	.04	.00	-.07	-.07	-.07	-.07	.49	8.3	84.8
	3	100	.59	-.06	-.07	.04	.00	-.07	-.07	-.07	-.07	.51	7.8	75.2
	3	500	.57	-.06	-.07	.04	.00	-.07	-.07	-.07	-.07	.50	7.7	70.8
$S^{o}]_{acr}$	1	50	1,212.0	-710.1	-711.4	275.1	3.9	-1,314.5	-924.5	-711.4	-497.0	-102.4	0.0	2.1
	1	100	1,212.0	-710.1	-711.4	275.1	3.9	-1,314.5	-924.5	-711.4	-497.0	-102.4	0.0	2.1
	1	500	1,212.0	-710.1	-711.4	275.1	3.9	-1,314.5	-924.5	-711.4	-497.0	-102.4	0.0	2.1
	2	50	1,206.4	-710.3	-712.0	275.3	3.9	-1,305.9	-924.4	-712.0	-496.6	-99.5	0.0	2.1
	2	100	1,206.4	-710.3	-712.0	275.3	3.9	-1,305.9	-924.4	-712.0	-496.6	-99.5	0.0	2.1
	2	500	1,206.4	-710.3	-712.0	275.3	3.9	-1,305.9	-924.4	-712.0	-496.6	-99.5	0.0	2.1
	3	50	3,178.6	21.4	177.5	377.0	5.3	-1,154.5	-289.5	177.5	351.2	2,024.1	-0.6	2.3
	3	100	3,199.7	17.3	149.2	376.1	5.3	-1,174.3	-289.6	149.2	351.3	2,025.4	-0.6	2.3
	3	500	3,196.5	14.1	140.6	379.9	5.4	-1,178.7	-293.8	140.6	351.9	2,017.7	-0.6	2.2

Table 20. Summary statistics for output probability distributions.—Continued

[Parameter descriptions are provided in table 4. Units for mobile outputs are grams per cubic meter ($C_{sw}{}^{P}]_{o,tf}$, $C_{sw}{}^{P}]_{o,t}$, $C_{sw}{}^{pl}]_{o,tf}$, $C_{sw}{}^{pl}]_{o,t}$). Units for stabile outputs are grams per square meter ($C_{pw}{}^{P}]_{acr}$, $S^{o}]_{acr}$, $S_{si}{}^{P}]_{acr}$, $C^{mp}]_{acr}$). SD, standard deviation; SE, standard error; Q, quartile]

Output	Level	Velocity (m/d)	Range	Mean	Median	SD	SE mean	Minimum	Q1	Q2	Q3	Maximum	Skew	Kurtosis
$S_{si}{}^{P}]_{acr}$	1	50	1.81	.66	.62	.34	.01	.06	.41	.62	.88	1.86	.6	3.0
	1	100	1.81	.67	.62	.34	.01	.06	.41	.62	.88	1.86	.6	2.9
	1	500	1.81	.67	.62	.34	.01	.06	.42	.62	.88	1.87	.6	2.9
	2	50	2.07	.66	.61	.35	.01	.04	.41	.61	.86	2.12	.8	3.4
	2	100	2.08	.66	.61	.35	.01	.04	.41	.61	.86	2.12	.8	3.4
	2	500	2.08	.66	.61	.35	.01	.05	.41	.61	.86	2.12	.8	3.4
	3	50	1.23	-.01	-.03	.09	.00	-.03	-.03	-.03	-.03	1.20	6.9	57.0
	3	100	1.23	-.01	-.03	.09	.00	-.03	-.03	-.03	-.03	1.20	6.8	56.2
	3	500	1.10	-.01	-.03	.09	.00	-.03	-.03	-.03	-.03	1.08	6.7	54.1
$C_{sw}{}^{pl}]_{o,tf}$	2	50	61.19	21.37	19.74	9.28	.13	6.04	14.28	19.74	26.21	67.22	1.0	4.1
	2	100	38.06	14.94	13.94	5.76	.08	5.02	10.55	13.94	18.06	43.08	1.0	4.0
	2	500	11.73	3.76	3.39	1.84	.03	1.02	2.29	3.39	4.85	12.75	1.0	4.0
	3	50	151.07	.77	.13	3.34	.05	.00	.00	.13	.80	151.07	26.8	999.8
	3	100	92.34	1.53	.72	3.48	.05	.00	.00	.72	2.08	92.34	12.3	244.0
	3	500	52.85	1.06	.83	1.86	.03	.01	.01	.83	1.55	52.86	10.1	200.4
$C_{sw}{}^{pl}]_{o,t}$	2	50	26.97	11.88	11.19	4.01	.06	5.11	8.84	11.19	14.01	32.08	1.0	4.4
	2	100	19.43	9.54	9.08	2.85	.04	4.57	7.39	9.08	11.06	24.00	1.0	4.3
	2	500	7.95	3.00	2.74	1.34	.02	.96	1.92	2.74	3.86	8.91	.9	3.4
	3	50	82.89	1.10	.60	2.28	.03	.00	.00	.60	1.60	82.89	14.8	414.6
	3	100	55.36	1.56	1.00	2.66	.04	.00	.00	1.00	2.31	55.36	7.3	104.8
	3	500	34.48	.97	.80	1.49	.02	.01	.01	.80	1.47	34.49	6.8	103.2
$C^{mp}]_{acr}$	3	50	7,380.8	-91.6	-212.2	382.2	5.4	-348.7	-348.7	-212.2	58.7	7,032.2	4.2	44.8
	3	100	4,772.3	-92.9	-208.1	361.1	5.1	-348.7	-348.7	-208.1	57.2	4,423.6	3.1	22.3
	3	500	7,388.1	-83.5	-192.2	388.5	5.5	-348.7	-348.7	-192.2	63.3	7,039.5	4.1	43.0

The consequences of these dynamics for the quantified uncertainty measures are deduced from the CDFs shown in figure 33. As expected, the CDFs for the stabile outputs are essentially unchanged. For $C_{sw}{}^{P}]_{o,tf}$, there is almost a 100-percent likelihood that velocities up to 100 m/d will result in almost zero surface-water SRP by the end of the 1-month simulation period. At 500 m/d, the CDF resembles that from a PDF with a β-distribution, as seen in the PDF and CDF for $S^{o}]_{acr}$ in level 1 (fig. 32). In that case, the only influence on the organic soil store is the oxidation rate, k_{ox}, which was given a β-distribution as shown in table 4, and the resulting output PDF would, thus, be expected to follow the same pattern. Given the earlier conclusion that increased velocity negated the limiting effect of depleted surface-water SRP on plankton growth, it is possible to assume that the plankton growth occurs largely at rates stipulated by the growth parameters, which themselves were also assigned β-distributions. With respect to $C_{sw}{}^{pl}]_{o,tf}$, if 10 g/m^3 was chosen as an arbitrary value of interest for plankton (suspended solids) output, then 100 percent of the simulations at 500 m/d would have outputs less than this, about 60 percent at 100 m/d, and about 40 percent at 50 m/d.

Level-3 Uncertainty

Velocity does not appear to substantially affect uncertainty results for any of the outputs except $C_{sw}^{P}]_{o,tf}$ (fig. 34). Along with $S^{o}]_{acr}$ and $C^{mp}]_{acr}$, however, $C_{sw}^{P}]_{o,tf}$ exhibits bimodality, which indicates that the system is characterized by a set of critical conditions (flow velocity, parameter values, and initial and boundary conditions) that, when exceeded, create distinct sets of results. Three of the six outputs ($C_{pw}^{P}]_{acr}$, $S_{si}^{P}]_{acr}$ and $C_{sw}^{pl}]_{o,tf}$) do not exhibit bimodality, and although their respective ranges are very large, the standard deviations are low, and consequently, the uncertainty is reduced by the increased complexity in this case. As in level 2, this seems somewhat contradictory, because increasing the number of uncertain parameters in a model typically increases the net uncertainty of the results. However, a large proportion of the simulations provide similar results, due to the collapse of one or more pools as the critical conditions mentioned above were exceeded, thereby reducing the range of final values and, thus, the net uncertainty.

$C_{sw}^{P}]_{o,tf}$ has two distinct phases in level 3 (fig. 34), one analogous to that shown in level 2 (fig. 33) where SRP results at 500 m/d are distinctly different to those at 50 and 100 m/d (and is now in fact negatively skewed), and another where results are consistently about 0.05 g/m^3, which is the value set for the initial and boundary conditions. The fact that the value has not changed by the end of the simulation implies that the plankton population is small. This explanation is supported by the PDF for $C_{sw}^{pl}]_{o,tf}$ in level 3 (fig. 33), which shows that a large proportion of the results was close to zero. The macrophytes, $C^{mp}]_{acr}$, also exhibit a bimodal response (fig. 34); a negative net accumulated mass appears to occur almost half of the time, which implies that conditions were such that the initial macrophyte store could not be maintained over the simulation and that a large proportion of the original mass was lost. The remainder of the simulations produced a more continuous set of results, ranging from negative to positive growth outcomes.

These trends are mirrored by results for $S^{o}]_{acr}$ (fig. 34), which show a large spike representing the many cases in which the macrophyte population failed to grow and the senesced material was deposited and incorporated into the organic soil store. The shallower portion of the PDF is more akin to the results for levels 1 and 2, and represents the cases in which macrophytes continued to grow and hold the bulk of their foliage. Results for $C_{pw}^{P}]_{acr}$ (fig. 34) provide further support for this explanation; almost all simulations resulted in completely depleted pore-water SRP. As presented in table 20, the median value at all velocities was -0.07 g/m^2 compared with the initial condition of 0.071 g/m^2. Under these conditions, macrophytes would have been limited by phosphorus, and could not have grown any faster than diffusion rates would permit SRP to reenter the soil, assuming surface-water SRP was not depleted at the time, or oxidation of the soil would release SRP into the pore water. It appears that in half of the cases, conditions were insufficient to support the initial macrophyte density, resulting in depleted pore-water phosphorus, minimal growth, and subsequent widespread senescence. In half of the cases, however, it appears that conditions were able to support a macrophyte population; such results must represent values for combinations of factors that might include higher soil oxidation rates (releasing more SRP into the pore water), lower growth rates or senescence rates, and even reduced adsorption and diffusion. In almost all simulations, adsorbed phosphorus was completely depleted (the median value for $S_{si}^{P}]_{acr}$ is -0.03 g/m^2, which equates to a loss of all 0.03 g/m^2 input as the initial condition), and implies that pore-water SRP must have been low for a long time.

The bimodality complicates interpretation of the uncertainty measures for many of the CDFs. The frequencies indicated by the PDF spikes are corroborated by the cumulative measures. In this hypothetical case, and almost 100 percent of the time, results for C_{pw}^{P} and S_{si}^{P} were about 0 g/m^2, regardless of velocity. The outputs $C_{pw}^{P}]_{acr}$ and $S_{si}^{P}]_{acr}$ were in deficit by amounts equal to their respective initial conditions. Plankton mass would be expected to drop to zero marginally less than 50 percent of the time at 500 m/d, just more than 50 percent of the time at 100 m/d, and about 80 percent of the time at 50 m/d. Regardless of velocity, there would be about a 55-percent probability that organic soil accretion ($S^{o}]_{acr}$) would be consistently in the region of 300 g/m^2, but about a 50-percent probability there would be no net gain in soil mass. Macrophytes would have almost a 100-percent probability of losing net mass in this system, with about a 50-percent likelihood of specifically losing about 300 g/m^2. Finally, there is nearly a 100-percent probability of surface-water SRP at the output being less than the initial and boundary condition input; if 0.045 g/m^3 is the chosen limit (initial/boundary condition is 0.05 g/m^3), there is a 50-percent probability that the output will be less at 50 and 100 m/d, but only a 20-percent probability at 500 m/d.

These results highlight the importance of initial conditions within the simulation lengths used in this study, particularly for plankton and macrophytes. If the initial population of plankton is too large, it will rapidly take up all of the SRP in the water column and then cease to grow any further, dying off until the end of the simulation or until a population level is reached that can be supported by the minimal phosphorus added to the water column through diffusion, assuming macrophytes have not depleted pore-water SRP. Similarly, an initial macrophyte population that is too large to be realistically supported will rapidly extract all of the phosphorus from the pore water and then similarly cease to grow and progressively senesce, adding to the soil much of the initial mass and that accumulated through the rapid but brief growth phase until a density is reached that can be supported by the soil pore-water SRP.

Summary and Conclusions

Phosphorus is an essential element for all life and frequently is the limiting nutrient in oligotrophic wetlands. Although many models exist for the simulation of wetland hydrology, few suitable computational models exist for nutrient modeling. The current study focuses on the conceptualization, development, and application of a spatially distributed water-quality model to simulate phosphorus dynamics and transport in wetlands. An integral component of this research involved the calibration and validation of the model, which was applied to the Everglades of southern Florida. A global analysis of sensitivity and uncertainty was also conducted.

Conceptually, the model considers physical and biogeochemical transfers between stores, and transports those elements that move with flowing surface water. Three main compartments can be defined containing stores that are modeled: biomass (phytoplankton, macrophytes, and biofilm), the water column (dissolved constituents, suspended solids), and soil (soil pore water and soil solids). Physical transfers include surface-water flow, atmospheric deposition, pore-water/surface-water interactions, settling and entrainment of particulate matter, sloughing and cohesion of biofilm, sorption and desorption, and mineral precipitation. Biological transfers include growth; senescence and decay of biological tissues; and soil oxidation, mineralization, and burial.

The model has been developed to be flexible in its application. Through the input interface, the user may choose which stores and processes to include or exclude, as well as what particular equation to use to describe a process. The model was calibrated for three different experimental datasets, representing three increasingly complex levels of potential application. For the simplest case (level 1), the model was calibrated to data from a laboratory soil core study, which measured SRP flux out of the soil and into the water column without the influence of macrophytes or phytoplankton. From this, a bioturbation factor was determined and found to control the model predictions when compared to the dataset. Data from an outdoor mesocosm study was used for an application of intermediate complexity (level 2). The model was calibrated against data for phosphorus released from flooded soil to the water column, under natural conditions, and for surface-water suspended solids and dissolved phosphorus. The third, most complex (level 3) case was a 147-ha field site—Cell 4 of STA-1W. This application incorporated new complexities such as through-flowing water, suspended and dissolved components, and active periphyton and macrophyte communities. Using some values obtained from calibration for the two simpler previous cases and data from a number of STA-1W studies, a successful calibration and validation for this field-site case was conducted. Finally, a spatially distributed application of the model on Cell 4 of STA-1W is presented using the same dataset referenced earlier. Overall the model was found to respond well to the case studies.

The model applications described herein have demonstrated a flexible modeling framework that enables simulation of phosphorus cycling using a variety of model complexity levels. For example, in level 1, phosphorus exchange was considered only between soil and water. The same general framework was extended in levels 2 and 3 to include phosphorus exchange with plankton and macrophytes. Furthermore, the level-2 applications demonstrated the ability of such a flexible framework to accurately capture phosphorus cycling dynamics in systems with different initial conditions. The first level-3 application showed that this phosphorus modeling framework can be applied even at the field scale. This application also showed the limitations of modeling field-scale systems as homogeneous units, because such approaches are unable to capture spatial trends that have been observed in field data. Finally, the second level-3 application demonstrated the potential utility of coupling hydrodynamic and biogeochemical models to simulate spatially and temporally varying processes. This model was able to capture general temporal trends in phosphorus import/export from a treatment wetland while also accurately simulating the transient spatial trends in soil phosphorus accrual.

Although sensitivity and uncertainty analyses are an essential part of the development and application of hydrologic and water-quality models, they are frequently overlooked. “One-at-a-time,” derivative-based techniques do not evaluate sensitivity over the entire parametric space of a given parameter, and their validity relies on linear output response. This is rarely encountered in hydrologic or water-quality models and, thus, an alternative “global” sensitivity approach is more appropriate. A modern model evaluation framework for hydrologic and water-quality models is applied to the new wetland phosphorus water-quality model for the purpose of conducting a comprehensive evaluation of the model sensitivity and uncertainty dynamics, and the susceptibility of these dynamics to effects from changing model structure or velocity. This framework combines two types of global sensitivity analysis techniques, a “Morris” screening method and a variance-based FAST technique, in conjunction with an uncertainty analysis that is based on extended FAST results.

One outcome of these analyses is quality assurance of the computer code generated from the conceptual model presented; that is, the model response to changes in input factors over their expected range matches the underlying conceptual model. This model assurance is generally difficult to achieve, because the users typically do not formally explore such a large number of combinations as those included in the global analyses.

For the purpose of calibration, the analyses provided the identification of the important model parameters. The Morris method efficiently screened the model parameters in levels 1 and 2, and predicted trends in sensitivity that were corroborated well with FAST results. For level 1, the organic soil oxidation rate, k_{ox}, was consistently ranked most important, followed by three other parameters: the diffusion coefficient, k_{df}; the soil bulk density, ρ_b; and the mass fraction of phosphorus in organic soil, $X_{so}{}^{P}$. These results are in agreement with current understanding of the physical system, because the principal source of new phosphorus to the level-1 system is from oxidation of the soil (controlled by k_{ox}), and the pore-water SRP (and, hence, the adsorbed phosphorus) is controlled by the other three parameters. The SRP in the water column is more sensitive to k_{df}, because this parameter represents the limiting process of diffusion through which the surface water gains new phosphorus. These trends persist across outputs in the level-2 results, with the only notable difference being the prominence of plankton growth parameters in the ranking for mobile outputs (outflow of surface-water SRP and plankton biomass). Level-3 results do not exhibit any pattern of parameter dominance across the different outputs. The Morris qualitative results for the more complex level 3 indicate that the majority of the level-3 variance is due to interactions and that a quantitative investigation of the output variance using the FAST analysis is required to more clearly understand the sensitivity dynamics. The stronger additivity of the model in the level-1 and level-2 cases suggests that an efficient calibration in most field situations is possible.

Model sensitivity to velocity is correlated with model complexity. Velocity had no discernible effect on the sensitivity of outputs for stabile components in levels 1 and 2. Mobile components were similarly unaffected in level 1; but in level 2, surface-water SRP was subject to variable effects from interactions, depending on velocity. Plankton mass was much more sensitive to plankton growth parameters at higher velocities and with soil parameters at lower velocities. Velocity effects in level 3 became apparent for stabile outputs, and remained important for mobile cases. Increasing the velocity increased the uncertainty in surface-water SRP, but reduced the uncertainty in plankton biomass. The first result is expected, given the direct relation between SRP transport as a solute and velocity in the dispersion term of the transport equation. The second result, however, is less intuitive and only became apparent through the uncertainty analysis. A nonlinear relation between plankton mass and velocity exists as plankton takes up SRP from the water column with growth, but is simultaneously transported much like the SRP itself.

The uncertainty analysis provided important support for accurate interpretation of the sensitivity results, and the combined analyses served as a powerful tool for analyzing wetland system dynamics. Increased velocity increased the uncertainty in surface-water SRP, but decreased the uncertainty in plankton mass. Uncertainty of stabile components is largely unaffected by velocity. Critical states of the system were apparent due to the observed decrease in uncertainty with increased complexity for many cases. Increasing the number of parameters, each with an inherent uncertainty, typically is expected to increase output uncertainty. However, PDFs and CDFs examined in the uncertainty analysis indicated that many of the simulations ended in the collapse of one or more stores to a fixed output value, thereby reducing the net range and deviation of the output distributions. This outcome was determined to be caused by the combined effect of sets of values for input parameters, in conjunction with initial conditions that together exceeded sustainable conditions for the system. The model sensitivity to initial conditions of the biological stores that accumulate mass and extract phosphorus is an important outcome of this process.

The results indicate that the inclusion of macrophytes in more complex representations of wetland systems of southern Florida substantially affect the model dynamics. When included, the macrophyte component tends to dictate much of the phosphorus dynamics, and can greatly reduce the role of plankton. A number of other important considerations can be drawn from these analyses. First, it is necessary to accurately measure the oxidation rates and the labile phosphorus content of the oxidizing soil and sediments in areas where surface-water phosphorus input is low and the oxidation of the organics soil is an important contributor of phosphorus, such as in Everglades National Park. Second, the role of plankton is expected to be different under faster flowing conditions, such as in sloughs, than under slower flow conditions. In areas with faster flow velocities, better measurements of plankton growth parameters would be more beneficial compared with plankton settling rates and phosphorus mass fractions in low-flow environments. Finally, plankton, to the exclusion of macrophytes, dominates few wetlands in the Everglades, but examples do exist, such as in the experimental stormwater treatment areas adjacent to the EAA. In most real applications, a system more similar to level 3 is expected, with both macrophytes and plankton present. However, because the same plankton growth parameters are important for SRP in the water column, particularly when velocities are high, such measurements would be beneficial at multiple complexity levels. Similarly, predictions of plankton would be improved substantially by more accurate values for plankton growth parameters at high velocities, particularly in the absence of macrophytes, and phosphorous mass fractions at low velocities. It appears that plankton settling rates are more important for plankton outputs when macrophytes are present than when they are absent.

References Cited

Ahn, H., and James, R.T., 2001, Variability, uncertainty, and sensitivity of phosphorus deposition load estimates in South Florida: Water Air and Soil Pollution, v. 126, p. 37-51.

Allison, R.V., 1956, The influence of drainage and cultivation on subsidence of organic soils under conditions of Everglades reclamation: Soil and Crop Science Society of Florida Proceedings, v. 16, p. 21-31.

Alvarez, R., Evans, L.A., Milham, P.J., and Wilson, M.A., 2004, Effects of humic material on the precipitation of calcium phosphate: Geoderma, v. 118, p. 245-260.

American Public Health Association, 1992, Standard methods for the examination of water and wastewater (18th ed.): American Public Health Association, Washington, D.C.

Ariathurai, R., and Arulanandan, K., 1978, Erosion rates of cohesive soils: Journal of the Hydraulics Division-Asce, v. 104, p. 279-283.

Asaeda, T., and Van Bon, T., 1997, Modelling the effects of macrophytes on algal blooming in eutrophic shallow lakes: Ecological Modelling, v. 104, p. 261-287.

Baca, R.G., and Arnett, R.C., 1976, A limnological model for eutrophic lakes and impoundments: Batelle Inc., Pacific Northwest Laboratories, Richland, Wash.

Bauer, I.E., 2004, Modelling effects of litter quality and environment on peat accumulation over different time-scales: Journal of Ecology, v. 92, p. 661-674.

Bavor, H.J., Roser, D.J., McKersie, S.A., and Breen P., 1988, Treatment of secondary effluent: Report to Sydney Water Board, Sydney, Australia.

Beven, K., 1989, Changing Ideas in Hydrology—The case of physically based models: Journal of Hydrology, v. 105, p. 157.

Beven, K., 2006, On undermining the science?: Hydrological Processes, v. 20, p. 1-6.

Borchardt, M.A., 1996, Nutrients, *in* Stevenson, R.J., Bothwell M.L., and Lowe, R.L., eds., Algal Ecology—Freshwater Benthic Ecosystems: San Diego, Calif., Academic Press, p. 31-56.

Bowie, G.L., Mills, W.B., Porcella, D.B., Campbell, C.L., Pagenkopf, J.R., Rupp, G.L., Johnson, K.M., Chan, P.W., and Gherini, S.A., 1985, Rates, constants, and kinetics: Formulations in surface-water quality modeling (2d ed): Athens, Ga., U.S. Environmental Protection Agency Environmental Research Laboratory, Office of Research and Development.

Bridgham, S.D., Updegraff, K., and Pastor, J., 1998, Carbon, nitrogen, and phosphorus mineralization in northern wetlands: Ecology, v. 79, p. 1545-1561.

Campolongo, F., Cariboni, J., Saltelli, A., and Schoutens W., 2005, Enhancing the Morris method, *in* Hanson, K.M., and Hemez, F.M., eds., Sensitivity analysis of model output: Proceedings of the 4th International Conference on Sensitivity Analysis of Model Output (SAMO 2004), Los Alamos, N.M., p. 369-379.

Carignan, R., and Kalff, J., 1980, Phosphorus sources for aquatic weeds—Water or sediments: Science, v. 207, p. 987-989.

Carignan, R., and Kalff, J., 1982, Phosphorus release by submerged macrophytes—Significance to epiphyton and phytoplankton: Limnology and Oceanography, v. 27, p. 419-427.

Carlton, R.G., and Wetzel, R.G., 1988, Phosphorus flux from lake-sediments—Effect of epipelic algal oxygen production: Limnology and Oceanography, v. 33, p. 562-570.

Carr, G.M., Duthie, H.C., and Taylor W.D., 1997, Models of aquatic plant productivity: A review of the factors that influence growth: Aquatic Botany, v. 59, p. 195-215.

Carrick, H.J., Aldridge, F.J., and Schelske, C.L., 1993, Wind influences phytoplankton biomass and composition in a shallow, productive lake: Limnology and Oceanography, v. 38, p. 1179-1192.

CH2M HILL, 2002, Periphyton-Based Stormwater Treatment Area Research and Demonstration Project: Phase 1 and 2 summary report: Deerfield Beach, Fla., Report Prepared for South Florida Water Management District.

Chen, C.W., and Wells, J.T. Jr., 1976, Boise River modeling, *in* Canale, R.P., ed., Modeling Biochemical Processes in Aquatic Ecosystems: Ann Arbor, Mich., Ann Arbor Science Publishers, p. 171-204.

Chen, X.J., and Sheng, Y.P., 2005, Three-dimensional modeling of sediment and phosphorus dynamics in Lake Okeechobee, Florida: Spring 1989 simulation: Journal of Environmental Engineering-Asce, v. 131, p. 359-374.

Chimney, M.J., and Goforth, G., 2001, Environmental impacts to the Everglades ecosystem: A historical perspective and restoration strategies: Water Science and Technology, v. 44, p. 93-100.

Choi, J., and Harvey, J.W., 2000, Quantifying time-varying ground-water discharge and recharge in wetlands of the northern Florida Everglades: Wetlands, v. 20, p. 500-511.

Collins, C.D., and Wlosinski, J.H., 1989, A macrophyte submodel for aquatic ecosystems: Aquatic Botany, v. 33, p. 191-206.

Comas, X., Slater, L., and Reeve, A., 2004, Geophysical evidence for peat basin morphology and stratigraphic controls on vegetation observed in a Northern Peatland: Journal of Hydrology, v. 295, p. 173-184.

Corstanje R., Grunwald, S., Reddy, K.R., Osborne, T.Z., and Newman, S., 2006, Assessment of the spatial distribution of soil properties in a northern Everglades marsh: Journal of Environmental Quality, v. 35, p. 938-949.

Costanza, R., Sklar, F.H., and White, M.L., 1990, Modeling coastal landscape dynamics: Bioscience, v. 40, p. 91-107.

Cukier, R.I., Fortuin, C.M., Schuler, K.E., Petschek, A.G., and Schaibly, J.H., 1973, Study of the sensitivity of coupled reaction systems to uncertainties in rate coefficients. I - Theory: Journal of Computational Physics, v. 59, p. 3873-3878.

Cukier, R.I., Levine, H.B., and Schuler K.E., 1978, Nonlinear sensitivity analysis of multiparameter model systems: Journal of Computational Physics, v. 26, p. 1-42.

Daroub, S.H., Stuck, J.D., Lang, T.A., and Diaz, O.A., 2002, Particulate phosphorus in the Everglades Agricultural Area: I – Introduction and sources: Gainesville, University of Florida Institute of Food and Agricultural Sciences, Soil and Water Science Department, Document SL 197.

Davis, J.H., Jr., 1946, The peat deposits of Florida, their occurrence, development and uses: Geological Bulletin, Florida Geologic Survey, v. 30.

DB Environmental, Inc., I.D., 2002a, Submerged aquatic vegetation/limerock treatment system technology: Follow-on study: Final Report Prepared for South Florida Water Management District and Florida Department of Environmental Protection, Contract No. C-E10660, West Palm Beach, Fla., 153 p.

DB Environmental, Inc., I.D., 2002b, Submerged aquatic vegetation/limerock treatment system technology: Follow-on study: STSOC Report Prepared for South Florida Water Management District and Florida Department of Environmental Protection, Contract No. C-E10660, West Palm Beach, Fla., 153 p.

DB Environmental, Inc., 2004, Vegetation Biomass and Nutrient Analysis for STA-1W (Appendix 4B-4), *in* 2004 Everglades Consolidated Report: South Florida Water Management District, West Palm Beach, Fla.

DeBusk, W.F., and Reddy K.R., 1998, Turnover of detrital organic carbon in a nutrient-impacted Everglades marsh: Soil Science Society of America Journal, v. 62, p. 1460-1468.

Dierberg, F.E., DeBusk, T.A., Jackson, S.D., Chimney, M.J., and Pietro, K., 2002, Submerged aquatic vegetation-based treatment wetlands for removing phosphorus from agricultural runoff: Response to hydraulic and nutrient loading: Water Research, v. 36, p. 1409-1422.

Dierberg, F.E., Juston, J.J., DeBusk, T.A., Pietro, K., and Gu B.H., 2005, Relationship between hydraulic efficiency and phosphorus removal in a submerged aquatic vegetation-dominated treatment wetland: Ecological Engineering, v. 25, p. 9-23.

Dingman, S.L., 1984, Fluvial Hydrology: New York, W.H. Freeman and Company.

Dodds, W.K., 2003, The role of periphyton in phosphorus retention in shallow freshwater aquatic systems: Journal of Phycology, v. 39, p. 840-849.

Dong, Q., McCormick, P.V., Sklar, F.H., and DeAngelis, D.L., 2002, Structural instability, multiple stable states, and hysteresis in periphyton driven by phosphorus enrichment in the Everglades: Theoretical Population Biology, v. 61, p. 1-13.

Fisher, M.M., and Reddy, K.R., 2001, Phosphorus flux from wetland soils affected by long-term nutrient loading: Journal of Environmental Quality, v. 30, p. 261-271.

Fisher, P.J., 1990, Hydraulic characteristics of constructed wetlands at Richmond, NSW, Australia, *in* Cooper, P.F., and Findlater, B.C., eds., Constructed Wetlands in Water Pollution Control: Oxford, Pergamon Press, p. 21-32.

Godshalk, G.L., and Wetzel, R.G., 1978, Decomposition of aquatic angiosperms - 2. Particulate components: Aquatic Botany, v. 5, p. 301-327.

Goldman, J.C., and Carpenter, E.J., 1974, A kinetic approach to the effect of temperature on algal growth: Limnology and Oceanography, v. 19, p. 756-766.

Grace, K.A., 2003, Phosphorus removal and soil stability within emergent and submerged vegetation communities in treatment wetlands: Gainesville, University of Florida, M.S. thesis.

Green, J.C., 2006, Effect of macrophyte spatial variability on channel resistance: Advances in Water Resources, v. 29, p. 426-438.

Grenney, W.J., and Kraszewski, A.K., 1981, Description and application of the stream simulation and assessment model: Version IV (SSAM IV): Fort Collins, Colo., Report by U.S. Fish and Wildlife Service Cooperative Instream Flow Service Group.

Grimshaw, H.J., and Dolske, D.A., 2002, Rainfall concentrations and wet atmospheric deposition of phosphorus and other constituents in Florida, USA: Water Air and Soil Pollution, v. 137, p. 117-140.

Grover, J.P., 1989, Phosphorus-dependent growth kinetics of 11 species of freshwater algae: Limnology and Oceanography, v. 34, p. 341-348.

Guardo, M., 1999, Hydrologic balance for a subtropical treatment wetland constructed for nutrient removal, Ecological Engineering, v. 12, p. 315-337.

Guardo, M., and Tomasello, R.S., 1995, Hydrodynamic simulations of a constructed wetland in South Florida: Water Resources Bulletin, v. 31, p. 687-701.

Haan, C.T., 1989, Parametric uncertainty in hydrologic modeling: Transactions of the ASAE, v. 32, no. 1, p. 137.

Haan, C.T., Storm, D.E., Al-Issa, T., Prabhu, S., Sabbagh, G.J., and Edwards D.R., 1998, Effect of parameter distributions on uncertainty analysis of hydrologic models: Transactions of the ASAE, v. 41, p. 65-70.

Hanlon, C.G., 1999, Relationships between total phosphorus concentrations, sampling frequency and wind velocity in a shallow, polymictic lake: Lake and Reservoir Management, v. 15, p. 39-46.

Hansen, K., Mouridsen, S., and Kristensen, E., 1998, The impact of Chironomus plumosus larvae on organic matter decay and nutrient (N,P) exchange in a shallow eutrophic lake sediment following a phytoplankton sedimentation: Hydrobiologia, v. 364, p. 65-74.

Harvey, J.W., Krupa, S.L., and Krest, J.M., 2004, Ground water recharge and discharge in the central Everglades: Ground Water, v. 42, p. 1090-1102.

Havens, K.E., Steinman, A.D., and Hwang, S.J., 2001, Phosphorus uptake by plankton and periphyton in relation to irradiance and phosphate availability in a subtropical lake (Lake Okeechobee, Florida, USA): Archiv Fur Hydrobiologie, v. 151, p. 177-201.

Hecky, R.E., and Kilham, P., 1988, Nutrient limitation of phytoplankton in fresh-water and marine environments—A review of recent evidence on the effects of enrichment: Limnology and Oceanography, v. 33, p. 796-822.

Heilman, R.E. 1995, Phosphorus uptake kinetics of cattail (*Typha spp*.) and sawgrass (*Cladium jamaicense*): Gainesville, University of Florida M.S. thesis, 79 p.

Hendry, C.D., Brezonik, P.L., and Edgerton, E.S., 1981, Atmospheric deposition of nitrogen and phosphorus in Florida, *in* Eisenreich, S.J., ed., Atmospheric Pollutants in Natural Waters: Ann Arbor, Mich., Ann Arbor Science Publishers, p. 199-215.

Herskowitz, J., 1986, Listowel artificial marsh project report: Ontario, Canada, Ontario Ministry of the Environment, Water Resources Branch.

Holdren, G.C., and Armstrong, D.E., 1980, Factors affecting phosphorus release from intact lake sediment cores: Environmental Science & Technology, v. 14, p. 79-87.

Hwang, S.J., Havens, K.E., and Steinman, A.D., 1998, Phosphorus kinetics of planktonic and benthic assemblages in a shallow subtropical lake: Freshwater Biology, v. 40, p. 729-745.

Irons, D.L., 2001, Phosphorus release from calcareous sediments as influenced by pH and redox conditions in a submerged aquatic vegetation wetland: Gainesville, University of Florida M.S. thesis.

James, A.I., and Jawitz, J.W., 2007, Modeling two-dimensional reactive transport using a Godunov-mixed finite element method: Journal of Hydrology, v. 338, p. 28-41.

Jørgensen, S.E., 1976, A eutrophication model for a lake: Ecological Modeling, v. 2, p. 147.

Jørgensen, S.E., Mejer, H., and Friis, M., 1978, Examination of a Lake Model: Ecological Modelling, v. 4, p. 253-278.

Jørgensen, S.E., Nielsen, S.N., and Jørgensen, L.A., 1991, Handbook of ecological parameters and ecotoxicology: Amsterdam and New York, Elsevier, 1,263 p.

Judson, W., Harvey, J.W., Newlin, J.T., Krest, J.M., Choi, J., Nemeth, E.A., and Krupa, S.L., 2004, Surface water and ground-water interactions in the central Everglades, Florida: U.S. Geological Survey Scientific Investigations Report 2004-5069, 88 p.

Jury, W.A., Gardner, W.R., and Gardner, W.H., 1991, Soil physics: New York, John Wiley & Sons, 328 p.

Kadlec, R.H., 1994, Detention and mixing in free-water wetlands: Ecological Engineering, v. 3, p. 345-380.

Kadlec, R.H., 1997, An autobiotic wetland phosphorus model: Ecological Engineering, v. 8, p. 145-172.

Kadlec, R.H., 1999, Phosphorus biogeochemistry in subtropical wetlands, *in* Reddy, K.R., O'Conner, G.A., and Schelske, C.L., eds., Transport of phosphorus in wetlands: Boca Raton, Fla., Lewis Publishers, p. 355-375.

Kadlec, R.H., and Hammer, D.E., 1988, Modeling nutrient behavior in wetlands, Ecological Modelling, v. 40, p. 37-66.

Kadlec, R.H., and Knight, R.L., 1996, Treatment Wetlands: Boca Raton, Fla., Lewis Publishers, 893 p.

Koda, M., McRae, G.J., and Seinfeld, J.H., 1979, Automatic sensitivity analysis of kinetic mechanisms: International Journal of Chemical Kinetics, v. 11, p. 427-444.

Kotz, S., and van Dorp, J.R., 2004, Beyond Beta: Singapore, World Scientific Publishing Co. Pte. Ltd., 283 p.

Krause-Jensen, D., and Sand-Jensen, K., 1998, Light attenuation and photosynthesis of aquatic plant communities: Limnology and Oceanography, v. 43, p. 396-407.

Krom, M.D., and Berner, R.A., 1980, Adsorption of phosphate in anoxic marine-sediments: Limnology and Oceanography, v. 25, p. 797-806.

Lehman, J.T., 1980, Release and cycling of nutrients between planktonic algae and herbivores: Limnology and Oceanography, v. 25, p. 620-632.

Li, W.C., Syers, J.K., Williams, J.D., Armstrong, D., and Harris, R.F., 1972, Rate and extent of inorganic-phosphate exchange in lake sediments: Soil Science Society of America Proceedings, v. 36, p. 279.

Li, Y.H., and Gregory, S., 1974, Diffusion of ions in sea-water and in deep-sea sediments: Geochimica et Cosmochimica Acta, v. 38, p. 703-714.

Luis, S.J., and McLaughlin D., 1992, A stochastic approach to model validation: Advances in Water Resources, v. 15, p. 15.

Martin, J.F., and Reddy, K.R., 1997, Interaction and spatial distribution of wetland nitrogen processes: Ecological Modelling, v. 105, p. 1-21.

Martinez, C.J., and Wise, W.R., 2003a, Analysis of constructed treatment wetland hydraulics with the transient storage model OTIS: Ecological Engineering, v. 20, p. 211-222.

Martinez, C.J., and Wise, W.R., 2003b, Hydraulic analysis of Orlando Easterly Wetland: Journal of Environmental Engineering-Asce, v. 129, p. 553-560.

Mayer, L.M., and Gloss, S.P., 1980, Buffering of silica and phosphate in a turbid river: Limnology and Oceanography, v. 25, p. 12-22.

McCormick, P.V., and Stevenson, R.J., 1998, Periphyton as a tool for ecological assessment and management in the Florida Everglades: Journal of Phycology, v. 34, p. 726-733.

McKay, M.D., 1995, Evaluating prediction uncertainty: NUREG/CR-6311: Los Alamos, N.M., U.S. Nuclear Regulatory Commission and Los Alamos National Laboratory.

McKay, M.D., Conover, W.J., and Beckman R.J., 1979, A comparison of three methods for selecting values of input variables in the analysis of output from a computer code: Technometrics, v. 21, no. 2, p. 239-245.

Miller, M.C., McCave, I.N., and Komar, P.D., 1977, Threshold of sediment motion under unidirectional currents: Sedimentology, v. 24, p. 507-527.

Mitsch, W.J., Cronk, J.K., Wu, X.Y., Nairn, R.W., and Hey, D.L., 1995, Phosphorus retention in constructed fresh-water riparian marshes: Ecological Applications, v. 5, p. 830-845.

Mitsch, W.J., and Gosselink, J.G., 2000, Wetlands (3d ed.): New York, John Wiley & Sons.

Moore, P.A., Reddy, K.R., and Graetz, D.A., 1991, Phosphorus geochemistry in the sediment-water column of a hypereutrophic lake: Journal of Environmental Quality, v. 20, p. 869-875.

Morgan, M.G., and Henrion, M., 1990, Uncertainty: A guide to dealing with uncertianty in quantitative risk and policy analysis: Cambridge, Cambridge University Press, 332 p.

Morris, M.D., 1991, Factorial sampling plans for preliminary computational experiments: Technometrics, v. 33, p. 161-174.

Moustafa, M.Z., 1999, Nutrient retention dynamics of the Everglades Nutrient Removal Project: Wetlands: v. 19, p. 689-704.

Muñoz-Carpena, R., Vellidis, G., Shirmohammadi, A., and Wallender, W.W., 2006, Evaluation of modeling tools for TMDL development and implementation: Transactions of ASABE, v. 49, no. 4, p. 961-965.

Muñoz-Carpena, R., Zajac, Z., and Kuo, Y.M., 2007, Evaluation of water quality models through global sensitivity and uncertainty analyses techniques: Application to the vegetative filter strip model VFSMOD-W: Transactions of ASABE, v. 50, no. 5, p. 1719-1732.

Murphy, J., and Riley, J.P., 1962, A modified single solution method for determination of phosphate in natural waters: Analytica Chimica Acta, v. 26, p. 31.

Murphy, T.P., Riley, K.J., and Yesaki, I., 1983, Coprecipitation of phosphate with calcite in a naturally eutrophic lake: Limnology and Oceanography, v. 28, p. 59-69.

Nepf, H.M., 1999, Drag, turbulence, and diffusion in flow through emergent vegetation: Water Resources Research, v. 35, p. 479-489.

Newman, S., Hagerthey, S., and Cook, M., 2005, Options for accelerating recovery of phosphorus impacted areas of the Florida Everglades: Section 2. Cattail Habitat Improvement Project: West Palm Beach, Fla., South Florida Water Management District report, 21 p.

Newman, S., and Pietro, K., 2001, Phosphorus storage and release in response to flooding: Implications for Everglades storm-water treatment areas: Ecological Engineering, v. 18, p. 23-38.

Noe G.B., and Childers D.L., 2007, Phosphorus budgets in Everglades wetland ecosystems: The effects of hydrology and nutrient enrichment: Wetlands Ecology and Management.

Noe G.B., Childers D.L., and Jones, R.D., 2001, Phosphorus biogeochemistry and the impact of phosphorus enrichment: Why is the everglades so unique?: Ecosystems, v. 4, p. 603-624.

Nungesser, M.K., and Chimney, M.J., 2001, Evaluation of phosphorus retention in a south Florida treatment wetland: Water Science and Technology, v. 44, p. 109-115.

Nyholm, N., 1978, Simulation-model for phytoplankton growth and nutrient cycling in eutrophic, shallow lakes: Ecological Modelling, v. 4, p. 279-310.

Otsuki, A., and Wetzel, R.G., 1972, Coprecipitation of phosphate with carbonates in a marl-lake: Limnology and Oceanography, v. 17, p. 763-767.

Persson, J., Somes, N.L.G., and Wong, T.H.F., 1999, Hydraulics efficiency of constructed wetlands and ponds: Water Science and Technology, v. 40, p. 291-300.

R.A. Smith and Associates, 1994, Wetlands to improve wind lake water quality: Report to Wind Lake Protection Association.

Raghunathan, R., Slawecki, T., Fontaine, T.D., Chen, Z.Q., Dilks, D.W., Bierman, V.J., and Wade, S., 2001, Exploring the dynamics and fate of total phosphorus in the Florida Everglades using a calibrated mass balance model: Ecological Modelling, v. 142, p. 247-259.

Reckhow, K.H., 1994, Water quality simulation modeling and uncertainty analysis for risk assessment and decision-making: Ecological Modelling, v. 72, p. 1-20.

Reddy, K.R., and Graetz, D.A., 1991, Phosphorus dynamics in the Everglades nutrient removal system: Final report 1990-1991: West Palm Beach, Fla., Report Submitted to South Florida Water Management District.

Reddy, K.R., Kadlec, R.H., Flaig, E., and Gale, P.M., 1999, Phosphorus retention in streams and wetlands: A review: Critical reviews in environmental science and technology, v. 29, p. 83-146.

Reddy, K.R., Wetzel, B.G., and Kadlec R.H., 2005, Biogeochemistry of phosphorus in wetlands, *in* Phosphorus: Agriculture and the environment: Madison, Wisc., American Society of Agronomy, p. 263-316

Richardson, C.J., 1985, Mechanisms controlling phosphorus retention capacity in fresh-water wetlands: Science, v. 228, p. 1424-1427.

Richardson, C.J., 1999, The role of wetlands in storage, release, and cycling of phosphorus on the landscape: A 25-year retrospective, *in* Reddy, K.R., O'Conner, G.A., and Schelske, C.L., eds., Phosphorus Biogeochemistry in Subtropical Ecosystems: Boca Raton, Fla., Lewis publishers.

Richardson, C.J., and Qian, S.S., 1999, Long-term phosphorus assimilative capacity in freshwater wetlands: A new paradigm for sustaining ecosystem structure and function: Environmental Science and Technology, v. 33, p. 1545-1551.

Richardson, C.J., and Vaithiyanathan, P., 1995, Phosphorus sorption characteristics of Everglades soils along a eutrophication gradient: Soil Science Society of America Journal, v. 59, p. 1782-1788.

Riis, T., and Biggs, B.J.F., 2003, Hydrologic and hydraulic control of macrophyte establishment and performance in streams: Limnology and Oceanography, v. 48, p. 1488-1497.

Rodgers, J.H., McKevitt, M.E., Hammerlund, D.O., Dickson, K.L., and Cairns, J., 1983, Primary production and decomposition of submergent and emergent aquatic plants of two Appalachian rivers, *in* Fontaine, T.D., and Bartell S.M., eds., Dynamics of Lotic Ecosystems: Michigan, Ann Arbor Science, p. 283-301.

Roesner, L.A., Giguere, P.R., and Evenson, D.E., 1981, Computer program documentation for the stream quality model QUAL-II: Athens, Ga., U.S. Environmental Protection Agency report EPA-600/9-81-014.

Rosendahl, P.C., 1981, The determination of Manning's roughness and longitudinal dispersion coefficients in the Everglades marsh: Paper presented at Symposium on Progress in Wetlands Utilization and Management, Orlando, Fla.

Ruiz, J., Macias, D., and Peters, F., 2004, Turbulence increases the average settling velocity of phytoplankton cells, *in* Proceedings of the National Academy of Sciences of the United States of America, v. 101, p. 17720-17724.

Saltelli, A., 1999, Sensitivity analysis: Could better methods be used?: Journal of Geophysical Research-Atmospheres, v. 104, p. 24013-24013.

Saltelli, A., 2002, Sensitivity analysis for importance assessment: Risk Analysis, v. 22, p. 579-590.

Saltelli, A., Ratto, M., Tarantola, S., and Campolongo, F., 2005, Sensitivity analysis for chemical models: Chemical Reviews, v. 105, p. 2811-2827.

Saltelli, A., Tarantola, S., and Campolongo, F., 2000, Sensitivity analysis as an ingredient of modeling: Statistical Science, v. 15, p. 377-395.

Saltelli, A., Tarantola, S., Campolongo, F., and Ratto, M., 2004, Sensitivity analysis in practice: A guide to assessing scientific models: Chichester, U.K., John Wiley & Sons, 219 p.

Sand-Jensen, K., and Borum, J., 1991, Interactions among phytoplankton, periphyton, and macrophytes in temperate freshwaters and estuaries: Aquatic Botany, v. 41, p. 137-175.

Scavia, D., and Park, R.A., 1976, Documentation of selected constructs and parameter values in the aquatic model cleaner: Ecological Modelling, v. 2, p. 33.

Schelske, C.L., Coveney, M.F., Aldridge, F.J., Kenney, W.F., and Cable, J.E., 2000, Wind or nutrients: Historic hypereutrophy in Lake Apopka, Florida: Archiv für Hydrobiologie—Advances in Limnology, v. 55, p. 543-563.

Scinto, L.J., and Reddy, K.R., 2003, Biotic and abiotic uptake of phosphorus by periphyton in a subtropical freshwater wetland: Aquatic Botany, v. 77, p. 203-222.

Shelef, G., Oswald, W.J., and Golueje, C.C., 1970, Assaying algal growth with respect to nitrate concentration by a continuous flow turbidostat: Advances in Water Pollution Research, v. 2, pap. 3-25, p. 1-9: Pergamon.

Shirmohammadi, A., Chaubey, I., Harmel, R.D., Bosch, D.D., Muñoz-Carpena, R., Dharmasri, C., Sexton, A., Arabi, M., Wolfe, M.L., Frankenberger, J., Graff, C., and Sohrabi, T.M., 2006, Uncertainty in TMDL models: Transactions of ASABE, v. 49, no. 4, p. 1033-1049.

Sklar, F.H., Fitz, H.C., Wu, Y., Van Zee, R., and McVoy, C., 2001, The design of ecological landscape models for Everglades restoration: Ecological Economics, v. 37, p. 379-401.

Slomp, C.P., and VanRaaphorst, W., 1993, Phosphate adsorption in oxidized marine-sediments: Chemical Geology, v. 107, p. 477-480.

Smith, D.J., 1978, Water quality for river-reservoir systems: Report prepared for U.S. Army Corps of Engineers by Resource Management Associates Inc., Lafayette, Calif.

Snyder, G.H., 2005, Everglades agricultural area soil subsidence and land use projections: Soil and Crop Science Society of Florida Proceedings, v. 64, p. 44-51.

Song, J., Luo, Y.M., Zhao, Q.G., and Christie, P., 2004, Microcosm studies on anaerobic phosphate flux and mineralization of lake sediment organic carbon: Journal of Environmental Quality, v. 33, p. 2353-2356.

South Florida Water Management District, 2003, Advanced treatment technologies, chap. 4C of 2003 Everglades consolidated report: West Palm Beach, Fla., 72 p.

Stairs, D.B., 1993, Flow characteristics of constructed wetlands: Tracer studies of the hydraulic regime: Corvallis, Oregon State University M.S. thesis.

Stuck, J.D., 1996, Particulate phosphorus transport in the water conveyance systems of the Everglades Agricultural Area: Gainesville, University of Florida Ph.D. dissertation, 404 p.

Sturm, T.W., 2001, Open Channel Hydraulics: New York, McGraw Hill.

Sutherland, T.F., Amos, C.L., and Grant, J., 1998, The effect of buoyant biofilms on the erodibility of sublittoral sediments of a temperate microtidal estuary, Limnology and Oceanography, v. 43, p. 225-235.

Sweerts, J., Kelly, C.A., Rudd, J.W.M., Hesslein, R., and Cappenberg, T.E., 1991, Similarity of whole-sediment molecular-diffusion coefficients in fresh-water sediments of low and high porosity: Limnology and Oceanography, v. 36, p. 335-342.

Thomann, R.V., Ditoro, D.M., and Oconnor, D.J., 1974, Preliminary model of Potomac Estuary phytoplankton: Journal of the Environmental Engineering Division-Asce, v. 100, p. 699-715.

Turner, B.L., Frossard, E., and Baldwin, D.S., eds., 2005, Organic phosphorus in the environment: Cambridge, Mass., CABI Publishing, 399 p.

Van Rees, K.C.J., Reddy, K.R., and Rao, P.S.C., 1996, Influence of benthic organisms on solute transport in lake sediments: Hydrobiologia, v. 317, p. 31-40.

Walker, W.W., 1995, Design basis for Everglades Stormwater Treatment Areas: Water Resources Bulletin, v. 31, p. 671-685.

Walker, W.W., and Kadlec, R.H., 2005, Dynamic model for Stormwater Treatment Areas: Accessed Sept. 30, 2005, at *http://www.wwwalker.net/dmsta.*

Wang, H.G., Jawitz, J.W., White, J.R., Martinez, C.J., and Sees, M.D., 2006, Rejuvenating the largest municipal treatment wetland in Florida, Ecological Engineering, v. 26, p. 132-146.

Wang, N.M., and Mitsch, W.J., 2000, A detailed ecosystem model of phosphorus dynamics in created riparian wetlands, Ecological Modelling, v. 126, p. 101-130.

Watanabe, F.S., and Olsen, S.R., 1965, Test of an ascorbic acid method for determining phosphorus in water and $NaHCO_3$ extracts from soil: Soil Science Society of America Proceedings, v. 29, p. 677-678.

Wauchope, R.D., and McDowell, L.L., 1984, Adsorption of phosphate, arsenate, methanearsonate, and cacodylate by lake and stream sediments—Comparisons with soils: Journal of Environmental Quality, v. 13, p. 499-504.

Wiberg, P.L., and Smith, J.D., 1987, Calculations of the critical shear-stress for motion of uniform and heterogeneous sediments: Water Resources Research, v. 23, p. 1471-1480.

Worman, A., and Kronnas, V., 2005, Effect of pond shape and vegetation heterogeneity on flow and treatment performance of constructed wetlands, Journal of Hydrology, v. 301, p. 123-138.

Wright, R.M., and McDonnell, A.J., 1986a, Macrophyte growth in shallow streams—Biomass model: Journal of Environmental Engineering-ASCE, v. 112, p. 967-982.

Wright, R.M., and McDonnell, A.J., 1986b, Macrophyte growth in shallow streams—Field investigations: Journal of Environmental Engineering-ASCE, v. 112, p. 953-966.

Wyss, G.D., and Jørgensen, K.H., 1998, A user guide to LHS: Sandia's Latin hypercube sampling software: Albuquerque, N.M., Sandia National Laboratories Technical Report SAND98-0210, p. 1-140.

Appendix 1. Model Nomenclature Used in this Study

This appendix describes the model nomenclature used in the stydy. The symbols and notation used to describe formulations of the model are presented in table A1. The chemical and material components used in the model are given in table A2. Finally, the parameters used in the model are presented in table A3.

Table A1. Symbols and notation used to describe formulations of the model.

Symbol	Description	Symbol	Description
Main symbols used in the model		Subscripts and superscripts for modeled processes[1]	
C	Solute concentration	*atm*	Atmospheric deposition: inflow → (*pn*, *pi*)
G	Growth	*bu*	Burial of soil: (*so*, *si*) → removal
J	Material flux	*ch*	Cohesion: *po* → *bf*
S	Soil concentration	*de*	Decay: (*fo*, *ro*) → (*po*, *so*)
X	Mass fraction	*df*	Diffusion of phosphorus: *sw* ↔ *pw*
Subscripts and superscripts for modeled stores		*en*	Entrainment of soil: *so* → *po*
P	Phosphorus	*gr*	Growth: (*sw*, *pw*) → (*pl*, *fo*, *ro*)
bf	Biofilm	*mn*	Mineralization of phosphorus: *so* → *pw*
bn	Benthic	*ox*	Oxidation of soil: *so* → removal
ep	Epiphytic	*ppt*	Precipitation: *sw* → *pi*
fo	Foliage	*sl*	Sloughing: *bf* → *po*
i	Inorganic (applied to soil *S*)	*sr*	Sorption/desorption: *si* ↔ *pw*
mp	Macrophyte	*st*	Settling: *po* → *so*
o	Organic (applied to soil *S*)	Flux and biomass growth notation[2]	
pi	Particulate inorganic material	G^M	Growth rate of material *M*: $k_g{}^M C^M C_W{}^P/([C_W{}^P]+k_{1/2}{}^M)$
pl	Phytoplankton (subset of *po*)	$J_{sr}{}^W$	Sorption from pore water onto soil: $[C_{si}{}^P] = k_d[C_{pw}{}^P]$
pn	Nonphytoplankton *po* (*po* - *pl*)	$J_{de}{}^{fo}$	Material lost from foliage by decay: $k_{de}{}^{fo} f_f C^{mp}$
po	Particulate organic material	$J_{de}{}^{ro}$	Material lost from roots by decay: $k_{de}{}^{ro} f_r C^{mp}$
pw	Pore water	$J_{df}{}^W$	Diffusion between $C_{sw}{}^P$ and $C_{pw}{}^P$: $k_{df}([C_{sw}{}^P]-[C_{pw}{}^P])/z_{df}$
ro	Roots	$J_{ox}{}^{so}$	Oxidation of organic soil: $k_{ox}{}^{so} S^o$
si	Inorganic soil	$J_{sn}{}^{mp}$	Macrophyte lost be senescence: $k_{sn}{}^{mp} C^{mp}$
so	Organic soil	$J_{sn}{}^{po}$	Particulate organic lost by senescence: $k_{sn}{}^{po} C^{po}$
ss	Suspended solids	$J_{st}{}^{po}$	Suspended organic material settled: $k_{st}{}^{po}[C_{sw}{}^{po}]$
sw	Surface water	$J_{en}{}^{si}$	Inorganic soil entrained into the water column: $k_{sl}{}^{po}[S^{si}]$
W	Water (generic)	$J_{en}{}^{so}$	Organic soil entrained into the water column: $k_{sl}{}^{po}[S^{so}]$

[1]Arrows denote the transfer/transformation from originating store to destination store that the model process represents

[2]Abbreviated notation used in equations. Dimensions and units are [M L^{-2} T^{-1}] and g/m^2/d, respectively

Table A2. Chemical and material components used in the model.

Symbol	Description	Location	Mobile or stabile
	Organic Material		
C^{bf}	Biofilm	Soil (upper surface)	Mobile
C^{mp}	Macrophytes	Water column	Mobile and/or stabile
C_{sw}^{pl}	Phytoplankton (subset of particulate organic material)	Water column	Mobile
C_{sw}^{pn}	Nonphytoplankton fraction of particulate organic material	Water column	Mobile
C_{sw}^{po}	Particulate organic material	Water column	Mobile
S^{o}	Organic soil	Soil	Stabile
	Inorganic Material		
C^{pi}	Particulate inorganic material	Water column	Mobile
S^{i}	Inorganic soil	Soil	Stabile
	Dissolved Solutes		
C_{pw}^{P}	Dissolved phosphorus in pore water	Soil (water phase)	Stabile
C_{sw}^{P}	Dissolved phosphorus in surface water	Water column	Mobile
	Particulate Solutes		
C_{pi}^{P}	Phosphorus in particulate inorganic material	Water column	Mobile
C_{pl}^{P}	Phosphorus in phytoplankton	Water column	Mobile
C_{pn}^{P}	Phosphorus in nonphytoplankton particulate organic material	Water column	Mobile
C_{po}^{P}	Phosphorus in particulate organic material	Water column	Mobile
	Soil		
S_{si}^{P}	Phosphorus in inorganic soil	Soil (solid phase)	Stabile
S_{so}^{P}	Phosphorus in organic soil	Soil (solid phase)	Stabile
	Biomass		
C_{bf}^{P}	Phosphorus in biofilm	Soil (upper surface)	Stabile
C_{mp}^{P}	Phosphorus in macrophytes	Water column	Mobile and/or stabile

Table A3. Parameters used in the model.

[Abbreviations for stores defined by subscript and superscript are provided in table A1. SRP, soluble reactive phosphorus]

Symbol	Description	Symbol	Description
Soil parameters		Rate constants [Dimension, [T^{-1}]; units, 1/d]	
k_d^{sr}	Sorption distribution coefficient	k_{ch}^{po}	Cohesion rate coefficient
z_{as}	Active soil depth	k_{de}^{fo}	Foliage decay rate coefficient
θ	Soil porosity	k_{de}^{ro}	Root decay rate coefficient
ξ	Bioturbation factor, BF	k_g^{fo}	Foliage growth rate coefficient
ρ_b	Bulk density	k_{sl}^{po}	Slough rate coefficient
Water-column parameters		k_g^{ro}	Root growth rate coefficient
b	Arrhenius constant	k_{ox}^{so}	Organic soil oxidation rate
D_m	Molecular diffusion coefficient	k_g^{pl}	Particulate organic (plankton) growth rate coefficient
k_{df}	Diffusion coefficient		
θ^2	Tortuosity	k_{sn}^{pl}	Particulate organic (plankton) senescence coefficient
I_0	Incident light		
k_{dr}	Particle drag coefficient	k_{sn}^{mp}	Macrophyte senescence coefficient
k_e	Light extinction coefficient	k_g^{bf}	Biofilm growth rate
k_{wb}	Light extinction coefficient due to biomass	Half saturation constants [Dimension, [M L^{-3}]; units, g/m^3]	
p_d	Sediment particle diameter	$k_{1/2}^{pl}$	Plankton half saturation constant
T	Temperature	$k_{1/2}^{bf}$	Biofilm half saturation constant
v_x	Surface water velocity in x-direction	$k_{1/2}^{fo}$	Foliage half saturation constant
v_y	Surface water velocity in y-direction	$k_{1/2}^{ro}$	Root half saturation constant
z_{df}	Depth of diffusive exchange	Soil and macrophyte fractions	
z_{wc}	Surface-water depth	f_f	Foliage fraction of macrophytes
z_{ws}	Distance below water surface	f_i	Inorganic soil fraction
ρ_s	Particle density	f_o	Organic soil fraction
ρ_w	Density of water	f_r	Root fraction of macrophytes (1 - f_f)
Mass fractions of phosphorus [dimensions, [MP MM^{-1}]; units, mg/kg (dry weight)]		Remaining mass flux quantities used in the model [Dimension, [M L^{-2} T^{-1}], units, g/m^2/s]	
X_{ep}^{P}	Mass fraction of phosphorus in epiphitic biofilm	J_{ppt}^{P}	Soluble reactive phosphorus deposited with rainfall (precipitation)
X_{fo}^{P}	Mass fraction of phosphorus in foliage	J_{en}^{S}	Material entrained from soil surface into water column
X_{so}^{P}	Mass fraction of phosphorus in organic soil	J_{atm}^{pi}	Atmospheric deposition of particulate inorganic phosphorus
X_{po}^{P}	Mass fraction of phosphorus in particulate organic	J_{atm}^{po}	Atmospheric deposition of particulate organic phosphorus
X_{ro}^{P}	Mass fraction of phosphorus in roots	J_{bu}^{S}	Loss of soil to deep burial
		J_{ppt}^{P}	Coprecipitation of SRP with particulate inorganics

Appendix 2. Model Parameter Values for Levels 1, 2, and 3

[Unit abbreviations: cm^2/s, square centimeter per second; m^3/g, cubic meter per gram; g/m^3, gram per cubic meter; m/s, meter per second; m, meter. Acronyms and other annotations: EAA, Everglades Agricultural Area; SAV, submerged aquatic vegetation; SFWMD, South Florida Water Management District; STA-1W, Stormwater Treatment Area 1 West; WCA; water conservation area; --, unknown or not applicable]

Parameter	Units	Values	Conditions	Reference
k_{df}	cm^2/s	7.91×10^{-6}	Assumed tortuosity = 1	Newman and others (2005); Moore and others (1991)
		7.34×10^{-6}	HPO_4^{2-}	Li and Gregory (1974)
		8.46×10^{-6}	$H_2PO_4^-$	Li and Gregory (1974)
		4.0×10^{-5}	--	Fisher and Reddy (2001)
		$.7 \times 10^{-5}$ - 1.5×10^{-5}	--	Sweerts and others (1991)
		3.53×10^{-6} - 3.33×10^{-6}	Calculated for $\theta = 0.7$ - 0.98	--
k_{ox}	1/day	.0016	Bog	Bridgham and others (1998)
		.0014	Acidic fen	Bridgham and others (1998)
		.0011	Intermediate fen	Bridgham and others (1998)
		.0019	Cedar swamp	Bridgham and others (1998)
		.0013	Tamarack swamp	Bridgham and others (1998)
		.0019	Meadow	Bridgham and others (1998)
		.00027	Fens and bogs	Bauer (2004)
		.00093	Fens and bogs	Bauer (2004)
X_{so}^P	%/100	.0008 - .0025	Soil and sediments	Daroub and others (2002)
		.0009 - .0025	Canal sediments in EAA	Daroub and others (2002)
		.0003	Dairy farm**	Reddy and others (1999)
		.001	Chandler slough	Reddy and others (1999)
		.00074	Lake sediment microcosm	Song and others (2004)
		.00063 - .0013	STA-1W	DB Environmental, Inc. (2002b)
		.00058	STA-1W cell 4 outflow	DB Environmental, Inc. (2002b)
		.0013	STA-1W cell 5 inflow	DB Environmental, Inc. (2002b)
		.00049 - .00053	STA-1W	DB Environmental, Inc. (2002a)
k_d	m^3/g	8.0×10^{-6} - 11.0×10^{-6}	Everglades soils	Richardson and Vaithiyanathan (1995)
		2.20×10^{-5}	Houghton fen peat	Richardson (1985)
		5.0×10^{-6}	Pocosin bog peat (Dare)	Richardson (1985)
		3×10^{-6}	Pocosin bog peat (Ponzer)	Richardson (1985)
		9×10^{-6}	Pocosin bog mineral-peat (Arapahoe)	Richardson (1985)
		81×10^{-6}	Swamp forest mineral-peat	Richardson (1985)
		600×10^{-6}	Colorado River sediments	Mayer and Gloss (1980)
		300×10^{-6}	Mississippi River floodplain sediments	Wauchope and McDowell (1984)
		25×10^{-6} - 35×10^{-6}	Lake sediments	Li and others (1972)
		50×10^{-6} - 3750×10^{-6}	Estuarine sediments	Krom and Berner (1980)
		7×10^{-6}- 436×10^{-6}	Marine sediments	Slomp and VanRaaphorst (1993)

Parameter	Units	Values	Conditions	Reference
k_g^{pl}	1/day	.02 - 2	--	Sand-Jensen and Borum (1991)
		.1-5.65	Extensive review	Jørgensen and others (1991)
		1-2.5	Total phytoplankton (20°)	Chen and Wells (1976)
		1.5	Total phytoplankton (20°)	Grenney and Kraszewski (1981)
		1-2.7	Total phytoplankton (T_{opt})	Scavia and Park (1976)
		1.5	Total phytoplankton (20°)	Nyholm (1978)
		1.8-2.53	Total phytoplankton (T_{opt})	Jørgensen and others (1978)
		.2-8	Calibrated	Baca and Arnett (1976)
		.2-8	Calibrated	Grenney and Kraszewski (1981)
		.58-3	Comprehensive review	Jørgensen (1976)
		.406	STA-1W	CH2M HILL (2002); SFWMD (2003)
$k_{1/2}^{pl}$	g/m^3	.0006-1.27	Freshwater phytoplankton	Borchardt (1996)
		.06	Periphyton	Dodds (2003)
		.0001-.0283	Shallow subtropical lake	Hwang and others (1998)
		.002-.035	Comprehensive review	Jørgensen and others (1991)
k_{st}^{pl}	m/s	.05-.5	Phytoplankton	Chen and Wells (1976)
		0-4	Phytoplankton	Bowie and others (1985)
		.05-.2	Phytoplankton	Thomann and others (1974)
		0-.9	Turbulent conditions	Ruiz and others (2004)
k_{st}^{pl}	m/s	.04-.6	Phytoplankton	Jørgensen (1976)
		.01-4	Calibrated	Baca and Arnett (1976)
		0-2	Calibrated	Smith (1978)
		.15-2	Calibrated	Roesner and others (1981)
		0-30	Comprehensive review	Jørgensen and others (1991)
		.1	From Kadlec and Knight (1995)	R.A. Smith and Associates (1994)
X_{pl}^{P}	%/100	.009-.015	Total phytoplankton	Daroub and others (2002)
		.015	Total phytoplankton	Chen and Wells (1976)
		.0088	Total phytoplankton	Jørgensen (1976)
		.01-.012	Total phytoplankton	Smith (1978)
		.016-.05	Calibrated	Baca and Arnett (1976)
		.0008-.0117	Comprehensive review	Jørgensen and others (1991)
k_g^{mp}	1/day	.004-.17	In Appalachian rivers	Rodgers and others (1983)
		.015	Calibrated for submerged aquatic vegetation	DB Environmental, Inc. (2002b)
$k_{1/2}^{mp}$	g/m^3	.005	Calibrated	Collins and Wlosinski (1989)
		.0047	Field data	Wright and McDonnel (1986a)
		.025	Calibrated for submerged aquatic vegetation.	DB Environmental, Inc. (2002b)
k_{sn}^{mp}	1/day	.03	Maximum	Collins and Wlosinski (1998)
		0-.045	Calibrated	Wright and McDonnel (1986b)
		.05	Maximum	Wright and McDonnel (1986b)
X_{mp}^{P}	%/100	.003-.005 g/g	Canal vegetation	Daroub and others (2002)
		.00017 - .00258	Cattail and sawgrass	Heilman (1995)
		.0008-.002	SAV STA-1W cell 4	DB Environmental, Inc. (2002a)
θ	Unitless	.88	Lake sediment microcosm	Song and others (2004)
		.8	Wetlands in general	Mitsch and Gosselink (2000)
		.93	Everglades	Harvey and others (2004)
		.98	Everglades	Harvey and others (2004)
		.91-.94	Peat soil	Comas and others (2004)

Parameter	Units	Values	Conditions	Reference
ρ_b	Unitless	.25	Lake sediment microcosm	Song and others (2004)
		.09	Everglades	Judson and others (2004)
		.049 - .070	WCA-2A	Fisher and Reddy (2001)
		.051	Bog	Bridgham and others (1998)
		.019	Acidic fen	Bridgham and others (1998)
		.088	Intermediate fen	Bridgham and others (1998)
		.118	Cedar swamp	Bridgham and others (1998)
		.103	Tamarack swamp	Bridgham and others (1998)
		.224	Meadow	Bridgham and others (1998)
		.095-.13	STA-1W	DB Environmental, Inc. (2002b)
λ_l	m	260	Based on Pe#: Cattail/open water	Kadlec (1994)
		250	Based on Pe#: Cattail	Stairs (1993)
		120	Based on Pe#: Cattail	Kadlec and Knight (1996)
		70	Based on Pe#: Cattail	Herskowitz (1986)
		270	Based on Pe#: Open water	Bavor and others (1988)
		150	Based on Pe#: *Myriophyllum*	Fisher (1990)
		70	Based on Pe#: Sawgrass	Rosendahl (1981)
λ_t	m	260	Assumed $\lambda_l = \lambda_t$	Kadlec (1994)
		250	Assumed $\lambda_l = \lambda_t$	Stairs (1993)
		120	Assumed $\lambda_l = \lambda_t$	Kadlec and Knight (1996)
		70	Assumed $\lambda_l = \lambda_t$	Herskowitz (1986)
		270	Assumed $\lambda_l = \lambda_t$	Bavor and others (1988)
		150	Assumed $\lambda_l = \lambda_t$	Fisher (1990)
		70	Assumed $\lambda_l = \lambda_t$	Rosendahl (1981)

*The values were not available at the time of initiating the sensitivity analysis.

Appendix 3. Equations and XML Input Files for Complexity Levels 1, 2, and 3

The equations and XML input files for complexity levels 1, 2, and 3 are presented in this appendix. The sources used for all three complexity levels include surface-water soluble reactive phosphorus (SRP), pore-water SRP, organic soil, and sorbed inorganic phosphorus. In addition to these souces, level 2 includes plankton biomass and level 3 includes plankton biomass and macrophyte biomass. Finally, two input files, Regional Simulation Model/Water Quality Model (RSM/WQ) XML equation file and RSM/WQ parameter definition files, are presented herein for each complexity level.

[Symbols are defined in appendixes 1 and 2]

Level-1 Equations

Surface-water SRP: Mobile [grams per cubic meter]

$$\frac{\mathrm{d}\ddot{C}_{sw}^{\ P}}{\mathrm{d}t} = +\left(\left.\frac{\mathrm{d}\ddot{C}_{sw}^{\ P}}{\mathrm{d}t}\right|_{diffusion}\right) = \frac{k_{df}}{z_w z_{df}}\left(\frac{C_{pw}^{\ P}}{z_{as}\theta} - \ddot{C}_{sw}^{\ P}\right)$$

Units check:

$$\left[\frac{M_P}{L^3 T}\right] = \left[\frac{L^2}{T}\frac{1}{L}\frac{1}{L}\left(\frac{M_P}{L^2}\frac{1}{L}\frac{L^3}{L^3} - \frac{M_P}{L^3}\right)\right]$$

Coded form:

$$\frac{\mathrm{d}(SRP\_sw)}{\mathrm{d}t} = \left[\left(\frac{(k\_df)(SRP\_pw)}{(depth)(z\_df)(active\_soil\_depth)(soil\_porosity)}\right) - \left(\frac{(k\_df)(SRP\_sw)}{(depth)(z\_df)}\right)\right]$$

Pore-water SRP: Stabile [grams per square meter]

$$\frac{\mathrm{d}C_{pw}^{\ P}}{\mathrm{d}t} = -\left(\left.\frac{\mathrm{d}C_{pw}^{\ P}}{\mathrm{d}t}\right|_{diffusion}\right) + \left(\left.\frac{\mathrm{d}C_{pw}^{\ P}}{\mathrm{d}t}\right|_{oxidation}\right) - \left(\left.\frac{\mathrm{d}C_{pw}^{\ P}}{\mathrm{d}t}\right|_{sorption}\right) = -\frac{k_{df}}{z_{df}}\left(\frac{C_{pw}^{\ P}}{z_{as}\theta} - \ddot{C}_{sw}^{\ P}\right) + X_{so}^{\ P} k_{ox} S^o - \frac{k_1 \rho_b k_d^{\ sr}}{\theta} C_{pw}^{\ P} + k_1 S_{si}^{\ P}$$

Units check:

$$\left[\frac{M_P}{L^2 T}\right] = -\left[\frac{L^2}{T}\frac{1}{L}\left(\frac{M_P}{L^2}\frac{1}{L}\frac{L^3}{L^3} - \frac{M_P}{L^3}\right)\right] + \left[\frac{M_P}{M_M}\frac{1}{T}\frac{M_M}{L^2}\right] - \left[\frac{1}{T}\frac{M_M}{L^3}\frac{L^3}{M_M}\frac{L^3}{L^3}\frac{M_P}{L^2}\right] + \left[\frac{1}{T}\frac{M_P}{L^2}\right]$$

Coded form:

$$\frac{\mathrm{d}(SRP\_pw)}{\mathrm{d}t} = \left[-\frac{(k\_df)(SRP\_pw)}{(z\_df)(active\_soil\_depth)(soil\_porosity)} + \frac{(k\_df)(SRP\_sw)}{(z\_df)}\right]$$

$$+\left[(chi\_org\_soil)(k\_ox)(org\_soil)\right]$$

$$+\left[-\frac{(k\_1)(bulk\_density)(k\_d)(SRP\_pw)}{(soil\_porosity)} + (k\_1)(soil\_inorg\_P)\right]$$

Organic soil: Stabile [grams per square meter]

$$\frac{\mathrm{d}S^o}{\mathrm{d}t} = -\left(\left.\frac{\mathrm{d}S^o}{\mathrm{d}t}\right|_{oxidation}\right) = -k_{ox}S^o \quad .$$

Units check:

$$\left[\frac{M_M}{L^2T}\right] = -\left[\frac{1}{T}\frac{M_M}{L^2}\right]$$

Coded form:

$$\frac{\mathrm{d}(org\_soil)}{\mathrm{d}t} = \left[-(k\_ox)(org\_soil)\right]$$

Sorbed inorganic phosphorus: Stabile [grams per square meter]

$$\frac{\mathrm{d}S_{si}{}^P}{\mathrm{d}t} = +\left(\left.\frac{\mathrm{d}S_{si}{}^P}{\mathrm{d}t}\right|_{sorption}\right) = \frac{k_1\rho_b k_d{}^{sr}}{\theta}C_{pw}{}^P - k_1 S_{si}{}^P$$

Units check

$$\left[\frac{M_P}{L^2T}\right] = \left[\frac{1}{T}\frac{M_M}{L^3}\frac{L^3}{M_M}\frac{L^3}{L^3}\frac{M_P}{L^2}\right] - \left[\frac{1}{T}\frac{M_P}{L^2T}\right]$$

Coded form:

$$\frac{\mathrm{d}(inorg\_soil\_P)}{\mathrm{d}t} = \left[\frac{(k\_1)(bulk\_density)(k\_d)(SRP\_pw)}{(soil\_porosity)} - (k\_1)(soil\_inorg\_P)\right]$$

RSM/WQ XML Equation File (eqs_one.xml)

```
<?xml version="1.0" ?>
<!DOCTYPE eqs SYSTEM "../../equations.dtd" [ ]>
<eqs version="0.1">
  <equation>
    <lhs>
      <variable>SRP_sw</variable>
    </lhs>
    <term action="add" type="first_order">
      <variable>SRP_pw</variable>
      <factor action="mult">k_df</factor>
      <factor action="div">z_df</factor>
      <factor action="div" type="physical">soil_porosity</factor>
      <factor action="div" type="physical">active_soil_depth</factor>
      <factor action="div" type="physical">depth</factor>
    </term>
    <term action="sub" type="first_order">
      <variable>SRP_sw</variable>
      <factor action="mult">k_df</factor>
      <factor action="div">z_df</factor>
      <factor action="div" type="physical">depth</factor>
    </term>
  </equation>
  <equation>
    <lhs>
      <variable>SRP_pw</variable>
    </lhs>
    <term action="sub" type="first_order">
      <variable>SRP_pw</variable>
      <factor action="mult">k_df</factor>
      <factor action="div">z_df</factor>
      <factor action="div" type="physical">soil_porosity</factor>
      <factor action="div" type="physical">active_soil_depth</factor>
    </term><term action="add" type="first_order">
      <variable>SRP_sw</variable>
      <factor action="mult">k_df</factor>
      <factor action="div">z_df</factor>
    </term>
    <term action="add" type="first_order">
      <variable>org_soil</variable>
      <factor action="mult">k_ox</factor>
      <factor action="mult">chi_org_soil</factor>
    </term>
    <term action="sub" type="first_order">
      <variable>SRP_pw</variable>
      <factor action="mult">k_1</factor>
      <factor action="mult" type="physical">bulk_density</factor>
      <factor action="mult">k_d</factor>
      <factor action="div" type="physical">soil_porosity</factor>
    </term>
    <term action="add" type="first_order">
      <variable>soil_inorg_p</variable>
      <factor action="mult">k_1</factor>
    </term>
  </equation>
  <equation>
    <lhs>
      <variable>org_soil</variable>
    </lhs>
    <term action="sub" type="first_order">
      <variable>org_soil</variable>
      <factor action="mult">k_ox</factor>
    </term>
  </equation>
  <equation>
    <lhs>
      <variable>soil_inorg_p</variable>
    </lhs>
    <term action="add" type="first_order">
```

```
      <variable>SRP_pw</variable>
      <factor action="mult">k_1</factor>
      <factor action="mult" type="physical">bulk_density</factor>
      <factor action="mult">k_d</factor>
      <factor action="div" type="physical">soil_porosity</factor>
    </term>
    <term action="sub" type="first_order">
      <variable>soil_inorg_p</variable>
      <factor action="mult">k_1</factor>
    </term>
  </equation>
</eqs>
```

RSM/WQ Parameter Definition File (level_one_wq.xml)

```
<?xml version="1.0" ?>
<wq version="0.1">
  <control
    tslen="30"
    tstype="minute"
    use_operator_splitting="true"
    postprocess="true"
    linear_solver_type="gmres"
    linear_preconditioner_type="ilu"
    chemistry_solver_type="gmres"
    chemistry_preconditioner_type="ilu"
    equation_filename="eqs_one.xml"
    fixed_velocity="true"
    x_vel="0.00579"
    y_vel="0.0"
    depth="1.0">
  </control>
  <components>
    <mobile>
      <name symbol="SRP_sw">SRP_sw</name>
      <initial_distribution type="constant"> 0.05 </initial_distribution>
    </mobile>
    <stabile>
      <name symbol="SRP_pw">SRP_pw</name>
      <initial_distribution type="constant"> 0.071 </initial_distribution>
    </stabile>
    <stabile>
      <name symbol="org_soil">org_soil</name>
      <initial_distribution type="constant"> 30000 </initial_distribution>
    </stabile>
    <stabile>
      <name symbol="soil_inorg_p">soil_inorg_p</name>
      <initial_distribution type="constant"> 0.027 </initial_distribution>
    </stabile>
  </components>
  <parameters>
    <chemical units="meter2_per_second">
      <name symbol="k_df">k_df</name>
<initial_distribution type="constant"> par1 </initial_distribution>
    </chemical>
    <chemical units="per_day">
      <name symbol="k_ox">k_ox</name>
<initial_distribution type="constant"> par2 </initial_distribution>
    </chemical>
    <chemical units="none">
      <name symbol="chi_org_soil">chi_org_soil</name>
<initial_distribution type="constant"> par3 </initial_distribution>
    </chemical>
    <chemical units="meter3_per_gram">
      <name symbol="k_d">k_d</name>
<initial_distribution type="constant"> par4 </initial_distribution>
    </chemical>
    <chemical units="per_day">
      <name symbol="k_1">k_1</name>
```

```
      <initial_distribution type="constant"> 1 </initial_distribution>
    </chemical>
    <chemical units="meter">
      <name symbol="z_df">z_df</name>
      <initial_distribution type="constant"> 0.04 </initial_distribution>
    </chemical>
    <physical units="none">
      <name>soil_porosity</name>
<initial_distribution type="constant"> par5 </initial_distribution>
    </physical>
    <physical units="none">
      <name>surface_porosity</name>
      <initial_distribution type="constant"> 1.0 </initial_distribution>
    </physical>
    <physical units="meter">
      <name>active_soil_depth</name>
      <initial_distribution type="constant"> 0.1 </initial_distribution>
    </physical>
    <physical units="none">
      <name>fraction_organic_soil</name>
      <initial_distribution type="constant"> 0.95 </initial_distribution>
    </physical>
    <physical units="none">
      <name>fraction_inorganic_soil</name>
      <initial_distribution type="constant">0.02</initial_distribution>
    </physical>
    <physical units="none">
      <name>bulk_density</name>
<initial_distribution type="constant"> par6 </initial_distribution>
    </physical>
    <physical units="meter">
      <name>long_disp</name>
<initial_distribution type="constant"> par7 </initial_distribution>
    </physical>
    <physical units="meter">
      <name>trans_disp</name>
<initial_distribution type="constant"> par8 </initial_distribution>
    </physical>
  </parameters>
  <mesh>
    <bc type="robin" section="o1" node_id_file="robin_nodes.dat">
      <for>SRP_sw</for>
      <data type="constant"> 0.05 </data>
    </bc>
  </mesh>
  <output>
    <monitor type="global" title="final monitor">
      <for>SRP_sw</for>
      <for>org_soil</for>
      <for>SRP_pw</for>
      <for>soil_inorg_p</for>
      <destination type="text"
                   time_format="no_time_printed"
                   every="-1"
                   spatial_format="indexed">./output/tp_final_output.dat</destination>
    </monitor>
    <monitor type="cell" id="0" title="cell 1 monitor">
      <for>SRP_sw</for>
      <for>org_soil</for>
      <for>SRP_pw</for>
      <for>soil_inorg_p</for>
      <destination type="text"
                   time_format="%Y-%B-%d %H:%M"
                   every="1"
                   spatial_format="indexed">./output/timeseries_cell1.dat</destination>
    </monitor>
    <monitor type="cell" id="40" title="cell 41 monitor">
      <for>SRP_sw</for>
      <for>org_soil</for>
      <for>SRP_pw</for>
```

```
      <for>soil_inorg_p</for>
      <destination type="text"
                   time_format="%Y-%B-%d %H:%M"
                   every="1"
                   spatial_format="indexed">./output/timeseries_cell41.dat</destination>
    </monitor>
    <monitor type="cell" id="80" title="cell 81 monitor">
      <for>SRP_sw</for>
      <for>org_soil</for>
      <for>SRP_pw</for>
      <for>soil_inorg_p</for>
      <destination type="text"
                   time_format="%Y-%B-%d %H:%M"
                   every="1"
                   spatial_format="indexed">./output/timeseries_cell81.dat</destination>
    </monitor>
    <monitor type="cell" id="120" title="cell 121 monitor">
      <for>SRP_sw</for>
      <for>org_soil</for>
      <for>SRP_pw</for>
      <for>soil_inorg_p</for>
      <destination type="text"
                   time_format="%Y-%B-%d %H:%M"
                   every="1"
                   spatial_format="indexed">./output/timeseries_cell121.dat</destination>
    </monitor>
    <monitor type="cell" id="39" title="cell 40 monitor">
      <for>SRP_sw</for>
      <for>org_soil</for>
      <for>SRP_pw</for>
      <for>soil_inorg_p</for>
      <destination type="text"
                   time_format="%Y-%B-%d %H:%M"
                   every="1"
                   spatial_format="indexed">./output/timeseries_cell40.dat</destination>
    </monitor>
    <monitor type="cell" id="79" title="cell 80 monitor">
      <for>SRP_sw</for>
      <for>org_soil</for>
      <for>SRP_pw</for>
      <for>soil_inorg_p</for>
      <destination type="text"
                   time_format="%Y-%B-%d %H:%M"
                   every="1"
                   spatial_format="indexed">./output/timeseries_cell80.dat</destination>
    </monitor>
    <monitor type="cell" id="119" title="cell 120 monitor">
      <for>SRP_sw</for>
      <for>org_soil</for>
      <for>SRP_pw</for>
      <for>soil_inorg_p</for>
      <destination type="text"
                   time_format="%Y-%B-%d %H:%M"
                   every="1"
                   spatial_format="indexed">./output/timeseries_cell120.dat</destination>
    </monitor>
    <monitor type="cell" id="159" title="cell 160 monitor">
      <for>SRP_sw</for>
      <for>org_soil</for>
      <for>SRP_pw</for>
      <for>soil_inorg_p</for>
      <destination type="text"
                   time_format="%Y-%B-%d %H:%M"
                   every="1"
                   spatial_format="indexed">./output/timeseries_cell160.dat</destination>
    </monitor>
  </output>
</wq>
```

Level-2 Equations

Surface-water SRP: Mobile [grams per cubic meter]

$$\frac{d\ddot{C}_{sw}^{\ P}}{dt} = +\left(\left.\frac{d\ddot{C}_{sw}^{\ P}}{dt}\right|_{diffusion}\right) - \left(\left.\frac{d\ddot{C}_{sw}^{\ P}}{dt}\right|_{plankton\_growth}\right) = \frac{k_{df}}{z_w z_{df}}\left(\frac{C_{pw}^{\ P}}{z_{as}\theta} - \ddot{C}_{sw}^{\ P}\right) - X_{pl}^{\ P} k_g^{\ pl} \ddot{C}_{sw}^{\ pl}\left(\frac{\ddot{C}_{sw}^{\ P}}{\ddot{C}_{sw}^{\ P} + k_{1/2}^{\ P}}\right)$$

Units check:

$$\left[\frac{M_P}{L^3 T}\right] = \left[\frac{L^2}{T}\frac{1}{L}\frac{1}{L}\left(\frac{M_P}{L^2}\frac{1}{L}\frac{L^3}{L^3} - \frac{M_P}{L^3}\right)\right] - \left[\frac{M_P}{M_M}\frac{1}{T}\frac{M_M}{L^3}\left(\frac{\frac{M_P}{L^3}}{\frac{M_P}{L^3} + \frac{M_P}{L^3}}\right)\right]$$

Coded form:

$$\frac{d(SRP\_sw)}{dt} = \left[\left(\frac{(k\_df)(SRP\_pw)}{(depth)(z\_df)(active\_soil\_depth)(soil\_porosity)}\right) - \left(\frac{(k\_df)(SRP\_sw)}{(depth)(z\_df)}\right)\right]$$

$$- \left[\left(\frac{(chi\_pl)(k\_pl\_growth)(plankton)(SRP\_sw)}{(SRP\_sw) + (k\_halfsat\_pl)}\right)\right]$$

Pore-water SRP: Stabile [grams per square meter]

$$\frac{dC_{pw}^{\ P}}{dt} = -\left(\left.\frac{dC_{pw}^{\ P}}{dt}\right|_{diffusion}\right) + \left(\left.\frac{dC_{pw}^{\ P}}{dt}\right|_{oxidation}\right) - \left(\left.\frac{dC_{pw}^{\ P}}{dt}\right|_{sorption}\right) = -\frac{k_{df}}{z_{df}}\left(\frac{C_{pw}^{\ P}}{z_{as}\theta} - \ddot{C}_{sw}^{\ P}\right) + X_{so}^{\ P} k_{ox} S^o - \frac{k_1 \rho_b k_d^{\ sr}}{\theta} C_{pw}^{\ P} + k_1 S_{si}^{\ P}$$

Units check:

$$\left[\frac{M_P}{L^2 T}\right] = -\left[\frac{L^2}{T}\frac{1}{L}\left(\frac{M_P}{L^2}\frac{1}{L}\frac{L^3}{L^3} - \frac{M_P}{L^3}\right)\right] + \left[\frac{M_P}{M_M}\frac{1}{T}\frac{M_M}{L^2}\right] - \left[\frac{1}{T}\frac{M_M}{L^3}\frac{L^3}{M_M}\frac{L^3}{L^3}\frac{M_P}{L^2}\right] + \left[\frac{1}{T}\frac{M_P}{L^2}\right]$$

Coded form:

$$\frac{d(SRP\_pw)}{dt} = \left[-\frac{(k\_df)(SRP\_pw)}{(z\_df)(active\_soil\_depth)(soil\_porosity)} + \frac{(k\_df)(SRP\_sw)}{(z\_df)}\right]$$

$$+ \left[(chi\_org\_soil)(k\_ox)(org\_soil)\right]$$

$$+ \left[-\frac{(k\_1)(bulk\_density)(k\_d)(SRP\_pw)}{(soil\_porosity)} + (k\_1)(soil\_inorg\_P)\right]$$

Organic soil: Stabile [grams per square meter]

$$\frac{\mathrm{d}S^o}{\mathrm{d}t} = -\left(\left.\frac{\mathrm{d}S^o}{\mathrm{d}t}\right|_{oxidation}\right) + \left(\left.\frac{\mathrm{d}S^o}{\mathrm{d}t}\right|_{plankton\_settling}\right) = -k_{ox}S^o + k_{st}{}^{pl}\ddot{C}_{sw}{}^{pl}$$

Units check:

$$\left[\frac{M_M}{L^2T}\right] = -\left[\frac{1}{T}\frac{M_M}{L^2}\right] + \left[\frac{L}{T}\frac{M_M}{L^3}\right]$$

Coded form:

$$\frac{\mathrm{d}(org\_soil)}{\mathrm{d}t} = \left[-(k\_ox)(org\_soil)\right] + \left[(k\_pl\_settle)(plankton)\right]$$

Sorbed inorganic phosphorus: Stabile [grams per square meter]

$$\frac{\mathrm{d}S_{si}{}^{P}}{\mathrm{d}t} = +\left(\left.\frac{\mathrm{d}S_{si}{}^{P}}{\mathrm{d}t}\right|_{sorption}\right) = \frac{k_1\rho_b k_d{}^{sr}}{\theta}C_{pw}{}^{P} - k_1 S_{si}{}^{P}$$

Units check:

$$\left[\frac{M_P}{L^2T}\right] = \left[\frac{1}{T}\frac{M_M}{L^3}\frac{L^3}{M_M}\frac{L^3}{L^3}\frac{M_P}{L^2}\right] - \left[\frac{1}{T}\frac{M_P}{L^2T}\right]$$

Coded form:

$$\frac{\mathrm{d}(inorg\_soil\_P)}{\mathrm{d}t} = \left[\frac{(k\_1)(bulk\_density)(k\_d)(SRP\_pw)}{(soil\_porosity)} - (k\_1)(soil\_inorg\_P)\right]$$

Plankton biomass: Mobile [grams per cubic meter]

$$\frac{\mathrm{d}\ddot{C}_{sw}{}^{pl}}{\mathrm{d}t} = +\left(\left.\frac{\mathrm{d}\ddot{C}_{sw}{}^{pl}}{\mathrm{d}t}\right|_{plankton\_growth}\right) - \left(\left.\frac{\mathrm{d}\ddot{C}_{sw}{}^{pl}}{\mathrm{d}t}\right|_{plankton\_senescence}\right) = k_g^{pl}\ddot{C}_{sw}{}^{pl}\left(\frac{\ddot{C}_{sw}{}^{P}}{\ddot{C}_{sw}{}^{P} + k_{1/2}{}^{P}}\right) - \frac{k_{st}{}^{pl}}{z_w}\ddot{C}_{sw}{}^{pl}$$

Units check

$$\frac{M_M}{L^3T} = \left[\frac{1}{T}\frac{M_M}{L^3}\left(\frac{\frac{M_P}{L^3}}{\frac{M_P}{L^3} + \frac{M_P}{L^3}}\right)\right] - \left[\frac{L}{T}\frac{1}{L}\frac{M_M}{L^3}\right]$$

Coded form:

$$\frac{\mathrm{d}(plankton)}{\mathrm{d}t} = \left[\frac{(k\_pl\_growth)(plankton)(SRP\_sw)}{(SRP\_sw) + (k\_pl\_half)}\right] - \left[\frac{(k\_pl\_settle)(plankton)}{(depth)}\right]$$

RSM/WQ XML Equation File (eqs_two.xml)

```
<?xml version="1.0" ?>
<!DOCTYPE eqs SYSTEM "../../equations.dtd" [ ]>
<eqs version="0.1">
  <equation>
    <lhs>
      <variable>SRP_sw</variable>
    </lhs>
    <term action="add" type="first_order">
      <variable>SRP_pw</variable>
      <factor action="mult">k_df</factor>
      <factor action="div">z_df</factor>
      <factor action="div" type="physical">soil_porosity</factor>
      <factor action="div" type="physical">active_soil_depth</factor>
      <factor action="div" type="physical">depth</factor>
    </term>
    <term action="sub" type="first_order">
      <variable>SRP_sw</variable>
      <factor action="mult">k_df</factor>
      <factor action="div">z_df</factor>
      <factor action="div" type="physical">depth</factor>
    </term>
    <term action="sub" type="monod_growth_function">
      <variable>plankton</variable>
      <limiter>SRP_sw</limiter>
      <k_half_sat>k_halfsat_pl</k_half_sat>
      <factor action="mult">chi_pl</factor>
      <factor action="mult">k_pl_growth</factor>
    </term>
  </equation>
  <equation>
    <lhs>
      <variable>SRP_pw</variable>
    </lhs>
    <term action="sub" type="first_order">
      <variable>SRP_pw</variable>
      <factor action="mult">k_df</factor>
      <factor action="div">z_df</factor>
      <factor action="div" type="physical">soil_porosity</factor>
      <factor action="div" type="physical">active_soil_depth</factor>
    </term>
    <term action="add" type="first_order">
      <variable>SRP_sw</variable>
      <factor action="mult">k_df</factor>
      <factor action="div">z_df</factor>
    </term>
    <term action="add" type="first_order">
      <variable>org_soil</variable>
      <factor action="mult">k_ox</factor>
      <factor action="mult">chi_org_soil</factor>
    </term>
    <term action="sub" type="first_order">
      <variable>SRP_pw</variable>
      <factor action="mult">k_1</factor>
      <factor action="mult" type="physical">bulk_density</factor>
      <factor action="mult">k_d</factor>
      <factor action="div" type="physical">soil_porosity</factor>
    </term>
    <term action="add" type="first_order">
      <variable>soil_inorg_p</variable>
      <factor action="mult">k_1</factor>
    </term>
  </equation>
  <equation>
    <lhs>
      <variable>org_soil</variable>
    </lhs>
    <term action="sub" type="first_order">
      <variable>org_soil</variable>
```

```
      <factor action="mult">k_ox</factor>
    </term>
    <term action="add" type="first_order">
      <variable>plankton</variable>
      <factor action="mult">k_pl_settle</factor>
      <factor action="div" type="physical">depth</factor>
    </term>
  </equation>
  <equation>
    <lhs>
      <variable>soil_inorg_p</variable>
    </lhs>
    <term action="add" type="first_order">
      <variable>SRP_pw</variable>
      <factor action="mult">k_1</factor>
      <factor action="mult" type="physical">bulk_density</factor>
      <factor action="mult">k_d</factor>
      <factor action="div" type="physical">soil_porosity</factor>
    </term>
    <term action="sub" type="first_order">
      <variable>soil_inorg_p</variable>
      <factor action="mult">k_1</factor>
    </term>
  </equation>
  <equation>
    <lhs>
      <variable>plankton</variable>
    </lhs>
    <term action="add" type="monod_growth_function">
      <variable>plankton</variable>
      <limiter>SRP_sw</limiter>
      <k_half_sat>k_halfsat_pl</k_half_sat>
      <factor action="mult">k_pl_growth</factor>
    </term>
    <term action="sub" type="first_order">
      <variable>plankton</variable>
      <factor action="mult">k_pl_settle</factor>
    </term>
  </equation>
</eqs>
```

RSM/WQ Parameter Definition File (level_two_wq.xml)

```
<?xml version="1.0" ?>
<wq version="0.1">
  <control
    tslen="30"
    tstype="minute"
    use_operator_splitting="true"
    postprocess="true"
    linear_solver_type="gmres"
    linear_preconditioner_type="ilu"
    chemistry_solver_type="gmres"
    chemistry_preconditioner_type="ilu"
    equation_filename="eqs_two.xml"
    fixed_velocity="true"
    x_vel="0.000579"
    y_vel="0.0"
    depth="1.0">
  </control>
  <components>
    <mobile>
      <name symbol="SRP_sw">SRP_sw</name>
      <initial_distribution type="constant"> 0.05 </initial_distribution>
    </mobile>
    <stabile>
      <name symbol="SRP_pw">SRP_pw</name>
      <initial_distribution type="constant"> 0.071 </initial_distribution>
    </stabile>
```

```
    <stabile>
      <name symbol="org_soil">org_soil</name>
      <initial_distribution type="constant"> 30000 </initial_distribution>
    </stabile>
    <stabile>
      <name symbol="soil_inorg_p">soil_inorg_p</name>
      <initial_distribution type="constant"> 0.027 </initial_distribution>
    </stabile>
    <mobile>
      <name symbol="plankton">plankton</name>
      <initial_distribution type="constant"> 0.043 </initial_distribution>
    </mobile>
  </components>
  <parameters>
    <chemical units="meter2_per_second">
      <name symbol="k_df">k_df</name>
<initial_distribution type="constant"> par1 </initial_distribution>
    </chemical>
    <chemical units="per_day">
      <name symbol="k_ox">k_ox</name>
<initial_distribution type="constant"> par2 </initial_distribution>
    </chemical>
    <chemical units="none">
      <name symbol="chi_org_soil">chi_org_soil</name>
<initial_distribution type="constant"> par3 </initial_distribution>
    </chemical>
    <chemical units="meter3_per_gram">
      <name symbol="k_d">k_d</name>
<initial_distribution type="constant"> par4 </initial_distribution>
    </chemical>
    <chemical units="per_day">
      <name symbol="k_1">k_1</name>
      <initial_distribution type="constant"> 1.0 </initial_distribution>
    </chemical>
    <chemical units="meter">
      <name symbol="z_df">z_df</name>
      <initial_distribution type="constant"> 0.04 </initial_distribution>
    </chemical>
    <chemical units="per_day">
      <name symbol="k_pl_growth">k_pl_growth</name>
<initial_distribution type="constant"> par5 </initial_distribution>
    </chemical>
    <chemical units="gram_per_meter3">
      <name symbol="k_halfsat_pl">k_halfsat_pl</name>
<initial_distribution type="constant"> par6 </initial_distribution>
    </chemical>
    <chemical units="meter_per_second">
      <name symbol="k_pl_settle">k_pl_settle</name>
<initial_distribution type="constant"> par7 </initial_distribution>
    </chemical>
    <chemical units="none">
      <name symbol="chi_pl">chi_pl</name>
<initial_distribution type="constant"> par8 </initial_distribution>
    </chemical>
    <physical units="none">
      <name>soil_porosity</name>
<initial_distribution type="constant"> par9 </initial_distribution>
    </physical>
    <physical units="none">
      <name>surface_porosity</name>
      <initial_distribution type="constant"> 1.0 </initial_distribution>
    </physical>
    <physical units="meter">
      <name>active_soil_depth</name>
      <initial_distribution type="constant"> 0.1 </initial_distribution>
    </physical>
    <physical units="none">
      <name>fraction_organic_soil</name>
      <initial_distribution type="constant"> 0.95 </initial_distribution>
    </physical>
```

```
    <physical units="none">
      <name>fraction_inorganic_soil</name>
      <initial_distribution type="constant"> 0.02 </initial_distribution>
    </physical>
    <physical units="none">
      <name>bulk_density</name>
<initial_distribution type="constant"> par10 </initial_distribution>
    </physical>
    <physical units="meter">
      <name>long_disp</name>
<initial_distribution type="constant"> par11 </initial_distribution>
    </physical>
    <physical units="meter">
      <name>trans_disp</name>
<initial_distribution type="constant"> par12 </initial_distribution>
    </physical>
  </parameters>
  <mesh>
    <bc type="robin" section="o1" node_id_file="robin_nodes.dat">
      <for>SRP_sw</for>
      <data type="constant"> 0.05 </data>
    </bc>
    <bc type="robin" section="o1" node_id_file="robin_nodes.dat">
      <for>plankton</for>
      <data type="constant"> 0.043 </data>
    </bc>
  </mesh>
  <output>
    <monitor type="global" title="final monitor">
      <for>SRP_sw</for>
      <for>org_soil</for>
      <for>SRP_pw</for>
      <for>soil_inorg_p</for>
      <for>plankton</for>
      <destination type="text"
                   time_format="no_time_printed"
                   every="-1"
                   spatial_format="indexed">./output/tp_final_output.dat</destination>
    </monitor>
    <monitor type="cell" id="0" title="cell 1 monitor">
      <for>SRP_sw</for>
      <for>org_soil</for>
      <for>SRP_pw</for>
      <for>soil_inorg_p</for>
      <for>plankton</for>
      <destination type="text"
                   time_format="%Y-%B-%d %H:%M"
                   every="1"
                   spatial_format="indexed">./output/timeseries_cell1.dat</destination>
    </monitor>
    <monitor type="cell" id="40" title="cell 41 monitor">
      <for>SRP_sw</for>
      <for>org_soil</for>
      <for>SRP_pw</for>
      <for>soil_inorg_p</for>
      <for>plankton</for>
      <destination type="text"
                   time_format="%Y-%B-%d %H:%M"
                   every="1"
                   spatial_format="indexed">./output/timeseries_cell41.dat</destination>
    </monitor>
    <monitor type="cell" id="80" title="cell 81 monitor">
      <for>SRP_sw</for>
      <for>org_soil</for>
      <for>SRP_pw</for>
      <for>soil_inorg_p</for>
      <for>plankton</for>
      <destination type="text"
                   time_format="%Y-%B-%d %H:%M"
                   every="1"
```

```
                spatial_format="indexed">./output/timeseries_cell81.dat</destination>
    </monitor>
    <monitor type="cell" id="120" title="cell 121 monitor">
      <for>SRP_sw</for>
      <for>org_soil</for>
      <for>SRP_pw</for>
      <for>soil_inorg_p</for>
      <for>plankton</for>
      <destination type="text"
                time_format="%Y-%B-%d %H:%M"
                every="1"
                spatial_format="indexed">./output/timeseries_cell121.dat</destination>
    </monitor>
    <monitor type="cell" id="39" title="cell 40 monitor">
      <for>SRP_sw</for>
      <for>org_soil</for>
      <for>SRP_pw</for>
      <for>soil_inorg_p</for>
      <for>plankton</for>
      <destination type="text"
                time_format="%Y-%B-%d %H:%M"
                every="1"
                spatial_format="indexed">./output/timeseries_cell40.dat</destination>
    </monitor>
    <monitor type="cell" id="79" title="cell 80 monitor">
      <for>SRP_sw</for>
      <for>org_soil</for>
      <for>SRP_pw</for>
      <for>soil_inorg_p</for>
      <for>plankton</for>
      <destination type="text"
                time_format="%Y-%B-%d %H:%M"
                every="1"
                spatial_format="indexed">./output/timeseries_cell80.dat</destination>
    </monitor>
    <monitor type="cell" id="119" title="cell 120 monitor">
      <for>SRP_sw</for>
      <for>org_soil</for>
      <for>SRP_pw</for>
      <for>soil_inorg_p</for>
      <for>plankton</for>
      <destination type="text"
                time_format="%Y-%B-%d %H:%M"
                every="1"
                spatial_format="indexed">./output/timeseries_cell120.dat</destination>
    </monitor>
    <monitor type="cell" id="159" title="cell 160 monitor">
      <for>SRP_sw</for>
      <for>org_soil</for>
      <for>SRP_pw</for>
      <for>soil_inorg_p</for>
      <for>plankton</for>
      <destination type="text"
                time_format="%Y-%B-%d %H:%M"
                every="1"
                spatial_format="indexed">./output/timeseries_cell160.dat</destination>
    </monitor>
  </output>
</wq>
```

Level-3 Equations

Surface-water SRP: Mobile [grams per cubic meter]

$$\frac{\mathrm{d}\ddot{C}_{sw}^{\ P}}{\mathrm{d}t} = +\left(\left.\frac{\mathrm{d}\ddot{C}_{sw}^{\ P}}{\mathrm{d}t}\right|_{diffusion}\right) - \left(\left.\frac{\mathrm{d}\ddot{C}_{sw}^{\ P}}{\mathrm{d}t}\right|_{plankton\_growth}\right) = \frac{k_{df}}{z_w z_{df}}\left(\frac{C_{pw}^{\ P}}{z_{as}\theta} - \ddot{C}_{sw}^{\ P}\right) - X_{pl}^{\ P} k_g^{\ pl} \ddot{C}_{sw}^{\ pl}\left(\frac{\ddot{C}_{sw}^{\ P}}{\ddot{C}_{sw}^{\ P} + k_{1/2}^{\ pl}}\right)$$

Units check:

$$\left[\frac{M_P}{L^3 T}\right] = \left[\frac{L^2}{T}\frac{1}{L}\frac{1}{L}\left(\frac{M_P}{L^2}\frac{1}{L}\frac{L^3}{L^3} - \frac{M_P}{L^3}\right)\right] - \left[\frac{M_P}{M_M}\frac{1}{T}\frac{M_M}{L^3}\left(\frac{\frac{M_P}{L^3}}{\frac{M_P}{L^3} + \frac{M_P}{L^3}}\right)\right]$$

Coded form:

$$\frac{\mathrm{d}(SRP\_sw)}{\mathrm{d}t} = \left[\left(\frac{(k\_df)(SRP\_pw)}{(depth)(z\_df)(active\_soil\_depth)(soil\_porosity)}\right) - \left(\frac{(k\_df)(SRP\_sw)}{(depth)(z\_df)}\right)\right]$$

$$- \left[\left(\frac{(chi\_pl)(k\_pl\_growth)(plankton)(SRP\_sw)}{(SRP\_sw) + (k\_halfsat\_pl)}\right)\right]$$

Pore-water SRP: Stabile [grams per square meter]

$$\frac{\mathrm{d}C_{pw}^{\ P}}{\mathrm{d}t} = -\left(\left.\frac{\mathrm{d}C_{pw}^{\ P}}{\mathrm{d}t}\right|_{diffusion}\right) + \left(\left.\frac{\mathrm{d}C_{pw}^{\ P}}{\mathrm{d}t}\right|_{oxidation}\right) - \left(\left.\frac{\mathrm{d}C_{pw}^{\ P}}{\mathrm{d}t}\right|_{sorption}\right) - \left(\left.\frac{\mathrm{d}C_{pw}^{\ P}}{\mathrm{d}t}\right|_{macrophyte\_growth}\right)$$

$$= -\frac{k_{df}}{z_{df}}\left(\frac{C_{pw}^{\ P}}{z_{as}\theta} - \ddot{C}_{sw}^{\ P}\right) + X_{so}^{\ P} k_{ox} S^o - \frac{k_1 \rho_b k_d^{\ sr}}{\theta} C_{pw}^{\ P} + k_1 S_{si}^{\ P} - X_{mp}^{\ P} k_g^{\ mp} C_{sw}^{\ mp}\left(\frac{C_{pw}^{\ P}}{C_{pw}^{\ P} + z_{as}\theta k_{1/2}^{\ pl}}\right)$$

Units check:

$$\left[\frac{M_P}{L^2 T}\right] = -\left[\frac{L^2}{T}\frac{1}{L}\left(\frac{M_P}{L^2}\frac{1}{L}\frac{L^3}{L^3} - \frac{M_P}{L^3}\right)\right] + \left[\frac{M_P}{M_M}\frac{1}{T}\frac{M_M}{L^2}\right] - \left[\frac{1}{T}\frac{M_M}{L^3}\frac{L^3}{M_M}\frac{L^3}{L^3}\frac{M_P}{L^2}\right] + \left[\frac{1}{T}\frac{M_P}{L^2}\right]$$
$$+ \left[\frac{M_P}{M_M}\frac{1}{T}\frac{M_M}{L^2}\left(\frac{\frac{M_P}{L^2}}{\frac{M_P}{L^2} + \frac{L}{1}\frac{L^3}{L^3}\frac{M_P}{L^3}}\right)\right]$$

Coded form:

$$\frac{\mathrm{d}(SRP\_pw)}{\mathrm{d}t} = \left[-\frac{(k\_df)(SRP\_pw)}{(z\_df)(active\_soil\_depth)(soil\_porosity)} + \frac{(k\_df)(SRP\_sw)}{(z\_df)} \right]$$

$$+\left[(chi\_org\_soil)(k\_ox)(org\_soil)\right]$$

$$+\left[-\frac{(k\_1)(bulk\_density)(k\_d)(SRP\_pw)}{(soil\_porosity)} + (k\_1)(soil\_inorg\_P) \right]$$

$$+\left[-\frac{(chi\_mp)(k\_mp\_growth)(macrophytes)(SRP\_pw)}{(SRP\_pw)+(active\_soil\_depth)(soil\_porosity)(k\_halfsat\_mp)} \right]$$

Organic soil: Stabile [grams per square meter]

$$\frac{\mathrm{d}S^o}{\mathrm{d}t} = -\left(\left.\frac{\mathrm{d}S^o}{\mathrm{d}t}\right|_{oxidation} \right) + \left(\left.\frac{\mathrm{d}S^o}{\mathrm{d}t}\right|_{plankton\_settling} \right) + \left(\left.\frac{\mathrm{d}S^o}{\mathrm{d}t}\right|_{macrophyte\_settling} \right) = -k_{ox}S^o + k_{st}{}^{pl}\ddot{C}_{sw}{}^{pl} + k_{sn}{}^{mp}C^{mp}$$

.

Units check:

$$\left[\frac{M_M}{L^2T}\right] = -\left[\frac{1}{T}\frac{M_M}{L^2}\right] + \left[\frac{L}{T}\frac{M_M}{L^3}\right] + \left[\frac{1}{T}\frac{M_M}{L^2}\right]$$

Coded form:

$$\frac{\mathrm{d}(org\_soil)}{\mathrm{d}t} = \left[-(k\_ox)(org\_soil)\right] + \left[(k\_pl\_settle)(plankton)\right] + \left[(k\_mp\_senesc)(macrophytes)\right]$$

Sorbed inorganic phosphorus: Stabile [grams per square meter]

$$\frac{\mathrm{d}S_{si}{}^P}{\mathrm{d}t} = +\left(\left.\frac{\mathrm{d}S_{si}{}^P}{\mathrm{d}t}\right|_{sorption} \right) = \frac{k_1\rho_b k_d{}^{sr}}{\theta} C_{pw}{}^P - k_1 S_{si}{}^P$$

Units check

$$\left[\frac{M_P}{L^2T}\right] = \left[\frac{1}{T}\frac{M_M}{L^3}\frac{L^3}{M_M}\frac{L^3}{L^3}\frac{M_P}{L^2}\right] - \left[\frac{1}{T}\frac{M_P}{L^2T}\right]$$

Coded form:

$$\frac{\mathrm{d}(inorg\_soil\_P)}{\mathrm{d}t} = \left[\frac{(k\_1)(bulk\_density)(k\_d)(SRP\_pw)}{(soil\_porosity)} - (k\_1)(soil\_inorg\_P) \right]$$

Planktonic biomass: Mobile [grams per cubic meter]

$$\frac{\mathrm{d}\ddot{C}_{sw}^{\ pl}}{\mathrm{d}t} = +\left(\left.\frac{\mathrm{d}\ddot{C}_{sw}^{\ pl}}{\mathrm{d}t}\right|_{plankton\_growth}\right) - \left(\left.\frac{\mathrm{d}\ddot{C}_{sw}^{\ pl}}{\mathrm{d}t}\right|_{plankton\_senescence}\right) = k_g^{pl}\ddot{C}_{sw}^{\ pl}\left(\frac{\ddot{C}_{sw}^{\ P}}{\ddot{C}_{sw}^{\ P} + k_{1/2}^{\ P}}\right) - \frac{k_{st}^{\ pl}}{z_w}\ddot{C}_{sw}^{\ pl}$$

Units check

$$\frac{M_M}{L^3T} = \left[\frac{1}{T}\frac{M_M}{L^3}\left(\frac{\frac{M_P}{L^3}}{\frac{M_P}{L^3} + \frac{M_P}{L^3}}\right)\right] - \left[\frac{L}{T}\frac{1}{L}\frac{M_M}{L^3}\right]$$

Coded form:

$$\frac{\mathrm{d}(plankton)}{\mathrm{d}t} = \left[\frac{(k\_pl\_growth)(plankton)(SRP\_sw)}{(SRP\_sw) + (k\_pl\_half)}\right] - \left[\frac{(k\_pl\_settle)(plankton)}{(depth)}\right]$$

Macrophyte biomass: Stabile [grams per square meter]

$$\frac{\mathrm{d}C^{mp}}{\mathrm{d}t} = +\left(\left.\frac{\mathrm{d}C^{mp}}{\mathrm{d}t}\right|_{macrophyte\_growth}\right) - \left(\left.\frac{\mathrm{d}C^{mp}}{\mathrm{d}t}\right|_{macrophyte\_senescence}\right) = k_g^{\ mp}C^{mp}\left(\frac{C_{pw}^{\ P}}{C_{pw}^{\ P} + z_{as}\theta k_{1/2}^{\ mp}}\right) - k_{sn}^{\ mp}C^{mp}$$

Units check

$$\frac{M_M}{L^2T} = \left[\frac{1}{T}\frac{M_M}{L^2}\left(\frac{\frac{M_P}{L^2}}{\frac{M_P}{L^2} + \frac{L}{1}\frac{L^3}{L^3}\frac{M_P}{L^3}}\right)\right] - \left[\frac{1}{T}\frac{M_M}{L^2}\right]$$

Coded form:

$$\frac{\mathrm{d}(macrophytes)}{\mathrm{d}t} = \left[\frac{(k\_mp\_growth)(macrophytes)(SRP\_pw)}{(SRP\_pw) + (active\_soil\_depth)(soil\_porosity)(k\_halfsat\_mp)}\right]$$

$$- \left[(k\_mp\_senesc)(macrophytes)\right]$$

RSM/WQ XML Equation File (eqs_three.xml)

```
<?xml version="1.0" ?>
<!DOCTYPE eqs SYSTEM "../../equations.dtd" [ ]>
<eqs version="0.1">
  <equation>
    <lhs>
      <variable>SRP_sw</variable>
    </lhs>
    <term action="add" type="first_order">
      <variable>SRP_pw</variable>
      <factor action="mult">k_df</factor>
      <factor action="div">z_df</factor>
      <factor action="div" type="physical">soil_porosity</factor>
      <factor action="div" type="physical">active_soil_depth</factor>
      <factor action="div" type="physical">depth</factor>
    </term>
    <term action="sub" type="first_order">
      <variable>SRP_sw</variable>
      <factor action="mult">k_df</factor>
      <factor action="div">z_df</factor>
      <factor action="div" type="physical">depth</factor>
    </term>
    <term action="sub" type="monod_growth_function">
      <variable>plankton</variable>
      <limiter>SRP_sw</limiter>
      <k_half_sat>k_halfsat_pl</k_half_sat>
      <factor action="mult">chi_pl</factor>
      <factor action="mult">k_pl_growth</factor>
    </term>
  </equation>
  <equation>
    <lhs>
      <variable>SRP_pw</variable>
    </lhs>
    <term action="sub" type="first_order">
      <variable>SRP_pw</variable>
      <factor action="mult">k_df</factor>
      <factor action="div">z_df</factor>
      <factor action="div" type="physical">soil_porosity</factor>
      <factor action="div" type="physical">active_soil_depth</factor>
    </term>
    <term action="add" type="first_order">
      <variable>SRP_sw</variable>
      <factor action="mult">k_df</factor>
      <factor action="div">z_df</factor>
    </term>
    <term action="add" type="first_order">
      <variable>org_soil</variable>
      <factor action="mult">k_ox</factor>
      <factor action="mult">chi_org_soil</factor>
    </term>
    <term action="sub" type="first_order">
      <variable>SRP_pw</variable>
      <factor action="mult">k_1</factor>
      <factor action="mult" type="physical">bulk_density</factor>
      <factor action="mult">k_d</factor>
      <factor action="div" type="physical">soil_porosity</factor>
    </term>
    <term action="add" type="first_order">
      <variable>soil_inorg_p</variable>
      <factor action="mult">k_1</factor>
    </term>
    <term action="sub" type="monod_growth_function">
      <variable>macrophytes</variable>
      <limiter>SRP_pw</limiter>
      <k_half_sat>mod_k_halfsat_mp</k_half_sat>
      <factor action="mult">chi_mp</factor>
      <factor action="mult">k_mp_growth</factor>
    </term>
```

```
  </equation>
  <equation>
    <lhs>
      <variable>org_soil</variable>
    </lhs>
    <term action="sub" type="first_order">
      <variable>org_soil</variable>
      <factor action="mult">k_ox</factor>
    </term>
    <term action="add" type="first_order">
      <variable>plankton</variable>
      <factor action="mult">k_pl_settle</factor>
    </term>
    <term action="add" type="first_order">
      <variable>macrophytes</variable>
      <factor action="mult">k_mp_settle</factor>
      <factor action="div" type="physical">depth</factor>
    </term>
  </equation>
  <equation>
    <lhs>
      <variable>soil_inorg_p</variable>
    </lhs>
    <term action="add" type="first_order">
      <variable>SRP_pw</variable>
      <factor action="mult">k_1</factor>
      <factor action="mult" type="physical">bulk_density</factor>
      <factor action="mult">k_d</factor>
      <factor action="div" type="physical">soil_porosity</factor>
    </term>
    <term action="sub" type="first_order">
      <variable>soil_inorg_p</variable>
      <factor action="mult">k_1</factor>
    </term>
  </equation>
  <equation>
    <lhs>
      <variable>plankton</variable>
    </lhs>
    <term action="add" type="monod_growth_function">
      <variable>plankton</variable>
      <limiter>SRP_sw</limiter>
      <k_half_sat>k_halfsat_pl</k_half_sat>
      <factor action="mult">k_pl_growth</factor>
    </term>
    <term action="sub" type="first_order">
      <variable>plankton</variable>
      <factor action="mult">k_pl_settle</factor>
    </term>
  </equation>
  <equation>
    <lhs>
      <variable>macrophytes</variable>
    </lhs>
    <term action="add" type="monod_growth_function">
      <variable>macrophytes</variable>
      <limiter>SRP_pw</limiter>
      <k_half_sat>mod_k_halfsat_mp</k_half_sat>
      <factor action="mult">k_mp_growth</factor>
    </term>
    <term action="sub" type="first_order">
      <variable>macrophytes</variable>
      <factor action="mult">k_mp_senesc</factor>
    </term>
  </equation>
</eqs>
```

RSM/WQ Parameter Definition File (level_three_wq.xml)

```
<?xml version="1.0" ?>
<wq version="0.1">
  <control
    tslen="30"
    tstype="minute"
    use_operator_splitting="true"
    postprocess="true"
    linear_solver_type="gmres"
    linear_preconditioner_type="ilu"
    chemistry_solver_type="gmres"
    chemistry_preconditioner_type="ilu"
    equation_filename="eqs_three.xml"
    fixed_velocity="true"
    x_vel="0.000579"
    y_vel="0.0"
    depth="1.0">
  </control>
  <components>
    <mobile>
      <name symbol="SRP_sw">SRP_sw</name>
      <initial_distribution type="constant"> 0.05 </initial_distribution>
    </mobile>
    <stabile>
      <name symbol="SRP_pw">SRP_pw</name>
      <initial_distribution type="constant"> 0.071 </initial_distribution>
    </stabile>
    <stabile>
      <name symbol="org_soil">org_soil</name>
      <initial_distribution type="constant"> 30000 </initial_distribution>
    </stabile>
    <stabile>
      <name symbol="soil_inorg_p">soil_inorg_p</name>
      <initial_distribution type="constant"> 0.027 </initial_distribution>
    </stabile>
    <mobile>
      <name symbol="plankton">plankton</name>
      <initial_distribution type="constant"> 0.043 </initial_distribution>
    </mobile>
    <stabile>
      <name symbol="macrophytes">macrophytes</name>
      <initial_distribution type="constant"> 500 </initial_distribution>
    </stabile>
  </components>
  <parameters>
    <chemical units="meter2_per_second">
      <name symbol="k_df">k_df</name>
<initial_distribution type="constant"> par1 </initial_distribution>
    </chemical>
    <chemical units="per_day">
      <name symbol="k_ox">k_ox</name>
<initial_distribution type="constant"> par2 </initial_distribution>
    </chemical>
    <chemical units="none">
      <name symbol="chi_org_soil">chi_org_soil</name>
<initial_distribution type="constant"> par3 </initial_distribution>
    </chemical>
    <chemical units="meter3_per_gram">
      <name symbol="k_d">k_d</name>
<initial_distribution type="constant"> par4 </initial_distribution>
    </chemical>
    <chemical units="per_day">
      <name symbol="k_1">k_1</name>
      <initial_distribution type="constant"> 1.0 </initial_distribution>
    </chemical>
    <chemical units="meter">
      <name symbol="z_df">z_df</name>
      <initial_distribution type="constant"> 0.04 </initial_distribution>
    </chemical>
```

```
    <chemical units="per_day">
      <name symbol="k_pl_growth">k_pl_growth</name>
<initial_distribution type="constant"> par5 </initial_distribution>
    </chemical>
    <chemical units="gram_per_meter3">
      <name symbol="k_halfsat_pl">k_halfsat_pl</name>
<initial_distribution type="constant"> par6 </initial_distribution>
    </chemical>
    <chemical units="meter_per_second">
      <name symbol="k_pl_settle">k_pl_settle</name>
<initial_distribution type="constant"> par7 </initial_distribution>
    </chemical>
    <chemical units="none">
      <name symbol="chi_pl">chi_pl</name>
<initial_distribution type="constant"> par8 </initial_distribution>
    </chemical>
    <chemical units="per_day">
      <name symbol="k_mp_growth">k_mp_growth</name>
<initial_distribution type="constant"> par9 </initial_distribution>
    </chemical>
    <chemical units="gram_per_meter2">
      <name symbol="mod_k_halfsat_mp">mod_k_halfsat_mp</name>
<initial_distribution type="constant"> par10 </initial_distribution>
    </chemical>
    <chemical units="per_day">
      <name symbol="k_mp_senesc">k_mp_senesc</name>
<initial_distribution type="constant"> par11 </initial_distribution>
    </chemical>
    <chemical units="none">
      <name symbol="chi_mp">chi_mp</name>
<initial_distribution type="constant"> par12 </initial_distribution>
    </chemical>
    <physical units="none">
      <name>soil_porosity</name>
<initial_distribution type="constant"> par13 </initial_distribution>
    </physical>
    <physical units="none">
      <name>surface_porosity</name>
      <initial_distribution type="constant"> 1.0 </initial_distribution>
    </physical>
    <physical units="meter">
      <name>active_soil_depth</name>
      <initial_distribution type="constant"> 0.1 </initial_distribution>
    </physical>
    <physical units="none">
      <name>fraction_organic_soil</name>
      <initial_distribution type="constant"> 0.95 </initial_distribution>
    </physical>
    <physical units="none">
      <name>fraction_inorganic_soil</name>
      <initial_distribution type="constant"> 0.02 </initial_distribution>
    </physical>
    <physical units="none">
      <name>bulk_density</name>
<initial_distribution type="constant"> par14 </initial_distribution>
    </physical>
    <physical units="meter">
      <name>long_disp</name>
<initial_distribution type="constant"> par15 </initial_distribution>
    </physical>
    <physical units="meter">
      <name>trans_disp</name>
<initial_distribution type="constant"> par16 </initial_distribution>
    </physical>
  </parameters>
  <mesh>
    <bc type="robin" section="ol" node_id_file="robin_nodes.dat">
      <for>SRP_sw</for>
      <data type="constant"> 0.05 </data>
    </bc>
```

```
  <bc type="robin" section="ol" node_id_file="robin_nodes.dat">
    <for>plankton</for>
    <data type="constant"> 0.043 </data>
  </bc>
</mesh>
<output>
  <monitor type="global" title="final monitor">
    <for>SRP_sw</for>
    <for>org_soil</for>
    <for>SRP_pw</for>
    <for>soil_inorg_p</for>
    <for>plankton</for>
    <for>macrophytes</for>
    <destination type="text"
                 time_format="no_time_printed"
                 every="-1"
                 spatial_format="indexed">./output/tp_final_output.dat</destination>
  </monitor>
  <monitor type="cell" id="0" title="cell 1 monitor">
    <for>SRP_sw</for>
    <for>org_soil</for>
    <for>SRP_pw</for>
    <for>soil_inorg_p</for>
    <for>plankton</for>
    <for>macrophytes</for>
    <destination type="text"
                 time_format="%Y-%B-%d %H:%M"
                 every="1"
                 spatial_format="indexed">./output/timeseries_cell1.dat</destination>
  </monitor>
  <monitor type="cell" id="40" title="cell 41 monitor">
    <for>SRP_sw</for>
    <for>org_soil</for>
    <for>SRP_pw</for>
    <for>soil_inorg_p</for>
    <for>plankton</for>
    <for>macrophytes</for>
    <destination type="text"
                 time_format="%Y-%B-%d %H:%M"
                 every="1"
                 spatial_format="indexed">./output/timeseries_cell41.dat</destination>
  </monitor>
  <monitor type="cell" id="80" title="cell 81 monitor">
    <for>SRP_sw</for>
    <for>org_soil</for>
    <for>SRP_pw</for>
    <for>soil_inorg_p</for>
    <for>plankton</for>
    <for>macrophytes</for>
    <destination type="text"
                 time_format="%Y-%B-%d %H:%M"
                 every="1"
                 spatial_format="indexed">./output/timeseries_cell81.dat</destination>
  </monitor>
  <monitor type="cell" id="120" title="cell 121 monitor">
    <for>SRP_sw</for>
    <for>org_soil</for>
    <for>SRP_pw</for>
    <for>soil_inorg_p</for>
    <for>plankton</for>
    <for>macrophytes</for>
    <destination type="text"
                 time_format="%Y-%B-%d %H:%M"
                 every="1"
                 spatial_format="indexed">./output/timeseries_cell121.dat</destination>
  </monitor>
  <monitor type="cell" id="39" title="cell 40 monitor">
    <for>SRP_sw</for>
    <for>org_soil</for>
    <for>SRP_pw</for>
```

```
      <for>soil_inorg_p</for>
      <for>plankton</for>
      <for>macrophytes</for>
      <destination type="text"
                   time_format="%Y-%B-%d %H:%M"
                   every="1"
                   spatial_format="indexed">./output/timeseries_cell40.dat</destination>
    </monitor>
    <monitor type="cell" id="79" title="cell 80 monitor">
      <for>SRP_sw</for>
      <for>org_soil</for>
      <for>SRP_pw</for>
      <for>soil_inorg_p</for>
      <for>plankton</for>
      <for>macrophytes</for>
      <destination type="text"
                   time_format="%Y-%B-%d %H:%M"
                   every="1"
                   spatial_format="indexed">./output/timeseries_cell80.dat</destination>
    </monitor>
    <monitor type="cell" id="119" title="cell 120 monitor">
      <for>SRP_sw</for>
      <for>org_soil</for>
      <for>SRP_pw</for>
      <for>soil_inorg_p</for>
      <for>plankton</for>
      <for>macrophytes</for>
      <destination type="text"
                   time_format="%Y-%B-%d %H:%M"
                   every="1"
                   spatial_format="indexed">./output/timeseries_cell120.dat</destination>
    </monitor>
    <monitor type="cell" id="159" title="cell 160 monitor">
      <for>SRP_sw</for>
      <for>org_soil</for>
      <for>SRP_pw</for>
      <for>soil_inorg_p</for>
      <for>plankton</for>
      <for>macrophytes</for>
      <destination type="text"
                   time_format="%Y-%B-%d %H:%M"
                   every="1"
                   spatial_format="indexed">./output/timeseries_cell160.dat</destination>
    </monitor>
  </output>
</wq>
```

Appendix 4. Fourier Amplitude Sensitivity Test (FAST) for Additional Model Outputs

A discussion of the FAST results for the remainder of the model outputs described in table 6 and not discussed in the main document is presented here. A threshold value of greater than 5 percent of total output variance was selected to separate sensitive from nonsensitive parameters. Values greater than 5 percent are highlighted as sensitive parameters in tables 14 to 19.

Surface-Water Soluble Reactive Phosphorus (SRP) Outflow

The quantitative FAST sensitivity analysis results for surface-water SRP outflow are presented in table 14 and figure 26. Both $C_{sw}{}^{P}]_{o,t}$ and $C_{sw}{}^{P}]_{o,tf}$ are tabulated, but given the strong similarity between their results, only surface-water SRP at the end of the simulation represented by $C_{sw}{}^{P}]_{o,tf}$ is discussed unless otherwise noted.

At level 1, the linear first-order effects of the parameters account for nearly all of the observed variance in the model output (about 89 percent of the total output variance across all velocities). At the 5-percent threshold level, four principal parameters collectively account for over 99 percent of first-order effects for all velocity cases. Of these four, k_{ox} is the most important, accounting for 35 to 38 percent of the total model variance. The second most important parameter, ρ_b, is responsible for 19 to 22 percent, followed by k_{df} and $X_{so}{}^{P}$, which are each responsible for about 16 percent of the total variance. The interactions are relatively insignificant, however, when compared with the large linear effects of these parameters, although all four of the parameters invoke higher order effects above 5 percent. There is little variation in sensitivity of the important parameters across the range of velocities as shown in figures 26A-B. The slight decrease in the first-order effects of k_{ox} and $X_{so}{}^{P}$ are minimal with increasing velocity, as is the small increase in ρ_b. The higher order effects exhibit no change with increasing velocity. As shown in figure 26, surface-water SRP at all levels exhibits some dependence on velocity, which is expected for a mobile component. As shown later, this trend is also present for the other mobile component (that is, plankton) and not evident in the stabile components for levels 1 and 2 (figs. 26-30).

In level 2, output measures for surface-water SRP indicate that plankton growth parameters $k_g{}^{pl}$ and $k_{1/2}{}^{pl}$ are the two primary controlling factors for surface-water SRP outflow (table 14). Both outputs show the effect decreases from 50 to 100 m/d, and then increases at 500 m/d (fig. 26C). At this level, surface-water SRP is dominated by first-order effects, which account for 75 to 95 percent of the observed output variance. In contrast with the other velocities, almost half of the output variance at the 100 m/d velocity is due to interactions.

Level 3 introduces substantially more nonlinearity in the model sensitivity to parameters. About 50 percent of the total variance can be attributed to first-order effects for all velocities (table 14). The first-order indexes quantitatively show that the four most important parameters are k_d, $k_g{}^{pl}$, $k_{1/2}{}^{pl}$ and $k_{st}{}^{pl}$, although their values change with velocity conditions. This indicates the relative importance of plankton dynamics and soil sorption on available surface-water SRP for the conditions simulated by the model. However, the first-order effects of these important parameters are always low and only gain some importance (15-20 percent of the total output variance) for the fastest flow velocity. The remaining first-order effects are spread thinly among all the other parameters, emphasizing the overall small total first-order effect shown for level 3. These figures are in contrast with the much larger numbers for the higher-order interactions in table 14, showing the dominance of the nonlinear effects at this level than typically found for lower complexity levels. For almost all of the parameters, at least 50 percent of the variance due to each can be attributed to its interactions with other parameters. The velocity dependence of some parameters is shown in figure 26E, where each of the important parameters exhibits some change between 50 and 500 m/d. In nearly all instances, an initial shift in sensitivity occurs, either up or down, as velocity increases; the shift then reverses direction with further velocity increase. This is especially true for $k_g{}^{pl}$ and $k_{1/2}{}^{pl}$, both of which exhibit an initial loss in sensitivity between 50 and 100 m/d, that reverses and increases rapidly between 100 and 500 m/d. In contrast, $k_{st}{}^{pl}$ showed the opposite trend. All parameters show a general reduction in higher order sensitivity effects with increasing velocity, although this is amplified somewhat for θ (fig. 26F).

Pore-Water Soluble Reactive Phosphorus (SRP) Variation

The sensitivity of pore-water SRP in level 1 is also strongly dominated by the first-order effects of a few parameters. Table 15 shows that k_{ox}, $X_{so}{}^{P}$, and ρ_b account for 96 percent of all first-order effects, which in turn account for 86 percent of the total variance in pore-water SRP. Consequently, the combined effect of all higher order interactions is only about 14 percent, highlighting the strong dominance of first-order effects evident at this level. The strongest influence on pore-water SRP is k_{ox}, which causes almost 44 percent of all the observed variance. The remaining two important parameters, $X_{so}{}^{P}$ and ρ_b, respectively contribute about 21 and 18 percent of the observed variance. As was the case for surface-water SRP, and apparent in figure 27A-B, velocity does not affect the sensitivity of any parameter for level 1.

Similar to level 1, the level-2 first-order effects are more important than the interactions, accounting for 83 percent of the variance at all velocities. The same three parameters that were identified in level 1 consistently have the greatest effect, and together account for 79 percent of the total variance in level 2. These parameters, k_{ox}, X_{so}^{P}, and ρ_b, respectively account for 42, 20 and 17 to 18 percent of the variance. Given the magnitude of these first-order effects, the interactions are considered relatively unimportant. No velocity dependence is apparent, with the major parameter effects remaining consistent over all three velocities (fig. 27C-D).

At level 3, total sensitivity is diffused over almost all the parameters, as was observed for surface-water SRP. About 49 percent of the total pore-water SRP variance is due to first-order effects (table 15), with k_g^{mp} and X_{mp}^{P} being the two most important parameters for all velocities.

For level 3, about 9 to 10 percent of the variance at any velocity is due to X_{mp}^{P}; this differs from k_g^{mp}, which is partly sensitive to velocity (fig. 27E). At 500, 100, and 50 m/d, velocity is responsible for 13, 17, and 12 percent , respectively, of the total output variance. At 50 m/d, k_{ox} contributes more than 5 percent of the variance, but this steadily declines with increasing velocity. These parameters collectively account for only about 50 percent of the total first-order variance, with the other half due to the cumulative effect of the remaining parameters.

With only about half of the variance explained by first-order effects, the importance of the higher-order interactions is evident at level 3. Higher order effects account for greater than 50 percent of the variance for all parameters (except for θ at 500 m/d), and in many cases, greater than 80 percent. This confirms that the cumulative interactions of almost every parameter create the variation, and this combined with the small but widespread first-order contributions of almost all the parameters, make it difficult to identify a few key parameters. With velocity change, some trends also appear in the interactions, in particular, with respect to X_{so}^{P} and θ (fig. 27F). This decrease in the importance of θ as velocity increases from 100 to 500 m/d was also observed earlier for surface-water SRP. The parameter X_{so}^{P} shows a bidirectional shift in higher order effects similar to the observed pattern of first-order effects for other parameters—a rapid change in one direction from 50 to 100 m/d, followed by a reversal in direction from 100 to 500 m/d. For X_{so}^{P}, the effect decreases between 50 and 100 m/d, but then rises between 100 and 500 m/d.

Organic Soil Accretion

The FAST analysis quantitatively identifies k_{ox} as the only important parameter for level 1 for the output of this model, with strong first-order dominance in its effect; that is, S_i = 99 percent for this parameter (table 16). Higher order effects are minimal, and although there is some change in significance at different velocities, as shown in figure 28A-D, the scale at which they occur is too small to have any importance. Figure 28A-B further confirms the strong linear dependency of the simulated soil organic accretion on k_{ox} and the absence of any velocity effects.

For level 2, total variance in organic soil also is due almost entirely to the first-order effects associated with k_{ox}, which again accounts for 99 percent of the variability. Velocity has no measurable influence on the effect of the parameter, which is the same result obtained for level 1 (figs. 28C-D). This indicates that adding the plankton component has little effect on organic soil accretion.

Level-3 first-order results for organic soil accretion show that only two parameters appear at the 5-percent significance level; namely, k_{ox} and k_{sn}^{mp} (table 16). The total contribution from first-order effects ranges from about 50 percent at 50 and 100 m/d, to 60 percent at 500 m/d. Of these parameters, k_{ox} has the strongest influence, accounting for between 13 and 15 percent of the total variance in linear effects. As velocity decreases, a progressive increase in the effect of k_{sn}^{mp} is evident as it rises from 4 to 9 percent at 50 m/d. The velocity relations at the first-order level are shown in figure 28E, where the effect of k_{sn}^{mp} increases at lower velocities. The dominance of k_{ox} also is evident, rising between 50 and 100 m/d, and decreasing slightly between 100 and 500 m/d. The prevalence of high interaction effects in table 16 again confirms the dominance of higher order effects at level 3, which exhibit minimal velocity dependence (fig. 28F). Only θ exhibits the typical reduction in higher order effects for the maximum velocity case. The plankton settling parameters, k_{st}^{pl} and X_{pl}^{P}, are two of the most consistently important parameters with respect to higher order effects. At 500 m/d, more than 80 percent of the effects for both parameters and X_{so}^{P} occur through interactions. At 100 m/d, k_{st}^{pl} and X_{pl}^{P} again are in the 80-percent range, as is λ_l. For the 50-m/d case, the plankton parameters are greater than 80 percent, along with k_{df} and $k_{1/2}^{mp}$. Most of the parameters have large higher order components, however, which inherently include overlapping effects; this makes it difficult to select dominant parameters other than k_{ox} and k_{sn}^{mp}.

Soil Adsorbed Phosphorus Variation

Level-1 first-order effects account for greater than 90 percent of the variance in soil-adsorbed phosphorus (table 17). Of this percentage, about 51 percent is attributed to k_{ox}, regardless of velocity. Almost 25 percent is attributed to X_{so}^{P} and 12 percent to ρ_b, both also independent of velocity. As shown in figures 29a and b, velocity does not substantially affect first-order or higher-order sensitivities.

For level-2 analysis, the same three parameters determined to be the most important for soil pore water are again the most important for soil adsorbed phosphorus. Total first-order effects are somewhat higher in this case than for pore-water SRP, reaching 90 percent. The effect of k_{ox} increases to 49 percent compared with the 42 percent for pore-water SRP, and X_{so}^{P} similarly increases to 26 percent compared to 20 percent for pore-water SRP. In contrast, the effect of ρ_b decreases to 13 percent. Again, no substantial velocity effect is observed at this level (figs. 29C-D).

At level 3, the first-order effects of all the parameters combined on soil inorganic phosphorus range from 54 to 56 percent with increasing velocity (table 17). Of these parameters, k_g^{mp} and X_{mp}^{P} have substantial first-order influence. The most dominant parameter is k_g^{mp}, which respectively accounts for 18 to 24 percent of the total variance in soil adsorbed phosphorus. Eleven percent of the variance is accounted for by X_{mp}^{P} at 500 m/d, and 9 percent at 50 and 100 m/d. The second parameter, k_{ox} also shows some first-order influence at 50 m/d, accounting for 6 percent of the variance through first-order effects. Although the level-3 higher order indexes are not specific to any single parameter (table 17), the overall effect is substantial, accounting for almost half of the total variance observed. Individual higher order effects for each parameter are all lower than 80 percent, but in almost all cases greater than 50 percent. Figure 29E shows that differences in velocity do not substantially affect the fraction of the total variance controlled directly by X_{mp}^{P} or k_{ox}. The same increase and decline identified for pore-water SRP, however, is observed for k_g^{mp}, where the first-order effect is greatest at 100 m/d. Figure 29E also shows the importance of k_g^{mp} and X_{mp}^{P}, as well as the smaller influence of k_{ox}. The collective interactive effect of all the parameters is again indicated. Two noteworthy changes with velocity are the reduced higher order importance of X_{so}^{P} at 100 m/d and θ at 500 m/d (fig. 29F).

Plankton Biomass Outflow

Planktonic biomass is first incorporated in level 2, and the observed variance at slower velocities is due entirely to first-order effects, with five primary contributors. The most important of the parameters is k_{ox}, which accounts for 40 percent of the observed output variance at both velocities (table 18). The parameters k_{df}, X_{so}^{P}, X_{pl}^{P} and ρ_b are each responsible for between 14 and 18 percent of the total variance. At the maximum velocity, a distinct change in the sensitivity is observed; none of the previous five parameters are significant above the 5-percent level, whereas $k_{1/2}^{pl}$ is now responsible for 18 percent of the variance and, most importantly, k_g^{pl} is responsible for 65 percent of the overall variance. This indicates that a marked change in the system dynamics occurs between 100 and 500 m/d, which is also indicated in figures 30A-B.

For level 3, five parameters have greater than 10-percent first order effects. At 50 and 100 m/d, three parameters are responsible for the first-order effects (table 18); k_{st}^{pl} accounts for 11 and 12 percent, X_{pl}^{P} for 16 and 8 percent, and k_g^{mp} for 5 and 12 percent, respectively. Both k_{st}^{pl} and X_{pl}^{P} exhibit some first-order influence, but most of the variance is due to k_g^{pl} and $k_{1/2}^{pl}$, which together account for 24 percent of the total variance in plankton. In this case, some difference in sensitivity to parameters was observed between $C_{sw}^{pl}]_{o,t}$ and $C_{sw}^{pl}]_{o,tf}$. The overall simulation average for plankton ($C_{sw}^{pl}]_{o,t}$) was more sensitive to X_{pl}^{P} at 100 m/d, and to both X_{pl}^{P} and k_{st}^{pl} at 50 m/d. In contrast, the end-of-simulation average ($C_{sw}^{pl}]_{o,tf}$) was more sensitive to k_g^{mp} at all velocities, but particularly the slower two. Overall, first-order effects accounted for 52 percent of the variance for the 100- and 500-m/d velocities, and as much as 70 percent at 50 m/d. As such, higher order effects are more substantial than previous outputs for the higher velocity cases, but are some of the lowest obtained for level 3 at 50 m/d. As discussed later, only macrophytes exhibit a stronger first order response. At level 3, higher order effects were similar for both plankton output measures ($C_{sw}^{pl}]_{o,t}$ and $C_{sw}^{pl}]_{o,tf}$). Because first-order effects account for only half the variance at 100 and 500 m/d, higher order effects are of similar magnitude to those obtained for other outputs at this level. At 50 m/d, however, only 30 percent of the total output variance is due to interactions (table 18), whereas the linear effects of all five of the important parameters identified at this level appear to vary widely with velocity (fig. 30C). With increasing velocity, X_{pl}^{P}, k_{st}^{pl} and k_g^{mp} lose some influence, whereas k_g^{pl}, $k_{1/2}^{pl}$ and X_{mp}^{P} gain influence. Although the effects generally follow the same trends for both plankton outputs, the final time-step average ($C_{sw}^{pl}]_{o,tf}$) shows X_{pl}^{P} gain and then lose influence with increased velocity, and k_g^{mp} lose influence over the 50- to 100-m/d range. By comparison with other outputs, the changes with velocity of higher order indexes for simulated plankton biomass are marginal (fig. 30D). Most parameters show some change in influence, although this is relatively minor except, perhaps, for X_{so}^{P} and ρ_b.

Macrophyte Biomass Accumulation

Macrophytes show some variation in their first-order response (table 19). At 50 m/d, 64 percent of the variance is attributed to first-order effects, and greater than 71 percent at 500 m/d, compared with only 43 percent at 100 m/d. The most important effect on macrophytes, and indeed on any output by any parameter at level 3, was by X_{mp}^{P} at 500 m/d. The first-order effect of X_{mp}^{P} accounted for almost 30 percent of the total observed variance, and at 50 and 100 m/d, it accounted for 16 and 10 percent of the change, respectively. The second most important parameter, k_{sn}^{mp}, exhibited first-order effects of 5, 7, and 12 percent with decreasing velocity. At all three velocities, k_{ox} contributed at least 5 percent of the total variance through first-order effects, and X_{so}^{P} showed similar but smaller effects. Because relatively high first-order effects are present at the 50 and (especially) 500 m/d velocities, interactions are less important at these extremes. At 100 m/d, however, interactions produced the majority of the total effects for all the important parameters, explaining 57 percent of the output variance. Figure 31A shows an initial drop and subsequent marked increase in X_{mp}^{P} that incorporates the important first-order effects just discussed. The progressive decrease in the effect of k_{sn}^{mp} with increasing velocity (from 12 to 5 percent) is also shown in figure 31A. Only k_{g}^{pl} (fig. 31B) shows any clearly discernible higher order sensitivity to velocity, with a pronounced minimum at 100 m/d.